METALLURGY AND METALLURGICAL ENGINEERING SERIES
ROBERT F. MEHL, PH.D., D.Sc., *Consulting Editor*

STRUCTURE
AND
PROPERTIES OF ALLOYS

In accordance with War Production Board regulations, this book is printed in a war-time economy format with reduced margins. However, the type page is standard for a book of this kind, and ease of reading is maintained.

At the end of the war when paper and binding materials are again plentiful, this book and other similar volumes will be reprinted in larger size with normal margins.

METALLURGY AND METALLURGICAL ENGINEERING SERIES

Barrett—Structure of Metals

Brick and Phillips—Structure and Properties of Alloys

Butts—Metallurgical Problems
Second Edition

Kehl—The Principles of Metallographic Laboratory Practice
Second Edition

Seitz—The Physics of Metals

STRUCTURE

AND

PROPERTIES OF ALLOYS

The Application of Phase Diagrams to the Interpretation and Control of Industrial Alloy Structures

BY

R. M. BRICK

Assistant Professor of Metallurgy, Yale University

AND

ARTHUR PHILLIPS

Professor of Metallurgy, Yale University

FIRST EDITION
THIRD IMPRESSION

McGRAW-HILL BOOK COMPANY, INC.
NEW YORK AND LONDON
1942

STRUCTURE AND PROPERTIES OF ALLOYS

THE MAPLE PRESS COMPANY, YORK, PA.

To

Champion Herbert Mathewson

PREFACE

The initiation of the Engineering, Science, and Management Defense Training Program, early in 1941, revealed a widespread interest in physical metallurgy applied to the control of metallurgical processes and the properties of industrial metals and alloys. Large plants with trained men adequate for normal production were forced to expand their technical staffs for increased production, and thus faced the problem of training new men for specialized control work. Smaller plants that managed to meet the requirements of their normal peacetime production without trained metallurgists found that government contracts, or subcontracts, with definite metal specifications required men with a knowledge of the response of metals and alloys to variations in chemical composition and to mechanical and thermal treatments. Interest generally was about equally distributed between nonferrous and ferrous metals although, among the latter, tool steels were of far more importance than is represented by their percentage of the total steel production.

A course covering this field has long been given to engineering students at Yale University and was well adapted for more general purposes. The "Metals Handbook" of the American Society for Metals has been employed as a general reference and textbook, which necessarily involved supplementary lectures, mimeographed sheets, and photomicrographs. Since correlation of structures with phase diagrams is essential to an understanding of the basis of physical metallurgy, and since no present textbook establishes that fundamental background in a manner readily understandable to the neophyte worker in metallurgy, it was felt that a book in this narrow field would be valuable, not only for defense training courses given to industrial employees, but for general engineering students who will use metals and should understand the basis for compositions, heat treatments, structures, and properties.

The original mimeographed material which forms the basis of this book was first written in 1922 and has been subsequently

revised at frequent intervals. Most of the large number of photomicrographs were prepared by Dr. D. L. Martin and Dr. R. G. Treuting, former graduate students in metallurgy. Many of the factual statements in the text were derived from research papers by individuals working in this field, but, in view of the character of the book, few specific references to the original literature have been included.

R. M. Brick,
Arthur Phillips.

Yale University,
New Haven, Conn.,
September, 1942.

CONTENTS

INTRODUCTION

" . . . we as individuals differ to a great degree in the depth of understanding that satisfies our intellectual curiosity. A lot depends on what we have learned to accept as facts, because of frequent observation, without asking ourselves why or without being able, having asked the question, to answer why."

JOHN L. CHRISTIE.

Physical metallurgy is concerned with the properties of metals and alloys, as affected by composition and by mechanical and thermal treatments. Although the technological advances associated with the development of an ever-increasing number of alloys, specifically adapted for industrial usage, have received popular recognition, there is too little appreciation of the scientific approach to the problems of metal behavior.

In the short period of approximately forty years, the metallurgist, by the accumulation and classification of voluminous data, has succeeded in establishing a systematization of knowledge which constitutes a science of metals. Certainly, present-day developments in physical metallurgy are motivated and directed by the systematic studies of the relationships between composition, structure, and properties of metallic substances. However, the status of metallurgy is not that of an independent science for its fundamental concepts have been derived by the intelligent application of three basic sciences, *viz.*, chemistry, physics, and crystallography.

The detailed and fragmental information acquired during the growth of a science generally leads to the adoption and standardization of forms and expressions for presenting the relatively few fundamental principles which are derived from an assembly and interpretation of experimental evidence. In physical metallurgy, the most basic expression is that embodied in the line drawings called *phase, equilibrium* or *constitutional diagrams.* Homogeneous parts of a system which are separated from one another by definite physical boundaries are often called *phases.* Although metallic phases, under nonequilibrium conditions, are

not necessarily homogeneous, every phase is characterized by a distinctive atomic configuration of the material in which there may be continuous chemical and physical variations. A discontinuous change in type or spacing of atom packing is necessarily a phase change. Thus, a metal may exist in one or more of three forms or phases; as a gas with no atomic bonds, as a liquid with loose or easily broken atomic bonds, and as a solid in which atomic bonds are strong and a fixed atomic structure exists. By using extremely high pressures, the ordinary atomic lattice or crystal structure of many pure metals may be altered, and this by definition constitutes a change in phase.

A binary alloy phase diagram shows for a system of two components (*e.g.*, chemically, water and salt, or metallurgically, copper and zinc) how changes in temperature of any specific alloy, or variations in the relative amounts of the two elements present, affect the number or composition of phases. A correlated knowledge of the crystallographic structures of the phases, of their preferred locations in the structure, and of their growth habits from the liquid or solid state makes it possible to predict in a qualitative manner the effect of temperature or concentration changes on the number, amount, size, or distribution of phases and thus the properties of the alloy. Actually, few industrial alloys consist of only two elements, since impurity elements are always present to some degree in commercial metals. However, the common impurities modify the phase diagrams only slightly, and most of the important alloys can be treated as binary.

The primary purpose of this text is to correlate, in a systematic manner, the alloy phase diagrams and property data that are available in many books, with selected photographs of the internal alloy structures at appropriate magnifications (enlarged 10 to 1,000 times). Not only are the alloy structures obtained under equilibrium conditions of extremely slow cooling, as required to conform with the phase diagrams, shown and discussed, but the more important nonequilibrium structures characteristic of many industrial alloys are reproduced. These illustrate the typical departures from a stable state frequently encountered when cooling conditions are rapid, on the order of or faster than those of sand-casting or air-cooling. When an understanding of the phase diagrams has been gained, it becomes possible to predict when the cooling rate is important and when it is not. Finally,

some typical micrographs illustrating defective structures have been included to demonstrate the usefulness of the phase diagrams, correlated with a knowledge of the fundamental principles governing metal structures, in interpreting alloy failures. The scope of the book does not permit discussion of all metal problems or difficulties; only those specifically related to internal structures are mentioned.

Illustrative data on physical or mechanical properties have been included, in most sections of the book, in tabular rather than graphical form. Although it is easier to grasp the significant trend of property changes with composition, etc., from drawings, the original data obtained by tests are always in tabular form, and it is believed the student may gain more by taking this material and plotting it himself than by studying charts. Questions appearing at the end of each section of this book may be answered either by reasoning from material included in the text or by referring to the "Metals Handbook."

The effort to focus attention upon the relationship between microstructures and properties, together with the actual application of phase diagrams in qualitatively predicting these effects, has led to a book with well-defined limits within which an attempt has been made to be reasonably comprehensive and complete, for student or more general uses. At the same time, to preserve a compact treatment, it appeared undesirable to attempt either a quantitative reproduction of all the data available on alloy properties or a detailed discussion of important, related manipulative techniques such as testing and temperature measurement. The "Metals Handbook," of the American Society for Metals, which contains the most complete compilation of data on metals and alloys but is lacking in respect to microstructural effects and their causes, should be available to anyone working with metals. It is employed throughout this text as the standard reference book.

For a detailed discussion of theory and practice in the field of physical metallurgy, Doan and Mahla's "Physical Metallurgy" or Sachs and Van Horn's "Practical Metallurgy" is recommended, or, in the field indicated by its title, Sisco's "Modern Metallurgy for Engineers." "Modern Uses of Nonferrous Metals" (A.I.M.E.) describes the development of useful metal and alloy products in a nontechnical, narrative style. Engineers

interested in metal specifications should consult the American Society for Testing Materials (A.S.T.M.) volumes of Tentative Standards or the Society of Automotive Engineers (S.A.E.) "Specifications Handbook." Finally, if some understanding of the fundamentals of physical metallurgy is obtained from this book, men working with metals will be in a position to profit from the many technical publications of the American Institute of Mining and Metallurgical Engineers (A.I.M.E.), the American Society for Metals (A.S.M.), and, in allied fields, publications covering foundry practice, heat treating, etc., or journals of general coverage such as *Metals and Alloys*.

STRUCTURE AND PROPERTIES OF ALLOYS

CHAPTER I

REQUISITE TOOLS OF THE METALLURGIST

Each section of this book devoted to specific alloy systems is subdivided into three parts entitled Phase Diagram, Structures, and Properties. An understanding of the material included under each of these headings requires a prior knowledge of methods of acquiring the significant data by direct or indirect measurements and observations. All methods employed to obtain data for the construction of phase diagrams, as well as the application of these diagrams in heat treatment procedures, require accurate measurement of temperature. Structures are visually observed, using polished specimens and a reflecting type of microscope. Properties are most commonly evaluated in terms of strength and hardness characteristics. The techniques used in each of these fundamental fields may influence the results obtained.

PYROMETRY

Temperatures of from −40 to 400°C. can be measured with thermometers having a liquid which expands in a calibrated pyrex glass capillary tube. For temperatures below −40°C. or up to about 1600°C., the thermoelectric pyrometer is generally used. This instrument includes a *thermocouple*, two wires of dissimilar metals or alloys usually welded together at one end which is placed at the point where a temperature measurement is desired. An instrument for measuring millivoltages is connected across the other ends of the wires. As the temperature of the welded end is increased, while that of the ends connected to the instrument is held constant, a current tends to flow in the wire. The voltage causing the flow increases with the

temperature of the hot junction. The voltage-temperature relationship is thus the basis of measurement of temperature. Because the relationship is not linear for the useful operating range of the wires employed, tables of voltages vs. temperature for each combination of dissimilar wires, or calibration of the setup, must be used. Calibration of the original thermocouple and instrument and repetition of this at intervals are always desirable for the following reasons:

1. The hot-junction weld may be imperfect and result in low voltage readings.

2. No two sets of wire, even from the same source, are necessarily identical in composition, and slight variations may be responsible for voltage differences equivalent to as much as 20°C.

3. The temperature-voltage relationship of thermocouples may change if the wires are contaminated by contact with certain gases (particularly carbon monoxide) or by alloying upon contact with liquid metals.

Calibration may be performed by comparison at various temperatures with a standardized instrument and couple, or by determining the indicated freezing point of substances with known freezing points. Pure metals are customarily used, and it is essential that the calibrating substance be of the same purity as the one whose temperature is known. For example, pure copper freezes at 1083°C., but when melted in air, the liquid metal dissolves oxygen and the copper-oxygen alloy may freeze at as low as 1065°C.

The "Metals Handbook" contains a detailed description of thermoelectric pyrometers, the different combinations of thermocouple wires available, and the two different types of voltage-measuring instruments commonly employed. There is also a discussion of optical and radiation types of pyrometers, used chiefly for measuring temperatures above 1000°C. The thermocouple type is by far the most widely used because of its relatively low cost, high accuracy (when properly employed), and the fact that its operating range permits it to be used in the control of most metallurgical processes. One last word as to its proper use deserves particular emphasis; the instrument records only the temperature of its "hot junction," which is not necessarily the same as that of the metal being treated. This difficulty

may be avoided by setting the hot junction of the couple in the center of the charge, if possible, or by circulating the heating medium (gas or liquid) so as to obtain temperature uniformity. The wires must be insulated from each other to insure that the active hot junction is at the welded tip. If a metal or refractory tube encloses the thermocouple to protect it from contamination by gases or liquid metals, time is necessary for the temperature to become equalized inside and outside the protection tube. There may be large differences in the temperature of metal at different points in a large furnace, or a large crucible, and for uniformity of heating, tests must be made to determine if gradients exist and their extent.

MICROSCOPY (METALLOGRAPHY)

The word *metallography*, formerly applied to the entire field of physical metallurgy, is now generally restricted to the field of microscopic work. The internal structure of metals and alloys is revealed by magnifying a polished or a polished and "etched" surface. The preparation of this surface is of great importance since variations in technique may distort or exaggerate essential parts of the structure.

Essentially, polishing for structural observations requires the attainment, or approximation, of a mirrorlike surface by cutting away normal irregularities rather than by causing high areas to flow into low areas, as in buffing. Flow distorts the surface and may lead to entirely erroneous conclusions as to the characteristics of the structure (*cf.* former concept of "primary" and "secondary" troostite or sorbite, page 143). The first stages of cutting the surface to a plane are usually accomplished by grinding with successively finer grades of abrasives cemented on paper. The direction of cutting is altered at each change to a finer abrasive to facilitate recognition of the stage when coarser or deeper scratches have been replaced by more shallow ones characteristic of the finer abrasive. In Plate I, Figs. 1, 2, and 3 show the surfaces of a cast brass, at a magnification of 50 diameters, after grinding with Nos. 0, 00, and 000 emery papers, respectively.

Finer abrasives than No. 0000 cannot be obtained mounted on paper, and it is frequently found that even this grade is not too uniform, with the result that coarser scratches may be present

than those left by the No. 000 paper. The final approximation to a mirror surface must be obtained by other means, usually by use of a rotating wheel covered with a special cloth that is charged with abrasive particles, carefully sized by levigation in water or equivalent methods. Two different wheels may be used; first, one with a relatively coarse abrasive; later, a wheel charged with a finer particle size.

It is impossible to learn how to prepare a specimen for good microscopic work by reading a book. Results are obviously affected by coarse dust particles in the air settling on fine papers or cloth laps, or equivalently, by carrying coarser particles on the specimen to the next finer paper or lap. Chemical changes may affect some abrasives; *e.g.*, fine magnesium oxide used as a final polishing abrasive may pick up carbon dioxide from the air or water to form coarse particles of magnesium carbonate that ruin the surface. The type of cloth is important and, when a metallographer finds a type particularly suited for his work, he will be wise to lay in a stock of it. Finally, the pressure used by the individual in holding the specimen on the cutting papers, or laps, has a considerable influence on the results. Too little pressure retards the rate of polishing and leads to pits in the final surface. Too much pressure causes local overheating and severe distortion to an appreciable depth. The correct degree of pressure varies for different metals, and this can only be learned by actual polishing (and for a considerable time, by repolishing!).

The method of polishing outlined above was used in the preparation of all structures reproduced in this book. It can give good results when employed by experienced operators. There are other methods which are superior in many respects to this one. Lead laps, charged with abrasives, may largely replace the abrasive papers with a gain in speed of polishing, flatness of the specimen, and preservation of small, brittle inclusions in the structure by minimizing the time required on the cloths. Practically complete freedom from distortion is possible by electrolytically removing the flat striated surface obtained from a No. 000 emery paper or its equivalent. The electrolytic method requires special equipment and considerable work in developing the optimum composition and temperature of the electrolyte, current density, and voltage. This method is a fairly recent development. At present, its chief advantage is the absence

of any surface distortion. It is, therefore, most valuable in polishing soft metals such as pure aluminum and zinc, or metals whose structures are particularly subject to alteration by distortion, such as stainless steels. The method is also being commercially employed to replace buffing where the shape of the part makes that operation difficult to perform; *e.g.*, at inside corners of rectangular sections.

The polished surface must be etched before any details of the structure become evident, unless there are moderately coarse sections of the surface whose hardness is very different from the remainder. If part of the structure is harder (oxide inclusions in metals, page 20), it will not wear away as rapidly as the softer matrix and will be left standing in relief. If it is softer (graphite in cast iron, page 196), it will wear away to a greater depth than the matrix and again be visible by a relief effect. Otherwise, the mirrorlike surface shows no structure until a liquid chemical that reacts somewhat with the metal is placed on the surface (or the specimen may be heated in air or vacuum in some cases). The chemical will differentially attack parts of different chemical composition, or reactivity, to reveal the structural condition. The chemical agent is called an *etchant* or etching solution. The "Metals Handbook" gives lists of the many solutions that may be used for commercially important metals and alloys, together with the specific applications of each. The time or depth of etching is determined mainly by the magnification at which the structure is to be examined. If it is to be studied by the naked eye, or at magnifications of less than 25 diameters (*macroscopic* examination), the specimen is usually etched deeply to increase the contrast in appearance of sections attacked at different rates. Structures magnified more than 25 diameters are called *micrographs*. If the magnification is in the range of 50 to 100 diameters, the specimen is usually given a moderately deep etch to obtain contrast. Very fine structures, that must be magnified 500 to 1,000 times, would be so roughened by a contrast etch, however, that details would be obscured. A relatively light etch is employed in these cases.

Plate I, Fig. 4, shows the structure of a cast α brass, at a magnification of 50 diameters ($\times 50$), after polishing on the emery papers (Nos. 0, 00, and 000), as pictured in Figs. 1, 2 and 3, polishing on two cloth laps to obtain a mirrorlike surface, and

etching. The appearance of the unetched specimen is not reproduced since its uniform surface did not reveal any structural details. Etching fairly deeply in a mixture of ammonia and hydrogen peroxide has revealed a coherent group of polygonal

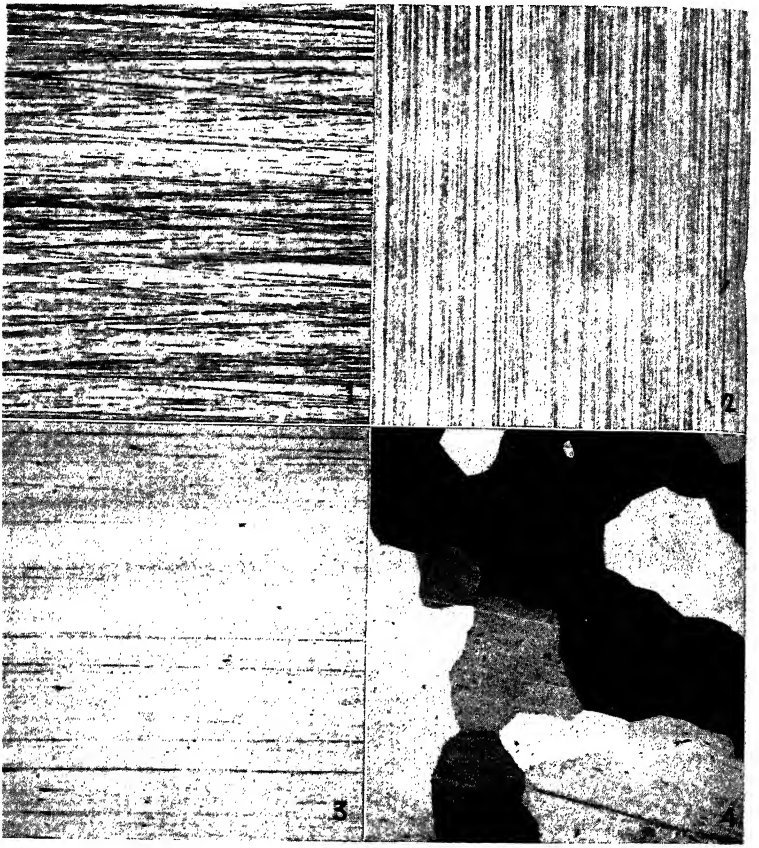

PLATE I.

areas, each shaded somewhat differently. The different areas are actually identical in composition and structure; each represents a crystal whose axes are at different angles with respect to its neighbors and the surface (see page 13). This particular etching solution attacks different crystal faces at a different rate and thus tends to outline a specific crystal face. A crystal in which the outlined face is parallel to the surface of polish has a

maximum flatness and relatedly, reflectivity for light, which causes it to have a bright appearance. If, in a different crystal, the outlined face is tilted away from the polished surface, that grain has a roughened or saw-tooth-type surface that does not fully reflect light to the observer's eye. Such crystals will appear dark to varying degrees, depending on the extent of etching and the actual angle of the outlined faces to the surface. Not all etching solutions have this effect of "darkening" crystals of differing orientations (see, for example, photographs of iron in the next section). Incidentally, Fig. 4 shows many striations, inclined slightly from the horizontal. These are scratches which were covered by flow during the final polishing and were then revealed by the etch which removed much of the distorted surface layer. The identification of the lines as scratches is primarily based on the fact that they cross crystalline grain boundaries with no change in direction.

Metallurgical microscopes differ only in details from those used in other types of scientific work. Light, from an electric bulb or a carbon arc, is focused by a lens (objective) on the specimen, reflected through the same lens, diverted from the original path by a prism or reflector, and passed through a second lens (ocular) to the observer's eye or to a photographic plate for permanent recording. Williams and Homerberg[1] include a detailed description of metallurgical microscopes. Assuming that the lenses are of good optical glass, ground to correct curvatures and corrected for distance and color distortions, the chief factor in preparing good photomicrographs is illumination with the proper quantity of light, correctly centered with respect to the lens system.

HARDNESS TESTS

The word *hardness* cannot be defined except by describing the test method, and since methods may vary considerably, hardness data obtained by one method cannot be expressed in terms of another measuring system, except by use of an empirical calibration. The hardness concept may signify resistance to cutting or abrasion, in which case a file or scratch test is applicable. The word may refer to energy absorption, in which event a rebound test of the scleroscope type will be informative. Usually,

[1] "Principles of Metallography," McGraw-Hill, 1939.

however, hardness is defined as the resistance of a metal to deformation. None of the usual test methods or machines successfully isolates and evaluates this property alone.

In the Brinell test, a hardened steel ball is forced by a known load into the metal being tested, the diameter of the impression is measured, and, using a formula or tables, converted into an empirical number called the Brinell hardness number or BHN. The Rockwell test is similar except that steel balls of various diameters or a diamond cone (Brale) may be used. The diameter of the impression of the cone is not measured; instead, its depth is automatically indicated on a dial. In both of these identation tests, the results are affected not only by the original resistance of the metal to deformation, but by the rate at which this resistance changes at the vicinity of the indentor during the tests (see deformation hardening, page 32). The results are also affected by elastic properties of the metal since the diameter or depth of the indentation is measured after the load has been released, with an accompanying elastic recovery or slight reversed dimensional change. Another variable that should be recognized is the relative volumes of metal displaced by varying depths of indentation of a sphere and a cone. The effect of work hardening and elastic recovery in the vicinity of the indentor makes it difficult to convert data obtained by one type of test into figures obtainable by a different test. Conversion tables, obtained empirically by tests of steels, may not be applicable for nonferrous metals with different work-hardening and elastic properties. Since two different combinations of load and indentor may result in different degrees of indentation by the Rockwell test, it is not possible to express hardness data obtained by one combination in terms of another, except after tests have established the correlation for the specific metal.

The empirical or arbitrary nature of the numerical hardness data and the limitations to conversion of data from one system to another have not prevented these hardness tests from being useful. The Brinell hardness number, for example, may be multiplied by 500 to obtain a fairly good approximation of the tensile strength of most carbon steels. The Rockwell test has the advantage of ease and rapidity of measurement and a small size of indentation, which does not noticeably mar the surface or affect the usefulness of the part after testing. Most of the

hardness data in this book, and in metallurgical literature, are expressed in terms of Brinell values (BHN) or Rockwell numbers (R with another letter designating the load and indentor used; for example, B = 100 kg. and $\frac{1}{16}$-in. ball, or C = 150 kg. and Brale).

TENSILE TESTS

The hardness test is the mechanical property measurement most quickly and easily made and is consequently the most common. Probably next in frequency as an engineering specification is the tensile test where a specimen, machined to a specific shape, is subjected to an axial load tending to stretch the bar. If the extent of stretch (*deformation*, *elongation*, or *strain*) is measured and correlated with the *stress* (load per unit area), the test will give data on the following:

1. Proportional Limit.—The stress beyond which strain is no longer directly proportional to load, or at which a plot of stress vs. strain (stress-strain chart) shows the first visible deviation from a straight line.

2. Elastic Limit.—The maximum stress to which a metal may be subjected without suffering some permanent or plastic deformation.

3. Yield Point.—The point on the stress-strain curve at which deformation starts to progress rapidly with no increase in load, or in some cases, a slight diminution in load.

4. Yield Strength.—By definition; (*a*) the stress corresponding to a total deformation of 0.5 per cent in the case of copper alloys, (*b*) the stress at which the stress-strain curve departs 0.2 per cent from the modulus line (see **8**) for aluminum alloys, heat treated steels, etc., (*c*) the stress at 0.1 per cent departure from the modulus line, in special cases.

5. Tensile Strength.—This is by custom, not by logic, the stress obtained by dividing the maximum load, sustained by the specimen before breaking, by the original cross-sectional area. It is a difficult test procedure to determine the actual specimen area at each increment of stress and particularly at the moment of maximum load, although this must be done to obtain the true stress values.

6. Elongation.—The increase in length divided by the original gauge length, $(L_1 - L_0)/L_0$; (L_0 = original length, usually 2 in.; L_1 = gauge length measured after fracture).

7. Reduction of Area.—The change in area divided by the original area, $(A_0 - A_1)/A_0$; (A_0 = original area = 0.2 sq. in. for a 0.505-in. diameter rod; A_1 = area at point of fracture).

8. Modulus of Elasticity in Tension (Young's Modulus).—The slope of the straight part of the stress-strain line, expressed in the same dimensions as stress (pounds per square inch) since it represents stress divided by strain.

In the above definitions, stress refers to the load shown by the test machine divided by the *original* cross-sectional area. Strain signifies deformation in terms of a pure number, *i.e.*, the change in length (inches) divided by the original length (inches). The strain, elongation, and reduction in area ratio values are usually multiplied by 100, to convert to percentages. Points 1, 2, 3, and 4 refer to the change from elastic to plastic behavior in metals.

The true proportional limit (1) can be determined only by using precision types of equipment for measuring strain; a sensitivity capable of detecting a change in length of one part in 100,000 may be required, and, at the same time, it is necessary that the load be uniform across the entire section being strained (axial loading) in order to calculate accurately the true stress at the point of strain measurement. With ordinary equipment, the measured proportional limit varies decidedly with the scale of plotting the stress-strain data. The elastic limit, as defined by point (2), can only be determined by loading the specimen to a given stress, relieving the load to see if the specimen returns to its original length, applying the load again with a slight increment above the previous value, again unloading to find if any permanent deformation occurred, and continuing in this manner until that point is reached. A yield point (3) is commonly found only in soft steels, and thus the yield strength (4) is most frequently encountered in engineering specifications as the indicator of elastic strength. Whenever yield strength is mentioned, the means of determination should be specified.

QUESTIONS

1. If distortion is encountered upon metallographic polishing with ordinary equipment, how may an undistorted surface be obtained (using the same equipment)?

2. What is the maximum hardness that may be determined with the regular Brinell test machine? Why?

3. In what respects is the Vickers Diamond Pyramid hardness test superior to both the Rockwell and Brinell tests and why, nevertheless, are the latter so widely used industrially?

4. What kind of thermocouple wires would you prefer for occasional temperature measurements employing a potentiometer to determine millivoltages in an oxidizing atmosphere at (*a*) 400 to 500°C., (*b*) 750 to 850°C., (*c*) 1200 to 1300°C.? If the thermocouple were in continuous use, or in a reducing atmosphere, would you change the wires for any of these applications?

5. Why do most tensile test specimens have a reduced cross section in the gauge length?

6. Why is the gauge length important in determining elongation values?

7. From the following data, plot a stress-strain curve and from this calculate values for the tensile test specifications 1 and 3 to 8 of page 9.

TABLE 1.

Load, lb.	Gauge length, in.	Load, lb.	Gauge length, in.
0	2.00000	17,000	2.0103
1,000	2.00033	18	2.0118
2	2.00067	19	0.0136
3	2.00100	20	2.0156
4	2.00134	21	2.0180
5	2.00167	22	2.0208
6	2.00200	23	0.0240
7	2.00234	24	0.0285
8	2.00270	25	2.038
9	2.00304	26	2.056
10	2.00340	27	2.088
11	2.00380	Maximum, 39	After fracture, 2.820
12	2.00425		
13	2.0047		
14	2.0052		
13.9	2.0065	Original diameter 0.505	
15	2.0079	Diameter at fracture 0.284	
16	2.0090		

REFERENCES

"Metals Handbook," sections entitled Pyrometry and Testing, including articles on the different hardness tests, Metallographic Polishing, Photomicrography.

WILLIAMS and HOMERBERG, "Principles of Metallography," McGraw-Hill, 1939.

VILELLA, "Metallographic Technique for Steel," A.S.M., 1938.

"Metals—How They Behave in Service," lectures published by A.S.M., 1939.

WILLIAMS, Metallurgical Factors in the Selection of Steels, *Metal Progress*, April, May, and June, 1941.

CHAPTER II

COMMERCIALLY PURE METALS

In addition to a knowledge of the requisite tools used in a given field of scientific work, it is necessary to acquire a familiarity with the words commonly employed in that field. Words having special metallurgical meanings will be defined when they first appear in this text in an effort to introduce gradually the special vocabulary of the metallurgist. Words having more than one common meaning are always sources of confusion and, in these cases, attempts will be made to limit the definition of terms, as far as possible, while retaining consistency with common usage.

TERMINOLOGY

A *metal* may be defined as a chemical element which in the solid form exists as a crystal or, in most cases, an aggregation of crystals characterized by two distinctive properties: free plasticity, or the ability to undergo considerable deformation without breaking; and relatively high electrical and thermal conductivity. Elements such as carbon, silicon, and boron which exhibit some conductivity but little or no plasticity are frequently called *metalloids*. A number of elements, including arsenic, antimony, and bismuth, are commonly classed as metals, although they are markedly deficient in these basic metallic properties in comparison with the metals of industrial importance.

The chemical processing of metal ores on a commercial scale usually produces the metallic elements with from less than 0.01 up to about 2.0 per cent[1] of foreign elements present. If the foreign elements are present in amounts residual from the refining process, they are called impurities. Although impurities always affect the properties of the metal to some extent, if the magnitude of the effect is small, the metal is commonly designated as *commercially pure*. On the other hand, a small amount of an

[1] Percentage by weight is used throughout the book.

element may be added deliberately, in controlled quantities, to obtain specific property effects, in which case the metal may be called commercially pure (*e.g.*, "A" nickel) or considered an alloy (*e.g.*, low-carbon steel).

The term *crystal* generally brings to mind a solid with flat, external faces at definite angles to each other. In a scientific sense, however, the word refers to a regular internal arrangement of atoms, repetitive in three chosen directions, and it is only in special circumstances that this is accompanied by external crystal faces. Metal crystals forming by solidification from the liquid state in a mold of fixed shape have to conform in external appearance to the container. If several crystals start to form in the liquid, they grow until each is in contact at some point; growth there necessarily ceases and continues at other parts of the crystal until contact at all points is completed. The size of each crystal is, of course, determined by the number in a fixed unit volume, and the shape of each is fixed by the zone of contact with surrounding crystals. Individual crystals, all of the same atomic symmetry, have their three directions (or axes) of symmetry at different angles to an external reference system, such as the surface and edge of a rolled strip. The relationship of symmetry axes to the external system is called the *orientation* of the crystal. Metal crystals, of irregular shape, in contact at all points with other similar crystals (contiguous) are called *grains*. The zones of contact are called *grain boundaries*. The word *crystallite* is commonly used synonymously with crystal or grain, but it might be desirable to confine its application to crystalline particles not in continuous contact with similar crystals. This would refer particularly to particles of a second phase for which there is, at present, no specific definitive word.

CRYSTAL STRUCTURE

The "Metals Handbook" has a section entitled Crystal Structure of Metals which adequately describes how metal atoms, by occupying the corners of imaginary cubes or other simple shapes, form crystals. Another atom, present in the center of each cube, forms what is called the *body-centered cubic* lattice, or, in the center of each of the six faces, forms the *face-centered cubic* structure. Here, it is necessary only to emphasize

that in any of the common crystalline forms, atoms are in a three-dimensional packing with distances between atom centers a constant repetitive value in each of the three directions.

The size of the unit cells of a metal lattice can be measured accurately by X-ray diffraction. For copper, the length of the edge of a unit cube is 0.000000014204 in. A straight line drawn parallel to the cube edge across a small crystal, perhaps $\frac{1}{10}$ in. in diameter, would include 7,040,300 atoms in perfect alignment. A three-dimensional copper crystal in the shape of a cube $\frac{1}{10}$ in. on the edge would include $3.49(10)^{20}$ unit cubes (a number making the national debt appear insignificant by comparison). There can be minute imperfections in the packing of this tremendously large number of atoms, but it is not possible to destroy the essential lattice structure, except by melting the metal.

The word *molecule* is not needed in discussing metal crystal structures since the forces holding atoms in the lattice originate within the individual atoms. The word *ion* may be substituted for *atom* since electrical conductivity requires free electrons which, in turn, means that some individual atoms must exist with positive charges. This is one point at which atomic physics and metallurgy converge, but it is outside the scope of this book and, it may be added, of its authors.

Far more informative than any number of words about crystal structure are simple experiments in packing spheres into a closed body. It is easy to pack marbles (those used in Chinese checkers will do nicely) in a small square box. It will be necessary to have extra pieces of board to vary the size of the square when changing from one type of packing to another. The three simplest packing methods will be found to correspond to the three commonest metal crystal forms; the body-centered cubic, the face-centered cubic, and the close-packed hexagonal. These structures appear, at first, to differ fundamentally in the character of their atomic arrangements, but closer study reveals that any one of them can be converted to either of the others by shifting the spacing of certain planes of atoms. For example, Fig. 1 (page 15) represents a unit cell of the close-packed hexagonal lattice, while Fig. 2 (page 15) shows two adjacent unit cells of the face-centered cubic structure. Certain atoms of the latter structure (specifically, those on two octahedral planes) have been drawn with black centers and interconnecting lines. This configuration

appears to be the same as the basal plane of the hexagonal packing, but there are two differences: (1) the distance between the basal plane of the hexagon and the one above, containing three atoms, is not fixed, while in the face-centered cube, it must be $\sqrt{2}/\sqrt{3}$ times the length of one edge of the hexagon, and (2) a third plane X (not shown in Fig. 2) intervenes between the three-atom plane and the next hexagonal plane; *i.e.*, the

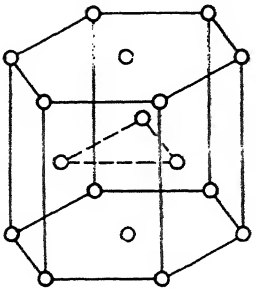

FIG. 1.—Unit cell of the close-packed hexagonal lattice (*e.g.*, Mg).

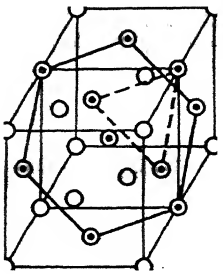

FIG. 2.—Two unit cells of the face-centered cubic lattice (*e.g.*, Al), with atoms on the octahedral plane indicated by black centers.

order is 6,3,X,6,3,X, etc., while the hexagon structure, Fig. 1, shows a sequence of 6,3,6,3, etc.

MICROSTRUCTURES (PLATE II)

Plate II, Fig. 1. Magnesium; photograph, at natural size, of large crystals formed directly from vapor, not by the solidification of liquid in a mold. Under this unique condition, the crystals develop external crystalline form with flat faces and true interfacial angles.

Plate II, Fig. 2. Iron (Armco ingot iron) with about 0.13 per cent total of impurities; ×50; 5 per cent HNO_3 in alcohol (Nital) etch. This structure shows polygonal outlines of grains of body-centered α iron (ferrite). At the plane of contact between two crystals of differing orientation, the atoms are not firmly held in either crystal lattice. This region, called the *grain boundary*, is one of relatively low stability or high energy; reactions will generally be initiated here (see page 214), and in this case chemical attack by the etching solution is greater. The narrow valley

PLATE II. FIGS. 1–6.

after etching appears as a dark line which, outlining the grain boundaries, makes the size of individual crystals readily apparent. The black spots are sites of oxide inclusions or of localized polishing pits. The micrograph represents a cross-sectional view of a hot-rolled bar.

Plate II, Fig. 3. Wrought iron; ×50; Nital etch. The matrix, or background structure, consists of ferrite grains similar to those of the ingot iron except that the dissolved impurities, particularly phosphorus, are present in somewhat greater amounts. (*Soluble impurities* means elements dissolved in the ferrite, hence not visible under the microscope and detectable only by chemical or spectrographic tests.) The dark elongated stringers are inclusions of slag, largely a mixture of FeO and SiO_2. The slag is present in amounts of from 1. to 2. per cent and is always elongated in the direction of flow from hot-rolling. Its distribution frequently is not very uniform; some areas show a lot, some very little; this micrograph is representative of a typical structure. There is no crystallographic or continuous atomic relation between atoms in the slag and in the ferrite crystals; consequently nothing but mechanical contact forces hold the metal and slag together at the contact area. The structure shows that the metal phase is much more continuous, *i.e.*, less interrupted, along a horizontal direction than along a vertical direction. As a result, strength and ductility are not uniform in all directions but depend on whether the axis of stress during testing is parallel or transverse to the direction of the slag filaments. This type of structure is fibrous and will have quite a different appearance, depending on whether the polished surface represents a section parallel, as in this picture, or perpendicular to the rolling direction.

Plate II, Fig. 4. Same as Fig. 3 at ×500. This shows the duplex structure of the slag (FeO and $FeSiO_3$). The slag is harder than the metal and thus, after polishing and etching, stands in relief above the metal surface. In this picture, the slag is in focus and the metal necessarily slightly out of focus. The markings in the ferrite grains appear after moderately heavy etching and are probably related to the distribution of dissolved metallic impurities.

Plate II, Fig. 5. Cast zinc (99.99 per cent Zn); ×50; etched with CrO_3, Na_2SO_4 solution. This structure consists of coarse

grains with lenticular (lenslike) markings that are mechanical twins. The word *twin* means that, within the lens-shaped area, the crystal orientation has shifted a fixed amount, equivalent to a rotation of 180 deg. about an axis normal to the crystal plane represented by the line bounding the twin. The direction of the twins thus reveals the position of a specific crystal plane in each grain. In the large dark grain, six different angular positions of the twins show six different directions of one type of lattice plane. The twin does not originate by rotation (the gross movements involved would be impossible to achieve) but from slight deformation after casting or surface flow during polishing, thus the qualifying adjective "mechanical." Carefully cast zinc polished in a manner avoiding surface distortion would show only the coarse grains.

Plate II, Fig. 6. Commercially pure aluminum (Alcoa 2S: 99. per cent Al + about 0.3 per cent each of Fe, Si and Cu); 0.5 per cent HF etch; ×500 (photomicrograph supplied through courtesy of the Aluminum Research Laboratories). This structure is that of the metal in the worked and annealed condition. It shows rather small grains of aluminum and black particles of an *aluminum-iron-silicon* compound, originating from the impurities. The direction of these insoluble particles represents the direction of prior deformation; they are elongated in the direction of flow, similarly to the slag particles of the wrought iron. The aluminum crystals are not elongated since they re-formed during the anneal following the deformation, (see Chap. III).

Plate II, Fig. 7. Cast tough-pitch electrolytic copper (99.95 per cent Cu; 0.03+ per cent O_2); ×50; NH_4OH-H_2O_2 etch. All metals solidify from the liquid state by the growth of crystals which, because of preferred growth in certain directions, form as open treelike structures called *dendrites* (see page 49). At a later stage in growth, when different dendrites are in contact, the open spaces between the dendrites are filled in with more of the crystalline element. If impurities are present, they will usually be of lower melting point, or form a structure of lower melting point, which means they will be concentrated in the parts last to freeze, *i.e.*, the open spaces between dendrites. This structure of a cast wire bar shows nearly pure copper in the

form of cells, actually the intersections of dendritic arms with the surface of polish. The oxygen impurity, present as Cu_2O (cuprous oxide) particles, forms with copper the dark structure of lower melting point, outlining the dendritic cells. The black spots are pores or holes in the cast metal.

Plate II, Fig. 8. Same as Fig. 7 at ×500. This shows in detail the dark structure outlining the copper dendrites. The cuprous oxide particles or crystallites are seen to be globular bodies dispersed in a copper background. Note that copper is continuous; that the brittle oxide, while forming a network, actually consists of separate, discrete crystalline particles. (This alloy structure is that of an hypoeutectic; see Chap. V.)

Plate II, Fig. 9. Same as Fig. 7 after hot-rolling; ×50; NH_4OH-H_2O_2 etch. The dendritic structure of Fig. 7, showing probably only two separate crystal (or dendrite) orientations, has been completely obliterated by the hot deformation. Now the specimen shows hundreds of very small, individual crystals. Parallel straight lines extending across many of the crystals outline *annealing twins* which appear after a metal has been deformed and annealed or equivalently deformed at a high temperature. (The ingot iron, Plate II, Fig. 2, shows what appears to be a well-defined annealing twin although body-centered cubic iron is not known to form this type of twin.) In addition to changing the grain size of the copper, the hot-rolling has destroyed the interdendritic network of Cu_2O particles and cause the oxide to be aligned as stringers of particles in the direction of hot-working (compare with the wrought iron, Plate II, Fig. 3, and 2S aluminum, Plate II, Fig. 6).

Plate II, Fig. 10. Same as Fig. 9 at ×500. It is apparent from a comparison of the size of these oxide particles with those in the as-cast structure, Plate II, Fig. 8, that the hot-rolling not only changed the distribution of Cu_2O but considerably increased the size and decreased the number of the individual crystallites. This is the result of attempts by the oxide to reach a state of minimum surface. It is possible by reason of a slight solid solubility (see page 20) of Cu_2O in copper; the smaller particles of oxide dissolve, and a corresponding amount must then go out of solution by crystallizing on a particle already present. Thus there is a general tendency for particles to grow

in size and decrease in number, but this is possible only when the metal is at an elevated temperature under conditions of slight solid solubility of the particle in the matrix.

Plate II, Fig. 11. Tough pitch copper; ×150; no etch. This structure represents a section across a tear found in cold-rolled copper sheet. Note that the tear represents a surface with a high cuprous oxide content on one side, and a low or normal content on the other. Localized regions of high oxide content may result from insufficient "scalping" (machining) of the cast set surface of the ingot, which frequently has an oxygen content approaching 0.4 per cent. It also may result from local overheating and melting during soaking at a high temperature for hot-working. In either event, the region adjacent to areas of high oxide content is susceptible to cracking under stress.

Plate II, Fig. 12. Oxygen-free, high-conductivity copper, heated in an oxygen-bearing atmosphere for 2 hr. at 900°C.; reheated 2 hr. at 900°C. in hydrogen; ×200; potassium bichromate etch. Although the original copper was free of oxygen, some entered the metal during the first heat treatment, to a content of about 0.008 per cent O_2. On reheating in hydrogen, atoms of hydrogen diffused into the copper. They reacted with cuprous oxide at the grain boundaries to form steam ($H_2 + Cu_2O \rightleftharpoons 2Cu + H_2O$) at a high pressure and temperature, and the steam created a network of fine holes along the grain boundaries. (Note that the twin bands do not contain any pores; this is further evidence of the continuity of the atomic lattice at twin bands and discontinuity at grain boundaries.) Copper in this condition may show a strength of only 5,000 p.s.i.[1] with zero elongation as compared to a normal 32,000 p.s.i. and 40 per cent elongation.[2] Tough pitch copper with 0.03 per cent oxygen instead of 0.008 per cent is equally susceptible to this "hydrogen embrittlement." Atmospheres containing carbon monoxide or another reducing agent plus water vapor may generate hydrogen ($CO + H_2O \rightleftarrows H_2 + CO_2$) and cause embrittlement, which formerly was attributed to the carbon monoxide gas. Naturally, oxygen-free copper is immune to this trouble, unless it is heated in air during processing. Embrittled metal can

[1] This designation is employed throughout the book for pounds per square inch.

[2] RHINES and ANDERSON, *Trans. A.I.M.E.*, **143**, 312, 1941.

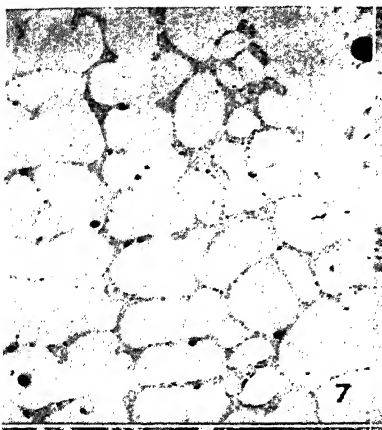
7


8


9


10


11

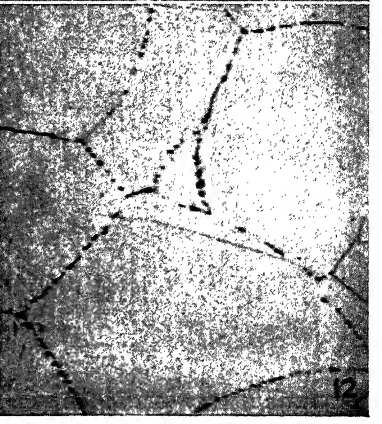
12

seldom be reclaimed except by remelting; it usually must be scrapped.

PROPERTIES

Metals in the pure state have relatively high plasticity or deformability and low strength. The degree to which they exhibit these properties is primarily a function of their crystal structures and the binding forces between atoms in the crystal. Drawings of the atomic lattice, such as those on page 15, are misleading in portraying atoms as small spheres widely spaced. This device is used only to permit representation of the three-dimensional lattice distribution of atoms. It should not be inferred that, having widely spaced atoms, metals might be readily compressed. They are compressible only to a slight extent, and large spheres in contact, as obtained by packing marbles in a box, better represent the actual structure. Even in this case, the stationary position of atoms is not a correct representation of the lattice, for these are only the statistical average positions of vibrating spheres. As the temperature is raised, the amplitude of atomic vibration increases and, although the configuration of atoms is unchanged, the average spacing increases and the forces between atoms become correspondingly less. Practically, this effect results in the expansion of metals and a loss in strength as the temperature increases from the theoretical absolute zero to the melting point. Although the strength-temperature relationship does not follow a straight line, it suggests that low-melting-point metals should be weaker (at room temperatures) than those with high melting points, and this is ordinarily true.

Plasticity of pure metal crystals is basically related to their atomic structures. Although it has been pointed out that the three common metal crystal structures (face-centered cubic, body-centered cubic, and close-packed hexagonal) are very similar, equivalent planes are not identical in respect to interplanar spacing and atomic density, two factors which determine the ease of deformability. Thus the (*octahedral*) planes, cutting off the corners of the face-centered cubic lattice, have atoms placed similarly to those on the basal plane of the close-packed hexagonal structure. However, there are four octahedral planes

in the cubic lattice at different positions with reference to any outside surface or direction while the hexagonal structure has only one. Thus, if a force is applied to the two different types of lattices, the cubic crystal is certain to have at least one plane in a position that will permit slip and deformation. (These processes are discussed in detail in Chap. III.) The hexagonal crystal, however, may have its single basal plane in such a position that it cannot function in the deformation process. Generally, it will then develop mechanical twins (see structure of zinc) which reorient the basal plane so that some deformation can occur. Certain positions of the basal plane with respect to the applied stress will result in cleavage of the crystal and, in general, the hexagonal metals must show considerably less plasticity than face-centered cubic metals. The body-centered cubic lattice has several potential planes of slip, like the face-centered cubic, but none so well defined, *i.e.*, densely packed and correspondingly well separated. Thus the body-centered cubic structure occupies an intermediate position in ease or possible extent of deformation.

These remarks are general comparisons of pure metal crystals. The presence of impurities can markedly alter expected plasticity, strength, or other properties, as is shown in the following specific examples.

Copper.—The common impurity, oxygen, slightly decreases plasticity, but this is not very noticeable, except at points of high oxide concentration (Plate II, Fig. 11) or when the copper is heated in atmospheres containing hydrogen or in which hydrogen may be generated. Oxygen-free copper can be produced by adding phosphorus to the liquid metal, but ordinarily, the residual phosphorus content reduces the conductivity of the metal below that required for electrical applications. Oxygen-free high-conductivity copper melted and cast in a carbon monoxide atmosphere (OFHC) will exhibit superior plasticity to the tough pitch grade, although it can also be embrittled by first heating in oxygen (or air) and then in hydrogen. One other particularly dangerous impurity is bismuth which, by forming a low-melting-point structure (with as little as 0.006 per cent Bi), causes the copper to lose all ductility at high temperatures (see hot-shortness, page 87). A lower concentration of bismuth can be tolerated on the basis of its slight solubility in solid copper.

Element	Symbol	Density, 20°C., g./cm.³	Coefficient of thermal expansion, 0 to 100°C., $\times 10^{-6}$ °C.	Electrical resistivity, at 20°C., microhm cm.³	Electrical conductivity (compared to copper), per cent	*Lattice type at 20°C. (or indicated temperature)	Lattice parameter (length of base of unit cell), $a, \times (10)^{-8}$ cm.
Aluminum	Al	2.70	24.0	2.65	64.	f.c.c.	4.0410
Antimony	Sb	6.62	11.3	39.	4.3	rh. hex.	4.4974
Beryllium	Be	1.85	11.8	12.2	13.7	c.p. hex.	2.281
Boron	B	2.3	2.	18.(10)[11]	.....	complex hex.	.....
Cadmium	Cd	8.65	29.4	7.59	22.	c.p. hex.	2.9727
Carbon	C	2.22	1.2	10.(10)[2]	0.17	(graph.) hex. (diamond) c.	2.46 3.5597
Chromium	Cr	7.14	6.1	13.1	12.8	b.c.c.	2.878
Cobalt	Co	8.92	12.8	6.36	26.4	(α)c.p. hex. (β-440° to 1150°C.) f.c.c.	2.507 3.546
Columbium	Cb	8.57	7.2	20.	8.4	b.c.c.	3.2941
Copper	Cu	8.94	16.7	1.68	100.	f.c.c.	3.6073
Gold	Au	19.3	14.3	2.42	70.	f.c.c.	4.0700
Iron	Fe	7.87	12.3	9.8	17.2	(α, δ) b.c.c. (γ — 908° to 1400°C.)f.c.c.	2.8610 3.60
Lead	Pb	11.34	28.3	20.65	7.2	f.c.c.	4.9389
Magnesium	Mg	1.74	26.0	4.46	38.	c.p. hex.	3.2030
Manganese	Mn	7.44	19.7	170.	1.	(α) complex c. (β—740° to 1160°C.) complex c. (γ—1160° to m.p.) f.c. tetrag.	8.901 6.305 3.767
Molybdenum	Mo	10.2	5.2	4.77	35.	b.c.c.	3.1403
Nickel	Ni	8.9	13.7	6.9	24.	f.c.c.	3.5170
Palladium	Pd	12.0	11.7	10.	16.8	f.c.c.	3.8817
Platinum	Pt	21.45	8.9	9.83	17.1	f.c.c.	3.9158
Rhodium	Rh	12.44	9.6	4.93	34.	f.c.c.	3.7957
Selenium	Se	4.81	37.	12.(±)	14.(±)	hex.	4.337
Silicon	Si	2.33	3.1	23.(10)[3]	0.007	diamond c.	5.4173
Silver	Ag	10.5	18.9	1.60	105.	f.c.c.	4.0782
Sulphur	S	2.07	67.5	19.(10)[16]	.....	f.c. orthorh.	10.48
Tantalum	Ta	16.6	6.6	14.6	11.5	b.c.c.	3.2959
Tellurium	Te	6.24	16.8	19.(10)[2]	0.09	hex.	4.445
Tin	Sn	7.30	23.5	11.5	14.6	b.c. tetrag. (below 18°C.) diamond c.	5.819
Titanium	Ti	4.5	8.2	.....	.....	c.p. hex.	2.953
Tungsten	W	19.3	4.6	5.48	30.6	b.c.c.	3.1585
Vanadium	V	5.68	....	26.	6.5	b.c.c.	3.033
Zinc	Zn	7.14	31.1	6.0	28.	c.p. hex.	2.6600
Zirconium	Zr	6.4	6.3	41.	4.1	c.p. hex.	3.223

*f.c.c.—face-centered cubic; rh—rhombohedral; c.p. hex.—close-packed hexagonal; b.c.c.—body-centered cubic; c—cubic; tetrag.—tetragonal. Polymorphic forms of the metals are given but not for the nonmetals S and Se. Some metals, as Cr and Ni, may exist in a different form when electrodeposited but do not show reversible, polymorphic transformations.

† Heats of formation of the oxides (from "Chemical Rubber Handbook," 22d ed.) are given in terms of a gram-molecular weight of the oxide formed. Dividing this value by the atomic weight of the element times the number of metal atoms per molecule of oxide will give relative heat data in terms of unit weight of metal oxidized.

Lattice parameter height of unit cell, c $\times(10)^{-8}$ cm.	Specific heat at room temperature cal. g. /°	†Heat of formation of lowest metallic oxide kilocal. g.-at.	Heat of fusion or crystallization, cal. g.	Melting point, °C.	‡Tensile strength of annealed metal, $\times 10^3$ p.s.i.	Tensile-test elongation of annealed metal, per cent	Brinell hardness of annealed metal, BHN	Minimum recrystallization temperature, °C.	Tensile strength of cold-worked metal reduction gen. = 80 per cent), $\times(10)^3$ p.s.i.	Young's Modulus of elasticity, $\times(10)^6$ p.s.i.	Symbol
.....	0.220)	380	92	660.	8. (Pure)	60.	16.	90.	....	....	Al
					13. (Com.)	45.	22.	150.	24.	10.3	
37°6'	0.051	165	30	631.	(Brittle)			.....	....	11.3	Sb
3.577	0.508	135.	262.	1284.	30.	0.	60.	.....	....	42.7	Be
.....	0.307	280.	...	2300.	(Brittle)		...	....	.....	....	B
5.6061	0.055	65.	13.	321.	13.	48.	20.	20.	....	....	Cd
6.69	0.165	26.	....	....	(Brittle)		....	.....	....	....	C
.....	0.112	267.	70.	1530.	(Can be ductile)		108.	.....	....	....	Cr
4.072	0.105	57.	67.	1467.	37.	...	124.	.....	100.	....	Co
.....	0.065	.....	....	1950.	(Can be ductile)		....	.....	....	....	Cb
.....	0.092	39.	49.	1083.	30. (Pure)	75.	....	90.	....	....	Cu
					32. (Com.)	48.	....	200.	64.	16.	
.....	0.031	−12.	15.	1063.	16.	45.	....	200.	30.	11.3	Au
.....	0.107	64.	65.	1530.	35. (Pure)	45.	65.	450.	....	30.	Fe
					41. (Com.)	42.	70.	490.	86.	30.	
.....	0.029	52.	5.	327.	1.6	68.	3.	10.	...	2.5	Pb
5.2002	0.242	146.	51.	651.	28.	17.	35.	150.	27.	6.2	Mg
.....	0.122	91.	64.	1242.	(Brittle)		30.	.....	....	....	Mn
3.536											
.....	0.062	131.	....	2500.	99.	21.	147.	900.	190.	50.2	Mo
.....	0.114	58.	70.	1455.	43. (Pure)	48.	54.	.....	....	....	Ni
					70. (Com.)	45.	107.	600.	120.	30.	
.....	0.059	21.	36.	1554.	20.	39.	46.	.....	47.	17.	Pd
.....	0.032	17.	27.	1773.	17.	30.	42.	400.	34.	21.4	Pt
.....	0.059	.....	....	1966.	(Can be ductile)		101.	.....	....	42.	Rh
4.944	0.078	56.	16.	217.	(Brittle)		....	.....	....	....	Se
.....	0.176	198.	....	1413.	13. (Comp.)	0.	....	.....	....	16.3	Si
.....	0.056	6.	24.	960.	22.	66.	28.	200.	57.	10.3	Ag
24.55	0.175	69.	9.	113.	(Brittle)		....	.....	....	...	S
.....	0.035	300.	....	2910.	48.	...	46.	1000.	169.	27.	Ta
5.912	0.048	78.	....	452.	(Brittle)		....	.....	....	....	Te
3.175	0.055	70.	14.	232.	2.	...	5.	15.	....	4.6	Sn
4.729	0.141	217.	....	1725.	(Can be ductile)		....	.....	....	....	Ti
.....	0.032	126.	....	3399.	145.	8.	290.	1000.	490.	60.	W
.....	0.115	209.	....	1720.	.....	...	....	.....	....	....	V
4.9379	0.093	84.	26.	419.	16.	55.	....	20.	22.	....	Zn
5.123	0.066	178	...	1927.	(Can be ductile)		....	.....	135.	....	Zr

‡ Tensile strength data are given for very pure Al, Cu, Fe, and Ni and also for the commercially pure metals (com.). The strength value for brittle silicon is for compression (comp.) loading. In addition to purity, the physical state of the metal, i.e., grain size and as-cast or wrought wire, rod, or sheet will markedly affect strength properties. Not all data here were on specimens in the same physical state, and therefore the values generally are only qualitatively comparable. Cr, Cb, Rb, Ti, and Zr, which are ordinarily brittle, can be produced in a ductile form, although strength data have not been published.

Most of these data were taken from the "Metals Industry [London] Handbook" for 1942, supplemented by the "ASM Handbook" (1939) and by recent research publications. Almost all the properties given here are influenced by the purity of the metal; *e.g.*, most handbooks show the melting point of Cr as 1550°C., a value obtained upon melting in air as a result of nitrogen absorption. Most properties are also crystallographically sensitive to the direction of measurement, particularly in the case of noncubic metals.

Magnesium has long been known to have relatively poor corrosion resistance, particularly to salt-water solutions or vapors. This resulted in extremely careful surface protection (or the abandonment of use of the metal) in many applications, for example, Naval aircraft. It has recently been found[1] that pure magnesium, and its important alloys, are very resistant to salt-water corrosion. By keeping the amounts of iron, copper, nickel, and cobalt impurities below certain tolerance limits (*e.g.*, 0.017 per cent Fe), or by balancing higher contents with other elements that neutralize the corrosion-stimulating effect, magnesium alloys may show far greater resistance to corrosion than was believed possible only a few years ago; *e.g.*, withstand three months' alternate immersion in a 3 per cent sodium chloride solution without significant loss of strength.

Zinc alloys when first used in die castings proved unsatisfactory particularly in warm, humid climates; castings would swell enough to jam mechanisms in which the castings were used, and the intergranular (between grains) corrosion, which caused the swelling, also greatly reduced the metal's strength. Research showed that by keeping the total content of lead and cadmium impurities below 0.01 per cent, the die castings would indefinitely resist intergranular corrosion. Thus, zinc for die castings must have a purity of 99.99 per cent, whereas that used for alloying with copper (to make brass) or for galvanizing iron has considerably higher permissible impurity limits.

Iron in the pure state has much better corrosion resistance than in the relatively impure form of steel, even low-carbon grades. Armco ingot iron finds its most important applications in enameled ware and in fields where better corrosion resistance than that of steel, but not particularly high strength, is required. (There appears to be some question as to the comparative corrosion resistance of relatively pure iron and ordinary low-carbon steel. It has long been believed that, in general, metals resist corrosion better when in a pure state, *e.g.*, magnesium and zinc. This generalization appeared to be true for iron, but recently some authorities have claimed that ingot iron's only special virtue is for enameling.)

[1] HANAWALT, NELSON, and PELOUBET, *Metals Tech.*, *A.I.M.E.*, **8**, September, 1941.

The commonest undesirable impurity element in all iron and steels is sulphur which, with iron, forms a low-melting-point constituent and thus causes hot-shortness (see page 87). The presence of manganese in amounts of about five times the sulphur content converts the sulphur to an innocuous (high-melting-point) manganese sulphide. When present in comparatively large amounts, the manganese sulphide, by interrupting the continuity of the plastic ferrite matrix, permits the steel to be machined faster, with less power, and with a better surface finish. Sulphur added to oxidized liquid steels does not seem to form the normal iron sulphide which, distributed along grain boundaries, causes hot-shortness. Ramsey and Graper[1] show that the machinability of deoxidized steels may be improved without large manganese additions by adding sulphur as a sulphite, Na_2SO_3, which, upon contact with liquid steels, decomposes to SO_2 and Na_2O. The SO_2 is absorbed by the steel, perhaps as a monoxide with the excess oxygen forming SiO_2 and Al_2O_3. These are slagged off by the Na_2O. The resulting oxysulphide inclusions, by being uniformly dispersed, increase machinability without causing hot-shortness.

Aluminum is slightly stronger and less ductile when the normal content of iron, silicon, and copper impurities are present (as in Alcoa 2S), but in most alloy applications these are relatively unimportant. They have some influence on alloy casting properties and heat-treatment temperatures (for details see page 82), and the amounts present should be controlled for reproducible optimum properties.

Nickel may contain a slight amount of sulphur from the fuel used in melting furnaces, which may form a continuous envelope of brittle sulphide at the grain boundaries and thus embrittle the entire structure. The amount of sulphide can be so small as to be undetectable by ordinary micrographic technique. The addition of about 0.05 per cent magnesium causes sulphide to form in an innocuous dispersion of particles and permits the metal to display its inherent plasticity or malleability. Similarly, lead may be present as an impurity in gold in amounts small enough to escape detection by the microscope and yet form a thin brittle envelope at grain boundaries which, being continuous or nearly so, embrittles the entire structure.

[1] *Metals Tech.*, **9**, April, 1942.

Beryllium, although having the same type of crystal structure as zinc and magnesium, has always been considered as a brittle metal since the purest laboratory grades have shown no malleability. Recently, commercial beryllium remelted under a vacuum (to eliminate nitrogen and other gaseous impurities), alloyed with small amounts (0.2 to 0.5 per cent) of titanium or zirconium, and then cast under vacuum, has been successfully hot-rolled. The titanium or zirconium seems to form disperse stable oxide particles which replace the former beryllium oxide films that initiated cracking. However, the hot-worked product is still deficient in cold malleability. Improvement in this direction would greatly increase the utility of this interesting metal. It is probable that small amounts of aluminum or other similar metals, by forming a low-melting phase, can make the metal hot-short in a manner similar to sulphur in iron or nickel, lead in gold, or bismuth in copper.

QUESTIONS

1. Are metals in the pure state in the best condition for ordinary service? Give several instances of pure metals, used as such, meeting certain specific requirements.

2. Express the electrical conductivity of Al, Au, Fe, Ni, and W as a percentage of that of Cu. Explain the anomaly of a value for commercial Cu in excess of 100 per cent.

3. What are the principal fields of utilization of wrought iron?

4. Explain the term "space lattice."

5. Classify the following metals on the basis of atomic arrangement. Which ones would be expected to show the best plasticity?

Iron	Magnesium
Copper	Cadmium
Tungsten	Lead
Tin	Silver
Nickel	Chromium
Gold	Beryllium
Zinc	Manganese
Aluminum	

6. Define the term *allotropic transformation* (or polymorphism). List three common metals that show such a transformation, and give the temperature at which it occurs, and the phases involved.

REFERENCES

"Metals Handbook," sections on Crystal Structure of the Elements; Properties of Iron, Commercially Pure Aluminum, Copper, Nickel, Zinc, Wrought Iron.

CHAPTER III

COLD-WORKING AND ANNEALING

Plasticity of metal crystals is synonymous with deformability—the ability to be strained or to undergo a considerable change in shape or dimensions without cracking or breaking. When the deformation occurs below a certain minimum temperature, the hardness and strength properties increase; *i.e.*, *strain hardening* occurs, while ductility properties correspondingly decrease and, under these conditions, the deformation process is generally called *cold-working*. Ductility may be restored to its initial value and the strain hardening eliminated by *annealing* the metal; *i.e.*, reheating above the minimum temperature previously mentioned. If the deformation proceeds at temperatures in the annealing range, no strain hardening occurs and the process is called *hot-working*.

MECHANICS OF DEFORMATION

It has already been pointed out that plasticity in metals is related to crystal structure; more specifically, it depends on the existence of parallel planes of high atomic density and correspondingly wide spacing, together with the special interatomic forces binding metal atoms in a lattice. Blocks of the crystal on either side of a specific plane, or group of planes, can move in opposite directions, come to rest with atoms on either side of the plane in *nearly* equilibrium positions, and thus change the external shape of the crystal without destroying it. The atoms cannot be in exactly normal positions after the deformation for then the properties of the crystal should be unchanged and no strain hardening would have occurred. Atomic conformity cannot have been entirely destroyed across the plane or subsequent movements at right angles would not be possible (see Plate III, Fig. 2). The mechanics of the movement are not known with certainty; it may occur by a shearing movement of entire blocks at adjacent planes, or by migration of atoms through vacant

sites of the lattice structure, starting at one side of the crystal and crossing it like a wave on the specific plane and in the requisite direction. In either event, the individual crystal is not isotropic, *i.e.*, it cannot flow in any direction, as do tar or other noncrystalline (amorphous) solids, but moves only according to the crystallographic slip planes and directions available. The slip process also requires a rotation of the slip plane and direction toward the direction of stress or plastic flow. (This rotation may be visualized by placing some flat pieces of a hard, sheet material in a ball of plastic clay and forcing the ball to elongate in a direction of about 45 deg. to the plates; they will be found to rotate during the deformation toward parallelism with the flow direction.) While the individual atomic movements during the plastic deformation of a single crystal are uncertain, the gross movements of large blocks of the crystal are predictable.

When a relatively fine-grained commercial metal is cold-rolled, the simple picture of slip and rotation becomes more complicated in that the operative slip systems of the aggregate are at different angles to the flow direction. The applied stress is resolved in each crystal to a stress on the slip plane and in the slip direction and another component normal to the plane. The normal stress tends to cause cleavage along the plane, and, since this does not ordinarily occur in ductile metals, the normal stress is generally ignored. The stress acting along the slip planes is the cause of shearing movements and flow. Since the resolved stress is a function of the orientation of each crystal and since a minimum elastic shearing stress limit must be exceeded before flow begins, it is apparent that all crystals do not start to flow at the same time and that, if the maximum stress is near the gross elastic limit, some crystals will have deformed plastically and some only elastically. This is one source of *residual or internal stresses* (on a micro scale) after releasing the applied stress and is also the reason most commercial metals do not show a sharp, well-defined, yield point (page 9). A second complication in the deformation of polycrystalline metals enters when neighboring crystals of differing orientation tend to flow in slightly different directions, yet must maintain contact at all points or a crack will form and spread. To ensure contact at all grain boundaries of an aggregate of crystals during flow, each crystal is forced to

use more than one slip system (one plane and one direction) and, consequently, some bending of the lattice structure is bound to occur, particularly at grain boundaries. Rotation of the slipping "blocks" will not be uniform and, as a result, deformation creates a series of crystal block fragments, often arranged in parallel, curved bands having slightly varying orientations within each band and mirror image rotations from band to band, all derived from an initial crystal of uniform structure.

A fine-grained metal containing crystals with a random distribution of orientations will, in most respects, behave as an isotropic substance despite the nonisotropic behavior of its individual component grains. After considerable plastic deformation, however, with crystallite fragments in each grain rotating toward a common position with respect to the flow direction, the metal ceases to be isotropic, both crystallographically and mechanically; it will show somewhat different properties depending on the direction of measurement, *i.e.*, the position of the axis of the test specimen with respect to the flow direction or direction of rolling.

In this discussion, deformational processes have been considered as applied to metals having a uniform crystal structure. This would include any pure metal or a metal where a second element is dissolved in the metal without altering the form of its crystal structure (page 47). Most of the actual structures employed to illustrate this discussion are of a solution-type alloy, α brass (in this case 70 per cent Cu, 30 per cent Zn), which has a crystal structure nearly identical to that of copper. It might also be pertinent to point out that a hard, insoluble constituent, such as Cu_2O in copper (Plate II, Fig. 10) or Al-Fe-Si compound in aluminum (Plate II, Fig. 6), will be strung out in the direction of flow without very seriously affecting the mechanics of deformation of the ductile matrix crystals.

MICROSTRUCTURES (PLATE III)

Plate III, Fig. 1. Single crystal of α brass strained 0.2 per cent in tension; $\times 200$. This specimen was polished, etched with ammonia peroxide, strained, and then photographed with the light at an oblique angle. The undisturbed surface of the crystal is dark, but light has reflected from the sides of steplike discontinuities or lines indicating the planes of block slip. The

single longitudinal line was scratched on the polished surface before straining. The slight deviation from the original straightness indicates that the amount of plastic displacement at each visible slip line amounts to about 700 to 800 atoms.

Plate III, Fig. 2. Polycrystalline annealed brass, polished, etched with ammonia peroxide, and then squeezed slightly in a vise; ×100. With normal illumination, the color variations of this grain structure are related to orientation differences (page 6). The parallel, dark lines are steplike discontinuities resulting from block slip. Note that when these reach grain boundaries, they stop or change direction. In some cases, they are parallel to annealing twins (the planes of slip in brass are also potential twinning planes). Where the active slip plane is not parallel to the twin but intersects it, note the change of direction at the twin and resumption of the original direction on the other side. This is further evidence of the change of orientation in twins and yet the atomic conformity between the twin and original crystal. Note also that the bottom crystal shows two sets of intersecting lines within some of the twin bands, indicating that more than one set of the potential slip planes functioned during this slight deformation. All of these markings appear only by reason of a difference in surface level on either side of the slip plane; repolishing of the specimen would remove the line markings.

Plate III, Fig. 3. Armco iron polished, etched with Nital, and then squeezed in a vise; ×100. Body-centered cubic iron has no single set of well-defined slip planes. That, rather than any lesser perfection of the crystal structure, is the probable explanation of these characteristically forked and wavy slip lines.

Plate III, Fig. 4. α brass cold-rolled to a 30 per cent reduction; NH_4OH-H_2O_2 etch; ×200. This structure of a surface parallel to the rolling plane (with the rolling direction vertical) shows grains somewhat elongated in the direction of rolling. The formerly straight twin bands now show curvature indicative of lattice bending. The curved, dark lines in the crystals are parallel to the active slip planes but appear for an entirely different reason than those of Plate III, Fig. 2; after the relatively high reduction of 30 per cent (Plate III, Fig. 2 was deformed less than 1 per cent) atomic nonconformity at the active slip planes, or possibly fragmentation or other localized atomic changes,

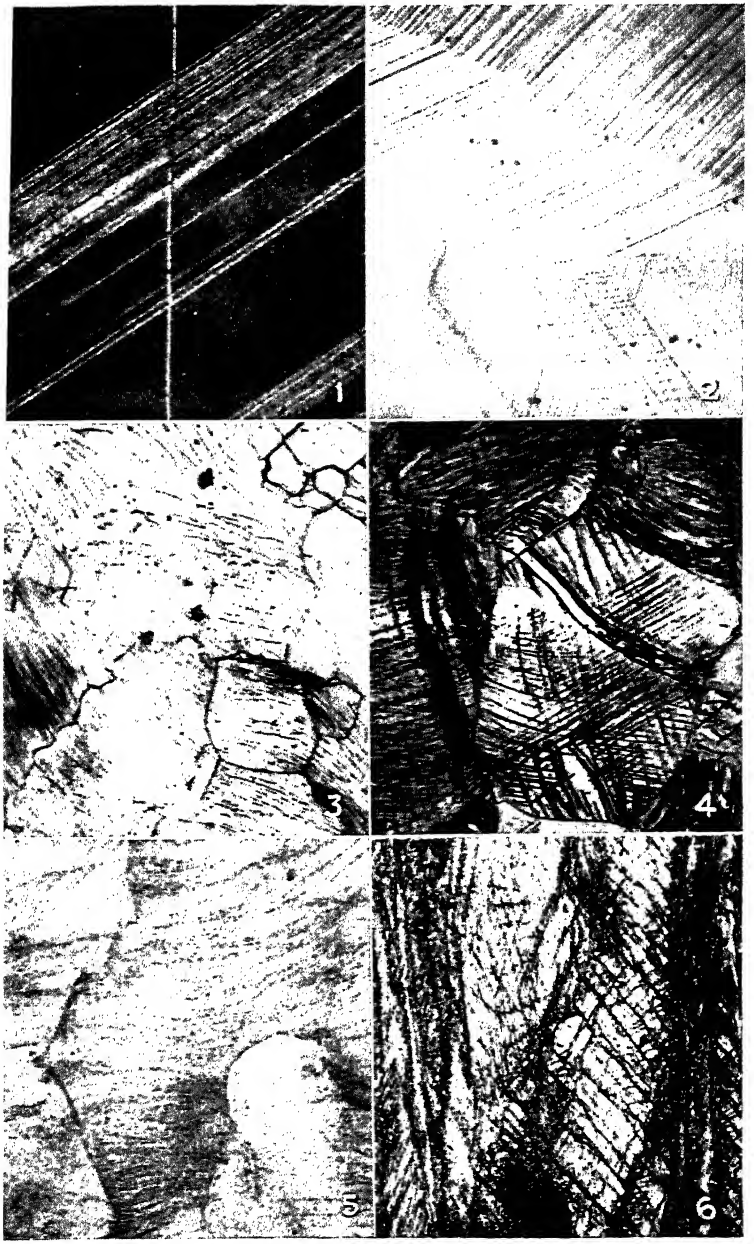

PLATE III. FIGS. 1–6.

has created a zone of high, localized instability where etching attack proceeds more rapidly, in a manner analogous to attack at grain boundaries. Three sets of markings in one crystal indicate that three different sets of octahedral planes were active in the deformation process. Since these markings cannot be removed by repolishing, they are called *noneffaceable deformation lines, etch markings*, or simply *strain markings*.

Plate III, Fig. 5. α brass cold-rolled to a 60 per cent reduction; NH_4OH-H_2O_2 etch; ×200. After a greater reduction, this structure of the rolling plane (rolling direction again vertical) shows strain markings that are less well defined and more wavy, curved, or branched, indicating greater lattice distortion and fragmentation. It is also evident that the strain markings (on the active slip lines), instead of being randomly disposed, grain to grain, as a result of random crystal orientation, are now tending to assume a common general position on the sheet surface, approaching perpendicularity to the rolling direction. Thus the rotation of individual crystals, or banded sections of crystals, into symmetry positions with respect to the direction of flow is generating a preferred orientation.

Plate III, Fig. 6. Same as Fig. 5 but photographed at ×200 on a plane parallel to the rolling direction and normal to the rolling plane (longitudinal section). The markings that tended to be perpendicular to the rolling direction in Fig. 5 are now seen to represent twisted and warped planes tilted at approximately 45 deg. to the surface of the rolled sheet.

PROPERTY CHANGES FROM COLD-WORKING

Strain hardening has already been defined as the change in mechanical properties, *i.e.*, increases in hardness and strength, decreases in ductility, which accompany cold deformation. There is no single, universally accepted explanation for strain hardening, but it seems certain that the visible distortion of the crystal lattice, manifested by curved and warped lines of deformation, and the accompanying fragmentation of the crystal must increase the force required to cause further deformation *on any set of slip planes*, as compared to the force required to initiate slip in a crystal with a relatively perfect lattice.

The extent of the various property changes is of more immediate importance in evaluating potential engineering applications

of cold-worked metals. Although both hardness and strength increase, they do not follow parallel courses when plotted against the reduction by cold-rolling (see Fig. 3; page 41). Strength generally increases more or less linearly, whereas hardness increases very rapidly in the first 10 per cent reduction and then

TABLE II.—ROCKWELL HARDNESS VALUES AND TENSILE PROPERTIES

Material and its initial condition	Per cent reduction by cold rolling						
	0	10	20	30	40	50	60
Armco Iron—Ann. 725°C	G2*	44	55	62	66	68	69
Aluminum 28—Ann. 400°C	H6	41	48	53	58	65	69
Copper T. P. Elec. (p. 18) Ann. 600°C	H15	73	81	86	90	91	92
Zinc (99.9% Zn)	Y6	8	10	9	8	8	7
Nickel silver (see page 52)—Ann. 950°C	B18	64	79	84	87	89	91
70:30 brass—fine grained 0.01 mm.	X18	70	88	93	97	99	101
70:30 brass—coarse grained (0.25 mm.)	X12	62	83	89	94	97	100
70:30 brass—tensile strength, pounds per square inch	43,000	48,000	53,000	60,000	70,000	80,000	90,000
70:30 brass—elongation (% in 2 in.)	70	52	35	20	12	8	6
60:40 brass—furnace-cooled (800°C.)	B8	65	77	84	89	91	92
60:40 brass—quenched (800°C.)	B37	76	83	87	90	92	93

* Rockwell scales; G = $\frac{1}{16}$ in., 150 kg.; B = $\frac{1}{16}$ in., 100 kg.; H = $\frac{1}{8}$ in., 60 kg.; X = $\frac{1}{16}$ in., 75 kg.; Y = $\frac{1}{8}$ in., 25 kg. The special Rockwell scale for the 70:30 brasses was required to keep all values in the regular range, 0 to 100. For initial structures of the 60:40 brass, see pages 102–104. Ann. = prior annealing temperature.

more slowly at successively higher reductions. Elongation (as determined in the tensile test) follows a course opposite to that of hardness, a large initial decrease in the first 10 per cent reduction and then a gradually slower rate, asymptotically approaching zero.

Typical data for hardness changes of several metals are reproduced in Table II.

The development of a preferred orientation in the cold-worked crystalline fragments is not noticeable, in most cases, until the metal has been given a reduction of from 40 to 50 per cent or more. Consequently, the preferred orientation bears no direct relationship to strain hardening. The extent of the preferred orientation, and relatedly, of the directionality of properties is not only affected by the degree of the last cold reduction but by the extent of all previous reductions and temperatures of annealing. The data of Table III represent changes in an α brass of 90 per cent copper and 10 per cent zinc ("Commercial Bronze"); elongation data are difficult to obtain and here are less significant than strength variations.

TABLE III.—DIRECTIONAL PROPERTIES OF COLD-ROLLED 90:10, COPPER-ZINC ALLOY

	Tensile strength			Per cent elongation in 2 in.		
	Angle, specimen axis to rolling direction					
	0 deg.	45 deg.	90 deg.	0 deg.	45 deg.	90 deg.
A. Light reductions and anneals + 37%	59,000	60,000	63,000	5.0	4.0	3.0
B. Moderate reductions and anneals + 56%	74,000	74,000	77,000	4.0	3.0	3.0
C. One heavy reduction, 95%	82,000	87,000	95,000	2.7	2.7	3.2

In addition to changes in mechanical properties, cold-working changes physical properties; *e.g.*, it has a deleterious effect on the magnetic properties of soft iron and decreases electrical conductivity of pure metals slightly (about 2 to 5 per cent) and of some alloys, such as α brass, strongly (about 20 per cent, see Fig. 3, page 41). The distorted lattice of cold-worked metals is of an unstable character and represents stored energy, which means that chemical reactivities of cold-worked metals are also affected (as shown by the increased rate of attack by etching solutions).

MECHANICS OF ANNEALING

The process of changing the distorted, unstable, cold-worked lattice, which may have residual macro- or microstresses, back to

a strain-free structure by the application of heat is termed *annealing*. *Macro-* and *micro-* have the same significance here as when applied to photographs of structures. The word *macro-stresses* refers to stresses existing, in a balanced state, over large areas of the metal. When the balance is upset by machining away part of the metal, the unbalanced stresses will redistribute themselves by a distortion of the metal; for example, a slit cold-drawn tube may open up at the cut, increasing the diameter of the tubing. On the other hand, microstresses, while also of necessity in a balanced state, are so localized in extent that they cannot cause a change of dimensions upon machining of the metal and are detectable only by X-ray diffraction or comparable methods.

At some relatively low temperature of heating, internal stresses are relieved; measurable macrostresses by plastic flow or creep, and microstresses by the movement of some atoms, forced out of stable lattice positions with respect to their neighbors, toward localized equilibrium positions. Since the gross lattice distortions are unaffected, hardness and strength may not be noticeably decreased; in fact, in some solid-solution alloys, such as the α brasses, the hardness and strength may increase slightly. (Placing a test specimen of cold-rolled brass on a hot radiator for a couple of hours may bring its strength up to specifications, if it originally was a little below the minimum. This slight increase in hardness and strength is believed by some to be caused by precipitation (see page 76) of a phase, soluble in the stable lattice and insoluble in the distorted lattice.) Heat treatment in this relatively low temperature range is called a *stress-relief* anneal. The internal stresses in a cold-worked metal may approach the strength of the material and exceed it, if localized surface notches are formed by the attack of certain specific corrosive agents, *e.g.*, ammonia or mercurous nitrate solutions for brasses. When the localized stresses exceed the strength of the material, cracks start forming. Since the corrosive attack usually creates notches at grain boundaries, the cracks start and propagate along grain boundaries, resulting in intergranular failure of the type known as *season-cracking* or, more accurately, *stress-corrosion cracking*. The temperature range of stress-relief annealing is called the *recovery* range. Besides the property changes already mentioned, there may be some very minor

structural changes but, at most, these will be only the partial disappearance of etch or strain markings. Their removal takes a considerably longer time than is possible to employ commercially, but the tendency illustrates the decrease in localized stresses that had given the original etching effect.

At the upper temperatures of the recovery range, hardness may start to decrease markedly. Simultaneously, minute new crystals, identical in composition and lattice structure to the original undeformed grains, make their appearance in the microstructure. These crystals are not elongated, as are the fragmented, deformed grains, but appear to be approximately *equiaxed; i.e.*, their diameters are about the same in whatever direction measured. The crystals appear first in the most severely distorted part of the worked structure, which would usually be at former grain boundaries. Presumably the re-formation of atoms into the uniform lattice of a new crystal requires a certain minimum energy, and since areas of maximum distortion are regions of maximum instability or of high energy content, they require less energy from an outside source. The atoms, or groups of atoms, from which the new grains start to form are *nuclei*, and the process of their formation and growth to a visible size is called *recrystallization.* The process is not completed instantaneously at a fixed temperature. As in all crystal structural changes involving nucleation and growth, the process is a function both of temperature and of time. The other variable to be considered is that of the initial instability, and factors affecting that are the degree of prior deformation and the prior grain size.

After recrystallization begins, the use of longer times at a specific temperature, or slightly higher temperatures (generally, doubling the time is equivalent to raising the temperature 10°C.), results in growth of the first new crystals from strained material surrounding them and the formation of additional nuclei in the somewhat less distorted sections of the cold-worked lattice. Strictly speaking, the word recrystallization refers only to the process by which nuclei form and grow, resulting in the gradual disappearance of the cold-worked structure. The temperature range in which this occurs is one of sharp changes of mechanical properties, unless the prior reduction was very small and the recrystallization range correspondingly wide. However, a multi-

tude of new crystals (Plate III, Fig. 7) usually will completely fill one area while an appreciable amount of the distorted lattice remains unaffected. In this case, some of the new crystals will grow larger at the expense of other new crystals adjacent to them. This process is called *grain-growth*, and it is clear that the grain growth and recrystallization processes overlap and cannot be cleanly separated in a temperature or time chart.

Grain growth in a completely recrystallized structure (or section of a structure) occurs by boundary migration; *i.e.*, atoms at the boundary plane between two crystals, *A* and *B*, are not in stable positions with respect to either crystal; if they become attached in normal lattice positions for grain *A*, the next adjacent layer of atoms is pulled slightly from symmetry positions with respect to *B*; the boundary then has migrated one atom distance, *A* has grown larger and *B* smaller. Which crystals are marked by what force to grow, and which to disappear, is an interesting question but unanswerable at the present time.

MICROSTRUCTURES (PLATE III)

All Etched with NH_4OH-H_2O_2 Solution

Plate III, Fig. 7. α brass, cold-rolled 60 per cent and heated to a temperature in the recrystallization range (30 min. at 300°C.); ×75. This structure shows masses of tiny new crystals, not very well resolved here, and some areas of the old deformed structure containing strain markings.

Plate III, Fig. 8. Same as Fig. 8 at ×500. The structure of the new crystals is somewhat better resolved at this magnification. The average diameter of the new crystals is about 0.002 mm.

Plate III, Fig. 9. Same specimen as Fig. 8 reheated 30 min. at 400°C.; ×75. After recrystallization has been completed and after some crystal growth, the average grain diameter is now about 0.020 mm.

Plate III, Fig. 10. Same specimen, reheated 30 min. at 500°C.; ×75. Additional growth has increased the average grain diameter to about 0.045 mm.

Plate III, Fig. 11. Same specimen, reheated 30 min. at 650°C.; ×75. The average grain diameter is now about 0.15 mm.

Plate III, Fig. 12. Same specimen reheated 30 min. at 800°C.; ×75. Inspection of a larger area at a lower magnification is required to determine that the average grain diameter is now about 0.25 mm.

All of these cold-worked and annealed brass structures show annealing twins. In making grain-size determinations, it is necessary to avoid mistaking twin-band boundaries for grain boundaries. The distinction is usually readily made on the basis of the straightness of twin-band edges and the fact it is a band, *i.e.*, has parallel sides. Use of an etch that differentially colors grains of different orientations facilitates grain-size determinations. These may be made in four different ways; (1) by taking a section of known area, counting all grains contained within that area. and adding half of those intersected by the edges; this gives the average number of grains per unit area; (2) the number of grains per unit area can be converted to a figure representing average grain diameter by making certain assumptions as to the shape of the grains; (3) the number of grains intersected by a straight line, of fixed length, drawn at random across the image (or micrograph) of the structure may be taken as representative of the grain size; this method, which is coming to be employed for tool steels (page 180), is useful in a qualitative sense; (4) the grain structure at a specific magnification can be compared with standard structures of known grain size (reproduced in the "Metals Handbook," A.S.T.M. Standards, etc.) at the same magnification or, by use of a conversion factor, at a different magnification. This last method is quickest and about as accurate as the other, more tedious methods. It is equally useful in most work since, by all methods, measurement is made on a two-dimensional view of a three-dimensional object, and the resulting data are not absolutely quantitative. Another method, less quantitative than the previously listed types, employs the appearance of a fractured specimen, usually obtained by impact stressing of a notched bar. If the notch prevents the localized deformation that usually accompanies a metal fracture, the appearance of the surface is indicative of the grain size. This quick test will give a very useful qualitative indication of grain size. A standard set of fractures of tool steels is available to enable a more quantitative description of results for these materials.

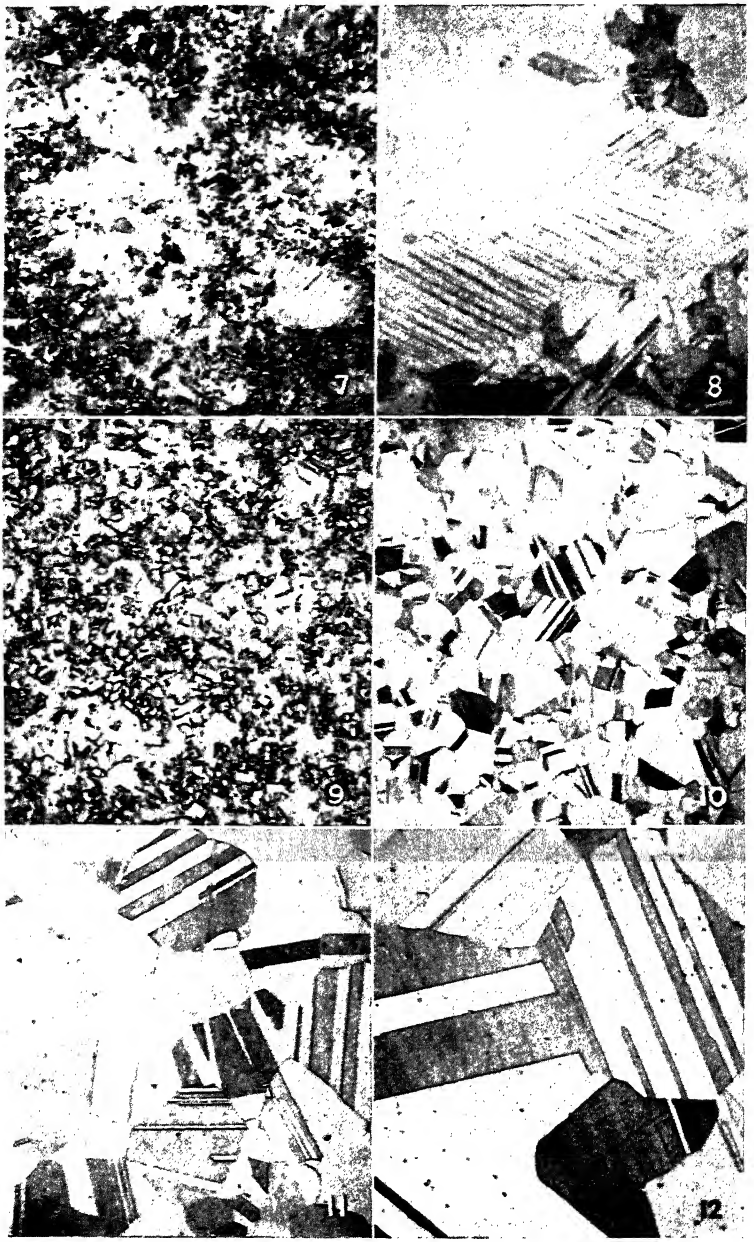

PLATE III. FIGS. 7–12.

PROPERTY CHANGES UPON ANNEALING

The recovery range of annealing has already been defined as one where hardness and strength are little affected, but stresses are at least partially removed and thus susceptibility to stress-corrosion cracking is diminished or eliminated. Residual stresses are undoubtedly related to nonuniform positions of individual atoms in the lattice with respect to one another (microstresses), or very large blocks of atoms to other blocks (macrostresses). In either case, the atomic displacements must be elastic. When the temperature is increased, the elastic strength of the metal is diminished, and the stresses cause plastic flow, or block movement toward equilibrium positions, that reduces the stress. The temperature-time relationships required to reduce the stresses to a given value may be calculated from creep (flow vs. time) data, but are more readily determined experimentally by forcing a strip of material to assume a specific curvature (using three pins with the center one out of line) with a resultant calculable tensile stress on the convex side, balanced by an equal compressive stress on the concave side. If the stresses are elastic, the beam will spring back to straightness when removed from the fixture. If the bent beam is heated for various times in the recovery range, the degree of stress relief can be measured by the tendency to "spring back" to straightness. When stresses are completely removed, the strip will remain permanently in the curved position.[1] It has been experimentally observed that the troublesome macrostresses in cold-worked metals can be largely diminished by plastic flow in the recovery range, without materially reducing the microstresses, altering the appearance of the cold-worked structure, or reducing strength and hardness properties.

The recrystallization range, in which the deformed structure is replaced by new, undistorted crystals of the same type, is a range of rapid transition of properties from those of a strained to a strain-free structure. Thus hardness and strength diminish, and ductility, as shown by elongation values in the tensile test, increases (Fig. 3). Higher annealing temperatures, which increase the grain size, correspondingly decrease the number of grain boundaries which, it will be recalled, offer discontinuities to

[1] KEMPF and VAN HORN, *Metals Tech.*, A.I.M.E., **8**, June, 1941.

slip or deformation. Thus, grain coarsening is accompanied by further decreases in strength and hardness and by increases in plasticity. The effects of the factors of prior deformation and temperature are shown in Table IV, and the effect of the time

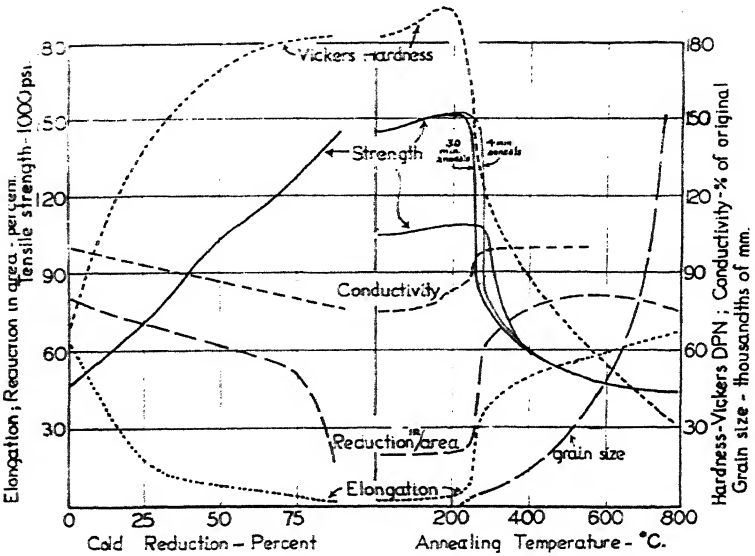

FIG. 3.—The effect of cold-working and annealing on some properties of common high brass (65 per cent copper, 35 per cent zinc).

factor may be indicated by saying that doubling the time would probably give about the same data for temperatures 10°C. lower than those shown.

A more detailed discussion of the factors affecting recrystallization temperatures and grain-growth characteristics is given in the "Metals Handbook." A summary of the more important influences follows:

1. Recrystallization starts at a lower temperature and is completed within a narrower temperature range:
   a. The heavier the prior deformation.
   b. The finer the prior grain size.
   c. The purer the metal.
   d. The longer the temperatures of annealing.
2. The recrystallized grain size will be smaller:
   a. The lower the temperature (above that required for recrystallization).
   b. The shorter the time at temperature.

c. The shorter the time heating to temperature (increased nucleation).
d. The heavier the prior reduction.
e. The more insoluble particles present, or the more finely they are dispersed.

TABLE IV.—ANNEALING OF SPECIMENS FROM TABLE II

Copper, T. P. Elec. 70:30 brass*

Annealing temp. and time	Prior reduction							
	30%	50%	80%	50% F.G.	50% C.G.	T.S.	El.	G.S.
None (cold-worked)	RH86	RH91	RH95	RX99	RX97	80,000	8.	
150°C. 30 min...	85	90	94	101	98	81,000	8.	
200°C. " ...	80	88	93	102	100	82,000	8.	
250°C. " ...	74	75	65	103	101	82,000	8.	
300°C. " ...	61	54	42	82	98	76,000	12.	
350°C. " ...	46	40	34	66	80	60,000	28.	0.02
450°C. " ...	24	22	27	50	58	46,000	51.	0.03
600°C. " ...	15	17	22	38	34	44,000	66.	0.06
750°C. " ...				20	14	42,000	70.	0.12
Final grain size....	0.15	0.12	0.10	0.08	0.12			

* F.G. = originally fine grained, C.G. = originally coarse grained; T.S. = tensile strength in pounds per square inch; El. = elongation, per cent in 2 in.; RH = Rockwell scale, $\frac{1}{8}$-in. ball, 60-kg. load; RX = $\frac{1}{16}$-in. ball, 75-kg. load; G.S. = grain size in millimeters.

It is evident from statements 1*c* and 2*e* that soluble impurities or alloying constituents, such as zinc in copper, raise the recrystallization temperature while insoluble constituents, such as Cu_2O in copper, do not noticeably affect the temperature of recrystallization but decrease the recrystallized grain size. This latter effect is widely used commercially to obtain fine-grained structures in annealed metals.

The grain size obtained after holding a specific time will be increased if the metal is reheated to a higher temperature, but will be stable, unaffected by all lower temperatures, unless the time is increased very considerably (*e.g.*, multiplied by about 1,000 for 100°C. lower).

The preferred orientations found in deformed metals after relatively high reductions are not obliterated by the recrystallization and grain growth accompanying subsequent anneals; in fact, the directionality of properties may be greater. It is certain to be more troublesome, since disks blanked from rolled and

annealed sheet are frequently drawn into cups or tubes, and, if the crystals are oriented in preferred directions, the *flowability* of metal will be greater in certain directions and, correspondingly, the drawn cups will not be uniform at the top edge but will have high sections (*ears*) of lesser wall thickness. The directional properties of different metals vary; upon cupping, some show four ears at 0 and 90 deg. to the rolling direction, others four ears at the 45-deg. position, while hexagonal and, occasionally, cubic metals may show six ears. Since the directional properties

TABLE V.—DIRECTIONAL PROPERTIES OF ANNEALED 90:10 CU:ZN ALLOY

	Tensile strength			Elongation			
	Angle, specimen axis to rolling direction						Height of ears, in.†
	0 deg.	45 deg.	90 deg.	0 deg.	45 deg.	90 deg.	
*A** Ann. 500°C; 0.01 mm. grain size	42,000	41,000	42,000	41	44	44	
A Ann. 800°C.; 0.07 mm. grain size	36,000	36,000	37,000	39	45	44	0.01
B Ann. 500°C.; 0.01 mm. grain size	47,000	45,000	45,000	37	41	42	0.01
B Ann. 800°C.; 0.04 mm. grain size	39,000	36,000	38,000	37	44	45	0.03
C Ann. 500°C.; 0.01 mm. grain size	48,000	45,000	44,000	38	41	40	0.01
C Ann. 800°C.; 0.05 mm. grain size	40,000	33,000	34,000	32	47	48	0.05

* *A*, *B*, and *C* are same specimens as listed in Table III, page 34.
† Ears on cups 0.6 in. deep by 1.12 in. diameter occurred at 45 deg. to the rolling direction.

generally increase, not only with increased prior reduction but with increased temperature of annealing, it would seem that not only do nuclei during recrystallization tend to show a preferred orientation but, more important, during grain growth, crystals oriented close to certain positions are favored and absorb their less fortunately situated neighbors. Data on the extent of the property variations, Table V (these are from the same commercial bronze as tested, in the cold-worked state, for the data of Table III), indicate that, in annealed metal, elongation values are more sensitive to directionality than strength.

The considerable amount of research in the field of preferred orientations in annealed metals has not defined in a quantitative sense the mechanism of their origin and development, but has revealed the conditions that tend to increase directionality; *i.e.*, heavy penultimate (next to last) reductions, and low penultimate annealing temperatures and high temperatures of final annealing.[1]

The change of properties with direction of testing is also known as *fiber* or *texture*. The "fiber" of these rolled and annealed metals, based on preferment of crystallographic orientations, should not be confused with the "fiber" of wrought iron, or similar metals, where the effect is mechanical, caused by the presence of slag stringers, all distributed in the rolling direction.

Large grain structures are frequently favored for their softness and ease of deformation. However, not only are they more likely to show directional properties, but the deformation process, necessarily operating in different crystallographic directions in each grain, causes some to rise and some to fall (from the original plane surface). This may result in a very undesirable surface roughening, or orange-peel effect, at least in sections where it is not suppressed by the deforming tool, *e.g.*, the roll surface.

It is now possible to define hot-working more positively; *i.e.*, deformation at temperatures above those required for recrystallization in the short times involved. The structural result of hot-working may be little different than that of cold-rolling and annealing; the final grain size in each will be largely determined by the degree of the reduction, the temperature of the metal after deformation is completed, and the time at that temperature. Metal crystal lattices are expanded at higher temperatures, and the specific planes that function in the deformation process at low temperatures are not the only ones participating in the flow process at elevated temperatures. For example, hexagonal metals, such as zinc and magnesium, are quite plastic at high temperatures, regardless of the crystal orientation, since slip is not confined to the basal plane but may also occur on pyramidal or prismatic planes. This and other factors, such as the lower atomic binding forces, mean that less force is required for initial deformation and this force does not increase during flow since no hardening occurs unless the rate of straining is very rapid.

[1] Burghoff and Bohlen, *Met. Tech. A.I.M.E.*, **9**, January, 1942. Palmer and Smith, *Met. Tech. A.I.M.E.*, **9**, June, 1942.

ENGINEERING APPLICATIONS

The nonferrous metals, copper, aluminum, nickel, and their alloys, are commonly furnished in various conditions of "temper" obtained by cold-working after annealing. Cold-working by rolling, drawing, etc., to decreasing thickness, is frequently measured in Brown and Sharpe gauge numbers, and the temper of brass mill products is commonly designated in terms of the reduction by gauge numbers.

B. & S. reduction	Temper designation	Reduction: sheet, per cent	Reduction: wire, per cent
1	Quarter hard	10.95	20.70
2	Half hard	20.70	37.11
4	Hard	37.11	60.45
6	Extra hard	50.13	75.12
8	Spring temper	60.45	84.36
10	Extra spring temper	68.63	90.16

Lead and tin do not strain-harden at ordinary room temperatures but recrystallize spontaneously following cold plastic deformation. Zinc, when very pure, behaves similarly, but commercial grades can be hardened somewhat by cold-working.

The plain carbon steels containing very little carbon, such as S.A.E. 1010 and 1015 (0.10 and 0.15 per cent carbon), are very commonly cold-worked to raise their strength, and this is also done with higher carbon steels in certain applications, such as cold-rolled shafting or cold-drawn wire for wire cable. The George Washington Bridge across the Hudson River, for example, is borne by four 36-in. cables, each composed of 61 strands of 434 wires each, 0.192 in. diameter, cold-drawn from ⅜-in. patented (sorbitic) rod containing about 0.8 per cent carbon. The rod had a tensile strength of about 170,000 p.s.i. and elongation value to 8 per cent before drawing, compared to 240,000 p.s.i. and 2 to 3 per cent, respectively, after drawing. In most other applications, however, steels containing 0.3 per cent or more carbon are usually heat-treated to develop optimum strength properties. The familiar 18-8 chrome-nickel (low-carbon) stainless steel is not improved by heat treatment but can be approximately doubled in strength by cold-working and is used extensively in this condition.

QUESTIONS

1. How can you distinguish between—(*a*) slip lines, (*b*) lines of deforma-

2. Draw curves showing effect of cold-work on the tensile properties of brass (from Table II).

3. Explain the course of the cold-rolling curve for zinc (Table II).

4. Arrange the following metals in the order of increasing temperatures of recrystallization; copper, tin, tungsten, lead, iron, nickel, aluminum.

5. Draw curves showing the effect on hardness, strength, per cent elongation, and grain size upon annealing spring brass (50 per cent reduction of initially coarse-grained material) at temperatures ranging from 100 to 700°C. (Table IV). Mark on this graph the *recovery*, *recrystallization*, and *grain-growth* temperature ranges.

6. What would be the best temperature range for annealing this brass (question 5) if it were to be used in making reflectors (drawn, polished, and plated)? Why?

7. Why would somewhat higher temperatures be used in intermediate annealing operations during cold-rolling in the mill?

8. Aluminum sheet, after cold-rolling and annealing, was found to be approximately 2 per cent oversize in thickness. Why would it be undesirable, or dangerous, to reroll to final gauge and then anneal at the high temperature which would be required to remove the effects of this slight cold reduction?

REFERENCES

"Metals Handbook," sections on Recrystallization; Plastic Deformation of Iron; Effect of Cold Work on Properties of Iron. Data on the many nonferrous metals which are cold-worked and annealed may be found in the appropriate sections of the handbook.

CHAPTER IV

SOLID SOLUTIONS: COPPER-NICKEL AND OTHER USEFUL SYSTEMS

Liquid solutions, *e.g.*, water and alcohol, are mixtures of two components where the temperature or the composition can be varied without the creation of a second phase. Analogously, solid solutions are mixtures of two metal elements in which concentration or temperature can be varied through a considerable range without changing the type of crystal structure of the alloy, a one-phase structure. Commercially important solid-solution alloys generally have the crystal characteristics of the element present in greatest amount, *i.e.*, the *solvent* metal. For example, in the α brasses discussed previously, up to about 38 per cent of zinc can be added to copper without changing the type of crystal structure and with only moderate, continuous changes in other basic characteristics of the copper. It is impossible to distinguish between the two elements in the ordinary solid-solution phase. In the usual *substitutional* type solutions, one type of atom, the *solute*, is substituted for the other, the *solvent*, at random points on its lattice. In the *interstitial* type of solution (see iron-carbon alloys, Chap. VIII), atoms of the added element are present in the interstices of the solvent lattice. It will be the practice throughout this book to refer to terminal solid solutions, which have the structure of one of their component metals, as *alpha* (or α) phases, with a subscript added to denote the solvent metal or element when more than one such solution appears on the diagram.

PHASE DIAGRAM

Charts showing the relationships between the phases present in an alloy system as a function of the temperature and composition are called *phase*, *constitutional*, or *equilibrium* diagrams. All the diagrams given in the "Metals Handbook" are "equilibrium" diagrams, meaning that the alloy phase condition

indicated for a given temperature and composition will show absolutely no change or tendency to change with time. The stable or equilibrium condition is dynamic; atoms are not stationary, but the gross summation of all movements is zero. The following generalizations will be helpful in applying abstract charts to specific alloy systems; *e.g.*, the copper-nickel system of Fig. 4:

1. Single-phase fields (for example, those marked *liquid* or α) must be separated by a two-phase field containing some of each single phase (*e.g.*, the field of *liquid plus* α). The upper line

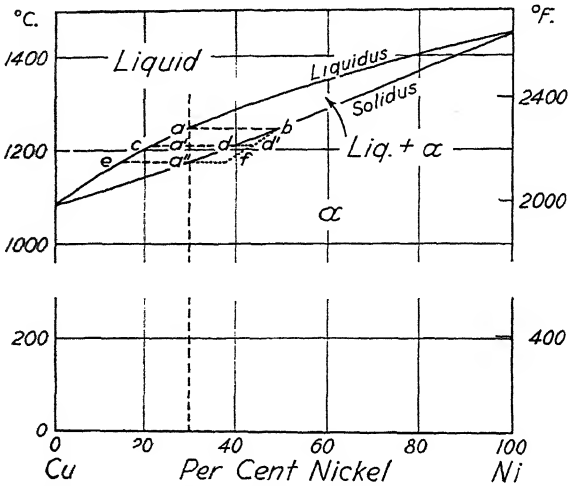

FIG. 4.—Phase diagram of the copper-nickel alloy system.

defining the *liquid* + α region is called the *liquidus* and the lower line, the *solidus*.

2. When an alloy of a fixed composition is heated or cooled past the temperature indicated on a diagram by a line, there is a partial (for sloping lines) or complete (for certain points on horizontal lines) change of phase and a concommitant absorbtion, or release of energy, in the form of heat. Thus, on cooling a 70:30 Cu-Ni alloy (composition *a*) past the liquidus, some solid crystals of the α phase start forming, and the release of their heat of formation causes a change in slope of the cooling curve. It is this effect which is utilized to determine the temperature at

which solidification begins, or the minimum temperature to which an alloy must be heated to insure complete melting.

3. In a two-phase field, the composition of each phase at a specific temperature is given by the intersections of a horizontal line, drawn at this temperature, with the phase field boundary lines. Thus, at the temperature indicated by the horizontal line *ab* the liquid has the composition of *a* (30 per cent Ni) and the solid the composition of *b* (50 per cent Ni); at the line *cd*, the liquid and solid phase compositions would be, respectively, 22 per cent nickel and 40 per cent nickel; etc.

4. The relative proportions of each phase in a mixture of two phases, knowing the temperature and composition of the alloy, is given by the *lever rule*. This states that, for an alloy in a two-phase field, the proportionate amount of each phase is given by the ratio of the *difference between the gross alloy composition and that of the other phase* to the *difference in composition of the two phases*. Thus, in the diagram, the 70:30 Cu-Ni alloy, at the temperature of the horizontal *cd*, contains α of composition *d* and liquid of composition *c*. The proportionate amounts of each would be:

$$\frac{d - a'}{d - c}(100) = \frac{40 - 30}{40 - 22}(100) = 55\% \text{ liquid}$$

$$\frac{a' - c}{d - c}(100) = \frac{30 - 22}{40 - 22}(100) = 45\% \ \alpha$$

Generalization 3 requires that the composition of the solid phase must change during the interval of solidification over a falling temperature. Under equilibrium conditions, this adjustment of composition would occur throughout the solid phase, which would be forming open, treelike crystals called *dendrites*. However, equilibrium is practically never achieved in commercial casting processes, and the first dendritic nuclei are richer in the higher-melting-point element than the successive layers formed at lower temperatures. The average composition of the total solid phase, in this case, will not be that shown by the phase diagram for a given temperature, *e.g.*, point *d* at temperature *cd* (see Fig. 4); it will contain more of the higher-melting-point element, perhaps that given by point *d'*. This difference in composition from center to edge of a dendrite may remain as a result of the slowness of atomic interchange or diffusion. (Chi-

nese bronzes over 3,000 years old show this dendritic composition difference.) The 70:30 alloy should be completely solid when it reaches the temperature of the lower phase field boundary line (at point a''), but under nonequilibrium conditions, the average solid-phase composition will be at some point near f and some liquid will remain; specifically,

$$\frac{f - a''}{f - e} = \frac{37 - 30}{37 - 15}(100) = 32\% \text{ liquid and } 68\% \text{ solid}$$

The presence of some liquid in a solid-solution alloy, cooled from the liquid state to the *solidus* line, results from the failure of diffusion, between the two types of atoms, to maintain the composition of the growing, solid-phase dendrites at the equilibrium concentration. The amount of liquid present here depends on the time permitted for diffusion during solidification. The more rapid the freezing, the farther will be the departure from equilibrium and the greater will be the amount of liquid present. Even under relatively slow cooling conditions, such as might be employed in thermal analyses for the determination of this phase diagram, the *solidus* temperature is never well marked on a cooling curve. After the solidification of the last liquid is completed, cooling may speed up slightly, but seldom is there a well-defined change in slope at a specific temperature. *Liquidus* temperatures may be depressed by undercooling because of slowness in the formation of the first dendritic crystal nuclei, but this effect can be minimized by agitating or stirring of the melt or, in some cases, by artificial nucleation. The pasty condition of the nearly solidified alloy prevents stirring and, although the required diffusion would be accelerated by deformation, that is difficult to accomplish with the alloy in a crucible or mold and still partly liquid. Solidus temperatures, however, may be readily determined by heating a *homogeneous* solid solution to successively higher temperatures. If the alloy is simultaneously subjected to a slight stress, it deforms plastically while entirely solid, but as soon as the solidus temperature is reached, liquid (enriched in the lower-melting-point element) forms at the grain boundaries, and the alloy breaks with an intercrystalline failure (hot-shortness). If the alloy is quenched from just above the solidus, evidence of the existence of the liquid phase at that temperature is preserved and can be identified micrographically by

reason of its different composition. This constitutes a second method of determining solidus lines.

MICRO STRUCTURES PLATE IV

All Etched with Potassium Bichromate and Ferric Chloride Solution

Plate IV, Fig. 1. 85 per cent Cu–15 per cent Ni, as chill-cast; ×50. This structure is composed of small dendrites of a single phase, the α solid solution. There is a very considerable difference in nickel content from the central axes of the dendrites to the midspace between axes, as predicted from the considerations previously described. This is a metastable structure which is commonly described as *cored* dendrites (from the continuous differences in composition from the interdendritic spaces to the cores). Upon etching, the nickel-rich, dendritic cores are not dissolved as rapidly as the copper-rich filling; thus the surface of the etched specimen consists of a series of "hills" and "valleys." The dendritic details obscure grain boundaries, although several differing grain orientations may be found by studying the directions of the dendrites.

Plate IV, Fig. 2. 85 per cent Cu–15 per cent Ni, as chill-cast and heated 3 hr. at 750°C.; ×50. The cored dendritic structure has changed only slightly. Counter diffusion of copper and nickel atoms between the nickel-rich cores and copper-rich fillings has decreased the composition differences somewhat and thus slightly reduced the height of the "hills" and depths of the "valleys." Careful examination of the structure shows some evidence now of grain boundaries.

Plate IV, Fig. 3. 85 per cent Cu–15 per cent Ni, as chill-cast and heated 9 hr. at 950°C.; ×50. This lengthy, high-temperature treatment has completely homogenized the cast structure, *i.e.*, equalized the composition at all points. Grain boundaries are clearly evident, and their irregular shape is frequently encountered in cast and homogenized solid solutions, the irregularity being related to interpenetration of dendrites growing in the liquid alloy. Black particles are copper oxide or nickel oxide inclusions. The grain size is no larger than in the original casting since grain growth does not occur in castings, except when

they have been previously strained by some stress (externally applied or originating from contraction during cooling).

Plate IV, Fig. 4. 85 per cent Cu–15 per cent Ni, as cast in a hot mold and slowly solidified; ×50. This dendritic structure is considerably coarser than that of the chill-cast alloy (Plate IV, Fig. 1). The cells represent nickel-rich areas (low hills) and the narrow, approximately parallel, lines outline the interdendritic copper-rich valley areas. The black, vaguely outlined areas are shrinkage cavities which, it should be noted, occur in the parts last to freeze, *i.e.*, the copper-rich areas. A single grain boundary, diagonally transversing the field along the interdendritic spaces, is also visible.

Plate IV, Fig. 5. 85 per cent Cu–15 per cent Ni, as cast in a hot mold, slowly solidified, and then reheated 15 hr. at 950°C.; ×50. In this homogenized structure, the grain size is considerably coarser than that of Plate IV, Fig. 3, more so than is evident in this photograph, which was taken at the intersection of three grains. Again, copper, or nickel, oxides are visible and also some shrinkage cavities. The time required for homogenization of the coarse dendrites was greater than that for the fine dendrites, in spite of the lesser initial composition differences across the coarse dendrites. The reason is that the distance through which copper and nickel atoms must diffuse is so much greater in the coarse structure.

Plate IV, Fig. 6. 64 per cent Cu–18 per cent Ni–18 per cent Zn; ×100. This is a longitudinal section of a wrought alloy, called "nickel silver" because its color approaches that of silver. It is frequently used as a base for plated silverware and other applications for which its color, corrosion resistance, and strength are adapted. This micrograph of commercial metal, in the hot-worked condition, shows that the cored dendritic structure has not been homogenized in spite of the fact that deformation accelerates homogenization. The increased softness of the homogeneous metal in these alloys is seldom worth the costs of the prolonged, high-temperature anneals necessary to obtain complete homogeneity.

CAST MACROSTRUCTURES

Upon very slow cooling of a liquid alloy with all of the metal maintained at a uniform temperature, solidification will start

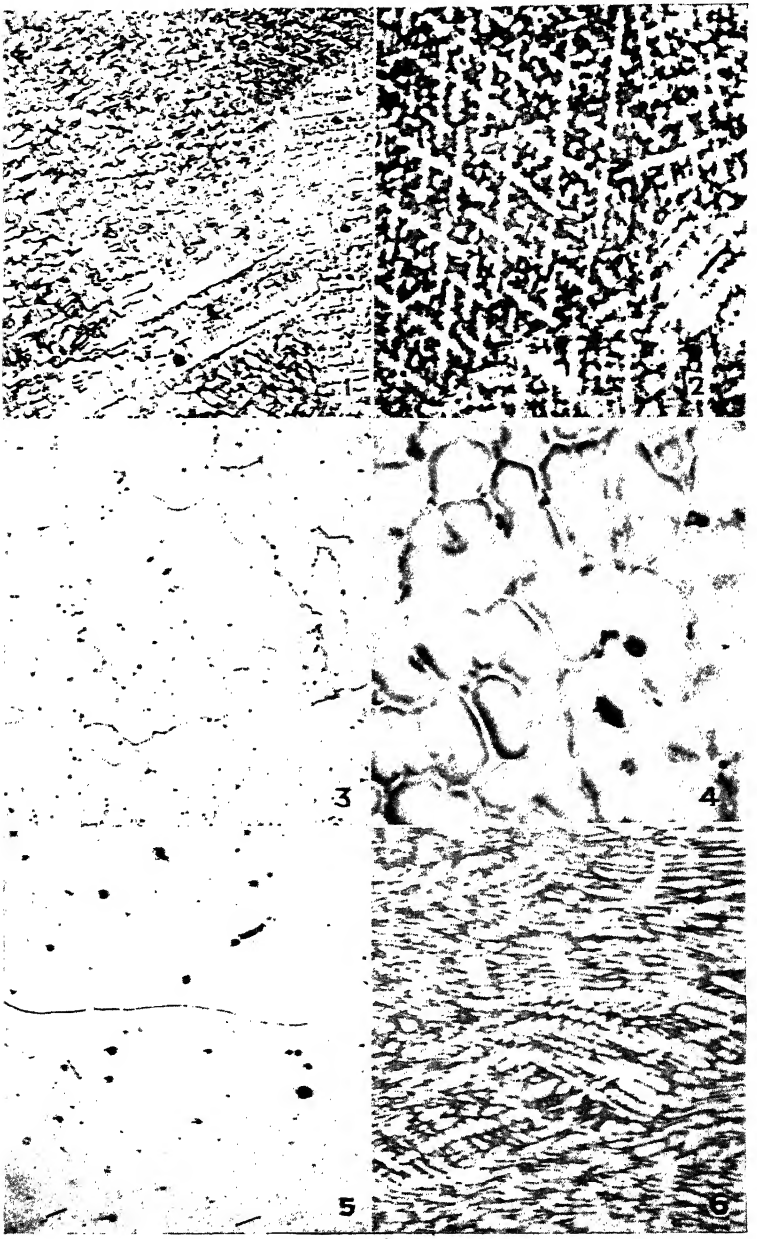

PLATE IV.

just below the temperature shown by the liquidus line of the phase diagram. A few nuclei, distributed throughout the liquid, will form, and each will grow in all directions (as dendrites) to form a coarse, equiaxed grain structure. If the entire liquid cools uniformly but rapidly, many more nuclei will originate in the melt and produce a finer grained equiaxed structure. If one part of the liquid cools rapidly and another slowly (as in industrial casting processes where a hot liquid is in contact with an originally cool mold), nuclei will form only where the liquidus temperature is first attained, *i.e.*, at the mold wall, and these nuclei will grow in the direction of the thermal gradient, giving elongated or columnar crystals. Later, the center, or hotter part, of the casting may reach the liquidus temperature before columnar crystals have grown into this section, and here equiaxed grains may be found. Thus, in castings, it is possible to have combinations of coarse and fine, columnar and equiaxed crystals. By controlling liquid and mold temperatures, thermal conductivities and relative masses, it is possible to exercise considerable control of cast structures. A fine equiaxed grain structure is usually desired for its greater strength and hardness (Chap. III). If impurities are present at grain boundaries, they will be more finely dispersed in a fine-grained structure and, therefore, less troublesome. This is particularly true when the casting is an ingot which is subsequently to be rolled; a coarse-grained structure is far more likely to crack in the early stages of working, and the brittleness is related to impurity concentrations at grain boundaries.

SEGREGATION

Dendritic segregation on a microscopic scale is called *coring* and may be explained by using the phase diagram in the manner already discussed. On a macrographic or full-size scale, a similar effect is noticed in that the first parts of a casting to freeze are enriched in the higher melting phase while the parts last to solidify (generally, top center sections) are enriched in the lower melting-point constituents. The effect is statistical in nature since both sections will exhibit coring. The resulting nonuniformity of chemical composition is known as *normal segregation* and differs only in dimensions from coring. A third type of segregation is the reverse of this; *i.e.*, the parts of the casting first to freeze are enriched in low-melting-point constituents.

The effect is called *inverse segregation*. It is primarily caused by the contraction of solidifying dendrites which tends to enlarge the interdendritic channels. As these open up, a resultant suction effect draws residual liquid metal, enriched in solute atoms (or low-melting-point constituents), through the channel to the surface. The action may be aided considerably by an internal pressure from the release of dissolved gases. Thus "tin sweat," exudations rich in tin, may form on the surface of tin bronze castings when the liquid metal contains appreciable amounts of dissolved hydrogen which is released as gas in a late stage of solidification and forces the tin-rich liquid at the center of the casting through the interdendritic channels to the surface.

Coring may be completely eliminated by diffusion (homogenization) treatments at high temperatures as shown by the photomicrographs. Normal and inverse segregation are little affected by such treatments because of the tremendous distances (on an atomic scale) involved.

PROPERTIES

The effect of solute concentration on some mechanical and physical properties of two copper-base solid-solution alloys, the copper-nickel and α brass series, is indicated by the data of Table VI.

The properties of annealed solid solutions are so affected by the grain size of test specimens and by soluble impurity elements that it is difficult to obtain comparable data for specimens representing concentrations across an alloy diagram. Recrystallization temperatures and grain-growth characteristics are affected by both solute concentration and impurities. Consequently, the data given here are not necessarily the same as would be obtained with industrial alloys and should be taken only as qualitatively indicative of the effects of dissolved elements. These, and other data not reproduced here, lead to the following general conclusions:

1. *Mechanical properties* show moderate, gradual changes, generally of considerably less magnitude than those effected by cold deformation. Strength and hardness (by indentation tests) are always increased, although not necessarily in a parallel manner. In a continuous series, such as the copper-nickel alloys, this requires maximum values for strength and hardness, although

TABLE VI.—PROPERTIES OF ANNEALED COPPER SOLID SOLUTION ALLOYS[1]

Solute concentration	Tensile strength, p.s.i.	Per cent elongation in 2 in.	Brinell hardness, 10 mm., 500 kg.	Lattice parameter, $\times 10^{-8}$ cm.	Electrical resistivity, microhms per cm.[3]	"Self-potential" (see page 59)
Per cent Ni:						
0	30,000	53	36	3.6073	1.7	− 65.mv.
10	35,000	47	51	3.5975	14.	− 45.
20	39,000	43	58	3.5871	27.	− 25.
30	44,000	40	67	3.5770	38.	+ 10.
40	48,000	39	70	3.5679	46.	+ 55.
50	50,000	41	73	3.5593	51.	+105.
60	53,000	41	74	3.5510	50.	+150.
70	53,000	42	73	3.5432	40.	+185.
80	50,000	43	68	3.5350	30.	+205.
90	48,000	45	61	3.5265	19.	+215.
100	43,000	48	54	3.5170	6.8	+225.
Per cent Zn:						
0	32,000	46	38	3.6073	1.7	
5	36,000	49	49	3.6176	3.1	
10	41,000	52	54	3.6275	3.9	
15	42,000	56	58	3.6378	4.7	
20	43,000	59	56	3.6488	5.5	
25	45,000	62	54	3.6612	6.3	
30	46,000	65	55	3.6735	6.6	
35	46,000	60	55	3.6864	6.7	
40($\alpha + \beta'$)	54,000	45	75	3.6940(α)		

the two maxima do not necessarily come at the same concentration. The changes in these properties are not linear in most cases. Considerable effort has been devoted to find an explana-

[1] Mechanical property data for high-purity copper-nickel alloys from Broniewski and Kulesza (*Metaux et Corrosion*, **12**, 67, 1937). Data in "Metals Handbook" show decidedly higher strengths for copper-nickel alloys because soluble impurities (*e.g.*, Mn) are present and the alloys probably had a finer grain size. Mechanical property data for brass alloys are from a Chase Brass & Copper Company *Bulletin* for commercial alloys of moderate grain size. Lattice parameter data (from Owen and Pickup) indicate changes in the size of the unit cells of the alloys effected by the solute atoms. "Self-potential" data for copper-nickel alloys and the discussion of related corrosion properties on p. 59 are from the Research Laboratory of the International Nickel Co. The 40 per cent zinc alloy marked ($\alpha + \beta'$) is a two-phase alloy, as hot-rolled (see p. 99).

tion for the differences in solid-solution hardening as effected by different solute elements. No consistent correlation has been found between the hardness increase and the type or size of the solute atom, although usually the hardening effect is greatest when the solubility is restricted. For example, to increase the hardness of pure copper from Vickers DPN 40 to 54, the following atomic concentration of each of the respective solute elements is required: Antimony, 0.6 per cent; arsenic, 3.6 per cent; manganese, 4.6 per cent; silicon, 4.6 per cent; aluminum, 4.7 per cent; zinc, 12.1 per cent; or nickel, 13.2 per cent (data by R. P. Angier on pure binary alloys annealed to a uniform, 0.035-mm. grain size).

It appears that the most rapid hardness increases are found when the potential solubility is least, although there are some exceptions to this generalization (*e.g.*, manganese).

Table VI shows that the effect of solid-solution elements may be to increase or decrease ductility insofar as that rather vaguely defined property is indicated by tensile-test elongation values. In most cases, the trend of elongation values probably varies inversely with that of strength and hardness, but silicon, zinc, or tin seems to increase the ductility of copper.

2. *Physical properties* also vary with solute concentration. Electrical conductivity is always decreased, or conversely, resistivity increased, although to a different extent by different solutes. In a complete alloy series, such as copper-nickel, this requires a maximum in resistivity at some intermediate alloy concentration. Other characteristics, such as the size of the lattice, as indicated by the length of the edge of the unit cube or *lattice parameter*, vary linearly or approach a straight-line relationship (Vegard's law). Both copper-nickel and copper-zinc alloys show a negative deviation from linearity, but the difference is not known to have any significance.

The lattice parameter relationship is important in consideration of the effect of coring, and its elimination, on mechanical properties. A specimen such as Plate IV, Fig. 1, with a fine dendritic, heavily cored structure cannot have a uniform slip system existing across one grain for, as the lattice periodically is contracted and expanded by the variation in nickel content, the potential slip planes must exhibit a related nonuniformity. Thus a greater stress is required to cause deformation, and the

metal is relatively harder and stronger than it would be in the homogenized condition with a uniform lattice. The coarse dendritic structure of the specimen in Plate IV, Fig. 4, would show intermediate strength or hardness values.

Solid-solution alloys are not customarily used where strength or hardness is of paramount importance. Their basic properties are ductility approaching or, in some cases, surpassing that of the pure solvent metals, plus moderately increased strength properties and other special properties derived from one or more of the components. α brasses are cheaper than copper (since the addition agent, zinc, is cheaper), stronger, and yet show good corrosion resistance and excellent ductility. Cupro-nickels have much improved corrosion resistance as compared to both copper and brasses. In all other cases, comparable compromises of special properties may be obtained in solid-solution alloys.

It is interesting to list alloy systems that show complete solid solubility at all temperatures. The more important ones, together with their lattice arrangements, include:

Ni-Cu, Ni-Co, Ni-Pt, Ni-Pd (face-centered cubic).

Ag-Pd, Ag-Au, Au-Pd, Pt-Rh, Pt-Ir (face-centered cubic).

W-Mo (body-centered cubic); Bi-Sb (rhombohedral hexagonal).

Another group of alloy systems includes elements which are completely soluble at some elevated temperature in the solid state but which, in some range of concentration, change structures at lower temperatures. Frequently, the structural change does not involve any change in lattice type, which remains that of original solid solution. However, in this lattice, the two types of atoms do not remain randomly dispersed but occupy preferred lattice sites. For example, the face-centered cubic lattice contains four atoms per unit cell, one corner atom (eight unit cells share the atom at each of the eight corners per cell) and three face-centered atoms (each of the six face-centered atoms is shared by two cells). In a random solid solution, the four atoms in each cell may be of either solute or solvent elements, but at a concentration of three atoms of element A to one of element B (*e.g.*, 75 atomic per cent Cu and 25 atomic per cent Au), three atoms of type A may, at some temperature, occupy the face-centered positions and the one atom of B may occupy the corner positions of each unit cube. This lattice is no longer a simple solid solution but is called an *ordered* solid solution.

Since ordering is strongest at simple atomic ratios and usually results in marked abnormalities of properties, usually an increase of electrical conductivity, of strength and a loss of ductility,[1] ordered structures are sometimes thought of as intermetallic compounds and their development considered to be a change in phase. The present tendency, however, is to use the specific descriptive term *ordered structure* or sometimes *superlattice* and to show the effect on phase diagrams by dotted lines, since a strict definition of the word *phase* does not require ordering to be a phase change. Systems which are completely soluble at elevated temperatures (below the solidus) but which show, at some concentration, either true phase changes or ordered structures include:

Fe-Cr, Fe-Mn, Fe-Ni, Fe-Co, Fe-V, Fe-Pt (solution range is either body-centered cubic or face-centered cubic, depending on the solute element).

Au-Ni, Au-Cu, Au-Pt, Pt-Cu (face-centered cubic).

ENGINEERING APPLICATIONS

The electropotential values for copper-nickel alloys, shown in Table VI, are the basis of a particularly interesting illustration of a compromise in properties that results in an alloy of specific industrial use. The data are not true self-potential values but actually represent, at each alloy concentration, the millivoltage difference, measured in an aerated 3 per cent sodium chloride solution, between a large clean sheet and a small sheet in contact with its products of corrosion.[2] The plot of potential vs. percentage of nickel gives a curve that passes through a zero value at a concentration near 70 per cent copper and 30 per cent nickel. Similarly, if a series of copper-nickel alloys were suspended in sea water near a harbor, and if the change in weight were determined and plotted against nickel concentration, it would be found that the copper-rich alloy lost weight through general corrosion, while the nickel-rich alloys had gained weight, by barnacle growth on the metal. Again, the 70:30 composition would show approximately no change in weight. The problem, like most corrosion effects, is quite complex but, stated in the simplest manner, may be explained in terms of the copper ion concentration required to prevent barnacle growth. The high-copper alloys

[1] Nix and Shockley, "Reviews of Modern Physics," **10**, 1938, p. 1.

[2] Research Laboratory, International Nickel Co.

corrode, or dissolve, rapidly enough to maintain the copper ion concentration sufficiently high at the surface to poison marine growths. The nickel-rich alloys do not dissolve as rapidly, and although pitting corrosion occurs at the point where barnacles attach themselves to the metal, there is a net gain in weight when that of the barnacles is included. Aside from the question of barnacle growth, the 70:30 copper-nickel alloy is specifically adapted for use in contact with salt water, *e.g.*, in marine condensers.

Nickel-base alloys are of great importance in the electrical field. Campbell's "List of Alloys" gives more than 100 titles of electrical resistance and oxidation-resistant alloys in which nickel is an essential constituent. Among these are various grades of *Chromel* or *Nichrome*, essentially a nickel-chromium-iron alloy; *e.g.*, Nichrome I contains these metals in the proportions, 60, 11, 25, with 4 per cent of manganese. An alloy of 80 per cent nickel, 20 per cent chromium is used for higher temperature (1000°C.) service, while for the highest temperatures (1350°C.) Kanthal-type alloys of iron-chromium-aluminum are now used.

The solution of one metal in the crystals of another increases the electrical resistivity, and alloys for rheostats or electrical heating appliances are always of this type; *e.g.*, the Nichrome alloys have resistivity of the order of 100 microhms per cubic centimeter, about ten to fifteen times that of nickel. The A.S.T.M. publishes various standard methods of testing such materials (accelerated life test, resistivity, change of resistivity with temperature and thermoelectric power).

There are also several grades of *Manganin, e.g.*, Cu 84, Mn 12, Ni 4, and many alloys of the "nickel-silver," or copper-nickel-zinc type in Campbell's list. The two classes of alloys are not clearly distinguishable. For example, Nichrome may be used for electrical heating or (in cast form) for annealing boxes or containers to withstand oxidation at high temperatures. There are many special nickel alloys containing iron, cobalt, tungsten, molybdenum, chromium, aluminum, or other metals, intended for high strength at elevated temperatures. Also, the cobalt-chromium-tungsten alloys (Stellite) are important in this respect. At present, this is a field of active experimentation, and the best alloy products for high-temperature service cannot be clearly specified.

In the field of magnetically soft materials, nickel is an indispensable constituent. For example, an alloy of iron with 78.5 per cent nickel, 78.5 *Permalloy*, shows a high ratio of flux density, B, to the magnetizing force producing it, H; more specifically, the permeability or ease of magnetization is initially very high, making this alloy an ideal material for the armatures and cores of sensitive relays. Other Permalloys show properties of the same type with minor modifications which adapt them for specific applications.

Perminvars are nickel-cobalt-iron alloys (*e.g.*, in the ratio of 45–25–30) possessing constant permeability over a range of low flux densities. Coils, with cores of this alloy, greatly reduce the amount of distortion in speech-transmission circuits.

Magnetic iron or commercially pure iron has relatively high permeability, but its low resistivity results in serious eddy-current losses in iron cores.

Silicon steel, iron with 4 per cent silicon in solution, has a higher permeability than magnetic iron at low flux densities and also five times the resistivity of the unalloyed metal.

Magnetically hard materials for use in permanent magnets are commonly hardened steels in which high residual induction and coercive force (or magnetic hardness) are related to metallurgical hardness. This is not achieved by simple solid-solution agents but by transformation hardening of plain and alloyed (chromium, tungsten, or cobalt) steels, or by dispersion or precipitation agents (aluminum in iron-nickel for Mishima alloys or molybdenum in iron-cobalt for Köster alloys). These alloys can be better understood after discussion of the pertinent phase diagrams.

QUESTIONS

1. Construct a metastable solidus line for the 70:30 copper-nickel alloy on the assumption that no diffusion occurs in the structure during solidification (a condition approached by extreme chill-casting) and that solidification proceeds by one-dimensional growth (*e.g.*, a plane advancing from the mold wall, a condition which is never an actuality but requisite to a solution of this problem). At what temperature is solidification complete?

2. Define "dendrites," "coring," and "solid solution."

3. What is the effect of rate of cooling on the structure of cast copper-nickel alloys? Do other solid-solution alloys show similar characteristics?

4. How can a cast copper-nickel alloy be homogenized? How does the time required for this treatment compare with that required for cast tin bronzes and α brasses?

5. What was the composition of United States nickel coins (up to January, 1942)? What reasons might be given for the choice of this alloy?

6. Name some of the reasons for adding nickel to copper.

7. How do the tensile strength, hardness, and percentage of elongation of the 30 per cent nickel alloy change with increasing degrees of cold-working?

8. Sketch the comparative hystersis loops of soft and hard magnetic materials.

REFERENCES

"Metals Handbook," sections on Constitutional Diagrams (General); Constitution and Properties of Cu-Ni and Cu-Ni-Zn; Magnetically Soft Materials; Alloys of Fe and Ni, etc.

ELLIS and SCHUMACHER, "Survey of Magnetic Materials in Relation to Structure," *Bell Telephone System Monograph* B837 (or *Metals and Alloys*, December, 1934, and January, 1935).

CHAPTER V

EUTECTIC ALLOYS: LEAD-ANTIMONY SYSTEM: BEARING METALS

There are at least two requirements that must be met for an alloy system to show *complete* solid solubility: (1) the two metals must have atomic lattices of the same type, *e.g.*, both should be face-centered cubic or body-centered cubic; and (2) the two atoms must be of nearly the same size. In the copper-nickel and gold-silver solutions, copper and nickel atoms differ in size by less than 3 per cent; gold and silver atoms differ by less than 1 per cent; and all four of these metals have face-centered cubic lattices. If the component metals of an alloy system do not meet the requirement of similar lattice types, complete liquid solubility is, of course, possible, but the alloy system must show two solid phases. These frequently originate in a reaction known as an *eutectic*. The alloys chosen here to demonstrate structures resulting from this reaction are composed of lead, with a face-centered cubic lattice, and antimony, which has a complicated hexagonal structure.

PHASE DIAGRAM

The α phase, at the left end of the horizontal line of Fig. 5, represents solid lead with about 3.5 per cent antimony in solid solution. This solubility decreases with temperature, as shown by the course of the left-hand line (solid solubility or *solvus* line) which drops steeply with temperature and also veers to the left, indicating a solubility limit at room temperature of 0.3 per cent antimony. Under equilibrium conditions, an alloy of lead with 2 per cent antimony will solidify as a solid solution (see copper-nickel alloys, Chap. IV) which is stable until the temperature falls to about 220°C. Upon further cooling, the alloy crosses the *solvus* line and enters a two-phase field with a resultant formation of α_{Sb} crystals in the solid $\alpha_{(Pb)}$ phase (see generalization 3 on page 48). The change from a one-phase solid to a two-phase

structure on cooling, as related to this type of solvus line, is essential for age-hardening (discussed in more detail in Chap. VI). Under equilibrium conditions, then, this 2 per cent antimony alloy would show a two-phase structure at room temperatures *but no eutectic.*

Means of determining the liquidus lines of a phase diagram by thermal analyses of slowly cooled liquid alloys, and of determining the solidus lines by reheating homogeneous solid solutions, have already been described. The temperature-concentration course of the solvus line cannot be determined by thermal analyses, since only a small amount of heat is liberated by the separation of a minute amount of a second phase, and the separation is very slow and subject to undercooling, requiring as it does diffusion of solute atoms through the solvent lattice to nuclei of the new phase. The solubility relationship may be determined micrographically by heating alloys of several concentrations at specific temperatures for long periods of time (in some cases, for weeks), quenching the specimen, and examining the structure for evidence of the presence of a second phase. If the change of solvent lattice parameter with solute concentration (page 57) is first measured (by X-ray diffraction), then, by reheating a saturated alloy at several temperatures in the two-phase field until equilibrium is attained, quenching, and measuring the lattice size of the solvent, the solute concentration at each temperature may be obtained. Finally, since electrical resistivity is strongly affected by an element in solid solution and only slightly by an element present as a disperse, second phase, resistivity measurements may be employed for solid-solubility determinations. The course of the solvus line, based on data from any of these methods, may be checked by the *log (solubility) vs. reciprocal of the temperature* plot described on page 75.

The $\alpha_{(Sb)}$ phase, at the right end of the horizontal line, represents solid antimony with some lead in solution. (It is called an α phase since the convention has been adopted, here, of calling all terminal solid solutions *alpha.*) The actual value of this solubility is not definitely known and is of no commercial importance since antimony, and thus the $\alpha_{(Sb)}$ phase, is relatively weak and brittle.

Along the horizontal line at 251°C.,[1] three phases may exist in equilibrium and, in accordance with Gibbs's phase rule, three

[1] Pellini and Rhines, *Metals Technology* (A.I.M.E.), September, 1942.

phases can exist in a binary system only at a constant temperature. This situation is best represented by the reversible reaction:

$$Liquid_{Pb-12\%Sb} \rightleftarrows \alpha_{Pb\ 3.5\%Sb} + \alpha_{Sb\ 3\%Pb} + heat$$

The reaction proceeds to the right upon cooling, releasing the heat of crystallization of the α_{Pb} and $\alpha_{(Sb)}$ phases, and, under equilibrium conditions, solidification takes place at a constant temperature, 251°C. (For many years, eutectics were thought to be

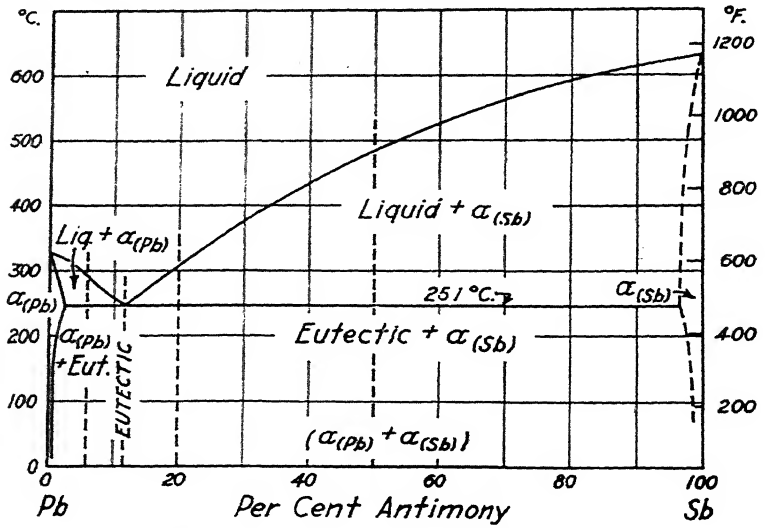

FIG. 5.—Phase diagram of the lead-antimony alloy system.

definite chemical compounds since they froze at a constant temperature and exhibited fixed concentrations, *i.e.*, in this case, Pb + 12 per cent Sb.) On heating, the reaction goes to the left, absorbing the heat of crystallization of $\alpha_{(Pb)}$ and $\alpha_{(Sb)}$ phases and forming the liquid phase containing 12 per cent of antimony. Since the eutectic alloy (12 per cent Sb) melts at a constant temperature, the Greek word *eutectic* meaning "well-melting" has come into use to describe this type of reaction or phase change. It has been logical, then, to apply the Greek prefix *hypo*, meaning "less than," to alloys having less than the eutectic concentration of an alloying element and more than the solid-solution limit (here, 3.5 to 12 per cent Sb), and to use the prefix *hyper*, meaning

"more than," to alloys to the right of the eutectic (here, 12 to about 97 per cent Sb).

Under equilibrium conditions, hypoeutectic alloys solidify from the liquid state as follows: (1) On reaching the liquidus, nuclei of *primary* crystals of $\alpha_{(Pb)}$ form, having the composition given by rule 3 on page 49; (2) cooling through the $\alpha_{(Pb)}$ + liquid field results in growth of the primary dendrites of $\alpha_{(Pb)}$ while their composition changes with temperature, as shown by the *solidus* line; and, at the same time, the formation of a lead-rich phase causes the residual liquid to become enriched in antimony, so that its composition changes along the liquidus line; (3) at 251°C., primary $\alpha_{(Pb)}$ crystals and liquid exist in the ratio given by the lever rule; the eutectic liquid freezes, forming $\alpha_{(Pb)}$ and $\alpha_{(Sb)}$ phases in a rather fine mechanical dispersion. The dispersion is called mechanical since there is no continuous atomic conformity nor necessarily any relationship between atoms of the two phases at their interfaces or planes of contact.

Under nonequilibrium conditions, freezing begins not at the liquidus line but at a temperature a few degrees under it (supercooling). The average composition of the primary crystals does not lie on the equilibrium solidus but on a "metastable" solidus (see page 48) and, consequently, the percentage of liquid at 251°C. will be somewhat greater than that shown by the diagram. The low concentration of alloying element in the primary dendrites requires a metastable, leftward prolongation of the eutectic horizontal to intersect the metastable solidus. As a result, an alloy containing only 1.5 per cent antimony, which should show no eutectic structure, usually will do so when solidified at rates encountered in normal castings. The eutectic freezing may be delayed by undercooling as well as the crystallization of the primary crystals; if one phase of the eutectic undercools more than the other, there can be a displacement of the eutectic concentration as well as temperature (see aluminum-silicon alloys, Chap. VI).

Undercooling of the eutectic liquid has a dual effect. Thermally, it causes the eutectic reaction to occur at a temperature of several degrees (perhaps 5 to 30°C.) under that shown by the equilibrium diagram. Structurally, it causes a refinement of the particle size of the phases participating in the reaction, in the same way as solid-solution dendrites (page 51) are refined by

chill-casting. When α_{Pb} containing 3.5 per cent of antimony and α_{Sb} containing about 97 per cent of antimony form from a homogeneous liquid, there must be a counterdiffusion of the two kinds of atoms in the liquid to each nucleus of the two phases. The rate of solidification when the liquid is suddenly chilled does not permit much time for even relatively rapid liquid diffusion and, simultaneously, there is a very great increase in nucleation points for the reaction. Both factors operate to change the size of crystallites in the eutectic.

MICROSTRUCTURES (PLATE V)

All Etched with 25 Per Cent HNO_3 Solution

Plate V, Fig. 1. Pb + 6 per cent Sb; ×50. This is a typical hypoeutectic structure consisting of primary $\alpha_{(Pb)}$ dendrites (black), plus an *interdendritic* filling of eutectic. The white particles are $\alpha_{(Sb)}$ crystals which, together with the black $\alpha_{(Pb)}$ in which they are embedded, comprise the two-phase structure. There is a difference in appearance of primary $\alpha_{(Pb)}$ and the eutectic α_{Pb}, but both form a continuous plastic structure.

Plate V, Fig. 2. Pb + 12 per cent Sb; ×50. At this concentration, the structure is completely eutectiferous with white brittle crystallites of $\alpha_{(Sb)}$ dispersed in a *continuous* matrix of plastic $\alpha_{(Pb)}$. Differently oriented "colonies" of $\alpha_{(Sb)}$ particles indicate different starting points for the eutectic reaction.

Plate V, Fig. 3. Pb + 12 per cent Sb; ×500. The eutectic structure in detail.

Plate V, Fig. 4. Pb + 20 per cent Sb; ×50. The hypereutectic structure shows primary α_{Sb} crystals in a eutectic matrix. The primary $\alpha_{(Sb)}$ crystals are angular rather than rounded like primary $\alpha_{(Pb)}$, presumably because of lower surface-tension forces. Note the clear-cut distinction in appearance, not in structure or composition, between the primary and the eutectiferous crystallites of antimony.

Plate V, Fig. 5. Pb + 50 per cent Sb; ×50. This hypereutectic alloy contains more of the primary $\alpha_{(Sb)}$ crystals in a eutectic matrix. Note that the primary crystals, although characteristically sharply angular, now show a distinctly dendritic pattern or arrangement.

Plate V, Fig. 6. Hard Babbitt of 84 per cent Sn, 7 per cent Cu, 9 per cent Sb; ×50. This hypereutectic *ternary* (three-compo-

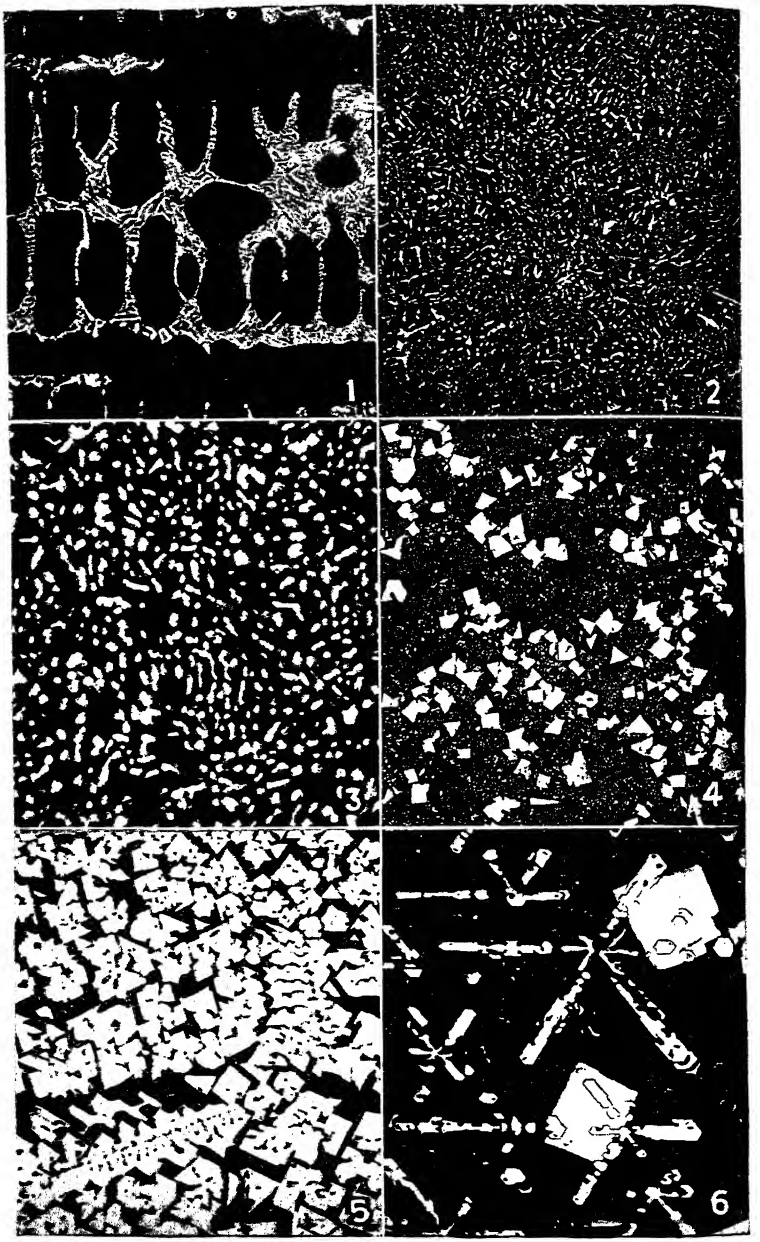

PLATE V.

ment alloy shows primary clusters of CuSn (an intermetallic compound) crystals, arranged in a star-shaped dendritic pattern, and large rectangular crystals of primary SnSb compound in a ductile ternary eutectic consisting of these compounds and a tin-rich solid solution. The CuSn compound has a higher freezing point than the SnSb, since it seems to exist inside the latter phase; *i.e.*, during solidification, the SnSb formed on some of the CuSn crystals already present.

PROPERTIES

The properties of a series of alloys across a eutectic horizontal will naturally be a function of the two solid phases present. In the lead-antimony system, and in a majority of all commercially important eutectiferous alloys, one phase is relatively weak and plastic, the other, relatively hard and brittle. As the antimony content is increased from 3 to about 97 per cent, the proportionate amount of $\alpha_{(Sb)}$ crystallites increases linearly, but the strength does not increase in the same way because of the difference in dispersion or size of the antimony solid-solution crystals, depending on whether they are primary or eutectiferous. There is a rapid rate of increase in strength from 3 to 12 per cent, and a diminution from 12 to 97 per cent antimony. In the former range, fine, eutectiferous crystallites of $\alpha_{(Sb)}$ are increasing in amount while in the latter range, the amount of small particles (or the amount of eutectic) is decreasing, with a corresponding increase in the number and size of large primary crystallites of antimony. The result is an inflection at the eutectic point in the plot of any mechanical property against alloy concentration across a eutectic series; in fact, it may not only be an inflection but a maximum, particularly of strength (the strength of cast Pb-Sb alloys, from 0 to 16 per cent Sb, is reproduced graphically in Fig. 7, page 88).

Examination of the microstructures shows that in all hypo- and hypereutectic alloys, the eutectic structure is continuous, as would be expected since, during freezing, eutectic liquid surrounds the primary dendrites. If in the eutectic structure the plastic phase is continuous, as in the lead, 12 per cent antimony alloy, then the entire series of alloys must have some plasticity. If, on the other hand, the brittle phase is continuous (see aluminum-copper alloys, Chap. VI), the entire series will be brittle. It

seems to be generally true that if one phase is present in a considerably greater proportion in the eutectic, that phase will be continuous in the duplex structure. Thus, if the eutectic concentration is much closer to that of a plastic phase, the eutectic generally will be plastic, and vice versa.

In addition to these considerations, an increase in cooling rates during solidification generally will result in smaller primary dendrites, a finer particle size (and perhaps different shape) in the eutectic, and perhaps a greater amount of eutectic. These factors may influence mechanical properties of eutectic alloys to a very considerable degree.

ENGINEERING APPLICATIONS

The familiar lead sheath used to protect the paper-wound conductors in telephone cables is strengthened by the presence of 1 per cent of antimony in the highly disperse form resulting from aging, after air-quenching from the extrusion temperature (see aging, page 76). Pure lead has a tensile strength of approximately 2,000 p.s.i. but the age-hardened 3 per cent antimony alloy may reach a strength of 10,000 p.s.i. Data showing the remarkable effect of calcium in hardening lead by this same method are given in the "Metals Handbook."

Specifications for bearing metals are based mainly upon composition, with compressive strength and hardness appearing as physical properties of particular importance in selecting the material. Unfortunately, no accepted short-time tests indicating the comparative value of bearing metals are available, and experience in connection with structural characteristics and strength properties must guide such selection. The well-known types of bearing metals are discussed in the "Metals Handbook." A.S.T.M. Specifications B23-26 cover the entire range of white-metal bearing alloys from high-tin to high-lead mixtures. Most of these alloys are eutectiferous, although they frequently contain three or more component metals.

Lead-base bearing metals may be hardened by metals other than tin, antimony, or copper, according to the references cited. "Oilless" and graphite bronze bearings may be made from copper-zinc-antimony-lead alloy strips with rolled-in indentations filled under pressure with graphite paste. Another type is made of powdered oxides of copper, tin, zinc, and lead mixed with

graphite, pressed, sintered, and partially reduced to a porous mass which absorbs oil by capillary attraction. This must be supported by a housing and is best shaped by grinding.

QUESTIONS

1. (*a*) Draw cooling curves for the four lead-antimony alloys whose structures are shown in micrographs 1, 2, 3, and 4. The significant temperatures should be properly correlated with the phase diagram (Fig. 5, page 65).

(*b*) Calculate the percentages of the structure elements (*i.e.*, primary $\alpha_{(Pb)}$, $\alpha_{(Sb)}$, or eutectic) present in each of these alloys.

2. What structural conditions are generally found in alloys for bearing metal service?

3. Name the common metals usually found in bearing alloys.

4. Distinguish between the "white metal" bearing alloys and the "bronzes" and between hard and soft Babbitt metal, on the basis of alloy composition and one significant property.

5. What is "type metal" and in what way is it similar to Babbitt metal?

6. What is Woods metal? Why does it have such a low melting point?

7. Tabulate the melting points of the pure metals, bismuth, cadmium, lead, and tin: also the compositions and melting points of their binary, ternary, and quaternary eutectics ("Metals Handbook," Low-melting Alloys).

REFERENCES

"Metals Handbook," sections on Copper-Lead-Tin Alloy: Lead (Constitution, Properties, Micrography); Constitution, Structure, and Properties of Tin-Antimony-Copper Alloys.

CORSE: "Bearing Metals and Bearings," A.C.S. Series No. 53.

GILLETT, RUSSELL, and DAYTON: "Bearing Metals," *Metals and Alloys*, 12, September, October, November, and December, 1940.

CHAPTER VI

AGE-HARDENING: CAST AND WROUGHT ALUMINUM ALLOYS

None of the industrially important aluminum alloys is strictly binary since the base metal, as commercially produced, always contains about 0.3 per cent each of copper, iron, and silicon. The iron and silicon usually combine with aluminum to form an intermetallic compound which is almost completely insoluble in solid aluminum and thus always visible in the microstructure (see Plate II, Fig. 6, page 16). The impurity compound not only complicates the appearance of the alloy microstructures but, since it forms a low melting eutectic with aluminum, the presence of iron and silicon affects melting point and heat treatment temperatures. However, the binary diagrams remain useful in discussing the general structural and property characteristics of most of these alloys.

PHASE DIAGRAMS

The aluminum-copper system diagram from 0 to 54 per cent copper, as reproduced in Fig. 6 (page 73), differs from the lead-antimony diagram (page 65) in only two essential respects: the eutectic contains more than 50 per cent of the right-hand phase, and this phase is not a terminal solid solution but an intermediate alloy structure θ, which is hard, brittle, and of a narrow range of compositions approximating that of the intermetallic compound $CuAl_2$, *i.e.*, a structure containing one atom of copper for every two atoms of aluminum. (The binding forces in intermetallic compounds differ from those holding chemical compounds in a specific crystal form. In salts, such as NaCl, the binding force arises from ionic or electrostatic fields resulting from exchanges of valency electrons. In intermetallic compounds, ordinary valency rules do not determine the atomic ratios.) The aluminum ends of the Al-Mg, Al-Ni, Al-Mn, and Al-Fe systems are like the aluminum-copper in showing eutectics between an aluminum

solid solution and an intermediate limited solid-solution phase or intermetallic compound, while the aluminum-silicon eutectic is between the two terminal solid solutions. All of these alloys show the same constitutional features that were discussed in detail in Chap. V (Pb-Sb alloys). In all except the aluminum-iron system, the solubility of the second phase in the $\alpha_{(Al)}$ solid solution is distinctly greater at the eutectic temperature than at room temperature, and, in the aluminum-copper and aluminum-

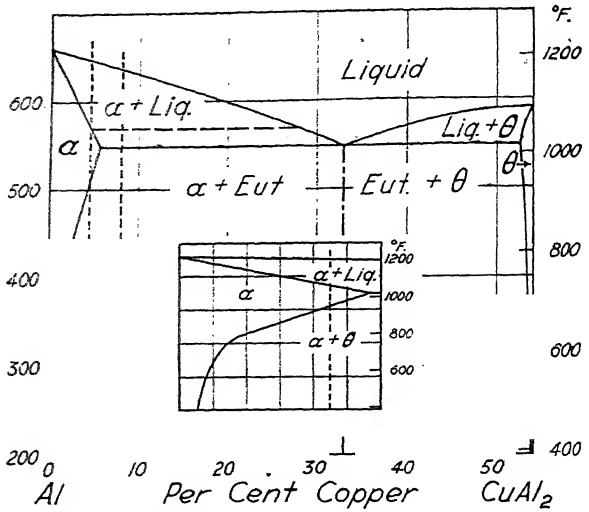

FIG. 6.—Phase diagram of the aluminum-copper alloy system, from 0 to 54 per cent copper.

magnesium systems, this feature is utilized to obtain high-strength alloys by a controlled dispersion of the second phase.

The extent of solid solubility of one element in another was stated on page 63 to depend on the relative types of lattices and atomic sizes of the solute and solvent metals. Atomic sizes are not fixed quantities; a large atom, randomly dispersed at lattice points of a solvent metal having a smaller atom, must contract somewhat to fit in the solvent lattice which, simultaneously, necessarily is expanded (Vegard's law, page 57). Contrariwise, a smaller atom may be enlarged if present in solid solution with a larger atom whose lattice is thereby contracted. The difference in sizes of solute and solvent atoms (measured when present in

their own form) is an important factor in determining the extent of solubility that may exist. If the two atoms differ by more than 15 per cent, extensive solid solutions are not usually found, although Table VII shows that the converse of this statement is not always true (for example, see titanium).

TABLE VII.—ATOM-SIZE FACTOR IN ALUMINUM-BASE SOLID SOLUTIONS

Solute		Reaction and and temperature, °C.	Maximum solubility		Atomic size,* Å	Per cent atomic size difference
Element	Lattice		Per cent by weight	Atom, per cent		
Al	f.c.c.†				2.86	
Zn	c.p. hex.‡	eutectic-380	82.	66.	2.75	− 3.8
Ag	f.c.c.	eutectic-558	57.	25.	2.88	+ 0.7
Mg	c.p. hex.	eutectic-451	14.9	16.3	3.19	+11.5
Cu	f.c.c.	eutectic-548	5.65	2.48	2.55	−10.8
Mn	complex c.	eutectic-659	1.82	0.90	2.37	−17.1
Si	diamond c.	eutectic-577	1.65	1.59	2.35	−17.8
Cr	b.c.c.§	peritectic-661	0.77	0.40	2.49	−12.9
Ti	c.p. hex.	peritectic-665	0.28	0.16	2.93	+ 2.4
Zr	c.p. hex.	peritectic-661	0.28	0.08	3.19	+17.7
Ni	f.c.c.	eutectic-640	0.05	0.023	2.48	−13.3
Be	c.p. hex.	eutectic-645	0.05	0.15	2.25	−22.7
Fe	b.c.c.	eutectic-655	0.02	0.009	2.48	−13.3
Co	b.c.c.	eutectic-657	0.02	0.009	2.50	−12.6

* From HUME-ROTHERY, "Structure of Metals and Alloys."
† f.c.c.—face-centered cubic.
‡ c.p.hex.—close-packed hexagonal.
§ b.c.c.—body-centered cubic.
‖ The peritectic reaction is described on p. 99.

It is quite evident that the lattice type and atomic size of the solute are not the only factors affecting the maximum solubilities. Generally, however, a high solid solubility appears to be favored either by a low eutectic temperature or by a favorable atomic-size ratio. The effect of a low eutectic temperature is shown by the close-packed hexagonal metals, zinc and magnesium, which have greater solubilities in face-centered cubic aluminum than face-centered cubic metals with a smaller atomic-size difference, silver and copper, respectively.

CORRELATION OF PHASE DIAGRAMS[1]

Since the phase diagrams of all alloy systems are based fundamentally on physical chemistry, many attempts have been made to verify equilibrium data by physical chemical laws. Reference has been made to Gibbs's phase rule (page 64) defining the number of variables F, usually temperature and concentration, which can be altered in an alloy having a known number of component metals C without changing the number of phases P present; ignoring the gas phase, the relation is

$$F = C - P + 1$$

A second equation, developed by LeChatelier, gives the relation between the concentration of an ideal solution (solid or liquid) and its temperature when the precipitating phase is of constant concentration (an element or compound):

$$\text{Logarithm (solute concentration in solvent)} = \frac{\text{constant}}{\text{temperature}} + \text{constant}$$

According to this equation, all solid solubility curves for ideal solutions should become straight lines when the logarithm of the solubility is plotted against the reciprocal of the temperature (Kelvin or absolute scale). The solid solubility or solvus curves for most of the aluminum alloys of Table VII have been so plotted and, in almost all cases, show a linear relationship. Furthermore, by definition of terms, this equation is equally applicable to hypereutectic liquidus curves, as has been demonstrated, at least for many aluminum alloys. A third equation, which will not be reproduced here, has successfully established a relationship between the eutectic concentration, the solid solubility at the eutectic temperature, and the actual temperature of the eutectic for many of the systems listed in Table VII. Other correlations of an empirical nature have been discovered in the aluminum-base-alloy phase diagrams. For example, the logarithm of the lowering to the eutectic temperature seems to be linearly related to the solute concentration of the α solid solution at the eutectic temperature and, furthermore, both of these quantities are linearly related to the slope of the solid solubility curve. These and other relationships satisfactorily generalize the data on a series of alloy

[1] FINK and FRECHE, *Trans. A.I.M.E.*, 111, 304, 1934.

systems. It is also evident that, where these relationships hold, the equilibrium diagrams at one end of an alloy system can be constructed with very few experimental data; two points on the hypereutectic (or hyperperitectic) liquidus, the eutectic temperature, and one point on the solid solubility curve could suffice.

THEORY OF AGE-HARDENING

Ordinarily, concentrations of the hardening constituent approaching maximum solid solubility in the $\alpha_{(Al)}$ phase at the eutectic temperature are chosen. The first step in the heat treatment is to heat the alloy to a temperature in the α phase field in order to obtain a solid solution of uniform composition. The saturated solution thus formed is quenched or at least cooled at too rapid a rate to permit the separation of the second phase that would normally occur with slow cooling. As a result of the rapid cooling, the alloy is in a state of supersaturation and is, therefore, thermodynamically unstable. The subsequent age-hardening of the alloy is a result of the decomposition of the solution, which in some alloys occurs at ordinary room temperatures but usually requires a relatively low-temperature heat treatment.

The hardening of Duralumin (basically, Al + 4½ per cent Cu), the alloy earliest known to be capable of age-hardening (1911), was first attributed (Merica et al., 1919) to the precipitation of the compound $CuAl_2$ in the form of particles too small to be visible under the microscope. According to the theory rather generally accepted prior to 1930, the particles of compound hardened and strengthened the alloy by making slip along crystallographic planes more difficult. In other words, the uniformly dispersed particles were considered to have a "keying" action, thereby obstructing movement along planes of ready slip.

As correlated data accumulated from age-hardening studies, this simple mechanical conception of hardening by compound precipitation appeared to become inadequate. Anomalous increases in electrical resistivity during aging at ordinary temperatures (resistivity should decrease as the concentration of solute atoms decreases, see page 57), intermediate peaks in hardness-time curves, and other comparable data led to postulates of preprecipitation changes such as the formation of "knots" of segregated solute atoms which affected the properties of the alloy independently of any subsequent precipitation.

Critical studies of the last few years have led to a more complete understanding of the age-hardening process, which appears to proceed in the following sequential order:[1]

1. Segregation of solute atoms on a specific crystallographic plane of the matrix (tetragonal $\theta_{(CuAl_2)}$ forms with its square, basal plane parallel to the cube plane of the α_{Al} phase, or the hexagonal γ precipitate in aluminum-silver alloys forms with its basal plane on the corresponding octahedral plane of the face-centered cubic matrix).

2. Formation of a new lattice of the precipitating phase. The precipitate is only from 2 to 50 atoms thick and may be from 20 to several hundred atoms long or wide; in other words, it is a thin plate. There must be atomic conformity between the lattices of the precipitating phase and the matrix, which requires that growth occur laterally along the plane of precipitation. The new phase, at this stage, is under high elastic stress (calculated to be about 115,000 p.s.i. in Al-Ag alloys) as a result of the enforced atomic conformity between lattices of somewhat different spacings, and thus it may have abnormal dimensions; it then is usually found to be a metastable or transition phase (θ' for Al-Cu alloys or γ' for Al-Ag alloys).

3. Growth of the transition phase causes the lateral elastic stresses to exceed a critical value, shearing occurs on the specific plane, atomic conformity over the entire plate ceases to exist, and the new phase changes to its stable dimensions and form, with the creation of an interface between it and the matrix lattice.

Property changes have not yet been correlated, in many alloys, with the above picture, but in general, anomalous conductivity effects occur in stage 1, maximum strength or hardness in 2, while 3 lies in the region of overaging or softening. The entire process, including stage 1, for simplicity may be termed *precipitation*, adopting the Merica theory in general terms. The sequence of changes during aging is of particular importance in alloys of the Duralumin type, which develop their useful properties without definite evidence of actual precipitation of the hardening phase. In a larger group of alloys, the optimum properties are obtained by heat treatments which produce visible evidence of precipitation, but even in these cases the visible precipitate particles are usually in the transition stage, or 2, with an abnormal lattice.

[1] BARRETT, GEISLER, and MEHL, *Trans. A.I.M.E.*, **143**, 134, 1941.

MICROSTRUCTURES (PLATE VI)

A. Etched with 0.5 Per Cent HF; *B.* Additional Etch in 20 Per Cent H_2SO_4 at 70°C.

Plate VI, Fig. 1. Al + 13 per cent Si + about 0.8 per cent Cu and Fe as impurities (Alcoa 47); ×75; *A*. This is a hypoeutectic structure showing a few primary dendrites of $\alpha_{(Al)}$ in a fine eutectic structure. Since the equilibrium eutectic composition is at 11.6 per cent silicon, this alloy would normally be hypereutectic, but the addition of 0.25 per cent sodium, 15 min. before casting, suppresses both the formation of primary silicon crystals and the eutectic reaction. The liquid cools until it reaches the temperature of the *metastable* prolongation of the hypoeutectic liquidus to form a few primary $\alpha_{(Al)}$ dendrites after which the eutectic reaction starts. The undercooled eutectic liquid forms a very finely dispersed two-phase structure (at about 564°C. rather than the equilibrium temperature of 578°C.).

Plate VI, Fig. 2. Same alloy (13 per cent Si) at ×1,000; *A*. Dark gray particles, such as that marked *A*, are eutectiferous silicon crystallites; lighter gray needles, marked *B*, are an aluminum-iron-silicon compound originating from the iron impurity. Note that the α aluminum phase is *continuous*, as predictable from the approximate relative proportions of $\alpha_{(Al)}$ (87 per cent) and silicon (13 per cent) in the eutectic.

Plate VI, Fig. 3. Al + 8 per cent Cu + about 1 to 1½ per cent Fe and Si as impurities (Alcoa 12); ×50; *AB*. This is a hypoeutectic structure consisting of cored primary $\alpha_{(Al)}$ dendrites (the dendritic characteristic is not very evident) surrounded by the eutectic of $\alpha_{(Al)}$ and θ (or $CuAl_2$).

Plate VI, Fig. 4. Same alloy (8 per cent Cu) at ×1,000; *AB*. A greatly magnified view of the $\alpha_{(Al)}$ and $\theta_{(CuAl_2)}$ eutectic shows that the brittle θ phase is continuous, probably because this eutectic consists of 58 per cent θ and 42 per cent $\alpha_{(Al)}$ (proportions calculated on a weight basis). The needles, extending through the eutectic (marked *C*), are an aluminum-copper-iron compound originating from the iron impurity. (Identification of all the common intermetallic phases found in aluminum alloys is possible by using various etching solutions, as specified in the "Metals Handbook.")

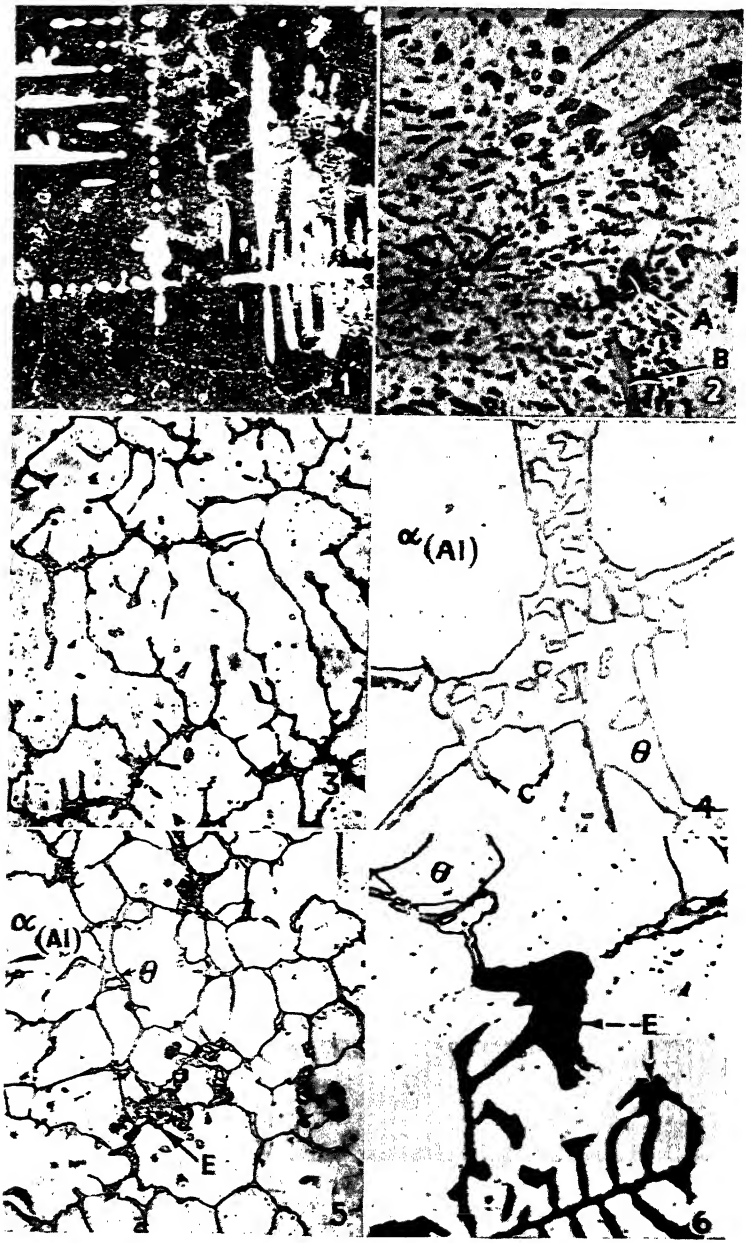

PLATE VI. FIGS. 1–6.

Plate VI, Fig. 5. Al + 4½ per cent Cu with controlled impurities (1 to 1½ per cent) of Fe and Si (Alcoa 195); ×75; *AB*. The as-cast structure reproduced here shows cored dendrites of $\alpha_{(Al)}$ surrounded by the $\alpha_{(Al)} + \theta$ eutectic and a eutectic structure of $\alpha_{(Al)}$ and aluminum-iron-silicon compound (*E*) originating from the impurities. Although the copper content of this alloy lies to the left of the $\alpha_{(Al)} + \theta$ eutectic horizontal, some eutectic is found in the cast structure because of the metastable position of the solidus on rapid cooling of the casting (page 48).

Plate VI, Fig. 6. Same alloy (4½ per cent Cu) at ×1,000; *AB*. The structural appearance of this particular aluminum-iron-silicon compound has led to use of the descriptive name "Chinese script." The θ present does not appear to be a part of a eutectic structure since the $\alpha_{(Al)}$ of the eutectic is not inside the θ but outside, in contact with and indistinguishable from the primary $\alpha_{(Al)}$. The θ and aluminum-iron-silicon compound appear to be isomorphous since there is a continuity from one structure to the other with a gradation in the coloring or degree of attack by the etchant.

Plate VI, Fig. 7. Same alloy (4½ per cent Cu) at ×75; *AB*; structure after heat treatment (A.S.T.M. No. 3) as follows: 15 hr. at 510°C. followed by a water quench; reheated 15 min. in high-pressure steam. This structure should be compared with that of Plate VI, Fig. 5; it is evident that the heat treatment at 510°C. has caused the $CuAl_2$ to dissolve in the $\alpha_{(Al)}$ matrix (thus the high-temperature treatment is called a *solution anneal* or *solution heat treatment*). Quenching in water, after the high-temperature soak, prevented precipitation of the dissolved θ upon cooling the alloy to temperatures at which two phases exist according to the diagram. Reheating this metastable or supersaturated solid solution has not caused particles of $CuAl_2$ to form in a size visible at this magnification. Particles of the aluminum-iron-silicon compound (*E*) are still present, since this phase has no measurable solubility in $\alpha_{(Al)}$ and remains unchanged through the heat treatment.

Plate VI, Fig. 8. Same alloy (4½ per cent Cu) at ×500; etched with HCl, HNO_3, and HF in water (Keller's reagent); structure after heating to 575°C. and quenching. According to the aluminum-copper phase diagram, when this alloy is heated above about 565°C., it is in a two-phase field, $\alpha_{(Al)}$ + liquid, and

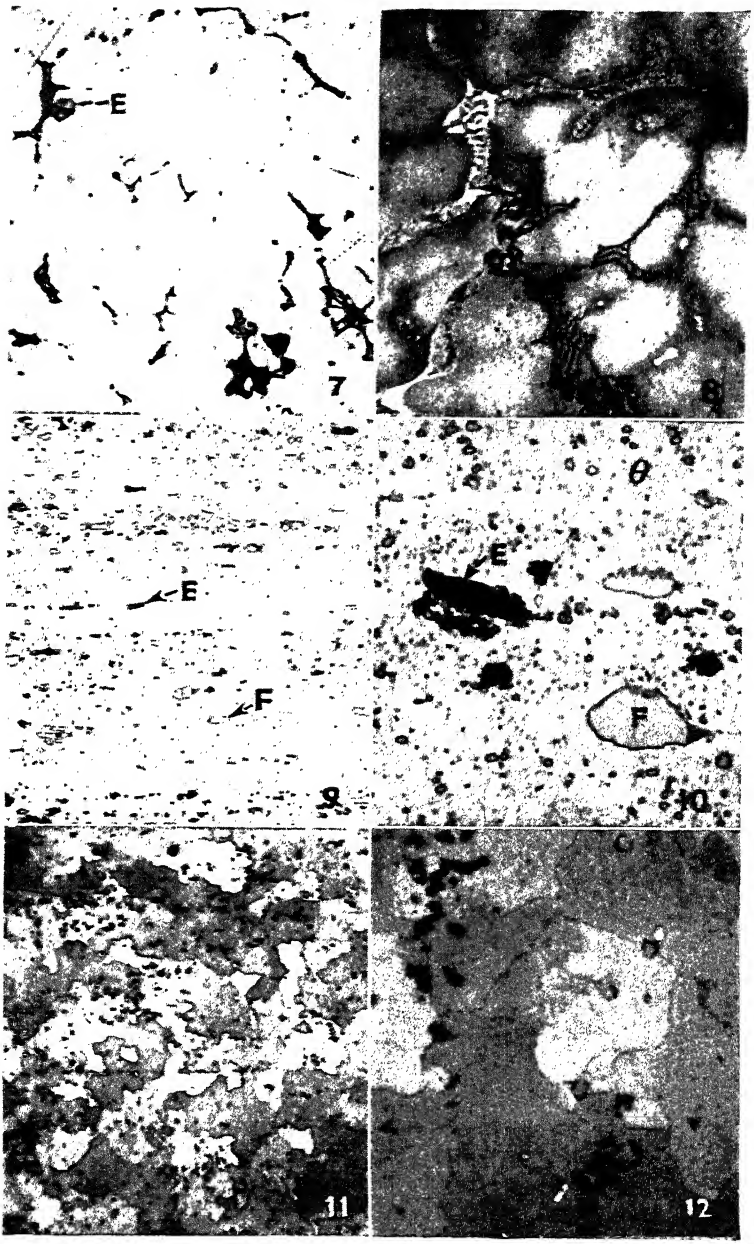

PLATE VI. FIGS. 7–12.

the liquid has an almost eutectic concentration of copper. The liquid phase forms at the $\alpha_{(Al)}$ grain boundaries and, upon quenching, must solidify there, in large part as a eutectic which, in this system, is brittle. With a nearly continuous brittle structure enveloping each grain, the total structure is now weak and brittle. The etch used for this micrograph has brought out coring in the aluminum matrix, *i.e.*, variations in the amount of dissolved copper. Although the binary aluminum-copper diagram shows the safe solution annealing temperature range to be 510 to 565°C., the presence of a eutectic network in the original casting of this alloy would set the upper limit at 545°C. More importantly, the presence of iron and silicon impurities means that a ternary or quaternary eutectic exists with a melting point of about 525°C., so that the safe heat-treatment temperature range is quite narrow, 505 to 520°C. The lower limit is set by the necessity for dissolving all the copper in order to obtain optimum properties, while the upper limit is set by the melting point of any eutectic present in the structure. The iron impurity content not only affects the minimum "burning" temperatures of the heat-treated aluminum-copper alloys but also markedly affects the optimum properties attained since the presence of iron results in the formation of an insoluble aluminum-copper-iron intermetallic compound (Plate VI, Fig. 4) and thus removes copper from an active participation in the aging process. High-purity aluminum-copper alloys may show very much better strengths than the commercial 195 alloy.

Plate VI, Fig. 9. Al + 4.2 per cent Cu, 0.5 per cent Mg, 0.5 per cent Mn, about 0.5 per cent Fe and Si as impurities (Duralumin or Alcoa 17S); ×75; *AB*. This structure represents that of the alloy in the as-extruded form, which means that it was hot-worked at a high temperature, probably in the $\alpha_{(Al)}$ solution field, and slowly cooled. The eutectic structure present in the original cast billet has been destroyed, and the insoluble constituents have been broken up into stringers extending in the direction of extrusion; *i.e.*, the black aluminum-iron-silicon impurity compound (*E*) and the clear, outlined particles of aluminum-manganese, aluminum-iron-manganese or aluminum-copper-iron-manganese compound (*F*). Manganese is added to Duralumin chiefly because the resultant insoluble constituent acts to restrict grain growth in the $\alpha_{(Al)}$ matrix during the solution heat treatment.

The copper and magnesium are in solution during the hot-working, but much of the copper has precipitated as the θ phase during the subsequent slow cooling. The fine precipitate gives the background a "salt and pepper" appearance at this low magnification.

Plate VI, Fig. 10. Same (Duralumin) at ×1,000; *AB*. At this magnification most of the θ precipitate, which formed at a relatively high temperature, is resolved, (θ). The indistinct markings in the background are probably particles of θ which formed last, as the alloy approached room temperature.

Plate VI, Fig. 11. Al + 4.4 per cent Cu, 1.5 per cent Mg, 0.6 per cent Mn, and about 0.5 per cent Fe and Si as impurities (Super-Duralumin or 24ST); the alloy in sheet form was quenched from 500°C. and aged at room temperature; ×75; HCl, HNO_3, and HF in water (Keller's etch). The etch employed in this case differentially attacks the aged aluminum solid-solution matrix to show the typical, irregularly shaped grains of the structure on a section parallel to the rolling plane. Insoluble manganese and iron-silicon intermetallic compounds are again extended in the direction of flow during hot-working. Only traces of copper or magnesium compounds are visible since they were almost completely dissolved during the heat treatment and now cannot be seen in the extremely fine precipitated form characteristic of the aged alloy.

Plate VI, Fig. 12. Same as Fig. 11 (24ST) at ×500. At the higher magnification, the clear, white particles of residual $CuAl_2$ are visible as well as the black and dark gray manganese and iron-silicon compounds. In addition, a series of small, dark particles along the grain boundaries are now resolved. They probably originated upon cooling the alloy somewhat too slowly from the solution treatment; *i.e.*, by quenching in hot water. The hot-water quench diminishes distortion and quenching stresses, but the grain boundary precipitate (of θ or $CuAl_2$) results in a susceptibility to intergranular corrosion. This may be avoided by coating the alloy with pure aluminum (Alclad 24ST).

Plate VI, Fig. 13. Same alloy (24ST) in the Alclad form; the sheet was carried through 900,000 cycles of stress (by bending) which attained a maximum intensity of about 18,200 p.s.i. at the surface; ×500; 0.5 per cent HF etch. The bottom of the micrograph shows the structure of the alloy core, and the upper $\frac{3}{4}$ in. shows the structure of the aluminum coating. The line of

delineation between the core and originally pure aluminum layer is based on the absence of the insoluble constituents in the latter zone. However, some copper and magnesium have diffused from the core into the coating during the hot-rolling and solution heat treatment stages of processing of the sheet. Aluminum in the diffusion zone is harder and has polished cleanly. The outer zone of the coating is probably still pure aluminum and so soft that polishing abrasive has adhered to this part of the specimen, resulting in a "dirty" appearance. It is important so to control the hot-rolling and heat-treatment times and temperatures that copper and magnesium atoms are not permitted to diffuse to the surface, or the benefits (see page 93) of the aluminum coating will be lost. In this micrograph, the rounded, clear particles in the core may be residual $CuAl_2$ or θ, left undissolved when the solution treatment was shortened sufficiently to avoid alloy diffusion to the surface.

The black lines, at approximately 45 deg. to the surface of the sheet, are shear cracks developed by repeated application of a stress with a maximum value far below the ordinary, axially determined tensile strength (62,000 p.s.i.) or even yield strength (40,000 p.s.i.). These cracks would eventually cause the sheet to break if the stressing was repeated often enough (this difficulty is minimized by design, see page 93). Failures of this type are called *fatigue* failures but are popularly (and erroneously) known as failures resulting from *crystallization* of the metal, since it is not generally realized that metals are always crystalline. The deformation accompanying an ordinary tensile fracture destroys the crystalline appearance of the broken surface. However, when a fatigue crack has reduced the effective cross-sectional area of the metal sufficiently, the remainder of the section breaks suddenly, without any noticeable deformation, and thus frequently has a crystalline appearance.

Plate VI, Fig. 14. Al + 5 per cent Cu; alloy of pure materials (less than 0.05 per cent of Fe + Si); quenched from 540°C., reheated 30 min. at 200°C.; ×1,000; 0.5 per cent HF etch. The heat treatment given this alloy resulted in maximum hardness (see Table VIII, page 90) but there is no readily visible precipitate. The grain boundary has etched more deeply than it would in the as-quenched (from 540°C.) structure and there are a few markings within the grains, indicative of some change in the solid

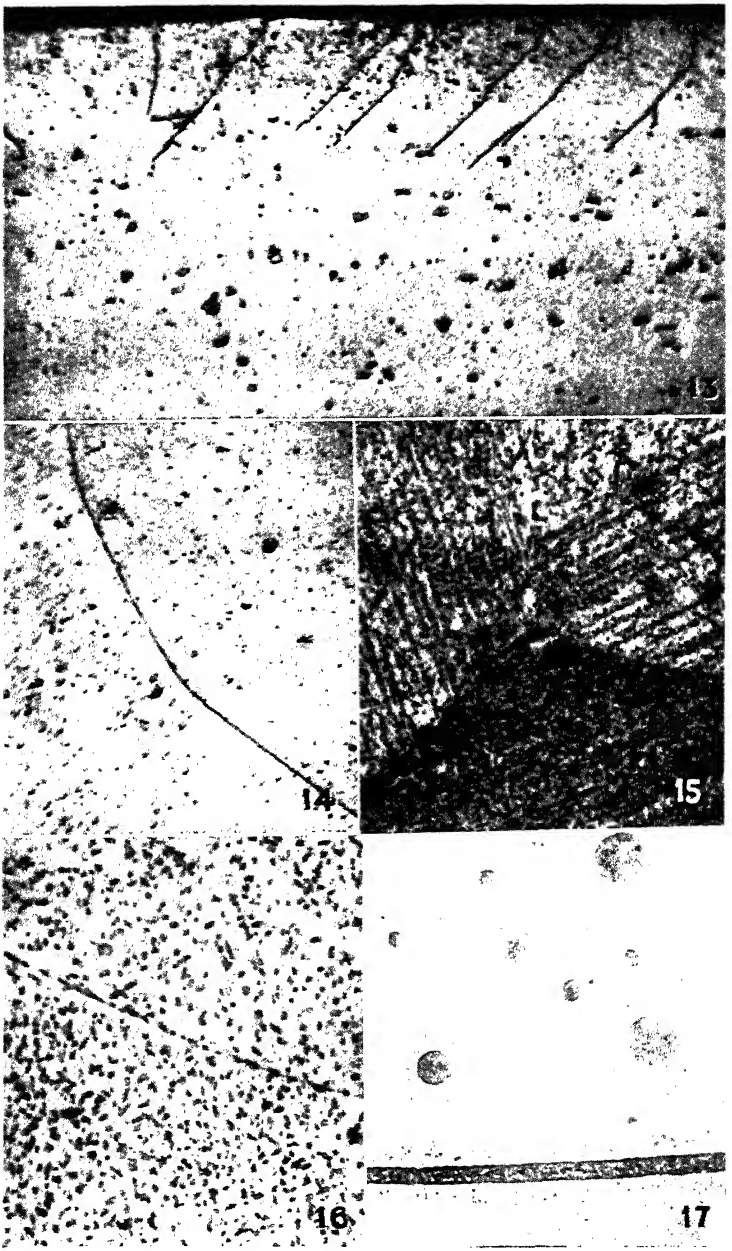

PLATE VI. FIGS. 13–17.

solution. Special etches have revealed more positive indications of precipitation in equivalent structures, but this is representative of the structure shown by the usual micrographic technique.

Plate VI, Fig. 15. Al + 5 per cent Cu; ×1,000; *A*. A specimen similar to Fig. 14 was quenched in cold water from a solution treatment at 540°C. and reheated 1 hr. at 250°C. Distortion from the cold-water quench caused a slight plastic deformation of the alloy matrix, and the subsequent aging treatment resulted in precipitation of the θ phase, which occurred preferentially on the slip planes that were active in the plastic movement. Nucleation of the precipitation (or more generally, of any solid phase change) occurs first at the least stable part of the matrix lattice, normally at grain boundaries but, in the case of prior or simultaneous plastic deformation, at slip planes. Note that precipitation is not uniform in all grains (in slight deformations, plastic movement is not uniform in all crystals). Particles of the precipitated θ are very fine and not clearly resolved here.

Plate VI, Fig. 16. Al + 5 per cent Cu; ×1,000; *A*. A specimen similar to Fig. 14 was quenched from 540°C. and reheated 1 hr. at 400°C. At this high aging temperature, the precipitated particles are very coarse and, partly as a result of their size and partly as a result of re-solution of θ (1.5 per cent of copper is soluble at 400°C. and only 0.6 per cent at 250°C.), there are fewer particles. Upon close examination, some needles are visible and these, in the third dimension, would of course be plates. The plates show the genetic relationship between matrix and precipitate lattice orientations, as mentioned in the previous section on theory of age-hardening. These visible plates, however, are tremendously larger than the "platelets" present at an early stage of aging. Notice the lineup of θ particles along the $\alpha_{(Al)}$ grain boundary.

Plate VI, Fig. 17. Same Al + 5 per cent Cu alloy, quenched from 620°C. and reheated at 400°C.; ×1,000; 0.5 per cent HF etch. The high-temperature treatment was well above the solidus temperature for this alloy (see Fig. 6, p. 73), and "burning" occurred. Not only did an eutectiferous liquid form at the grain boundary (the horizontal eutectic structure), but a similar liquid formed in spherical globules within the grains, resulting in the circular eutectic "rosettes" shown above the boundary. Coring in the adjacent solid solution is revealed by the precipitate

adjacent to the boundary eutectic and the rosettes; the $CuAl_2$ was precipitated in these regions upon the subsequent reheating to 400°C. The thin lines visible in parts of the structure are new grain boundaries, formed by recrystallization, at 400°C., of metal plastically deformed during the previous quench.

HOT-SHORTNESS AND BURNING

Any tensile stress applied to an alloy while it is in the two-phase, *solid* + *liquid*, condition will naturally cause the metal crystals to separate where there is no solid to solid contact. The stress may come from rolling, forging, or other form of hot-work, or it may originate in the contraction or shrinkage of a hollow casting about a strong core. In the latter case, the amount of liquid is critical, and Sachs and Van Horn show that with more than about 15 per cent present, the structure is sufficiently open for more liquid to flow or be sucked in from hotter portions (*e.g.*, the riser) to fill any openings. This susceptibility to damage while at the high temperature of the α + *liquid* field is known as *hot-shortness*.

The structure shown by Plate VI, Fig. 8, is commonly called a *burnt* structure; the word as here used does not signify an oxidation reaction but heating into a two-phase, *solid* + *liquid*, field during solution heat treatments or hot-working operations. Deformation within this temperature range, of course, will cause the alloy to crack and be ruined. If the alloy has a plastic eutectic, as in the aluminum-silicon alloys, the damage to the quenched metal (in the absence of deformation) is negligible. If the eutectic envelopes around the grains are brittle, as in the aluminum-copper alloys, both strength and ductility are seriously impaired. While the bad effects could largely be eliminated by a solution anneal, the time required to redissolve the eutectic is so long that it is not generally profitable commercially to do other than scrap the overheated alloy.

PROPERTIES

The properties of the eutectiferous alloys can be qualitatively evaluated on the basis of the proportionate amounts of primary crystals and eutectic structure and the physical characteristics of the eutectic:

The aluminum-silicon phase diagram has not been reproduced here since it is almost a duplicate of the lead-antimony diagram (Fig. 5) with regard to concentration limits of the plastic α phases of Pb or Al), the brittle α phases (Sb or Si), and the eutectic composition; although the temperatures of liquidus, solidus, and eutectic lines are naturally higher. The normal aluminum-silicon eutectic temperature and composition are 578°C. and 11.6

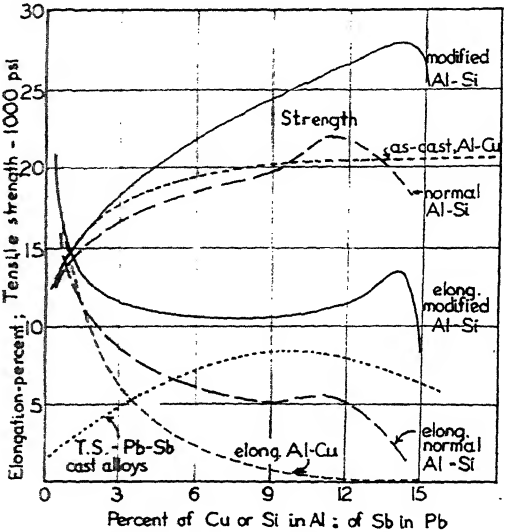

FIG. 7.—Strength properties across the hypoeutectic sections of the aluminum-copper, aluminum-silicon, and lead-antimony systems; effect of modification on the strength and elongation of the aluminum-silicon alloys.

per cent Si, respectively. However, chill-casting or a sodium treatment of the liquid alloy before casting may suppress the formation of primary silicon crystals in a normally hypereutectic structure, say of 14 per cent Si, and cause it to solidify as a eutectic alloy at 564°C. rather than at 578°C. In addition to shifting the eutectic composition and temperature, the chill-casting or sodium treatment, called *modification*, notably refines the structure of the eutectic, particularly the silicon crystallites. The effect of this on strength and elongation values of the aluminum-silicon alloys is shown in Fig. 7; note the maximum of all properties at the eutectic concentration, about 11.5 per cent Si in the normal alloys and 14 per cent Si in the modified alloys.

All of the aluminum-silicon alloys show some ductility since aluminum is the *continuous* phase in the eutectic. The superior ductility of the modified alloys is related to the shape as well as the size of the eutectiferous silicon crystallites; in the normal alloys, they tend to be angular plates whose sharp edges act as internal notches in the structure, whereas this effect is nearly absent with the rounded silicon particles of the modified alloy (Plate VI, Fig. 2).

The aluminum-copper system (Fig. 6, page 73) has a eutectic composition nearer the brittle θ phase ($CuAl_2$) than the plastic $\alpha_{(Al)}$ phase, and thus the $\alpha_{(Al)} + \theta$ eutectic structure is inherently brittle. The effect of fairly rapid cooling in casting and the related position of the metastable solidus results in some eutectic in cast alloys with as little as 2 per cent copper present. Figure 7 (page 88) shows that there is a moderate increase in strength and strong decrease in ductility (as shown by test elongation values) as the amount of copper in aluminum is increased. When the eutectic structure becomes continuous (Plate VI, Fig. 3; 8 per cent Cu) the strength is almost at a maximum and the ductility nearly zero. Further increases in the amount of eutectic have little effect on the strength properties, within the range of commercial alloys of aluminum and copper, although the 12 per cent Cu alloy has greater hardness and wear resistance as a result of the increased amount of θ present in the structure.

Strength, ductility, and hardness properties of two-phase alloys are related to the size, number, distribution, and properties of the crystals of both phases. The effect of matrix grain size was discussed in Chap. III, of an added element in solid solution in Chap. IV, and of a relatively coarse dispersion of a second phase in Chap. V. Very fine dispersions cannot be obtained from the liquid state but can form in the solid by reason of the greater order of magnitude of nucleation in the latter case. The process involved has been discussed from the standpoint of the phase diagram under theory of age-hardening. Three structures have been shown, Plate VI, Figs. 14, 15, and 16, which should be examined with relation to the data of Table VIII.

It is evident that, even when the precipitate is as fine as that shown in Plate VI, Fig. 15, the alloy has passed its point of maximum hardness and would be in a condition known as "overaged," while the coarse precipitate of Plate VI, Fig. 16, would represent a

structure of minimum strength and hardness, designated as the "annealed" or "S0" condition by the Alcoa system. The precipitate present in the condition of optimum strength and hardness is not readily detected by ordinary micrographic technique for many alloys, although special care in polishing and the use of special etches generally will reveal some structural alteration as compared to the initially as-quenched supersaturated condition.

TABLE VIII.—AGING OF AL–5 PER CENT CU ALLOY
As Quenched from 540°C. RF61

Time	Temperature, °C.	Hardness	Time	Temperature, °C.	Hardness
0	25	RF61	1 hr.	150	RF80
2 hr.	25	RF72	1 hr.	200	RF90
1 day	25	RF85	1 hr.	250	RF84
1 week	25	RF87	1 hr.	300	RF73
1 month	25	RF88	1 hr.	350	RF56
1 year	25	RF88	1 hr.	400	RF44
¼ hr.	200	RF78	¼ hr.	300	RF83
1 hr.	200	RF90	1 hr.	300	RF73
5 hr.	200	RF87	5 hr.	300	RF65
24 hr.	200	RF83	24 hr.	300	RF43

Strength properties generally show the same trends as hardness, but ductility may not show the usual inverse trend. The decrease in tensile-test elongation values during early stages of aging may be slight. At about the point of maximum hardness or slight overaging, a sharp drop in ductility values is frequently observed. This stage seems to correspond to a very heavy and almost continuous grain-boundary precipitation of the brittle θ. When the precipitate has coarsened considerably, brittleness diminishes and, at the point of minimum strength and hardness, the alloy again shows good ductility, the boundary precipitate now consisting of a few discrete, large particles of θ (Plate VI, Fig. 16). As the heat treatment temperature is further increased, to the vicinity of the solvus line, re-solution of the θ phase causes a slight additional increase in ductility and a simultaneous increase in strength.

Aluminum alloys are subject to distortion and residual stresses when quenched in cold water as a result of the temperature gradients developed during cooling. Contraction of the more rapidly cooling surface compresses the interior which plastically deforms to conform to the shrunken exterior. As the center cools to the same temperature as the surface, it attempts to contract, but by this time the surface metal is cold and not very plastic. As a result, it is under an elastic compressive stress, and since the rigidity of the surface prevents the interior from attaining its stable dimensions there is a balancing tensile stress in the central region.[1] To mimimize the distortion and internal stresses resulting from drastic quenches, many alloys are quenched in hot water which cools the metal more slowly and, relatedly, mimimizes the temperature gradients that cause residual stresses. The slower rate of cooling is still rapid enough to retain the solute in a supersaturated matrix solution *except at grain boundaries.*

Grain-boundary precipitation during cooling (or aging) may not adversely affect the mechanical properties attained by the alloy but may have serious consequences on its resistance to corrosion and on the physical properties shown by corroded specimens. A uniform chemical composition throughout the structure generally assures a uniform rate of corrosion which, in aluminum alloys, is quite slow. Alloys of aluminum with 4 to 5 per cent of copper, as quenched in cold water, are substantially in this condition, for if precipitation occurs, it takes place throughout the structure upon the planes of plastic movement during the quenching (see Plate VI, Fig. 15), and as a result, corrosion is uniform. When these alloys are quenched in hot water to avoid distortion and stresses, the subsequent precipitation is concentrated at grain boundaries, with a related concentration gradient of copper from the boundary regions to the remainder of the grains. The boundary area, of purer aluminum (since precipitation of copper is more complete), acts as an anode in an electrolyte, with the large area of the grain acting as a cathode, when this alloy is subjected to corrosion. As a result, the attack is chiefly at grain boundaries and, if the alloy is in relatively thin sheet, as in aircraft structures, it can be seriously embrittled. The difficulty can be overcome by having the alloy coated with pure aluminum, which, by the

[1] KEMPF, HOPKINS, and IVANSO, *Trans. A.I.M.E.*, 111, 158, 1934.

electrolytic effect mentioned above, tends to protect the alloy, even at the edges of the sheet or at regions of cracks or other surface damage.

ENGINEERING APPLICATIONS

Most of the common metals can be improved by age-hardening. A partial list of important alloys of this type would include: Al-Mg, Al-Cu, Al-Cu-Mg-Si, Al-Mg-Si, Cu-Be, Cu-Cr-Si, Cu-Sn-Ni, Cu-Ni-Al (Cu-Co-Si experimental), Pb-Sb, Pb-Ca, Ag-Cu, Ni-Cu-Al, Ni-Cu-Si, Mg-Al, Mg-Al-Zn. Other cases of age-hardening include precious-metal dental alloys of Au-Ag-Cu (Zn) in which platinum or palladium may be substituted in part or in whole for the gold, although all alloys usually contain at least 50 atomic per cent of precious metal. In these alloys of soft elements, strengths up to 175,000 p.s.i. are attained, combined with good ductility. Copper with 2½ per cent beryllium may have its strength increased from 35,000 to 175,000 p.s.i. Iron with 20 per cent cobalt and 20 to 30 per cent tungsten, quenched from 1400°C. and reheated at 700°C., may have a hardness equal to that of high-speed steel and maintain that hardness at 700°C., a temperature which rapidly softens the high-speed steel. Finally, deep drawing steel containing small amounts of carbon, oxygen, and nitrogen may be subject to age-hardening by any, or all three, of these elements. This is a case of an undesirable and unwanted aging effect.

Commercially pure ingot aluminum (2S) is produced with approximately 1 per cent of impurities, chiefly iron and silicon, which are always present in commercial aluminum alloys. Alloys, in the Aluminum Company designations, have a numeral indicating the composition, a suffix *S* signifying wrought material, and another letter designating the temper: *H* for alloys hardenable only by cold work and *O*, *W*, and *T* for heat-treatable wrought alloys, where these letters respectively signify: annealed, quenched from a solution treatment, and quenched and aged to maximum strength.

Commercially pure aluminum (2S) and alloys 3S (1¼ per cent Mn) and 4S (1 per cent Mg, 1¼ per cent Mn) are hardenable only by cold-working, ranging from soft (SO) to rather hard (SH). The alloys exhibit very good corrosion resistance. Typical properties and applications are listed in the "Metals Handbook."

The other wrought alloys are the so-called "strong alloys," containing copper and or magnesium and silicon as hardening agents, in which the optimum properties are developed by heat treatment. These alloys show a range of strength of 48,000 to 65,000 p.s.i. with about 20 per cent elongation in 2 in.

Alloy 17S (4 per cent Cu, 0.5 per cent Mn, 0.5 per cent Mg) is the ordinary Duralumin, available in sheets, plates, tubing, bars, rods, wire, or shapes, and used extensively in the construction of motor coaches, trucks, and aircraft. The magnesium acts in some unknown way to facilitate the precipitation reaction at room temperatures in this alloy after quenching. The element is visible in cast duralumin as a compound, Mg_2Si, which later dissolves in the α_{Al} phase although subsequent precipitation seems to involve the compound Mg_2Al_3. Manganese is present primarily to restrict grain growth during heat treatments. The silicon, present as an impurity in the primary aluminum, is also essential to the development of the best properties in this alloy.

Alloy 24S (4.4 per cent Cu, 1.5 per cent Mg, 0.5 per cent Mn) resembles ordinary Duralumin except for the increased magnesium content. This alloy is considerably stronger than 17S but is also more difficult to fabricate. Extruded and heat-treated rounds have shown tensile strengths of as high as 80,000 p.s.i.

Alloy 25S (4.5 per cent Cu, 0.8 per cent Mn) was developed as a strong alloy that could be more readily forged than the Duralumin types. Not having any magnesium present, it must be aged at an elevated temperature after the solution heat treatment to develop optimum properties.

Alloy 51S (0.6 per cent Mg, 1.0 per cent Si) is the nearest to pure aluminum in composition, corrosion resistance, and plasticity at high temperatures, and yet by a solution heat treatment (dissolving the compound Mg_2Si) and subsequent aging, a strength of about 48,000 p.s.i. may be developed. At high temperatures, this alloy is soft enough to be forged into very intricate shapes.

The Duralumin alloys, 17S and 24S, are available in the form of sheet with a surface coating of pure aluminum (Alclad) which represents about 10 per cent of the cross-sectional area (not counting the zone into which copper and magnesium have diffused, page 84). Alloy 24ST in the Alclad form is the basic alloy for aircraft structures. The aluminum coating prevents inter-

crystalline corrosion, even when the alloy is quenched in hot water. The strength of the composite is only slightly decreased (by about 5 per cent) when loads are uniform across the section, as in direct tension. The strength is more seriously affected by bending stresses, particularly repeated loads such as may be encountered under vibratory conditions, in which the maximum stress comes at the weakest part of the structure, the aluminum surface, and may result in surface shear cracks (Plate VI, Fig. 13). Difficulties on this score, however, have been overcome by design, *e.g.*, the use of channel sections in which the neutral axis is not at the center of the sheet and stresses are completely tensile or compressive across the section involved.

Most of the cast alloys are primarily copper or silicon alloys that are used without any heat treatment. The common alloy for general purposes is the No. 12 alloy, containing 8 per cent of copper. By control of iron and silicon impurities, the sand-casting characteristics may be improved as in the case of alloy No. 112 (7 per cent Cu, 1.7 per cent Zn, 2.0 per cent Si, 1.2 per cent Fe) and No. 212 (7.5 per cent Cu, 1 per cent Si, 1 per cent Fe).

The high-silicon alloys, such as No. 47 or Silumin, have better casting characteristics and corrosion resistance than the copper alloys but should be modified, by sodium treatment or chill-casting, to obtain a finer grain structure and better properties. The 5 per cent silicon alloy, No. 43 or S.A.E. 35, requires no modification treatment and is widely used, particularly for making leak-proof sand castings with excellent corrosion resistance.

The high-silicon alloy is being displaced in this country by sand-cast alloys which may be heat-treated to develop superior mechanical properties, *e.g.*, No. 195. Another alloy which is more difficult to cast but which, upon proper heat treatment, develops the highest strength and hardness among the present casting alloys is No. 220 or S.A.E. 324, containing about 10 per cent magnesium. It is also the lightest available aluminum-base alloy.

Ordinary automobile pistons are usually cast in permanent iron molds of alloy No. 122 (10 per cent Cu, 1 per cent Fe, 0.2 per cent Mg) or more rarely 142 (4 per cent Cu, 1.5 per cent Mg, 2 per cent Ni). These alloys may be heat-treated to develop maximum strength and hardness and then given a "degrowthing" heat treatment in which the metal is heated to slightly above its

operating temperature to insure a stabler precipitate and, therefore, dimensional stability.

A newer alloy, known as LO-EX or No. 132 (13 per cent Si, 1 per cent Cu, 1 per cent Mg, 1.5 per cent Ni) is becoming predominant for piston service. For airplane or Diesel motors, it may be produced in the more expensive wrought form (as 32S) to ensure optimum properties. It may be heat-treated to develop excellent strength and hardness values while retaining a low coefficient of expansion, enabling closer piston fitting in motors. As is true of other high-silicon alloys, machining costs are high, and usually tungsten carbide tools are required.

Aluminum-base die castings are primarily silicon or silicon-copper alloys such as No. 5 (Si, 12.5 per cent), which is resistant to salt-water corrosion and has a tensile strength of about 33,000 p.s.i., or No. 81 (Cu 8 per cent, Si 1.5 per cent) of about the same strength, a cheap general-purpose alloy which has been used in the United States more than any other aluminum die-casting alloy and is generally known as No. 12 (the Stewart Die Casting Corporation's number).

All aluminum alloys may be anodically treated to develop a hard, inert surface oxide coating. On pistons, the increased hardness reduces wear or scuffing. On architectural aluminum spandrels and other exposed surfaces, the oxide coating reduces staining and weathering. On die castings and drawn shapes, the rough oxide provides a base ensuring adherence of lacquers or other colored finishes.

QUESTIONS

1. List the common physical and mechanical properties of commercially pure aluminum.

2. What is the basis of the corrosion resistance of aluminum and its alloys?

3. Give the approximate hardness and tensile properties of Duralumin (17S) as (*a*) annealed, (*b*) heat-treated and aged, (*c*) heat-treated, aged, and cold-rolled.

4. What are the comparative advantages and disadvantages of aluminum copper and aluminum-silicon sand-casting alloys?

5. What is Alclad? What is the basis for its use in aircraft?

6. Compare the tensile strength, elongation, and impact strength of aluminum-base and zinc-base die castings.

7. Plot the hardness data of Table VIII and choose the most desirable aging time and temperature for commercial practice. Justify your choice from the viewpoint of costs, properties, and ease of control.

REFERENCES

"Metals Handbook," sections on Constitution, Properties, etc., of aluminum alloys.

EDWARDS, FRARY, and JEFFRIES, "The Aluminum Industry," McGraw-Hill, 1930.

SACHS and VAN HORN, "Practical Metallurgy," Am. Soc. Metals, 1940 (many references to researches in the field of age-hardening).

CHAPTER VII

PHASE TRANSFORMATIONS: COPPER-ZINC ALLOYS

Copper-zinc alloys or brasses containing up to about 35 per cent zinc are one-phase solid solutions whose structural and property characteristics were described in Chaps. III and IV. The phase transformations occurring with temperature changes in brasses of higher zinc content are of industrial importance in their own right but, furthermore, introduce the subject of transformations in the solid state which are of fundamental significance in studies of the structural features of steels. Only the copper-zinc system will be treated directly, but the principles governing these alloys may be applied to structural studies of copper-tin bronzes or other copper-base alloys.

PHASE DIAGRAM

The solid solubility of zinc in copper follows a course opposite to that shown by age-hardening alloys; it increases with decreasing temperatures from 32.5 per cent at 905°C. to about 38 per cent at 453°C. (see Fig. 8). There is some recent, but inconclusive, evidence that it changes course and decreases below this temperature, but since there is no evidence of age-hardening in 38 per cent zinc brasses after quenching from 450°C. (except in "recovery" anneals of unstable, cold-worked alloys, see page 35), the solubility limit has been indicated by a dashed line in the low-temperature range. The line on the phase diagram showing this solubility limit as a function of temperature is approximately paralleled by another line showing the solubility limit of a solid phase labeled β above 453°C. and β' below this temperature. Between the uniform α solid solution and the β solid solution, there is a field of mixed α and β phases.

The horizontal line bisecting the $\alpha + \beta$ field at 453°C. is dotted to indicate that it is not related to a true phase change and thus need not conform to the phase rule generalization (page 64) of three phases existing in equilibrium at constant temperature. At

this temperature, β becomes unstable and changes to β'. The latter phase has a crystal structure identical to that of its parent, β, a body-centered solid solution, but whereas above 453°C., zinc and copper atoms are dispersed at random on points of the lattice, below 453°C. the copper and zinc atoms tend to occupy specific, fixed positions relative to each other, *e.g.*, copper atoms at the

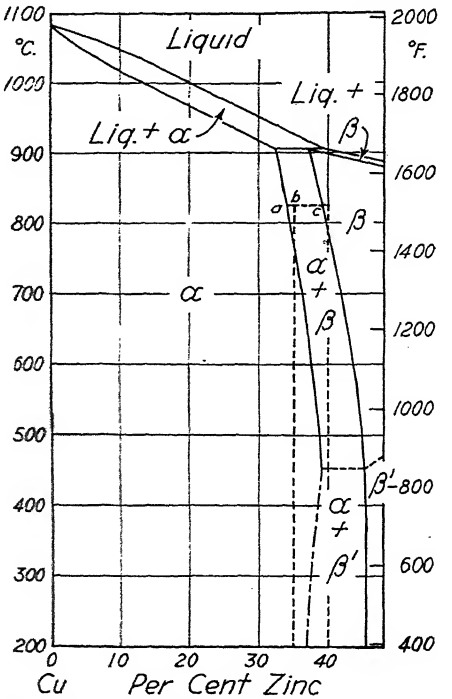

FIG. 8.—Phase diagram of the copper-zinc system, from 0 to 50 per cent zinc.

corners of the unit cubes, zinc atoms at their centers. The latter condition is termed an *ordered* solid solution (see page 58). The ordered structure is one of smaller free energy and therefore of greater stability and, in this case, has considerably different properties from the equivalent "random" solid solution, particularly, much less plasticity.

In liquid alloys containing from 32.5 to 38.5 per cent zinc, the β phase originates at 905°C. with a composition of 37 per cent zinc, as a result of a reaction between α (32.5 per cent Zn) and liquid

(38.5 per cent Zn) written in the form $\alpha + liquid \rightleftharpoons \beta$. It is called a *peritectic*, from the Greek form *peri* which means "around," since, during the reaction, α crystallites will be surrounded by the reaction product, β, which in turn is surrounded by liquid. It is very unusual, however, for a peritectic structure to be visible in the microstructure as such. Consequently, it does not rank in industrial importance with the eutectic. Alloys containing from 50 to 95 per cent zinc contain other phases resulting from peritectic reactions, but these brittle structures are not useful industrially. For this reason only half of the copper-zinc phase diagram, from 0 to 50 per cent zinc, has been reproduced.

An alloy of 65 per cent copper, 35 per cent zinc, under equilibrium conditions, consists of homogeneous grains of α up to about 780°C. Upon heating above this temperature, the alloy enters the two-phase field, $\alpha + \beta$, which means that β crystals of a higher zinc content (about 39 per cent Zn) form with a corresponding decrease in zinc content of the remaining α. On heating to increasingly higher temperatures, the amount of α decreases and that of β increases, as may be quantitatively estimated by use of the lever rule (see page 49). At the same time, the concentration of zinc in both phases changes in accordance with the slope of the phase boundary limits. At 905°C., some α remains

$$\%\ \alpha = \frac{37 - 35}{37 - 32.5}\,(100) = 44\%;\ +56\%\ \beta$$

and, by supplying additional heat, the peritectic decomposition of the β forms more α and some liquid,

$$\%\ \alpha = \frac{38.5 - 35}{38.5 - 32.5}\,(100) = 58\%;\ +42\%\ \text{liquid}$$

All of these changes are reversible under equilibrium conditions as approached by very slow cooling.

The 60 per cent copper, 40 per cent zinc alloy contains some β (or β') at all temperatures; at room temperatures, this amounts to about $[(40 - 38)/(45.5 - 38)]\,(100)$ or 26 per cent, but on heating above 453°C. the proportion of β increases while that of α decreases and the zinc concentration in both phases decreases. At about 780°C., the alloy enters the single β phase field and it will remain a completely β structure up to the temperature of the

solidus line where melting begins in the manner previously described as "burning." Again, these changes are reversible under equilibrium conditions of cooling, or the nearest approach to that almost unattainable state. It is unattainable during a cooling cycle because the diagram requires that, under equilibrium conditions, both the relative amounts of α and β and, simultaneously, their composition (or zinc contents) shall change. This requirement means that zinc and copper atoms must travel continually through the lattice (in opposite directions); not merely at the boundaries of the two phases, but through each large crystallite in order to maintain homogeneity of the phases. The metastable position of the solidus line (page 48) encountered in the simple solid-solution diagram has already been described as originating from incomplete diffusion, or atomic interchange, between two elements in a single phase. In a similar manner, the boundaries of the $\alpha + \beta$ field are subject to displacement to the left under ordinary cooling conditions. Thus the 60:40 alloy, after cooling in air to room temperature, may show considerably more than the calculated 26 per cent of the β' phase. In addition, an alloy of 67.5 per cent copper, 32.5 per cent zinc, which according to the diagram should show no β', will probably contain some on air-cooling relatively small sections.

Since normal cooling rates tend to result in metastable positions of the phase field boundaries of the diagram, very fast cooling rates, by preventing diffusion, may make them appear vertical; *i.e.*, the equilibrium structural condition for a high temperature may be at least partially preserved, by quenching, for observation at room temperature.

An alloy of 62.5 per cent copper and 37.5 per cent zinc is of particular interest in that, under equilibrium conditions, it has a completely β structure at 900°C., and a uniform α structure below about 500°C. Upon extremely slow cooling from 900°C., it will gradually transform to α on passing through the $\alpha + \beta$ field, and this transformation will be of a diffusion type, *i.e.*, accompanied by continual changes in the zinc concentration of the α and β phases. On more rapid cooling to room temperature, there will be some residual β (or β') in a metastable condition, and the amount of β will increase with increase in cooling rate. However, an extremely drastic quench from 900°C. into an iced brine solution results in an entirely different structure. There is no

opportunity for the time-consuming diffusion type of α formation in the temperature range 900 to 500°C., but the unstability of β at the low temperature causes it to transform, at about −14°C., to a face-centered structure similar to α but differing in that one edge of the cube is longer than the other two; it is then called a face-centered tetragonal structure. The high-temperature β and the room-temperature α are of the same composition, and the change from body-centered cubic β to face-centered cubic α requires only a slight contraction of the lattice in two directions and an expansion in the third. If the dimensional readjustment is incomplete (because of lattice rigidity at low temperatures), the intermediate, unstable tetragonal lattice is found.

The atomic adjustments required may be visualized by reference to the sketch of Fig. 9 showing four unit body-centered cubic cells, *i.e.*, four cells of the β structure, drawn in light lines. The

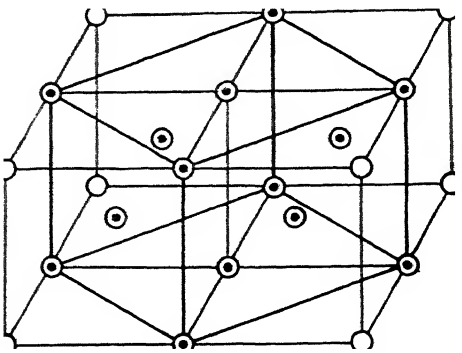

FIG. 9.—Four unit cells of the body-centered cubic structure (β) with specific atoms marked with black centers to indicate the structure might also be considered as face-centered tetragonal.

face diagonal of each cube on the top and bottom of the structure, with connecting vertical lines, will be found to outline a tetragonal structure where the length of the side of the base (face diagonal of the cube) is $\sqrt{2}$ times the height of the tetragon. Furthermore, the body-centered atoms of each of the four β cubes may also be considered as centered in the four side faces of the tetragon, while the top and bottom shared corner atoms of the cubes may be considered as centered in the top and bottom faces of the tetragon (the atoms which make up the tetragonal structure are shown with black centers). Thus a body-centered cubic structure may

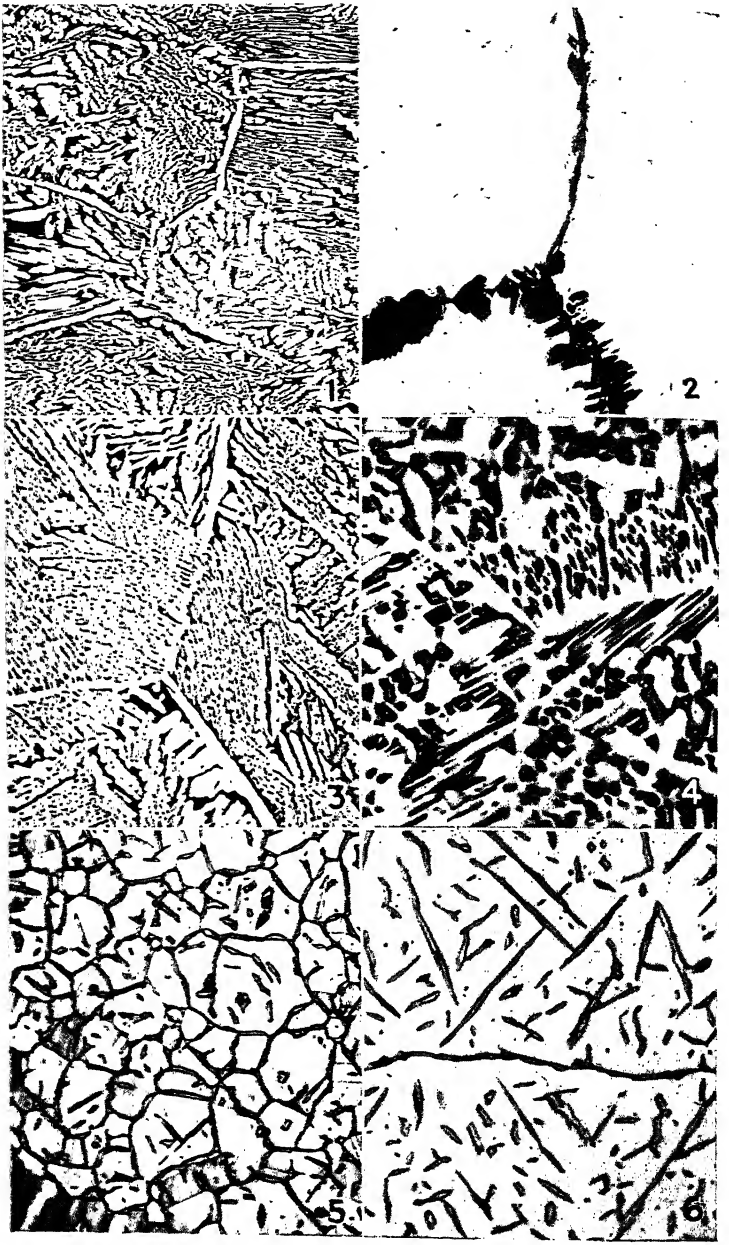

PLATE VII.

be considered as a face-centered tetragonal structure; it is merely customary to designate it by its more symmetrical form (see page 14).

The diffusionless transformation of the 62.5:37.5 brass is of no commercial importance since the requirement of heating to within a few degrees of the melting point gives very coarse grains and the drastic quench required can only be attained in relatively thin metal sections. However, the structure and its origin are quite similar to the martensitic structure of steels (page 145) which is of paramount industrial importance.

MICROSTRUCTURES (PLATE VII)

Plate VII. Fig. 1. Extruded and air-cooled section of 60 per cent Cu, 40 per cent Zn alloy (Muntz metal); ×50; $FeCl_3$ etch (black phase is β'). At the extrusion temperature, the alloy was completely β and, upon deformation and cooling, α (white) formed in the β structure, first at the β grain boundaries and then inside the β grains. The α formation at the β boundaries indicates the size of the β grains at the high temperature; parts of about six of the *former* β grains are visible. The α crystals, during initial formation in the β structure, must have their atoms in conformity with atoms of the β crystals. This is a general rule for the formation of any new solid phase in a solid matrix of different crystal structure (*cf.* precipitation of θ_{CuAl_2} from $\alpha_{(Al)}$ during age-hardening, page 77).

Usually, only one type of plane of the matrix and one type of plane of the new phase have atoms in a similar pattern when compared in a specific direction. For example, Fig. 9 shows that the base plane of the face-centered tetragon (cube plane when it shifts to face-centered cubic α) matches the cube plane of the body-centered cubic β when the edge of the base of the tetragon is in the direction of the face diagonal of the body-centered cube. This conformity results in an alignment of the new phase, α, in only certain planar directions of the β phase. Sometimes these planes are clearly outlined by the new phase, and the structure may then be said to show a *Widmanstätten pattern*,[1] as is evident

[1] The orientation of the lattice in a new phase, forming from a parent solid phase, is related crystallographically to the lattice of the parent phase. On a polished and etched surface, the traces of the plates, needles, or polyhedra of the new structure exhibit a geometrical pattern. Familiarly seen in cast

here to some extent. Frequently, later growth stages of the new phase may form an equiaxed shape which obscures its crystallographic relationship to the matrix.

Plate VII, Fig. 2. The same Muntz metal quenched (in a $\frac{1}{8}$-in. thick section) in water from 825°C.; ×50; etched with NH_4OH-H_2O_2 so that α is dark and β' light (colors reversed from previous specimen). At the high temperature, this structure was completely β (see phase diagram). The quench preserved most of the β but did not suppress completely the formation of α, particularly at the β grain boundaries. Note the directional character of the α forming as plates extending from the boundary into the β' grains (a Widmanstätten characteristic). The relationship is also shown by a few, very small, isolated platelets of α within the β' grains. The β grain size is very coarse, as a result of grain growth in the single-phase range, 780° to 825°C.; it was difficult to find sections showing as many as three grains for this micrograph.

Plate VII, Fig. 3. Same specimen as above (quenched from 825°) after reheating 1 hr. at 450°C.; ×50; etched with $FeCl_3$ (colors again reversed so that α is light and β' dark). The unstable β' of the quenched alloy changed over to α upon heating in the low-temperature range, resulting in the attainment of approximately equilibrium proportions of the two phases. The initial platelets of α at the grain boundaries have grown further into the former β grains, and their shape, as plates, is still evident by the shape of residual β crystallites between the α plates. The very small plates or needles of α visible in Plate VII, Fig. 2, have grown in a similar manner so that the quenched and annealed structure resembles that of the extruded stock (Plate VII, Fig. 1).

Plate VII, Fig. 4. A different 60:40 Cu-Zn alloy quenched from 825°C. and reheated at 500°C.; ×200, $FeCl_3$ etch. This structure differs from Plate VII, Fig. 3, in that while α crystals initially grew in a needlelike structure from the β grain boundaries, at a later stage, the α formed in more or less equiaxed shapes and the residual β' crystallites do not show any crystallographic pattern or relationship of origin. This is frequently although not universally true: that the new phase formed at a

steel or overheated wrought steel but a possibility in any alloy subject to a phase change in the solid state. ("Metals Handbook.")

high temperature under equilibrium cooling conditions will show a crystallographic pattern while that formed by annealing a quenched metastable structure is equiaxed (*cf.* carbide structures from various heat treatment of steels, page 153). Almost always, however, it is fairly easy to distinguish between structures formed at high or low temperatures. Note the twin bands, faintly visible, in the α crystals of this structure, formed as a result of strain accompanying the transformation.

Plate VII, Fig. 5. Worked and annealed 65 per cent Cu, 35 per cent Zn alloy (common high brass) quenched from 825°C.; ×50; ammonium persulphate etch. As ordinarily worked and annealed, this brass will have a uniform α structure showing annealing twins and a grain size characteristic of the specific rolling and annealing schedule. However, upon heating to 825°C., it enters the $\alpha + \beta$ field (see phase diagram). The new phase, β, forms predominantly at the α grain boundaries and, to a somewhat lesser extent, within the α grains. That forming inside the grains shows the crystallographic relationship required of β forming in α; the β is in lens-shaped plates on specific crystal planes of the α. Quenching from the high temperature has preserved most of the β as β'.

Plate VII, Fig. 6. A cast 65:35 brass quenched from 825°C.; ×50; ammonia peroxide etch. The very coarse-grained cast structure shows no twins, but the Widmanstätten pattern of β' platelets in two grains of α is beautifully illustrated.

PROPERTIES

The mechanical properties of brass specimens with the microstructures shown here can be qualitatively estimated on the basis that α is rather soft and plastic, particularly when moderately coarse grained, that β' is a rather hard and brittle phase, and that the *continuous* phase will have an effect out of proportion to the relative amount present. Instead of discussing properties of the individual specimens, data pertaining to corresponding structures are reproduced in Table IX, as typical of the properties developed upon heat treatment of small sections.

Annealing the 60:40 brass at low temperatures following the 825°C. quench results in an increase in hardness. At first it might seem anomalous for this alloy to become harder as the amount of the soft α phase increases. However, when the α

TABLE IX

Heat treatment	60 : 40 Brass (arsenical)	65 : 35 Brass		
	Rockwell E hardness ⅛ in., 100 kg.	Rockwell E	Tensile strength	Per cent elongation in 2 in.
Quenched 650° (10 min.)	76	32	44,000	64
Quenched 700 (10 min.)	83	27	43,000	67
Quenched 760 (10 min.)	86	23	42,000	70
Quenched 825 (10 min.)	93	40	50,000	52
Quenched 825° + 250° (60 min.)	106	38	49,000	58
Quenched 825 + 325 (60 min.)	100	34	47,000	62
Quenched 825 + 400 (60 min.)	93	30	45,000	65
Quenched 825 + 450 (60 min.)	85	27	44,000	67
Quenched 825 + 500 (60 min.)	79	24	43,000	69

forms at very low temperatures in a very disperse form, it causes precipitation hardening of the β' matrix. There is a continual decrease in hardness as the α particles increase in size. Low-temperature annealing of the 65:35 brass, quenched from 825°C., is accompanied by a gradual decrease in the amount of β' although minute amounts are still present after the 500°C. anneal. The properties change more rapidly than the change in the amount of β present because these anneals first tend to interrupt the continuity of the β network (*cf.* Plate VII, Fig. 5) while longer times or higher temperatures are required to eliminate completely the disperse β' particles.

ENGINEERING APPLICATIONS

Although face-centered cubic α brass is considerably softer and more plastic than the ordered body-centered β' at temperatures up to about 450°C., at very high temperatures, the β structure is much more plastic than the α and is, therefore, preferred for hot-working. If up to 3 per cent lead is added for machinability, it is present as insoluble globules and, presumably, as a result of the change of crystal structure of the 60:40 brass with temperature, the lead does not impair hot-working properties. In α brass, however, as little as about 0.04 per cent lead will make the metal hot-short since it is present as an intercrystalline film in the cast billet

The many other alloys of copper cannot be discussed in detail but, for binary alloys at least, the phase diagrams and property data in the "Metals Handbook," together with a knowledge of the metallurgical principles covered in this and preceding sections, make it possible to visualize probable structures and the effect of variations in casting, working, and heat treatment on mechanical properties.

Brass screws and various small fittings machined from rod in high-speed automatic machines are usually of Muntz metal (60:40) containing several per cent of lead. For hot forgings, a similar alloy is employed although the lead content will be somewhat lower and the copper content a little higher—chiefly to ensure better ductility at room temperatures while retaining hot-working properties and machinability. If higher strength is desired, Muntz metal is alloyed with 1 per cent tin (Naval brass). The regular hot-forging grade may show 45,000 p.s.i. tensile strength, 18,000 p.s.i. yield strength, and 25 per cent elongation, while the Naval brass will run about 54,000 p.s.i. tensile, 22,000 p.s.i. yield strength, and 25 per cent elongation.

For still higher strength in brass mill products, a 10 per cent aluminum bronze or the newer silicon bronzes are available. The aluminum bronze may be quenched from an elevated temperature and reheated at a low temperature, with an accompanying change of properties as follows: tensile strength increased from 65,000 to 80,000 p.s.i., yield strength increased from 25,000 to 50,000 p.s.i., elongation decreased from 15 to 4 per cent.

Brass for extensive cold-drawing operations must have an entirely α structure. The properties of the α structure from 0 to 38 per cent zinc do not change linearly nor even follow a smooth curve, as was shown by Table VI in Chap. IV; the 70:30 alloy, cartridge brass, shows slightly higher strength than the 65:35 alloy, common high brass. Low or red brass, 15 to 20 per cent zinc, contains enough copper to give the alloy a red tint and is used where color, freedom from stress corrosion or season cracking, and superior corrosion resistance are factors of sufficient importance to justify the higher cost. Commercial bronze, an alloy of copper with 10 per cent zinc, has a bronze color and is widely used, together with the 95:5 alloy, in applications for which the color, softness, or corrosion resistance of the metal is suited.

Pipes and tubes are made of various copper-zinc compositions: Muntz metal, high brass, or red brass according to requirements, mainly in the direction of corrosion resistance. Red brass is generally best for water conduction, particularly if dezincification (removal of zinc from surface), or pitting, are likely to be encountered from hot, impure waters. Condenser tubes may be made from Muntz metal, cartridge brass, the same 70:30 alloy with 1 per cent tin replacing a similar amount of zinc (admiralty metal), or 70:30 with 1 to 2 per cent aluminum replacing part of the zinc. The tin or aluminum remains in solid solution and does not significantly affect the appearance or microstructure of the alloy but does noticeably improve its corrosion resistance, and aids in obtaining a finer grain and immunity from season cracking. The 80:20 and 70:30 cupro-nickels are superior to any of the brasses in respect to corrosion resistance and strength, and are particularly important for marine condenser service (page 59).

QUESTIONS

1. What would be the relative advantages and disadvantages in the use of 60:40 or 70:30 brass for (*a*) cartridge cases (*b*) large forgings.
2. Describe two methods of varying the relative amounts of α and β phases in a 60:40 brass by heat treatment.
3. Why should 64:36 brasses be slowly cooled from a high temperature? If cooled too rapidly, how may the condition be remedied?
4. Explain the course of the hardness vs. temperature data for the 65:35 brasses and the 60:40 brasses, as quenched from 650° to 825°C. (Table IX).
5. How does lead function to increase the machinability of Muntz metal?
6. What is the maximum copper content brass alloy that will develop some β constituent upon annealing at very high temperatures (consult phase diagram)?
7. How can β' be distinguished from α in a duplex structure of the two constituents?

REFERENCES

"Metals Handbook," section on Copper—Constitution and Properties of Copper Alloys.

CHAPTER VIII

IRON-CARBON ALLOYS: NORMALIZED AND ANNEALED STEELS

Commercial steels are never binary alloys of iron and carbon, for manganese, silicon, sulphur and phosphorus are always present in the iron-carbon alloy, as produced from pig iron by any of the industrial refining processes. Plain carbon steels, produced in the open-hearth furnace using from 25 to 50 per cent scrap metal, may also contain residual elements such as copper, nickel, chromium, and tin, to name but a few, in amounts up to 0.1 per cent. All of these elements will affect some property of the steel but, in general, the effects are small. The iron-carbon phase diagram is not noticeably changed by the presence of any of these residual impurities, or addition agents, such as manganese or silicon, in the amounts usually found in carbon steels. Modifications in the diagram, in the properties of steels, or in their response to heat treatment, as affected by larger additions of other elements, will be discussed in later sections.

PHASE DIAGRAM

The phase diagram, Fig. 10, has been reproduced with the carbon-concentration scale plotted so as to expand the area including commercial steels, 0 to 1.4 per cent carbon, and compress the area of cast irons, 2. to 4. per cent carbon, in which the exact carbon content is of lesser importance. The basis of the differentiation between steels and cast irons is found in the phase diagram and may be expressed in two ways. From a practical standpoint, steels have such a high melting point (above 1440°C.) that special and expensive equipment is required to melt them, whereas cast irons melt at 1350°C. or less, a temperature much more readily attained with inexpensive equipment. However, since the decrease in melting point (or liquidus temperature) with increase of carbon content is continuous from 1525 to 1142°C., this reasoning, while of practical importance, leads to no specific

demarcation limit. A second means of distinguishing between the two classes of materials is on the basis of structure and properties; iron containing up to 1.7 per cent carbon[1] can be heated to a temperature at which it will show only one phase,

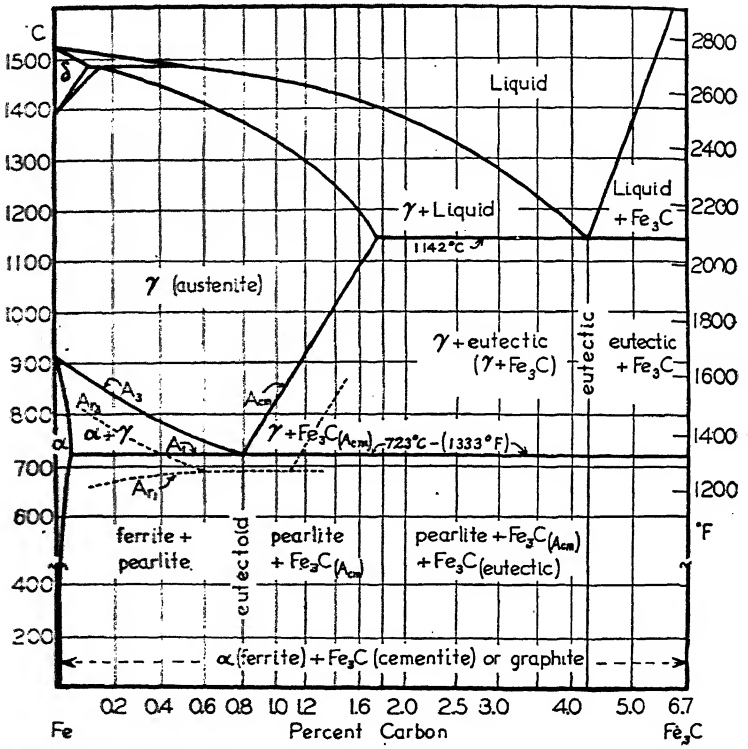

FIG. 10.—Phase diagram of the iron-iron carbide (metastable) alloy system.

face-centered cubic γ, while alloys containing more than 1.7 per cent carbon always contain γ + Fe_3C eutectic structure. The eutectic has some 50 per cent by weight (more by volume) of the brittle Fe_3C phase which tends to be continuous, and thus alloys

[1] Recent work by Gurry (*Metals Tech.*, 9, April, 1942) indicates that the A_{cm} line of Fig. 10 may be incorrect. The saturation solubility limit of carbide in austenite at the eutectic temperature, universally accepted as 1.7 per cent carbon for many years, appears to be about 2.0 per cent carbon. The low value ordinarily obtained is a result of incomplete homogenization of austenite (see p. 139, or compare with the general effect of a metastable solidus in eutectic systems, p. 66).

above 1.7 per cent carbon, containing eutectic at all temperatures, are somewhat brittle. The eutectic in alloys of less than 1.7 per cent carbon, resulting from undercooling, can be dissolved in γ which, being face-centered cubic, is plastic. This distinction, that steels can be hot-rolled and cast irons can not, is not absolutely clear-cut, however nicely it ties up with the phase diagram. For example, cast irons (white) of about 2.25 per cent carbon, which contain only 20 per cent of the eutectic and 80 per cent of the γ phase at about 1100°C., can be hot-rolled if the initial soaking at the high temperature before rolling is effective in breaking the continuity of the carbide in the eutectic (by agglomeration, see page 166), and if the initial breakdown passes are moderate. Alloys in the range from 1.5 to 2.5 per cent carbon, then, are intermediate between steels and cast irons. This should not lead to their being termed semisteels (page 203) for the reason that the latter designation has been used for such a wide variety of iron-carbon alloys that it has become practically meaningless.

The phase diagram shows three horizontal lines, each representing a reaction involving three phases and occurring at a constant temperature. The reactions may be represented as

(1) At 1490°C., δ (0.08% C) + liquid (0.55% C) $\rightleftarrows$ γ (0.18% C)
(2) At 1142°C., Liquid (4.3% C) $\rightleftarrows$ γ (1.7% C) + Fe_3C (6.7% C)
(3) At 723°C., γ (0.80% C) $\rightleftarrows$ α (0.034% C) + Fe_3C (6.7% C).

The solidification process, through the peritectic range (0.1 to 0.5 per cent C), solid-solution range (0.5 to 1.7 per cent C), or hypoeutectic range (1.7 to 4.3 per cent C) of carbon content, proceeds as it does in any alloy system showing comparable conditions. For example, an alloy of iron and 1.2 per cent carbon upon cooling from the liquid state to 723°C. behaves exactly like an aluminum, 4 per cent copper alloy; solidifies in the form of a solid solution, γ, and, as this cools past the line marked A_{cm}, the decrease of solubility of Fe_3C causes the carbide phase to precipitate from solid solution in γ which correspondingly becomes depleted in carbon. The carbide precipitation occurs chiefly at the γ grain boundaries, although, if a large amount of Fe_3C must separate, it forms Widmanstätten plates within the grains. When the γ phase reaches a carbon content of 0.80 per cent at 723°C. (under equilibrium conditions), reaction (3) occurs. This reaction is missing from the aluminum-copper diagram although,

again, the construction of the phase diagram is identical if the γ field is taken to represent liquid alloys. Because of the essential similarity of reaction (3) to the eutectic (2), the former is known as an eutect*oid*. Whereas an eutectic represents the formation of a mechanical dispersion of two new solid phases, here $\gamma + Fe_3C$, from a liquid, a eutectoid represents the formation of a dispersion of two new solid phases, $\alpha + Fe_3C$, from a solid, γ. In both cases, the two-phase dispersed structure has a distinctive appearance as compared with either phase which may have formed in a different manner.

The term hypoeutectoid has the same significance as hypoeutectic. On cooling a 0.4 per cent carbon steel past the line equivalent to the liquidus in eutectics, here called the A_3 line, crystals of α begin to form at the γ grain boundaries and continue forming until, at 723°C., they represent $(0.80 - 0.40)/0.76 = 53$ per cent of the structure (under equilibrium conditions), after which the residual γ of 0.80 per cent carbon content goes through the eutectoid reaction. Hypereutectoid alloys behave in an identical manner, except that the phase separating from γ at its grain boundaries is Fe_3C.

Note that the solubility of Fe_3C in the α phase decreases from 0.04 per cent carbon at 723°C. to about 0.007 per cent at room temperatures. This indicates that low-carbon alloys are susceptible to age-hardening when cooled rapidly from the vicinity of the eutectoid temperature (page 92), an effect known as *quench-aging*.

TERMINOLOGY

The iron-carbon diagram was one of the first metallic systems to be studied, and this fact, plus the predominant commercial production and use of steels among all alloys, has led to the application of special names for phases and structures, in addition to the basic Greek-letter designations. The common ones are:

γ = *austenite*, the face-centered cubic structure which can dissolve up to 1.7 (or perhaps 2.0) per cent carbon at 1142°C.

α = *ferrite*, body-centered cubic iron dissolving a maximum of 0.04 per cent carbon at 723°C.

Fe_3C = *cementite* = iron carbide or simply "carbide."

$\gamma + Fe_3C$ = *eutectic* = ledeburite (see cast irons, page 195).

$\alpha + Fe_3C$ = *eutectoid* = pearlite, the distinctive two-phase structure, formed from 0.8 per cent carbon austenite on slow cooling past 723°C.

and sulphur than basic open-hearth grades. In addition to this difference in the content of normally reported impurities, phosphorus and sulphur, the three major types of steel can be differentiated by the concentration of an impurity not usually determined analytically, *i.e.*, oxygen, present in the combined form as an oxide. Naturally, the oxygen content will vary inversely with the carbon content, no matter how the steel is produced. By processes, however, the degree of oxidation of the liquid steel and, relatedly, the amount of residual oxides in the final product, will decrease in this order: acid Bessemer (high), basic open-hearth, and basic electric (low by reason of the finishing slag). A description of the skill and knowledge required to control the form, size, and dispersion of the solid oxide in the final steel is beyond the scope of this book, but the importance of this final form is paramount in many applications. Oxides or oxide mixtures (FeO, MnO, and SiO_2) with relatively low melting points are certain to segregate at the original austenitic grain boundaries of the cast metal and, if present in any considerable amount, impair the impact properties (see page 131). The same effect is true for sulphides or oxysulphides, both brittle compounds. The amount of oxides in the finished steel depends not only on the steelmaking process, but also on the operating conditions for a given process. The physical form in which oxygen is present may vary in carbon or alloy steels according to its chemical form, *i.e.*, whether present as FeO and MnO, SiO_2, Cr_2O_3, Al_2O_3, TiO_2, or Zr_2O_3. Combinations of oxides forming low-melting-point constituents, particularly of an acid (SiO_2) and base (FeO), tend to agglomerate and form large "inclusions" while the highest melting-point oxides (Al, Ti, and Zr oxides) solidify while the steel is liquid and are ultimately dispersed in the much less objectionable, or, in respect to grain size, beneficial, form of very fine particles.

The size, amount, and dispersion of oxides (or sulphides) affect mechanical properties as previously mentioned. For example, bending properties may be adversely affected when the bending axis is parallel to elongated stringers of inclusions (bending with the "fiber"). In addition, the welding characteristics of a steel are markedly affected. Bessemer steel strip (skelp) welds much better than an equivalent open-hearth grade in pipe making by lap and butt welding, although it is not certain whether this is due to low-melting-point inclusions or some other characteristic. On

the other hand, an unusually high oxide content in high-quality electric steel used for making aircraft propellers by welding may cause defects in the weld deposit as a result of the reaction between carbon and oxides in the liquid weld metal. Finally, a critical dispersion of very small oxide particles may inhibit grain growth in the austenitic state and considerably raise the temperature at which coarsening begins. Thus, when dispersed aluminum, titanium, or zirconium oxides are formed by additions of one of these elements to the liquid steel containing dissolved oxygen as FeO, the final solid steel is usually fine grained. This condition is of importance in carburizing at high temperatures (page 121) or in attaining improved physical properties in either carbon or low-alloy structural steels (page 136).

GRAIN REFINEMENT OF STEELS

Once a steel is in the solid form, the grain-size factors discussed in Chap. III become operative. The effect of oxide inclusions was covered in a general manner by stating that insoluble phases seemed to retard grain growth. Upon heating steels to temperatures below the A_{c_1} line, the ferrite grain size may be increased, although this is noticeable only in relatively low-carbon steels (under about 0.30 per cent carbon) since the pearlitic areas of higher carbon steels interfere with boundary movements.

Heating above the A_{c_1} line causes the ferrite and carbide phases to go through the eutectoid reaction and form austenite. At the A_{c_1} temperature, austenite of eutectoid carbon content forms in the pearlite. Several austenite grains may be formed in each pearlitic area and the number formed is determined by the degree of overheating. Rapid heating through the A_{c_1} temperature results in more austenite nuclei and thus smaller austenitic grains when all the pearlite has subsequently disappeared. This effect is complementary to that generally observed, since rapid cooling encourages greater nucleation and a finer grain. In a hypoeutectoid steel, heating just above the A_{c_1} line merely forms austenite in the pearlite areas while the ferrite grains remain in an amount determined by the carbon content. The ferrite grains may grow in size at each other's expense in zones of mutual contact, and since this phase is stable down to room temperatures, the ferrite will not be affected if the steel is now cooled below the

A_{c_3}. To change the ferrite grain size and distribution, it is necessary to continue heating the steel past the A_{c_3} temperature, thus forcing the austenite grains to absorb the ferrite. The initial austenitic grain size achieved upon heating above the upper critical temperature (A_{c_3}) is, then, a function of the amount of carbon present, which determines the amount of pearlite areas in which the austenite forms, the size of the ferrite and pearlite areas originally present in the steel, and the rate of heating through the critical temperatures. Once in the one-phase γ field, grain growth may result in coarsening the austenite grains, and it is in this range of heating that oxide inclusions affect the grain size resulting from heating to specific temperatures.

When the steel is cooled below the A_{r_3} temperature, ferrite crystals start to form at the austenitic grain boundaries. As cooling continues to the A_{r_2}, the first ferrite crystals grow and more form, chiefly at the grain boundaries of the γ phase, although in low-carbon steel some form within the γ grains. At the A_{r_1} line, the steel consists of austenite crystals surrounded by ferrite crystals. These latter are unaffected by the eutectoid reaction, during which the austenite transforms to pearlite. The ferrite grain size consequently is determined by (1) the austenitic grain size from which it originated (fine-grained austenite has more boundaries, thus more sites for nuclei), and (2) the cooling rate, specifically from the A_{r_3} to the A_{r_1}. For optimum grain refinement, the steel should be heated to just above the A_{c_3} and then cooled as rapidly as the section size or hardness and residual stress specifications (see page 150) permit. However, since an initially very coarse structure would still not give as fine-grained a structure as a less coarse one, a repetition of this treatment can result in further refinement. The high temperature, above the A_{c_3}, to which the steel must be heated, sets a minimum for the attainable grain size, usually met upon a second treatment.

Hot-forging is a general term applied to the hot-working of metals by means for forging machines, hammers, and presses. Steel ingots may be forged with the object of improving the structure and properties of the ingot for subsequent working; the

[1] These designations were defined on p. 113 as lines on the phase diagram, but they are usually employed to designate a specific temperature whose value may be a function of the carbon content or heating and cooling conditions.

forging at elevated temperatures promotes diffusional activities, thereby favoring chemical homogeneity, refines the grain, and, in certain highly alloyed steels, is effective in destroying the continuity of troublesome carbide segregates. Forging is also an important process for converting a block of metal to the approximate dimensions of a finished article, and forgings, in many cases are competitive with castings. The direction of flow of the metal during forging to a specific shape is of considerable importance since the physical properties of the final product are noticeably better in a direction parallel to that of flow than they are in a transverse direction. This "fiber" effect may result from alignment of oxide inclusions in the direction of flow or from an alignment of segregated areas of incompletely homogenized austenite.

When steel is being hot-worked in the austenitic range, the deformation may give a finer γ grain size than would be attained otherwise, particularly if the steel is deformed at a temperature within the critical range (A_{r_3} to A_{r_1}). The ferrite forming in a deformed austenite has a considerably higher degree of nucleation, *i.e.*, many more sites at which to originate and, subsequently, the ferrite grains are also deformed and spontaneously recrystallized. Thus a very much finer ferrite grain size is attainable than that achieved by purely thermal treatments. If the "hot" working is continued below the A_{r_1}, however, the time and temperature relationships may not result in recrystallization of the ferrite, and the deformation then is in reality cold-working. After forming, the forging may be heat-treated to produce the desired structures and properties by treatments essentially the same as those applied to castings of the same composition.

MICROSTRUCTURES (PLATE IX)

Plate IX, Fig. 1. Section from an I beam; ×100; Nital etch. The structure represents ferrite, with a moderately fine grain size, and pearlite in an amount which might represent about 0.15 per cent carbon. The actual ferrite grain size in any of the common structural steels is chiefly determined by the finishing temperature of the hot-rolling process and by the size of the finished section or, more fundamentally, by the cooling rate through the critical range. An analysis of this steel shows a manganese content of about 0.40 per cent and a silicon content of 0.15. Its mechanical properties are: yield point, 40,000 p.s.i.; tensile strength, 60,000

p.s.i.; elongation, 35 per cent (2 in.), and reduction in area, 62 per cent.

Plate IX, Fig. 2. Section from a low-alloy, high-strength structural steel (see page 136); ×100; Nital etch. The analysis of this steel (0.13 per cent C, 0.70 per cent Mn, 0.80 per cent Si, 0.23 per cent Cu, 0.60 per cent Cr, 0.15 per cent Ni, 0.10 per cent Mo, 0.12 per cent Zr) accounts for the fine grain size of the ferrite, particularly the zirconium employed to deoxidize the liquid steel. Its strength properties in an I beam (Plate X, Fig. 1), would be yield point, 56,000 p.s.i.; tensile strength, 78,000 p.s.i.; elongation, 36 per cent (2 in.); reduction in area, 72 per cent.

Plate IX, Fig. 3. Section from alloy structural steel (railway generator shaft) containing 1.25 per cent Mn and 0.10 per cent V; ×100; Nital etch. The alloying elements, particularly vanadium, have made this steel very fine grained, a desirable condition for its particular service. The carbon content appears to be about 0.40 per cent but is actually only about 0.30 per cent. The smaller amount of ferrite is partly a result of a rapid cooling rate through the critical temperature and partly a result of the lower equilibrium carbon content of the eutectoid when the manganese content is raised. Thus with 1.25 per cent manganese, the equilibrium concentration of the eutectoid is displaced from 0.80 to 0.72 per cent carbon.

The structure of the rod is not uniform in respect to ferrite; some areas contain more ferrite and less pearlite than others. The high- and low-ferrite areas are both parallel to the rolling direction. The resulting *banded* structure is frequently encountered in steels. It is related to a segregation of certain elements in the original ingot that is not removed during hot-working. Areas of austenite high in phosphorus are elongated into bands parallel to the rolling direction. Since phosphorus raises the critical points, specifically, the A_{r_3} temperature, ferrite starts forming first in areas high in phosphorus, and this tends to displace carbon toward adjacent areas. The final result is a banded structure having a nonuniform distribution of ferrite and pearlite with respect to the rolling direction. Phosphorus is not the only element that can produce this effect; any nonuniformity of composition of the austenite may cause it to some degree. If carbon were segregated (this generally would occur only by surface decarburization since carbon diffuses readily in austenite), areas

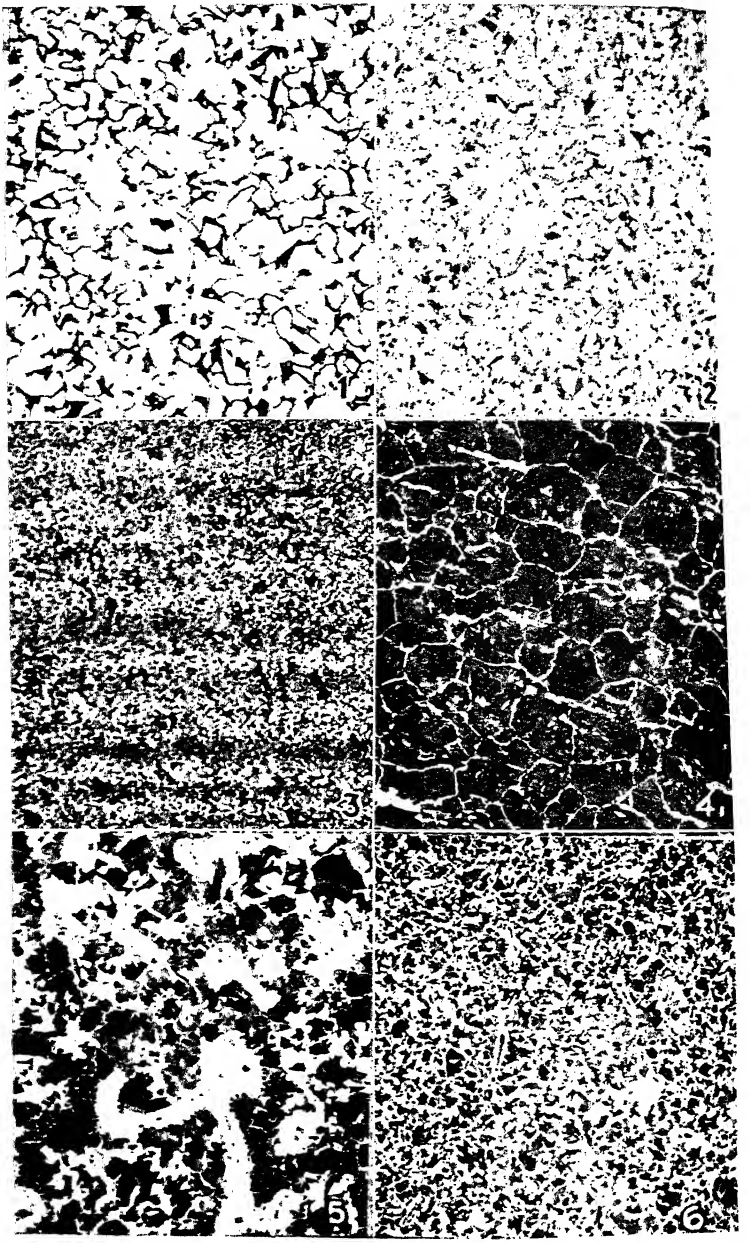

PLATE IX.

low in carbon would start to transform first, since the A_3 increases with decrease in carbon content. As ferrite formed, it would displace the carbon originally present in the area where it was growing toward the adjacent austenite. If manganese were segregated, ferrite would start forming first in areas low in manganese, since this element depresses the A_{r_3}, and again banding would result.

Plate IX, Fig. 4. Section from a steel rail; ×100; Nital etch. Rails require greater strength and hardness than ordinary structural steels and are generally made of steels approaching the eutectoid in carbon content. This particular rail appears to contain about 0.75 per cent carbon, although actually somewhat less than that is present (0.68 per cent); the abnormally small amount of ferrite resulted from fairly rapid cooling in air with a related depression of the A_{r_3} temperature (page 140). There are a few elongated streaks of ferrite not completely confined to an austenitic grain boundary. These show the direction of rolling of the rail and are related to phosphorus segregation as in the banded structure of the manganese-vanadium steel. Some of the ferrite bands show elongated nonmetallic inclusions of either sulphides or oxides (of a darker color than the ferrite).

Plate IX, Fig. 5. Section from a large steel casting; ×50; Nital etch. This structure represents *a defective casting*, not one found in good cast steels. It contains about 0.35 per cent carbon and has probably been given one heat treatment, since in some areas a moderately fine-grained ferrite and pearlite structure is visible. However, other areas have large aggregates of ferrite and, in the midst of these, a string of small globules is visible. At one point, there is an eutectic-appearing mixture of particles at the intersection of three former austenitic grains. These are oxysulphide inclusions which formed in the last part of the structure to freeze, the austenitic boundaries. The large sections of ferrite probably resulted from phosphorus segregation in the same, last-freezing areas. The appearance of ferrite inside the former austenite grains suggests that one heat treatment, an inadequate one, was given the casting. The gross ferrite areas cause this steel to have poor strength properties while inclusions at the original austenitic grain boundaries are conducive to poor impact and fatigue strength.

Plate IX, Fig. 6. Same casting as Fig. 5 after double heat treatment; ×50; Nital etch. The poor structure has been elimi-

nated by a double anneal. First, the steel was heated 200°F. above the A_{c_3}, to 1750°F. (950°C.), and held for 2 hr. to homogenize the austenite. After furnace cooling, the structure was uniform but not particularly fine grained because of coarseness of the high-temperature austenite grains. The steel was then reheated to about 25°F. above the A_{c_3}, held only long enough to ensure completely austenitizing the structure, and subsequently air-cooled. The final structure is uniformly fine-grained and would show good strength. However, the distribution of inclusions has not been changed; they are not readily visible now but still retain an envelope type of dispersion. While the resistance to impact stresses and the fatigue strength of this structure are superior to the values shown by the original steel, they are inferior to those of good castings. The form of the inclusions can be changed only by modifying the original melting, deoxidizing, and casting procedure. For example, the addition of an element which would raise the freezing point of the inclusions and cause them to solidify before the steel, would produce a uniform rather than intergranular dispersion.

PROPERTIES AND ALLOYING EFFECTS

Most common structural grades of carbon or low-alloy steels are used in the hot-rolled condition, for heat treatment of long sections is difficult and expensive. The effect of carbon content and of finishing temperature on the amount of pearlite and the ferrite grain size has already been discussed, as well as many of the other variables relating to these two structural conditions which determine the strength properties. Steel castings, after being heat-treated for grain refinement of their structures, resemble structural steels, of comparable analyses, in most properties.

When cost considerations permit, other elements may be added to the carbon steels, or the usual small amounts of elements such as manganese or silicon may be increased sufficiently to noticeably alter the normal mechanical properties obtained with a specific carbon content. This in effect comprises the usual definition of an alloy steel. Alloying elements in structural or cast steels, not heat-treated for any purpose other than grain refinement, generally are elements that strengthen the metal by entering into solid solution in the ferrite, thus giving a normal solid-solution strengthening effect. Nickel and silicon both fall into

this classification. Manganese partly dissolves in ferrite and partly enters the carbide, displacing some of the iron to form $(Fe - Mn)_3C$. All these elements, but particularly manganese, also act to strengthen the steel by decreasing the carbon content of the eutectoid, which causes a given carbon concentration to result in more pearlite and less ferrite.

Some elements, such as chromium, molybdenum, and vanadium, enter almost entirely in the carbide phase. Their strong carbide-forming tendency is related to the stability of the carbide formed, and the stability results in a slow rate of solution in austenite with a related tendency for fine grain size. These elements are more generally used in heat-treated steels (Chaps. X and XI) although they may be utilized for structures or castings operating at elevated temperatures. Here, stable carbides cause the entire structure to be more stable or to change (by growth of carbide particles) more slowly with time.

ENGINEERING APPLICATIONS

In the fields of civil engineering and building construction, large structures, such as bridges and buildings, require steels of moderate cost, as specified by the A.S.T.M., in structural grades of plain carbon, so-called (low) silicon steel, and the more expensive 3.5 per cent nickel steel. The yield point of the nickel structural steel is at least 50 per cent greater, and of the silicon steel about 40 per cent greater, than that of the carbon steel. This is, of course, partly because around 0.4 per cent carbon is specified in the former steels while only 0.2 to 0.3 per cent carbon would be used in the plain carbon steel to obtain the properties designated.

Medium-manganese steel containing, *e.g.*, 1.60 per cent manganese, with 0.33 per cent carbon and 0.18 per cent silicon, as used in the main compression members of the Kill van Kull Bridge,[1] is in competition with the other high-strength structural steels used in the as-rolled condition. On cooling after hot-rolling, it tends to develop an extremely fine pearlite structure which probably accounts in large measure for its strength—yield point over 58,000 p.s.i. and tensile strength over 100,000 p.s.i.

In addition to the structural steels used in the as-rolled condition, heat-treated mild carbon grade steels, of comparatively high

[1] Additional information on the steels employed in bridge structures may be obtained by consulting the article from which these data were abstracted, *viz.* D. B. STEINMAN, *Metal Progress*, June, 1931.

strength, have been available to bridge engineers since 1915. Heat-treated eye bars, for use at a unit stress 50 per cent higher than that specified for ordinary structural steel, were adopted for the principal tension members of the Carquinez Strait cantilever bridge in California. Their cost was approximately one cent a pound above the cost of ordinary structural steel eye bars. Silicon steel was used for the towers and compression members of this bridge and for the towers, floor, and anchor girders of the George Washington Bridge over the Hudson River at Fort Lee. It also cost about 1 cent per pound more than ordinary structural steel as against some 2.5 cents per pound for the standard 3.5 per cent nickel steel, which, in spite of high cost, has been specified for important members in many bridges, such as stiffening trusses in the Manhattan Bridge (8,000 tons from a total of 44,000 tons of steel in the entire bridge).[1]

Heavy steel rails are typically of eutectoid composition, with a minimum of about 0.50 per cent carbon for the lighter rails. They were formerly always used in the approximately normalized condition produced by air-cooling after hot-rolling. In recent years, however, rails subject to particularly heavy service have come to be heat-treated. They are usually allowed to cool from the hot-rolling operation to below the critical temperature, then reheated to the austenitic condition and the ends quenched in an air blast. Subsequently the entire rail is permitted to cool slowly in air and, in this stage, heat flows from the main body of the rail and tempers the air-cooled ends. Structural variations, from moderately coarse to fine pearlite, will be found in the various parts of the rail, *i.e.*, the head, web, and flange, according to the differing cooling tendencies in these regions, while a very fine pearlitic structure is found at the ends (page 146). The heat-treated structure shows a somewhat higher hardness at the rail ends, which are subjected to a greater battering effect by the passage of trains. In addition, the main part of the rail, although slightly softened by the slow cooling, shows very much increased resistance to impact loads and to failures from transverse fissures and other internal defects.

Specifications for steel castings cover a rather wide range including carbon steels and alloy steels for general industrial, or railroad and marine, structural purposes, as well as alloy steels for

[1] See footnote on page 133.

valves, flanges, and fittings for service at temperatures up to about 600°C. (dull red).

The carbon content of the plain carbon steel castings is left to the discretion of the manufacturer, but it is not intended that heat treatment (such as liquid quenching or spraying, and tempering), other then annealing or normalizing, shall be required in order to develop the specified strength properties. On this basis, the carbon would normally run from 0.2 to 0.3 per cent in the soft castings to 0.5 or 0.6 per cent in the hardest. The chemical compositions range from 0.5 to 1.0 per cent of manganese and from 0.2 to 0.75 per cent of silicon to ensure satisfactory deoxidation of the liquid steel, while phosphorous and sulphur are not allowed above 0.05 and 0.06 per cent, respectively, by reason of their embrittling effect.

The alloy steel castings specified by A.S.T.M. for structural purposes are divided into three classes according to the following criteria:

The tension requirements for Class A castings are intended to apply to castings of such design and dimensions that they may be regarded as unsuitable for any method of heat treatment other than one that includes slow furnace-cooling from above the critical temperature. In Class B castings, the properties are obtained by air-cooling, which is regarded as a safe procedure for the great majority of alloy-steel castings, developing in them the highest tensile-strength and yield-point values that can be obtained from the materials by any method of heat treatment except liquid quenching. In Class C castings, liquid quenching followed by tempering is the approved treatment.

The chemical specifications limit only the phosphorus and sulphur to 0.05 and 0.06 per cent, respectively, and the manufacturer may use carbon, silicon, manganese, and other alloying constituents at his discretion in obtaining the requisite physical properties in all three classes of castings, which range from 75,000 to 150,000 p.s.i. tensile strength, and from 40,000 to 125,000 p.s.i. yield point, with elongation in 2 in. never below 10 per cent and reduction of area never below 25 per cent.

Under these specifications, many types of low-alloy steel may be offered, such as vanadium, chromium, chromium-vanadium, nickel, nickel-chromium, chromium-molybdenum, or manganese steel.

The alloy steels intended for service at temperatures from 400 to 600°C. (A.S.T.M. A157–41) are divided into two classes; ferritic steels of nine kinds, specifically, C-Mo, Cr-Mo, Ni-Cr, Ni-Cr-Mo, 4 to 6 per cent Cr, 4 to 6 per cent Cr-Si-Mo, 8 to 10 per cent Cr-Mo, 13 per cent Cr, and two austenitic steels, 18 Cr and 8 Ni or 8 Cr and 20 Ni. The ferritic steels may be annealed, annealed and drawn (heated 150°F. above the service temperature), normalized and drawn, or normalized and annealed. The austenitic steels are given a subcritical stabilizing treatment; *i.e.*, they are heated to a temperature and held there for a sufficient time to ensure a stable carbide structure.

LOW-ALLOY HIGH-STRENGTH STEELS

The advent in the steel industry of continuous rolling mills, with a high productive capacity for sheet steel at a low unit cost, has stimulated investigations into new means of utilizing the product. One innovation of this character has been the development of a new type of steel having a considerably greater strength than carbon steels in the equivalent hot- or cold-rolled condition. The increased physical properties are achieved in most cases by the same type of structural modifications that have been previously discussed, *i.e.*, by refinement of the ferrite grain size and solid-solution strengthening of the ferrite structure. The new aspect of this development enters by reason of the use of small amounts of expensive alloys, such as nickel or chromium, and an extensive use of low-cost alloying elements, such as manganese, silicon, copper, or phosphorus. The effect of phosphorus on the properties of steel for many years was believed to be an embrittlement at low temperatures. This misconception arose originally from the many brittle failures encountered with high-phosphorus-content steel rails during the first winter of operation on the Trans-Siberian Railroad. In the latter part of the nineteenth century, phosphorus was known and utilized as a strengthener of steel. Recent work on the low-alloy (and relatively low-cost) high-strength steels has rediscovered this fact and outlined the conditions under which low-temperature embrittlement will or will not appear. In general, the phosphorus content of a steel may be considerably increased if the carbon content is low, and vice versa.

The increased strength of the low-alloy steels has permitted use of the thinner sections that may be readily produced by a continuous mill, and despite the higher steel cost per unit of weight, the lesser weight of the final structure may result in direct metal-cost economies as well as obvious but less determinate savings possible when the lighter structure is one that is moved (*i.e.*, a freight car, truck body, etc.). However, the use of thinner sheet metal required a compensating improvement in corrosion resistance to prolong the useful life of the structure. The addition of copper (and phosphorus) is effective in somewhat improving the resistance to weathering as well as increasing strength, but generally painting must still be relied upon for adequate protection.

QUESTIONS

1. How would it be possible to differentiate between three hot-rolled steel specimens of identical shape, size, and carbon content, if one had been produced by the acid Bessemer, one by the basic open-hearth, and one by the basic electric process?

2. What might be the difference found in the structure and properties of rivets heated to about 2000°F. and then hammered (*a*) at 1900°F., (*b*) at 1325°F., (*c*) at 600°F.?

3. What is the difference, if any, between the strength of large- and small-section commercial hot-rolled steel shapes? Why?

4. Cast or forged carbon steels of the same composition can be heat treated, *i.e.*, normalized and annealed, to attain approximately the same Brinell hardness and tensile strength. What would be their relative positions with regard to ductility and directionality of properties?

5. Why is the structure of cast hypoeutectoid steel coarse when in the as-cast condition? What structural elements are present?

6. How would you refine the grain of cast steel containing 0.30 per cent carbon? 0.60 per cent carbon?

7. When should a double annealing heat treatment be given steel castings and when would it be unnecessary? Would it be as necessary for large as for small sections?

REFERENCES

"Metals Handbook," sections on Technology of Iron and Steel, Shaping and Forming of Metals, High-strength Low-alloy Steels, Properties of Forgings, Heat Treatment of Steel Castings. "Modern Steels"—Manufacture, Inspection, Treatment, and Uses (ASM) 1941.

CHAPTER X

THEORY OF HEAT TREATMENT OF STEELS

Steels may be heat-treated in order to accomplish one or more of the following objectives: (1) the elimination of hydrogen, dissolved during pickling or electroplating, which causes brittleness; (2) relieving microstresses in the atomic lattice that increase brittleness (tempering or drawing); (3) relieving macrostresses that may cause distortion upon machining or failures in service (stress-relief annealing); (4) eliminating the effects of cold-work (subcritical or process annealing); (5) changing the structure to a more uniform condition (normalizing); (6) changing the structure to a softer or more machinable condition (annealing, full or spheroidizing types); or (7) enhancing the strength and hardness properties to a marked extent (hardening, usually followed by a tempering treatment). Of these heat treatments, type 1, performed at 250 to 450°F., is accompanied by no visible change in the microstructure and, with 4, is not included in this discussion.

FORMATION OF AUSTENITE

Almost all steels, except the highly alloyed austenitic types, consist of the stable phases, ferrite and carbide, when they are machined or otherwise formed to shape prior to final heat treatment. The first step in the heat treatment is to *austenitize* the steel; *i.e.*, heat the metal to a temperature above the A_{c_1}, or above the A_{c_3} if it is of hypoeutectoid composition. The austenite does not immediately form as a homogeneous phase throughout the structure. Some time is required for the initial austenite nuclei to grow by absorbing the surrounding ferrite and carbide crystals. Even after the structure has completely transformed to austenite, it is not necessarily homogeneous; areas which were formerly ferrite may be somewhat low in carbon, and those formerly carbide may be high in carbon concentration. In the case of a hypoeutectoid steel, some time may be required for carbon to diffuse into areas which were previously large masses of ferrite. Hypereutectoid steels are hardened from a temperature between

the A_{cm} and the A_1 lines; hence some undissolved carbides remain in the austenite, and the austenite in the vicinity of these carbides does not immediately have the same carbon content as it has elsewhere.

The time required to obtain homogeneous austenite varies with the maximum temperature reached and the structural characteristics of the original ferrite-carbide matrix. The higher the temperature to which the steel is heated in the γ field, the shorter will be the time required for carbon diffusion to erase nonuniformities in carbon distribution. For example, a normalized eutectoid carbon steel requires about 5 sec. at 780°C. or 100 sec. at 730°C. to transform about 99.5 per cent to austenite. However, it requires about 200 sec. at the 780°C. to dissolve all carbides, and in the vicinity of 10,000 sec. (nearly 3 hr.) to attain a completely homogeneous austenite. At 810°C., homogeneous austenite is obtained in 1,000 sec. about 17 min.).[1] A finely spheroidized carbide structure austenitizes most rapidly, next a fine pearlitic structure, then, most slowly, a coarse pearlitic or spheroidized structure.

If the prior structure consists of large masses of ferrite or contains coarse crystallites of cementite, the austenitizing time is noticeably longer at any specific temperature. If the carbide phase is not simply Fe_3C but contains chromium, molybdenum, vanadium, or tungsten carbides which are relatively stable and slow to dissolve, then homogeneous austenite is rarely attained by the ordinary times and temperatures utilized in industrial practise. A higher temperature that would completely dissolve the alloy carbides and homogenize the austenite is undesirable for reasons of possible and undesirable austenitic grain growth or quenching stresses (page 150) or, relatedly, danger of distortion or cracking upon quenching. However, the subsequent discussion of heat treatment is predicated upon starting with homogeneous austenite except when the contrary is explicitly stated. Furthermore, the discussion applies only to carbon steels except when otherwise specified.

ISOTHERMAL TRANSFORMATION OF AUSTENITE

In the iron-carbon diagram of Fig. 10 (page 110), the equilibrium line indicating the temperature at which austenite eutectoidally

[1] MEHL, *Trans. A.S.M.*, **29**, 813. 1941.

transforms to the ferrite-carbide aggregate known as pearlite is called the A_1 line. The diagram also shows a lower position of this same line labeled the A_{r_1}, where austenite transforms to pearlite upon cooling at a rate faster than that required to maintain equilibrium conditions. The A_1 temperature has a fixed equilibrium value, but the A_{r_1} temperature (and also the A_{r_3}), resulting from undercooling, varies with the speed of cooling.

A similar displacement of lines in phase diagrams has been mentioned, qualitatively, in every other system discussed so far. The effect in iron-carbon alloys, however, is of such direct importance in practical heat treating that a more quantitative treatment is desirable. Such a treatment is experimentally possible by quenching small sections, from a temperature in the homogeneous austenitic range, into a bath at a temperature below the A_1 line and noting the time required for transformation to start and the time necessary for completion. When this procedure, *isothermal or constant-temperature* transformation, is carried out at a number of temperatures from the A_1 line to room temperature, a temperature-time graph, such as that shown in Fig. 11, is obtained.

At the top of this graph, the horizontal line directly below the designation *stable austenite* represents the A_3 temperature of a hypoeutectoid steel or the A_{cm} temperature of a hypereutectoid steel. The actual value of this temperature, in either case, would, of course, be a function of the carbon content of the steel. The next horizontal line represents the A_1 temperature of 723°C. Under equilibrium conditions, this temperature range (A_3 or A_{cm} to A_1) would call for austenite and ferrite in steels with less than 0.8 per cent carbon, or austenite and carbide for steels with more than the eutectoid carbon content. The dashed line traversing this intermediate field, in a right, upward direction, shows the time required for ferrite or carbide to start separating from the austenite at any specific temperature between the A_3 (or A_{cm}) and A_1 points.

The roughly parallel *S*-shaped lines below the A_1 define the time required for the $\gamma \rightleftarrows \alpha + Fe_3C$ reaction to start (marked START) and be completed (marked END) at any specific temperature in the indicated range. The transformation is slow to start and be completed at temperatures just under the critical, but the delay in starting and the time required for completion decrease as the temperature drops to about 550°C. (about 1000°F.). In this

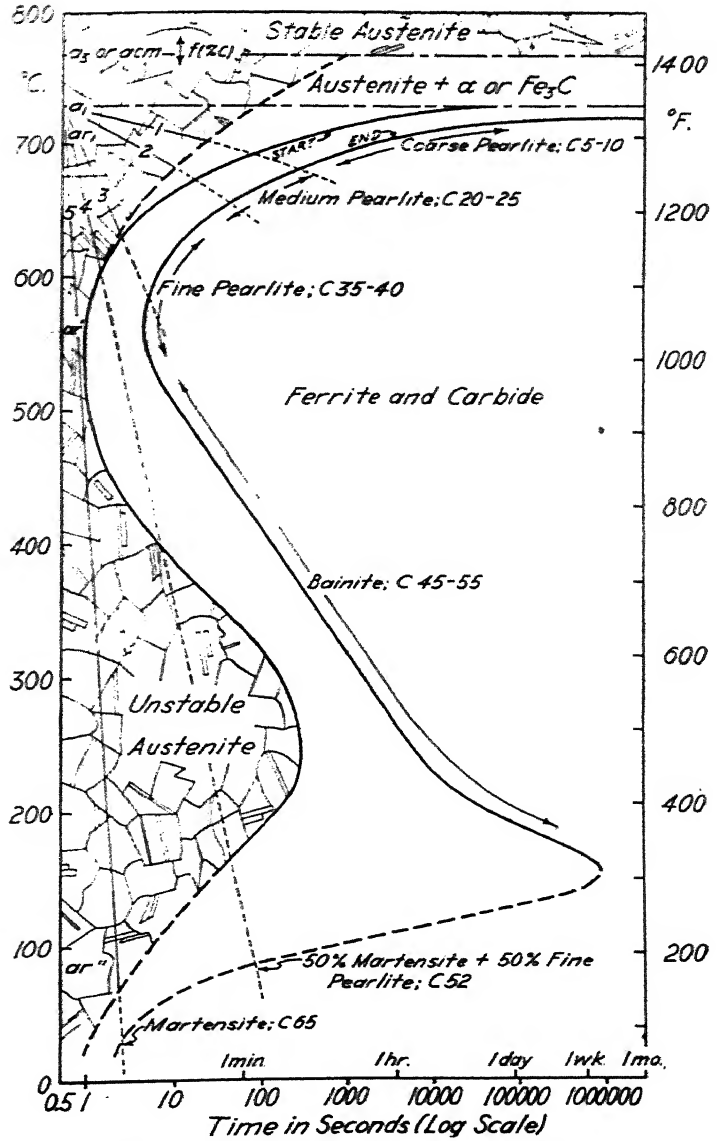

FIG. 11.—Chart (*S* curve) showing the effect of temperature on the time required for the transformation of eutectoidal austenite and the structures obtained in various ranges. The diagram is roughly applicable to hypo- or hypereutectoid steels.

range, the greater the degree of undercooling, the more unstable austenite becomes, or in other words, the greater is the urge to transform. Down to about 550°C., this effect is dominant over the associated difficulty in transformation resulting from the formation of two phases of far different carbon contents, α (0.04 per cent C) and Fe_3C (6.7 per cent C), from a homogeneous solution. The transformation in this range results in a pearlitic aggregate of the two phases, and their formation involves diffusion of carbon. If the degree of unstability is low and the rate of reaction slow, plenty of time is available for diffusion. The ferrite and carbide then form coarse, lamellar pearlite with an associated low hardness. As the temperature of austenitic transformation decreases (toward 550°C.), the rate increases, the time available for carbon diffusion is less, and, consequently, the pearlite lamellae become increasingly finer, or closer together, with a related increase in hardness.

The mechanics of the transformation in this range is partially known. Carbide formation initiates the process, and presumably, as carbide forms, the adjacent austenite becomes depleted in carbon, thus less stable (*e.g.*, note the course of the A_3 line with carbon concentration) and ultimately an adjacent layer of ferrite forms. As the α phase forms with little (0.04 per cent) carbon in solution, that element diffuses to the adjacent austenite which eventually becomes supersaturated, carbide again forms, and so forth. The formation of coarse pearlite at high temperatures seems to conform to this description in that the structure apparently develops by alternate deposition of ferrite and carbide, but finer pearlites seem to show simultaneous growth of both phases at their open ends in contact with austenite (Plate X, Figs. 4 and 5). Crystallographic relationships seem to be well defined for the coarse pearlite in which the carbide-ferrite lamellae are quite straight. As the lamellae become finer, they are subject to greater distortion and bending with a loss in obvious crystallographic relationships.

If the steel is of hypo- or hypereutectoid carbon content, then before austenite transforms to pearlite, it must reject excess ferrite or carbide at its grain boundaries until the carbon content reaches the limiting pearlite concentration for the temperature involved. This process will occur between the A_3 (or A_{cm}) and the A_1 temperatures, leaving residual stable austenite. At tem-

peratures successively lower than the A_1, the time permitted for rejection of excess ferrite or carbide decreases, the amount formed before the pearlite reaction starts becomes less, and, consequently, the carbon content of pearlite is not fixed but is a function of the temperature of transformation and carbon concentration in the austenite.

The pearlite transformation is initiated at austenitic grain boundaries. If hypo- or hypereutectoid steels are very slowly cooled so that the reaction occurs just below the A_1 temperature, pearlite usually grows into only one austenite grain since excess carbide or ferrite is present at the boundary. In eutectoid steels, with no excess phase at the austenite boundaries, the pearlite nodules tend to grow across the boundaries and become larger than the former γ grains. Upon more rapid cooling with the eutectoid reaction occurring near the Ar' point or in the 550°C. range, pearlite grows from an austenitic boundary, in a roughly spherical form, into all adjacent austenite grains, since in many hypo- or hypereutectoid steels (0.6 to 1.2 per cent C) there is no excess phase at the γ grain boundaries to prevent this growth. The large number of nuclei, however, now cause the pearlite nodules to be much smaller than the original austenite grains. In a polished section, the pearlite has a nodular form, and exceptional micrographic technique is required to resolve the individual ferrite-carbide lamellae. This structure was, until recently, called primary troostite, but the term should no longer be applied to this structure which differs only in fineness or degree, not in kind, from the higher temperature, coarser pearlites.

At temperatures between about 550 and 200°C. (1000 to 350°F.), more time is required for the transformation of austenite to start, and the subsequent rate of transformation decreases. In this range of temperatures, while the degree of "unstability" of the austenite continues to increase, the retardation force, arising from very slow diffusion of carbon and the greater rigidity of the austenite lattice, becomes increasingly important and overbalances the increased urge to transform. Structures in this range vary from a feathery aggregate of ferrite and very fine carbides at around 450°C. to groups of dark-etching, lens-shaped (but more angular) needles with no visible carbides at around 200°C. All of these structures are called "bainite." They are basically different from pearlites; *e.g.*, the ferrite in pearlite has

one crystallographic relationship to austenite, while in bainite it has quite a different relationship, actually one similar to that shown by hypoeutectoid ferrite separating from austenite. The difference presumably indicates that, whereas pearlite formation is initiated by carbide separation, bainite is initiated by ferrite separation.[1]

Below 200°C., the rate of isothermal transformation of austenite apparently again increases. The experimental evidence on this point is controversial; some suggests that below the 200°C.

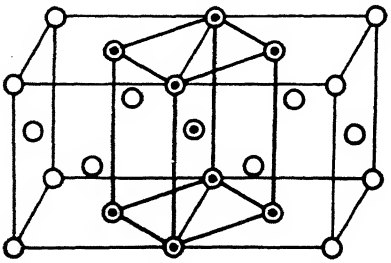

FIG. 12.—Two unit cells of the face-centered cubic lattice (γ Fe) with specific atoms marked with black centers to indicate the structure might also be considered as body-centered tetragonal.

temperature, austenite is stable as long as the temperature is uniform but transforms as soon as the temperature falls. Other work seems to indicate the contrary, that the rate of transformation does increase while the time required to start decreases. Since there is no theoretical reason for the rate to increase, yet it effectively seems to, the *S* curve showing the start and end of the transformation in this temperature interval has been drawn as a dashed line.

The structures formed below about 200°C. are also lens-shaped needles, similar in shape and appearance to the bainites formed at slightly higher temperatures, but have slower etching characteristics and, therefore, are usually lighter in color. The structure, as freshly formed, is called *white martensite*. Whereas carbide is readily visible in pearlite and detectable by X-rays in bainite, no carbides have been found in freshly formed martensite by any experimental means now available. The lens-shaped, angular needle structure of martensite is frequently called *acicular* (from the Latin word meaning needle-shaped). The structure shows an

[1] SMITH and MEHL, *A.I.M.E. Tech. Pub.* 1459, 1942.

apparently clear-cut crystallographic relationship to a specific set of planes of the austenite (see Plate X, Fig. 13) which, however, is not a simple plane such as the octahedral (plane of slip and twinning).[1]

Freshly formed martensite has been found to have a body-centered structure which is not cubic but tetragonal. A simple but unfortunately, inaccurate) explanation of this structure appears in Fig. 12. If the atoms in the center of the top and bottom faces of two unit cells of the face-centered cubic austenite lattice are linked with the five atoms on the plane joining the two cells, these nine atoms are found to constitute a body-centered tetragonal structure. If, as in this case, the height of the tetragon happens to be $2\sqrt{2}$ times the edge of its base, the structure is designated by its more symmetrical form, face-centered cubic. Thus, to change from a face- to a body-centered cube ($\gamma \rightleftharpoons \alpha$) the lattice need only contract in one dimension and expand in the other two. At one time it was believed that, when martensite formed at a lower temperature, this process of *compression* halted before reaching completion. This explanation of the mechanism of martensite formation, first proposed by Bain, while simple and logical, is not in accord with the known crystallographic data and thus the actual process must be more complicated. The transformation mechanism best accounting for the observed crystallographic relationship between martensite and the parent austenite is that proposed by Kurdjumow and Sachs, which involves a shearing movement of atoms on specific planes of the austenite in a manner analogous to the shearing movements accompanying mechanical twinning.

The reason for martensite etching white, while low-temperature bainite etches dark, probably is related to the distribution of carbon. During the formation of martensite, there is neither time nor sufficient atomic mobility for carbide to form (to a detectable size); the transformation occurs with no measurable diffusion and presumably the carbon atoms are trapped to form a very supersaturated solution in the body-centered lattice or it may form a highly disperse, perhaps colloidal, precipitate of carbide. Bainite, forming more slowly and at a higher temperature, permits the carbide to precipitate in a disperse form which causes the structure to etch rapidly and have a black appearance.

[1] GRENINGER and TROIANO. *Trans. A.I.M.E.*, **140**, 307, 1940.

The lines on the diagram (Fig. 11, page 141) marked 1, 2, 3, 4, and 5 represent cooling curves superimposed on the isothermal transformation graph. The curves are started at the A_1 line since, at least for an eutectoid steel, the rate of cooling from the austenitizing temperature to the A_1 line is of no significance. The austenite is stable and of uniform composition above this critical temperature. *Line* **1** represents a typical cooling rate obtained by permitting the steel to cool in the furnace, assuming the heat supply is turned off and the furnace is left closed. This *annealing* treatment permits soft, moderately coarse pearlite to be formed at the A_{r_1} temperature (about 690°C.) with an almost equilibrium amount of excess ferrite or carbide, depending on the carbon content. During the transformation to moderately coarse pearlite, the release of the heat of the eutectoid reaction (*recalescence*) prevents the temperature from dropping continuously as is indicated by Line 1, and it may rise somewhat. Generally the temperature at the approximate end of the reaction will at least be nearly the same as at the start; in this case, the reaction would probably be completed at about 690°C. (1275°F.). Once the reaction is complete, the cooling rate is of little importance since the phases present in the structure are stable. The only effect of quenching after about 300 sec. at 690°C., for example, would be to develop some stresses of the same type as were discussed for aluminum alloys (page 91). Long holding at 690°C., on the other hand, would only result in an eventual spheroidization of the lamellar carbides with some related softening of the structure.

Line **2** represents a typical cooling rate obtained by air-cooling a fairly heavy section. This might be a normalizing treatment, giving moderately spaced pearlitic lamellae of an intermediate hardness, and a smaller amount of the excess phase. Again, the cooling rate after the pearlite forms (in about 100 seconds at 670°C.) is of little consequence. *Line* **3** represents a typical cooling rate obtained by air-cooling a thin section (or oil-quenching a heavy section) resulting in a fine pearlitic structure with a fairly good hardness. This completely black etching structure was *formerly called primary sorbite* since no lamellar characteristics can be observed by ordinary examination of the structure. This is the lowest temperature of transformation to a completely pearlitic structure and the temperature at which it occurs is called

the A_1. Very little time is available for the separation of excess ferrite or cementite so the carbon content of this very fine pearlite is variable; it may be from about 0.6 to 1.2 per cent, depending on the carbon content of the steel. *Line* **4** represents the cooling curve obtained by oil-quenching a moderately sized section of a water-hardening carbon steel. It will be noted that at around 550°C., it reaches a point about midway between the "start" and "end" of the transformation to fine pearlite, which means that about 50 per cent of the austenite thus transforms. The residual austenite remains unchanged until the cooling curve intersects the *S* curve at around 150°C. at which time the γ phase transforms to martensite. Although the cooling curve traverses the completely austenitic field between 400 and 150°C., ferrite and carbide formed below the A_1 line are stable and can not retransform to austenite. *This graph is not a phase diagram.* The steel now consists of nodular, fine pearlite (formerly called primary troostite) outlining the former austenitic grains with white martensite representing the remainder of the structure. The aggregate has a hardness intermediate between that of fine pearlite and that of martensite. This condition indicates an unsuccessful quench, if a completely hardened, martensitic structure was desired. Since part of the austenite transforms at a high temperature (A_1') and part at a low temperature (A_1''), the resulting structure is said to have originated from a *split transformation.*

Line **5** represents the probable cooling curve obtained by water-quenching a small-sized section. The structure is completely martensitic except for the possible presence of some untransformed austenite. The maximum amount of residual austenite found in quenched carbon steels increases with carbon content, from approximately zero at 0.55 per cent carbon to perhaps 15 or 20 per cent in a 1.30 per cent carbon steel. Throughout this range of carbon content, the martensitic hardness is about the same, C65-67, although when the amount of residual austenite approaches 15 to 20 per cent, the hardness may be very slightly lower, *e.g.*, C63-64.

It should now be clear that successful hardening requires cooling, *particularly from* 723°C. *to* 550°C., in a time less than that required for fine pearlite to form at the "nose" of the *S* curve. Since heat is abstracted directly by the cooling medium only from the surface of the steel, the cooling rate at various depths

below the surface, in conjunction with the time position of the nose of the *S* curve, will also determine the depth of the completely martensitic structure. The depth of hardening under controlled experimental conditions is called the *hardenability;* the word does not refer to the *degree* of hardness but the *depth* of useful hardness. The entire control of hardenability is based on control of the time required for initiation of the transformation to fine pearlite at the A_r' temperature of about 550°C. (1000°F.). Factors affecting this time are:

1. Austenitic grain size. Since the fine pearlite starts to form at austenitic grain boundaries, fine-grained austenite transforms more quickly at around 550°C. Steels with fine-grained austenite then tend to be shallow hardening while those with coarse-grained austenite harden to a greater depth.

2. Austenitic homogeneity. Since the pearlite reaction is nucleated by carbide formation, residual carbides or localized areas of austenite rich in carbon cause the pearlite reaction to start sooner and thus contribute to shallow hardening. For example, it has been found[1] that the rate of nucleation at 680°C. may vary by a factor of 1,000 between 5 and 90 min. of austenitizing (at 900°C.), resulting in a change of reaction time from 1 to 7 min. However, at the significant A_r' point, this factor is less important.

3. Austenitic composition. Alloying elements which, in addition to carbon, must diffuse during pearlite formation, necessarily slow up the rate of its formation and increase the time required for diffusion to establish the conditions permitting the reaction to start. The chief distinction between water-, oil-, and air-hardening steels is in the position of the nose of the *S* curve. In the graph shown here (for carbon steels) only water-cooling, *line* 5, completely avoids the high-temperature transformation at the A_r' region. If some manganese, nickel, or chromium is added, the *S* curve may be displaced to the right sufficiently for *line* 4 to exceed the critical cooling rate. Finally, appreciable amounts of these elements or combinations of them with perhaps others, such as molybdenum, might so slow up the rate at around 550°C. that even air-cooling, such as shown by *line* 3, would permit the steel to form martensite. Isothermal transformation curves of these alloyed steels may be considerably more complicated[2] than the

[1] MEHL, *loc. cit.*

[2] DAVENPORT, *Trans. A. S. M.* 27, p. 837, 1939.

one shown for carbon steels (*e.g.*, some of the *bainite* structure can form upon direct cooling of some alloy steels), but their significance is similar.

VOLUME CHANGES AND RELATED STRESSES ACCOMPANYING TRANSFORMATIONS

The transformation of austenite into pearlite or martensite is accompanied by an expansion of the steel and the release of thermal energy. The critical temperatures (A_1 and A_r values) may be determined by measuring dimensional changes with temperature (by use of a dilatometer) or by cooling or heating curves (thermal analysis). A simple demonstration of both dimensional and thermal changes may be made by stringing a piano wire, which is always made of approximately eutectoid steel, between two supports with electrical contacts.[1] (A 12-ft. length of 0.034-in. wire can be used directly across an ordinary 110-volt alternating-current power supply.) A current is passed through the wire to raise its temperature above the A_{c_1}, and then the current is shut off to permit the wire to cool in air. It sags during heating, but, since the rate of heating is seldom uniform along its length, the transformation to austenite at the A_{c_1} temperature is not readily detected. As it cools, however, the sagging wire rises steadily as the austenite contracts with drop in temperature. Because of rapid cooling of the thin section in air, the steel does not transform until it reaches a dark-red color, corresponding to a temperature of about 550 to 600°C. As it then transforms to fine pearlite, the wire becomes visibly hotter, an effect commonly called *recalescence*. The expansion, resulting both from the transformation and the rise in temperature, causes the wire to sag suddenly. Then, as the transformed structure continues to cool, the suspended wire resumes its slow contraction and steady rise to its original position.

Upon slow cooling, as in a furnace, there is not any great temperature difference or gradient between the outside and center of even fairly heavy sections; all of the transformation occurs at a high temperature (the A_{r_1}), and the expansion accompanying the transformation is accommodated by deformation of the plastic metal. Under these circumstances, there cannot be any appreciable residual stresses. When a heavy section, such as a steel roll

[1] United States Steel Corporation, Research Laboratory.

casting 1 ft. thick, is cooled in air or a liquid medium, the outside may reach the transformation temperature and expand while the center is much hotter and still completely austenitic. To accommodate the surface expansion, the metal in the central region is pulled toward the surface and the ends may be forced in and become slightly concave. Well after the surface section has transformed and resumed its normal contraction, the central section reaches its transformation temperature and starts expanding. In order to conform to an expansion of the interior, the surface layers must expand. Since they are contracting at this time, the enforced expansion takes place by plastic flow, but at a much lower temperature and in metal having less plasticity than was the case upon furnace-cooling. If the roll has been quenched, this stage of the cooling cycle may find the surface in a brittle martensitic condition, not able to deform plastically, and surface sections may spall off, sometimes with explosive violence. Assuming that the surface plastically conforms to the expanding core, the final stages of cooling find the center, which transformed at a higher temperature and consequently is hotter, contracting more than the surface and now tending to pull it inward. This tensile pull of the center is balanced by the compressive elastic strength of the surface so that, when the metal is uniformly at room temperature, there is a residual tensile stress in the center and a residual compressive stress at the surface.

The presence of residual stresses is not confined to steel sections 1 ft. in thickness; it may be found in all metals (see page 91 for aluminum alloys) and in sizes less than 1 in. thick, if cooling from a high temperature was sufficiently rapid to produce a marked temperature differential between the surface and center sections. A high quenching temperature usually results in greater temperature gradients and thus introduces greater stresses with a related increase in the danger of cracking or distortion. The stresses described above act in a circumferential direction on cylindrical specimens, but these are also accompanied by longitudinal (lengthwise on the surface) and radial (from surface to center) stresses. The stresses result in a displacement of the normal atomic spacing. If the crystal lattice is more or less uniform, they may be detected by X-ray measurements. They may also be detected mechanically by machining off surface layers (or splitting tubes, etc.) since, when part of the metal in a balanced

elastic stress system is removed, the remaining unbalanced stresses cause some deformation or distortion.[1] This is frequently a problem of considerable magnitude in machine shop work.

Residual stresses may be relieved thermally by heating to a temperature sufficiently high to permit plastic deformation. The elastic limit of metals decreases rapidly at elevated temperatures and, since stresses are elastically balanced, they are diminished by internal flow. They are also reduced by an external or gross deformation; stretching the rod causes more flow in sections previously under tensile stresses and may eventually reverse the stress in sections under originally compressive forces, resulting in an equalization effect upon release of the external force.

Martensite, forming in relatively cold austenite, may be subject to stress of a much greater magnitude (since the elastic limit is higher) but on a much smaller scale. The first plates of martensite forming in plastic austenite may expand without trouble. When the adjacent austenite later transforms to martensite, the accompanying expansion is opposed by contact with the previously formed martensite. Thus the first martensitic needles are under a high, localized, elastic tensile stress with their newer neighbors balanced in compression. Minute cracks have been detected in the martensitic structure after etching and examining at a high magnification. The cracks may be a stress-corrosion (etching) effect, but they do suggest one cause for the brittleness of martensite.

TEMPERING OF MARTENSITE

Freshly formed martensite has been described as a body-centered tetragonal structure, under high microstresses, and greatly supersaturated with carbon or containing very disperse carbides. Reheating of martensite would be expected to permit a reversion to the stable body-centered cubic lattice, internal readjustments to relieve stresses, and, on the basis of the previous discussion of age-hardening, precipitation of carbide particles followed by growth or agglomeration of these carbides, as permitted by temperature and time. Upon *tempering or drawing* at successively higher temperatures for a constant time of 1 hr., the

[1] SACHS and VAN HORN, "Practical Metallurgy," A.S.M., 1940.

whole process can be divided up into stages on a rather arbitrary basis which, nevertheless, has a practical significance.

150 to 230°C. (300 to 450°F.); the tetragonal lattice becomes cubic, residual austenite transforms (probably on cooling from the draw), carbide precipitation causes the martensite to etch more rapidly and to a blacker structure called *tempered* or *black* martensite. Hardness may increase slightly in the lower end of the range, but, despite the transformation of residual austenite, growth of carbides in the upper temperature range decreases hardness slightly, from C65 to C60–63. Carbides remain too small, however, to be resolved by the microscope.

230 to 400°C. (450 to 750°F.); growth of carbides in a globular form continues, although they still may be unresolvable by the microscope. Their general distribution causes the entire structure to etch rapidly and to a black mass which is called *troostite*. Hardness continues to decrease, from about C62 to about C50.

400 to 650°C. (750 to 1200°F.); growth of carbides continues to the point where they can be resolved at high magnifications although the structure appears dark and indistinct at magnifications up to about 500 diameters. The structure is called *sorbite* and includes hardnesses in the range C45 to C20.

650 to 723°C. (1200 to 1335°F.); continued growth of carbides brings them to a size that may be resolved at ×500 although their form may be better seen at ×1,000. They appear as globular particles in a continuous ferrite matrix which now becomes visible as a separate phase for the first time although grain growth of the ferrite has undoubtedly accompanied carbide growth in earlier stages. The structure is called *spheroidite*, and it is naturally soft, from C20 to C5, tough, and "gummy" to machine. (Spheroidal carbide structures may also be obtained by heating pearlitic structures in the same temperature range, since carbides tend to assume the shape having least surface area or lowest energy. A long time is required to spheroidize pearlites, and the minimum size of the ultimate spheroids is limited by the size of the lamellae from which they develop.)

SUMMARIZING OF THEORY

Pearlite is the lamellar aggregate of ferrite and carbide *formed only from austenite* upon slow to moderately fast cooling rates, between the A_1 and A_r' temperatures. The faster the cooling

rate, the more rapidly is the pearlitic structure developed, with a related increase in fineness of the lamellae and hardness of the aggregate. The more rapidly pearlite is formed, the less time is available for the separation of excess ferrite or carbide, with the result that pearlite is of a fixed carbon content only when formed under very slow cooling conditions. Further increase in the cooling rate of austenite causes at least some of it to remain unchanged until acicular white martensite forms at the A_r'' temperature, and, after attaining or exceeding a critical rate, only martensite is formed. Reheating of martensite causes precipitation and growth of *granular* carbides in a ferrite matrix with a continuous change in hardness. The terms, tempered martensite, troostite, sorbite, and spheroidite, apply to certain ranges of structural aggregates of ferrite and granular carbides, arbitrarily selected on the basis of hardness, etching behavior and micrographic appearance.

MICROSTRUCTURES (PLATE X)

Plate X, Fig. 1. Austenitic, 18 per cent Cr–8 per cent Ni, steel; ×200; 1:2:3 proportions of HNO_3:HCl:glycerin etch. A highly alloyed grade of steel is required to demonstrate the structure of austenite since that phase cannot be successfully preserved at room temperature in a carbon steel even by drastic quenching. This structure of wrought stainless steel, quenched from 1900°F. (1050°C.), is directly comparable to that of any face-centered cubic metal after deformation and annealing; it shows polygonal grains containing a few annealing twin bands. (Some undissolved carbides are present as a result of the short holding time of 10 min. at 1900°F.)

Plate X, Fig. 2. Same 18-8 steel, reheated 20 hr. at 1250°F. (680°C.); ×1,000; same etch. This steel is of a commercial grade known as Type 302, containing 0.12 per cent carbon. Carbon is soluble up to 0.20 per cent at 1950°F. but only to about 0.03 per cent at 1250°F. Reheating in the range 1150 to 1400°F. (620 to 760°C.) permits carbides to precipitate at the austenitic grain boundaries (see next section on properties). The arrowhead-shaped plates of a different color represent ferrite which separated from the austenite (at 1250°F., equilibrium calls for γ, α, and carbide phases to be present).

Plate X, Fig. 3. Razorblade steel with 1.2 per cent C, austenitized at 1000°C. (1830°F.), held 50 sec. at 710°C. (1310°F.) and quenched in water; ×1,000; Picral etch (page 116); hardness C65. This specimen has been held long enough to cross the dotted line of the isothermal transformation graph (Fig. 11, page 141) but not to reach the line indicating the start of pearlite formation. Carbides outline the former austenitic grains which transformed to white martensite in the water quench. Note the comparatively large size of the austenitic grains.

Plate X, Fig. 4. Same 1.2 per cent C steel, austenitized at 1000°, held 100 sec. at 710°C., and then quenched; ×1000; Picral etch; hardness C40. The transformation of austenite to moderately coarse pearlite is about one-third completed. Note in the upper left corner of this structure that pearlite is growing into an austenitic grain in two directions, at the sides and at the ends of the lamellae. Pro-eutectoid (excess) carbide is visible at the austenitic boundaries.

Plate X, Fig. 5. Same 1.2 per cent C steel, austenitized at 1000°, held 20 sec. at 680°C. (1250°F.), and then quenched; ×1,000; Picral etch; hardness C46. The reaction at this lower temperature, yielding a finer pearlite, is about one-third complete in a much shorter time. The front of the pearlite "nodules" shows that growth is chiefly at the *ends* of the pearlite lamellae at this temperature. Growth is mainly from the former austenite boundaries into one adjacent grain. At this temperature, only a trace of pro-eutectoid carbide has been able to form at the grain boundaries of the γ phase.

Plate, X, Fig. 6. Same 1.2 per cent C steel, austenitized at 1000°, held 5 sec. at 650°C. (1200°F.), and then quenched; ×1,000; Picral etch; hardness C55. The transformation, here about 15 per cent complete, has started much sooner at this temperature near the nose of the *S* curve, and the pearlitic structure is much finer, so fine that it is not resolved in this slightly overetched structure. The martensitic needles, in areas which were austenite before quenching, are more evident here because of the overetching. Note the nodular appearance of the fine pearlite areas (which formerly were called primary troostite) and their characteristic radiation into two austenitic grains from the boundary. This structure is typical of a steel quenched at somewhat less than the critical cooling rate. The short time at 600°C.

PLATE X. FIGS. 1–6.

has not permitted excess carbide to form at the austenitic grain boundaries, but the austenite grain size is revealed by the fine pearlite nodules at the boundaries.

Plate X, Fig. 7. Same 1.2 per cent C steel, austenitized at 850°C. (1540°F.), held 5 sec. at 710°C. (1310°F.), and quenched; ×1,000; Picral etch; hardness C65. In this and the following structures, the same steel was austenitized below the A_{cm} line, in a commercial hardening temperature range at which the spheroidized carbides are not completely dissolved. Cementite has started to form at the austenitic grain boundaries much sooner than in the comparable specimen (Plate X, Fig. 3) which was austenitized at a much higher temperature. Note the fine austenitic grain size in the present specimen, austenitized at a lower temperature.

Plate X, Fig. 8. Same 1.2 per cent C steel, austenitized at 850°C., held 10 sec. at 710°C., and quenched; ×1,000; Picral etch; hardness C65. After a somewhat longer holding time, cementite at the grain boundaries and residual particles have thickened, but the pearlitic reaction has not yet started.

Plate X, Fig. 9. Same 1.2 per cent C steel, austenitized at 850°C., held 30 sec. at 710°C., and quenched ×1,000; Picral etch; hardness C41. By now, the pearlite reaction has reached a stage of about 40 per cent completion. Note that coarse pearlite has grown from the grain boundary into just one austenitic grain. Comparison of this structure with that of Plate X, Fig. 4 shows that while the fine-grained austenite transforms more quickly, the resulting pearlite spacing is similar.

Plate X, Fig. 10. Same 1.2 per cent C steel austenitized at 850°C., held 100 sec. at 710°C. and quenched; ×1,000; Picral etch; hardness C21. The transformation is complete but not simply to pearlite. While some grains show this lamellar structure, others show merely coarse globular carbides. This is one form of a so-called "abnormal" but very frequently encountered type of structure. In the abnormal structure, carbides continue to form on carbides already present, which here were globular, so that the transformed structure contains large globular carbides and ferrite. Sometimes the excess grain boundary carbides become very thick with a correspondingly thick ferrite envelope next to them and with perhaps a little pearlite in the center of the former austenite grains.

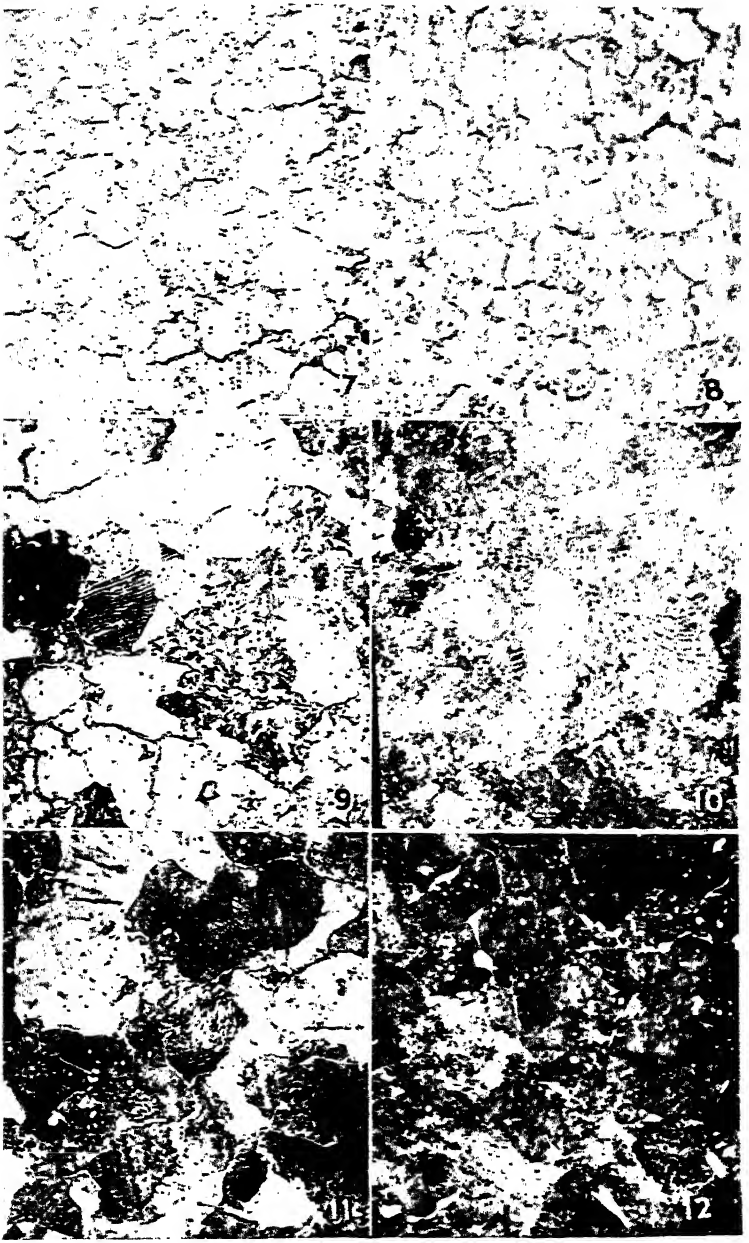

PLATE X. FIGS. 7–12.

Plate X, Fig. 11. Same 1.2 per cent C steel, austenitized at 850°C., held 10 sec. at 680°C. (1250°F.), and quenched; ×1,000; Picral etch; hardness C49. The austenite transformation is about 60 per cent complete and, although some excess carbide formed first at the austenitic grain boundaries, considerably less is present than in the equivalent 710°C. specimen. The pearlite is distinctly finer and not as well resolved.

Plate X, Fig. 12. Same 1.2 per cent C steel, austenitized at 850°C., held 50 sec. at 680°C., and quenched; ×1,000; Picral etch; hardness C30. The steel has completely transformed to rather fine pearlite with some excess carbides. The pearlite is not resolved in some grains but is readily visible in others where the angle of the lamellae to the surface is more favorable.

Plate X, Fig. 13. Forged steel of 0.70 per cent C (S.A.E. 1070), quenched from 925°C. (1700°F.) in cold water and tempered 1 hr. at 100°C. (212°F.); ×1,000; etched 2 min. in 4 per cent Picral; hardness C64. The structure after this very low tempering treatment is still essentially a *white martensite*. Only three directions of the acicular or needle-like martensitic plates are apparent in this micrograph, indicating that this entire field was only part of one austenitic grain. The temperature from which this specimen was quenched was about 250°F. above that ordinarily employed in commercial practice. The high temperature results in a coarse structure, well adapted to show the nature of martensite but too brittle for most service applications, (*cf.*, Plate XI, Fig. 5, p. 177).

Plate, X, Fig. 14. Same as Fig. 13, reheated 1 hr. at 200°C. (390°F.); ×1,000; etched 40 sec. in 4 per cent Picral; hardness C60. The somewhat higher temperature draw has caused the martensitic structure to etch more rapidly and darker. It is now called *tempered martensite*. The horizontal line at the right center section represents a small oxide inclusion (see page 125).

Plate X, Fig. 15. Same as Fig. 13, reheated 1 hr. at 350°C. (630°F.); ×1,000; etched 25 sec. with 4 per cent Picral; hardness C50. General precipitation of fine carbides, below a resolvable size, causes the specimen to appear to be a black aggregate in which the martensitic plate directions are still evident. This structure is normally called *troostite*.

Plate X, Fig. 16. Same as Fig. 13, reheated 1 hr. at 600°C. (1080°F.); ×1,000; etched 25 sec. with 4 per cent Picral; hardness

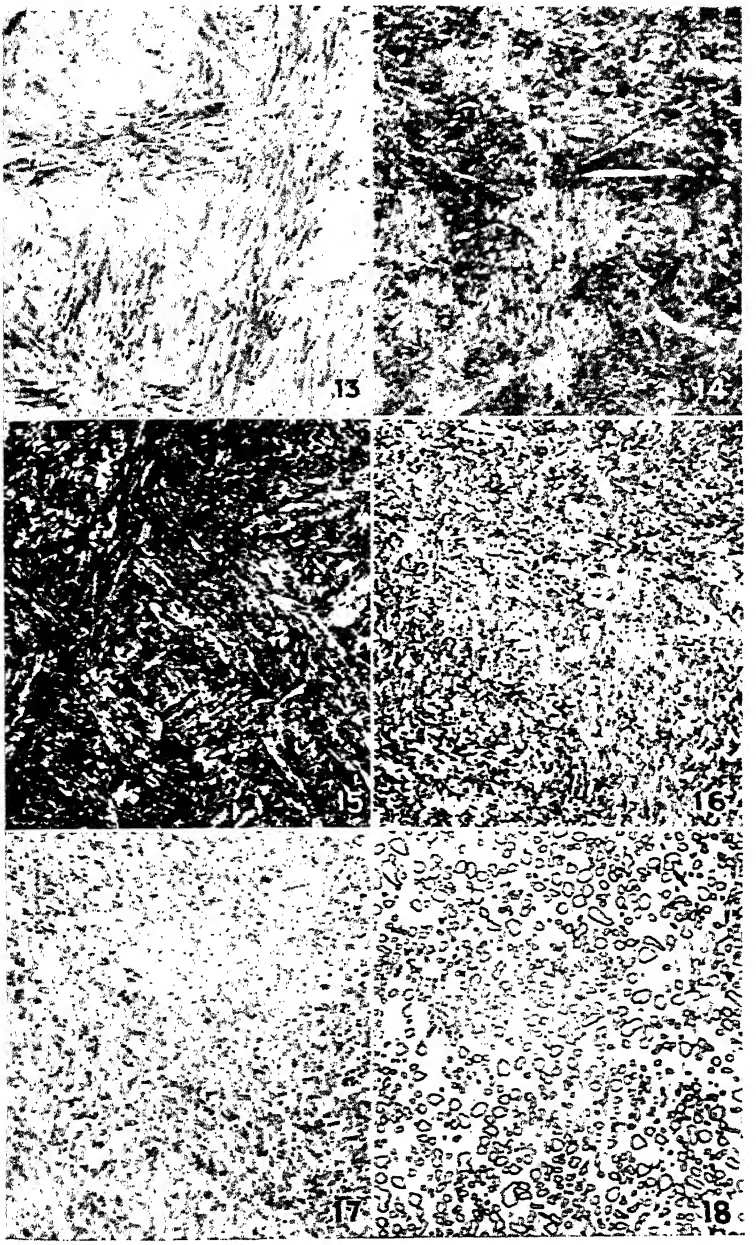

PLATE X. FIGS. 13–18.

C30. Carbides have grown to a size just about resolved at this magnification, and the ferrite matrix is now evident. The structure is termed *sorbite*.

Plate X, Fig. 17. Same as Fig. 13, reheated 4 hr. at 720°C. (1330°F.); ×1,000; etched 25 sec. with 4 per cent Picral; hardness C8. The continued growth of carbides has made them clearly resolved so that this structure is much whiter and clearer than the preceding one. It would be called fine *spheroidite*. Note that alignment of the carbide particles still reveals the sites of the former martensitic needles.

Plate X, Fig. 18. A commercial steel (S.A.E. 52100) which gave machining difficulties; ×1,000; Nital etch. This structure, with its rather coarse carbide particles widely spaced in a ferrite matrix, could have originated only by an extremely long subcritical spheroidizing anneal.

PROPERTIES

Commercial austenitic steel may be of the Hadfield type (1. to 1.5 per cent C and 10. to 14 per cent Mn) or of the chromium-nickel stainless type. Both are completely austenitic as quenched from around 1900 to 2000°F. (1050 to 1100°C.) and remain in that relatively soft, plastic condition while undisturbed at room temperature. Cold-work tends to induce both to transform, to some extent, to the body-centered lattice. In the relatively high-carbon Hadfield steel, the cold-worked structure becomes hard and abrasion resistant. The steel cannot ordinarily be machined since localized deformation in the vicinity of the tool soon develops a localized hardened structure that resists further cutting. The 18-8 grade of stainless also presents machining difficulties, although with a low carbon content, the transformed, somewhat magnetic, structure is not as hard as martensite. (Ferrite is strongly magnetic below 768°C., but austenite is almost completely nonmagnetic.) This partial transformation of the austenite is probably responsible for the high work-hardening capacity of the chromium-nickel stainless.

Both the Hadfield and 18-8 stainless steels, commonly designated as austenitic, actually contain austenite, ferrite, and an alloy carbide as stable phases under equilibrium conditions at room temperatures. The metastable quenched austenitic state,

however, will change only upon cold working or long-time treatments at relatively low temperatures (Plate XI, Fig. 2).

Carbide precipitation, as shown in Plate X, Fig. 2, may occur in the vicinity of welds or wherever temperature and time permit. The carbide is not Fe_3C but is predominantly a chromium carbide (containing up to 90 per cent chromium). The chromium for the precipitate must come from the austenite in the vicinity of the zones of precipitation, the grain boundary areas, which are consequently depleted of much of their nominal 18 per cent chromium. A corrosive solution in contact with the metal in this condition may act as an electrolyte, the depleted boundary zones as anodes, and the mass of the crystals as cathodes. The result is a marked intergranular electrolytic type of attack that may actually reduce the metal to a crystalline powder, or at least greatly diminish its strength. A similar difficulty in Duralumin alloys was mentioned on page 91. The problem has been solved for most commercial applications by the addition of a more powerful carbide-forming element than chromium, for example titanium or columbium (Stainless Types 321 or 347), which forms stable carbides and thus leaves the matrix with a uniform chromium content. The trouble has also been minimized by maintaining the carbon content below the solubility limit in the precipitation range (below 0.08 per cent in Stainless Type 304) or by reheating all welded sections to 1900°F. (1050°C., a temperature at which precipitated carbides redissolve in the austenite) and quenching. The last method is obviously impractical for large welded assemblies.

The presence of carbide envelopes in hypereutectoid carbon steels has already been mentioned as a source of brittleness. In the pearlitic structures, while the ferrite is continuous and occupies about 90 per cent of the structure, the 10 per cent carbide, disposed in thin lamellar plates, interrupts the continuity of the ferrite much more than the same amount of carbide disposed in the spherical or globular dispersion characteristic of sorbite. Consequently, although fine pearlite and sorbite may have the same hardness and appear to have similar black, unresolvable structures upon examination at moderate magnifications, the lamellar structure developed directly from austenite always shows less impact strength, particularly in the notch bar test which requires good local plasticity, than the globular

structure of the same phases, developed by quenching and tempering.

TABLE XI.—TENSILE PROPERTIES OF THE PRODUCTS OF AUSTENITE TRANSFORMATION[1]

Reaction temperature	Hardness, RC	Yield strength (0.2% offset), 1,000 p.s.i.	Tensile strength, 1,000 p.s.i.	Per cent elongation in 2 in.	Red. area, per cent	Pearlite spacing, Å.
700°C.	19	59	120	13	20	6,300
650	30	95	155	16	35	2,500
600	40	135	190	14	40	1,000
550*	38	132	185	12	30	
500	36	130	180	16	46	
450	40	150	190	18	54	
400	44	170	210	16	52	
350	48	190	230	13	44	

* Data variable in this temperature range.

Some typical tension test data, on specimens with a 0.25-in. diameter and a 1-in. gauge length (comparable to the usual 0.505-by-2-in. specimen), are presented in Table XI. These show a linear increase in strength properties with decrease in the reaction temperature (or decrease in the logarithm of the pearlitic spacing), from the A_1 to the A_1' temperature. There is a discontinuity of property changes in the vicinity of the nose of the S curve at around 550°C., but in the bainite region there again is a linear increase in strength with decrease in temperature. There appear to be two maxima in ductility, as shown by elongation or reduction in area values, one in the middle of the pearlite range and one in the middle of the bainite range. No data are included on martensitic specimens since it is almost impossible to get uniform loading and representative test data for this brittle structure. Data on the mechanical properties of tempered martensites are given in the "Metals Handbook."

More precise generalizations expressing the relation of structure to properties have been made (reference of Table XI) as follows:

[1] Data from Gensamer, Pearsall, Pellini, and Low, *A.S.M. Preprint* No. 19, 1941. Obtained on a eutectoid plain carbon steel (0.80 C, 0.74 Mn, 0.24 Si); corrected for recalescence during transformation.

1. Strength properties vary linearly with the austenite reaction temperature and the logarithm of the lamellar spacing of the resulting pearlite, and this spacing is proportional to the diffusivity of carbon at the reaction temperature.

2. The resistance to deformation of a metallic aggregate consisting of a hard phase dispersed in a softer one is proportional to the logarithm of the average length of straight path through the continuous phase. This rule has been found to apply to both pearlitic and spheroidized structures and extrapolation leads to reasonable carbide particle sizes for the finest, unresolvable, spheroidal carbide (tempered martensite) structures.

AUSTEMPERING

This is the name of a special heat-treating process which consists essentially of isothermally transforming austenite at a temperature between the range of fine pearlite formation (A_r' on the *S* curve) and martensite formation (A_r'').[1] The structures developed in this range are called *bainites* (page 143) which, in carbon steels, cannot develop in any specimen *cooled continuously* from the A_1 line to room temperature, whatever the rate. The transformation graph (Fig. 11, page 141) shows the range of hardness of bainite structures. At least in the lower part of the temperature range bainite has a hardness directly comparable to that of tempered martensite. Since this structure forms directly from austenite at an appreciably higher temperature than martensite, the microstresses developed in bainite are of a much lower magnitude (*cf.* microcracks in martensite, page 151). Bainite structures with a hardness of C50 have shown phenomenally high plasticity for hardened steel; 0.18-in. sections have shown a reduction of area of 35 per cent in tensile tests or absorbed 35 ft.-lb. of energy in impact tests, whereas tempered martensite, at the same hardness, shows less than 1 per cent reduction in area or only 3 ft.-lb. impact strength. However, it is only in this hardness range that the bainite structures show superior properties and then only in the case of carbon steels. In the range C40–45, the sorbitic structure is superior for the same reasons that it is superior to fine pearlite. In the hardness range required for cutting tools, C60–65, the bainite structures cannot be obtained. Other limitations of the process involve the size

[1] LEGGE, *Metals and Alloys*, **10**, 228, 1939.

requirements; sections must be thin enough to cool past the A_r' point rapidly enough to avoid the formation of fine pearlite, more expensive equipment is required to quench into a bath at around 250 to 400°C. and hold there a fixed time, and finally, normal variations among different heats of steel result in variable time requirements for transformation in the required temperature range.

QUESTIONS

1. Why is Hadfield manganese steel so well suited for applications requiring both abrasion resistance and toughness; *i.e.*, rock crushers, etc.? Why would the steel not be suitable for the nozzles of sand-blasting guns?

2. How might a spheroidized carbide structure be converted to (*a*) fine pearlite, (*b*) coarse pearlite?

3. Why is a sorbitic structure preferable to pearlite of equal hardness for use as an automotive connecting rod?

4. How might an 0.40 per cent carbon steel be treated to show (*a*) large masses of ferrite with islands of ferrite and spheroidized carbides. (*b*) uniformly distributed spheroidized carbides?

5. On the basis of photomicrographs shown in this section, state quantitatively the difference in time required for transformation of coarse austenite and fine austenite plus residual carbides at 710°C. (1310°F.). Which prior structure would give the finer lamellar spacing in the pearlite formed?

6. If a quenched high-carbon (martensitic) steel were placed in a furnace at 1500°F. (820°C.), what would be the effect of the prior structure on (*a*) the required austenizing time, (*b*) possibility of cracks from stresses associated with thermal gradients?

REFERENCES

"Metals Handbook," Heat Treatment of Metals, Relation of Design to Heat Treatment, Mass Influence in Heat Treatment, Principles of Heat Treatment of Iron and Steel.

Sachs and Van Horn, "Practical Metallurgy," A.S.M., 1940; (particularly for methods of analysis of residual stresses).

Thum, "Book of Stainless Steels," A.S.M., 1935.

The references cited in the text contain bibliographies which will lead to most of the important researches on the subject of austenite transformations. Many of the older textbooks (and, indeed, some of fairly recent publication) employ a terminology which differs from that used here and thus may tend to confuse the student. The older terminology, particularly usage of the terms *primary* and *secondary troosite* or *sorbite*, originated prior to researches of Bain and Davenport (published in the *Trans. A.S.M.* and *A.I.M.E.*, 1932–1940) which definitely established the mode of austenite transformation at different subcritical temperatures.

CHAPTER XI

HEAT-TREATED AUTOMOTIVE AND TOOL STEELS

The heat treatment of steels to obtain great hardness or other desired properties was an art practiced for literally thousands of years before any scientific knowledge of the process was available. However, a knowledge of the theory of structural changes, *i.e.*, a correlation of the iron-carbon diagram, the *S* curve, and the martensite tempering curve makes it possible to dispense with memorized "formula" for the treatment of each different type of steel. An appreciation of these three aspects of theoretical reasoning, as summarized on page 152, enables the metallurgist, confronted with a specific, undesirable microstructure, to prescribe a heat treatment, or an intelligently minimized series of tests for the determination of a treatment, that will produce any one of the large number of possible microstructures.

MACHINABILITY

Some steels are heat-treated before machining if the desired physical properties do not require high hardness. Most machining operations cannot be readily performed on steels of hardnesses greater than Rockwell C20–25 (BHN 200–250) although, by use of rugged, modern equipment for holding the work and tool rigid, simple cutting operations have been successfully accomplished on steels at hardnesses of C45 (BHN 425). In most cases where final hardness is to be above C25 and in the manufacture of all cutting tools, the metal is first machined to shape, then hardened to a martensitic structure, and finally tempered or drawn by reheating to the temperature required to give the specified physical properties. In these cases, the structure of the steel prior to machining is of considerable importance in determining the ease of cutting, tool wear, and the final surface finish on the machined part. It is not proposed to discuss here the variables of tool design, physical characteristics of tool steels, the rigidity of the work-holding device, and tool lubricants or coolants, although these factors might affect machinability more than the structure

of the steel being cut. Assuming that these conditions are all properly adjusted, a pearlitic structure will usually cut better than a sorbitic or a spheroidized structure. The lamellar structure is more brittle and the metal tends to shear immediately in front of the tool (along the line of cut) and the chips break off more readily, resulting in a cleaner type of cut. On the other hand, a very fine pearlitic structure is harder, requires more strength at the tool edge, and thus necessitates use of more powerful and rigid machines. The type of cutting operation is also a variable; the best structure for an intricate milling operation may not be best for drilling or thread-cutting operations.[1] A frequent compromise in structure is the use of a partially spheroidized pearlite, frequently called a *wormy* structure. The structures shown by Plate XI. Figs. 1 and 2, illustrate extreme divergences.

Methods of obtaining different types of structures are implicitly explained in Chap. X, a coarse pearlitic structure by slow furnace-cooling of austenite and finer pearlites by somewhat more rapid cooling. Spheroidized structures are, of course, obtained by tempering of martensite, but when this structure is desired for machining purposes it is usually obtained by reheating fine pearlite (normalized structure) below the A_1 temperature. This method depends on the surface tension forces of the carbide phase which effectively break up the lamellar distribution and gradually agglomerate the carbide to approximately spherical shapes. Moderately short times only partly spheroidize the lamellae; quite long times are required to complete the process. The spheroids formed are somewhat related in size to the pearlite; specifically, a coarse pearlite cannot be treated to give a fine spheroidite. Heating slightly above the A_1 and then cooling below will naturally break up a coarse pearlitic structure more rapidly. Finally, isothermal transformation treatments have been successfully employed to obtain more machinable structures; *i.e.*, heating into the austenitic range, furnace-cooling to 1150 to 1250°F. (620 to 680°C.), holding there 1 to 4 hr., and then air-cooling.

EFFECT OF ALLOYING ELEMENTS

Elements other than carbon and iron in steel may be present either in solution in ferrite (copper, nickel, aluminum, silicon), in

[1] WOLDMAN, *Iron Age*, **147**, No. 25, p. 37, No. 26, p. 44, 1941.

the carbide when sufficient carbon is present (tungsten, molybdenum, titanium, vanadium), distributed in both basic phases (manganese and chromium), or present as special compounds (sulphides, selenides, oxides, etc.). These elements all have some effect on the positions of boundary lines in the iron-carbon diagram, specifically on the carbon content of the eutectoid and the critical temperatures. For example, 6 per cent chromium added to iron shifts the eutectoid concentration to about 0.45 per cent carbon and raises the A_1 temperature to about 750°C. (1380°F.). The effect on critical temperatures may appear to be anomalous in many steels; while nickel depresses both the A_r and A_r temperatures, molybdenum raises the A_r temperatures and depresses the A_r temperatures. The reason for this effect is related to the increased sluggishness of the eutectoid reaction in steels in which the alloying element both dissolves in ferrite and forms a stable carbide that is slow to dissolve in, or precipitate from, austenite. Published data for critical points, *e.g.*, those in the 1940 ed., "S.A.E. Handbook," are generally based on the transformation temperatures obtained on fairly rapid heating or cooling. They do not apply for heat treatments in which the steel is held at temperature for an appreciable time. For example, a highly alloyed (British) aircraft steel of 4 per cent nickel, 1.25 per cent chromium, and 0.5 per cent molybdenum with 0.25 per cent carbon was reported to have an A_{c_1} of 1320°F. and an A_{c_3} of 1395°F. It was found that, upon heating $^1/_2$-in. sections to a series of temperatures and holding for 2 hr., the steel became a mixture of austenite and ferrite at 1225°F. (thus, it was above the A_1 temperature) and became completely austenitic at 1300°F. (necessarily, it was above the A_3 temperature). A similar difference of from 25° to 100°F. between the A_r temperatures on a continuous heating cycle and those obtained on holding at temperature is found in most published temperature data on critical points of alloy steels.

Associated with an effect on critical temperatures, a pronounced alteration in the microstructures is frequently observed. For example, a hacksaw steel, containing 1 per cent carbon and about 1 per cent tungsten, does not develop a pearlitic structure upon isothermally transforming between the A_1 and A_r' temperatures. The presence of a strong carbide-forming element, such as tungsten, apparently prevents any development of the lamellar

carbide structure, and the carbide phase comes out of austenite in the form of irregular masses. On the other hand, this effect may result from incomplete homogenization of the austenite, since tungsten carbide is difficult to dissolve completely, and residual carbides may serve as nuclei upon which the eutectoidal carbide forms, resulting in the abnormal structure. This may also be true of molybdenum, but the equivalent chromium steel, S.A.E. 52100 with 1 per cent carbon and about 1 per cent chromium, forms pearlite by use of normal austenitizing times and temperatures.

The theory of the effect of alloying elements on hardenability has been considered on page 148. If the purpose of alloying is merely to increase the depth of useful hardness or permit the same depth to be obtained by a slower quench (therefore with less residual stress), it has been found that the addition of small amounts of many elements is more effective than a large addition of one element, particularly the use of combinations of manganese, chromium, molybdenum, or vanadium. (The addition of many elements generally is more effective in raising the strength and hardness of solid solutions than an equivalent total addition of a single element.) The reason for this behavior is that large amounts of these elements form sluggish carbides which, since they do not dissolve fully in austenite, do not contribute to any retardation of transformation at the A_r' whereas small amounts dissolve fully and complicate the diffusion process necessarily accompanying the pearlite reaction. In addition, the hardenability effects of several elements are multiplicative, while increased amounts of one element are additive in increasing hardenability. An idea as to the relative effects of different alloying elements on hardenability is suggested by the amounts required to increase by 50 per cent the size of a section hardening all the way through when other factors, such as austenitic grain size and quenching rate, are constant. Of individual elements, this would require: 0.002 per cent boron, 0.05 per cent vanadium, 0.14 per cent manganese, 0.16 per cent molybdenum, 0.20 per cent chromium, about 0.70 per cent silicon, and about 1.40 per cent nickel. Vanadium contents above 0.15 per cent may actually decrease hardenability, *i.e.*, contribute to shallow hardening, owing to the relative stability or slow rate of solution in austenite of vanadium carbides. On the other hand, manganese seems to

linearly increase hardenability up to quite high manganese contents; about 1.8 per cent permits a steel to harden throughout a section five times as thick as a comparable 0.20 per cent manganese steel. The required amounts of silicon and nickel are only approximate since they are based on lengthy extrapolations of limited data.[1]

QUENCHING RATES

The effect of cooling rate is of sufficient importance to demand inclusion of the following table (from Grossman) in which the higher numbers represent more severe quenching. The table demonstrates, more or less quantitatively, the value of movement of the cooling medium in speeding up the quenching rate, particularly the rate in the important temperature range of 723 to about 550°C.

	Oil—60°C.	Water—20°C.	Brine—20°C.
No circulation of liquid or agitation of piece	0.2	1.0	2.0
Mild circulation (or agitation)	0.3	1.1	2.1
Good circulation	0.4	1.4	
Strong circulation	0.6	1.8	
Violent circulation	1.0	4.0	5.0

Differences in the efficiency of the several types of quenching baths in conducting heat from the metal are related to the "wetting" tendency of the liquid, its vaporization characteristics or tendency to form vapor blankets which insulate the steel, its ability to remove scale which also acts as an insulator, and to other physical variables. Naturally the temperature of the medium is of importance, particularly with reference to its boiling point; *e.g.*, hot water cools steel more slowly than does hot oil.

There are noticeable differences among various types of oils, depending on their relative viscosities, vapor-forming characteristics, and the chemical changes occurring with continued use. There are differences between waters, particularly between fresh tap water which contains dissolved air, and water that has been used for some time (or distilled water) with no air to come out of

[1] GROSSMAN, *A.I.M.E. Tech. Pub.* 1437, 1942.

solution at the steel surface and thereby slow up heat transfer. Finally, the concentration of a brine or caustic solution is of importance, and tests have shown that 9 per cent sodium chloride or 3 per cent sodium hydroxide solutions are most favorable for elimination of soft spots caused by vapor pockets at the steel surface in the early stages of cooling. Incidentally, the increased speed of cooling of brines does not depend on the use of lower temperatures of the bath but is related to its action in removing surface oxide or scale and in suppressing vapor formation at the steel surface.

FLAME-HARDENING AND WELDING

The theoretical discussion of structural and property changes accompanying the heating and cooling of steels applies not only to heat treatment of complete sections but also to intentional heating of localized surface areas, as in induction-hardening[1] and flame-hardening processes. No structures are reproduced here for they would be found nearly to duplicate those produced by normal heat treatments of similar steels. In both processes, uniform control of actual temperatures in the austenitic field may be somewhat difficult to achieve, but the very short time at temperature minimizes grain growth of the structure. Hardenability is seldom an important factor since a depth of hardening of about $\frac{1}{4}$ in. is the maximum usually desired. Distortion is frequently troublesome in flame hardening since the entire surface to be hardened cannot always be brought to temperature at once. When large sections are treated, the flame proceeds slowly over the surface, with the quenching liquid following closely behind the torch. Considerable experience is required in regulating flame intensity, rate of movement, and sequence of movement over the surface so as to austenitize to a sufficient depth for proper hardening, to minimize distortion, and to avoid overlapping with a structural discontinuity at the junction of two successive passes. The induction-hardening process where applicable, avoids this difficulty by heating the entire surface simultaneously. This method is limited by the cost of the requisite electrical equipment and by the simplicity of shape required in parts to be treated. It is being very successfully employed for rounds, particularly the bearing surfaces of automotive or aircraft crankshafts.

[1] CONE. *Metals and Alloys*, **9**, p. 1, 1938.

Welding is essentially a chill-casting process involving small amounts of liquid metal, which, in contrast to ordinary castings, is fused to the "mold" or, in this case, the section being welded. The fusion requirement means that the base metal in contact with the weld deposit is at least momentarily heated to the proximity of its melting point with a consequent temperature gradient from this zone to a distant point in the base section at which the temperature rise is insignificant. Thermal gradients have already been mentioned as sources of distortion or internal stresses, or both, and it is for this reason that welded joints are given a stress-relief anneal if service requirements are severe. When possible, the entire welded section may be heated into the stress-relief annealing temperature range (1100 to 1300°F.), but in large assemblies, it is possible only to "flame-anneal," *i.e.*, reheat locally with a torch. If the steel has air-hardening characteristics, resulting from the presence of alloying elements, the zone adjacent to the weld may become partially martensitic as a result of being heated into the austenitic field and cooled rapidly by the flow of heat into adjacent cooler sections. High stresses in a localized martensitic zone are very likely to cause crack formation and failure under ordinary service conditions (see Plate XI, Fig. 7). This difficulty can be avoided by preheating the entire structure, before welding, to about 500 to 700°F. The warm base metal slows up the quenching effect of heat flow from the zone next to the weld into the adjacent colder metal.

HIGH-SPEED STEELS

There are several thousands of different tool steels if classified by trade names, several hundreds if classified by composition, and perhaps twenty or so if classified by *types* of alloy composition. The structures and properties of a majority of these are explicable on the basis of the material already presented. The so-called "high-speed" steels depart significantly in many ways from plain carbon, low or moderately alloyed grades. The following discussion applies generally to the common types of steel that can maintain their hardness at low red heats; *viz.*, **I**, 14 to 18 per cent W, 4 per cent Cr, 1 to 2 per cent V; **II**, 4 to 6 per cent W, 4 to 6 per cent Mo, 4 per cent Cr, 1 to 2 per cent V; **III**, 0 to 3 per cent W, 6 to 8 per cent Mo, 4 per cent Cr, 1 to 2 per cent V. All of these types contain from 0.6 to 0.8 per cent carbon and also may be

made with 5 or 8 per cent cobalt present. Carbon contents on the high side of the range and the presence of cobalt decrease toughness and increase abrasion resistance. Chromium and vanadium are common to all grades, and either tungsten, molybdenum, or a combination of both, in the amounts noted, is requisite for development of the red-hardness property. Within the composition ranges shown, it is evident that 1 per cent of molybdenum is roughly equivalent to 2 per cent of tungsten.

An equilibrium phase diagram of alloys as complicated as these types of steel cannot be drawn and explained in a simple manner, but if the left hand of the Fe-Fe_3C system (page 110) be considered as (Fe + 18W + 4Cr + 1V) and a diagram drawn for this metallic mixture with carbon additions, the system may be portrayed simply and not too inaccurately. In this case, the A_{c_1} temperature would be about 1540°F. for the 6:6 steel (II); the eutectoid carbon content might be close to 0.2 per cent, the saturation solubility of carbon in austenite at the eutectic temperature would be about 0.5 per cent, and the eutectic temperature at approximately 2350°F. The eutectic is between austenite and an alloy carbide (Fe, W, Mo, Cr, V)$_6$C and the eutectoid between an alloyed ferrite and the same carbide. This hypothetical diagram explains the necessity of using austenitizing (or hardening) temperatures close to the eutectic temperature. If the steel were hardened from just above the A_{c_1}, the resulting martensite would contain only about 0.2 per cent carbon and, consequently, would not be very hard. The higher the temperature is raised, the more carbides go in solution, but they are not completely dissolved at any temperature below the eutectic. If this temperature is exceeded, the carbides enter the liquid phase and then, upon cooling, form a brittle eutectic envelope around the austenite grains (*cf.* "burning" of aluminum alloys, page 82). The high-speed steels can be heated close to the eutectic temperature without excessive grain growth because residual stable carbides, which restrict grain coarsening, are present in large amounts until the temperature approaches 2300°F.

If steel specimens are quenched from 2275°F. into salt or lead baths at temperatures from 1500 to 200°F., and isothermally transformed in a manner comparable to carbon steels (Fig. 11, page 141), the high temperature of most rapid transformation is 1400°F., equivalent to the A_r' point. Here, the austenite trans-

formation starts after approximately 10 min. has elapsed and is completed in about 4 hr. to a dark-etching structure showing small carbide spheroids in ferrite. In the range, 1000 to 700°F. (equivalent to just above the A_r''), austenite has been found to be unchanged at the end of 12 days when tests were stopped.[1] At 600°F. and below, the transformation product is acicular and hard; C55 in the range 600 to 500°F. and C65 below 300°F. Normal quenching from 2275° in oil gives a structure which consists of about 25 per cent residual austenite and 75 per cent tetragonal martensite, with a hardness of C60–65. The lower as-quenched hardness is obtained when the austenitizing treatment is performed near the upper limit of the normal temperature range. This treatment results in coarser austenitic grains, which contain more dissolved carbon and consequently transform more slowly and leave more residual austenite.

Tempering of the quenched high-speed steel is at first analogous to the drawing of a quenched carbon steel at low temperatures (below 350°F.). The residual austenite in the high-speed steel remains unchanged, tetragonal martensite changes to the cubic form, and cementite, Fe_3C, precipitates and agglomerates in this martensite with a decrease in hardness of the structure.[2] This process continues up to temperatures in the vicinity of 750°F. The precipitation of cementite, rather than the complex alloy carbide, is explained by the very slow diffusion of the alloying elements, particularly tungsten, molybdenum, and vanadium, which forces the carbide to form from the element that is most readily available, iron. On raising the temperature to 1050°F., the carbon tends to go over to its more stable carbide, the complicated (Fe, W, Mo, Cr, V)$_6$C, which forms as a fine dispersion and increases the hardness of the structure, an effect known as *secondary hardness*. The increase is more marked in specimens quenched from the highest temperature since these contain the most dissolved carbon. This effect in the case of a Type II steel is:

Quenching temperature	As-quenched hardness	Secondary hardness
2225°F. (2 min.)	C66	C63 (1 hr. at 1050°F.)
2275°F. (2 min.)	65	65 (1 hr. at 1050°F.)
2325°F. (2 min.)	62	67 (1 hr. at 1050°F.)

[1] HAM, PARKE and HERZIG, *Trans. A.S.M.*, **29**, 623, 1941.

[2] COHEN, *Trans. A.S.M.*, **27**, 1015, 1939.

The secondary hardness is also increased by the breakdown of residual austenite upon cooling from the tempering treatment. Since the martensite so formed involves an expansion in a rigid structure, the danger of cracking may be greater on cooling from the draw than on cooling from the high-temperature quench, at which time martensite forms in a plastic austenitic structure.

The stability of the highly alloyed austenite at about 1000°F., shown by the isothermal transformation work (no change for 12 days at this temperature), is commercially important in two ways. If a heavy or complicated section is quenched from about 2300°F., quenching stresses alone (apart from those associated with martensitization) may occasionally cause trouble. In this event, it would be advisable to quench from 2300°F. to a bath at 1000°F., hold until temperature equilibrium is achieved, and then quench to room temperature. This procedure would minimize quenching stresses and still achieve the same results as a direct quench. Second, if the steel is not cooled to room temperature, no appreciable austenite decomposition will occur and, on tempering at 1050°F., no appreciable alloy carbide precipitation will be obtained. If, as in this case, the austenite remains substantially unchanged, the advantages of secondary hardness are not gained.

Straightening operations are most safely and readily performed while a relatively large amount of plastic austenite is present in the structure, *i.e.*, while the metal is still warm after quenching from the high temperature. Cracking after the draw is most likely to occur if the steel is permitted to stand too long before tempering.

MICROSTRUCTURES (PLATE XI)

Plate XI, Fig. 1. Alloy steel (1.0 per cent Ni, 0.5 per cent Cr, 0.5 per cent C); ×1,000; Picral etch. This steel is used for small screws in an aircraft engine, and specifications require an extremely good surface on the threads and at the base of the threads to ensure adequate fatigue strength. The structure shown represents stock that was readily cut and from which few parts were rejected. It shows excess ferrite surrounding moderately coarse pearlite, both derived by slow cooling of a coarse grained austenite.

Plate XI, Fig. 2. Same alloy steel (1.0 per cent Ni, 0.5 per cent Cr, 0.5 per cent C); ×1,000; Picral etch. Stock from a different

source for the same aircraft screws machined with difficulty. Over 50 per cent of the parts made were rejected as having an inferior finish, although tooling was identical to that employed for the previous steel. This spheroidized structure has exactly the same hardness (Rockwell B90) as that above, but the continuity of the ferritic structure here confers greater plasticity to the aggregate. The spheroidal structure can be changed to a pearlitic type, but a high temperature (1700°F. for ½ hr.) is required to dissolve the carbides in austenite, presumably because of the chromium content, although in any case a moderately coarse spheroidal structure must be heated to a higher temperature, or held a longer time, to transform to homogeneous austenite.

Plate XI, Fig. 3. Carbon tool steel (1.20 per cent C); ×500; Nital etch. This structure of the raw stock, before hardening, shows finely spheroidized carbides in a ferritic matrix although details are not too evident at this relatively low magnification. However, traces of the former austenitic grain boundaries are visible by reason of a greater carbide concentration at these areas. This structure must have originated as follows: the steel was normalized (from above the A_{cm} line) and then reheated below the critical temperature for spheroidization of the fine, lamellar carbides. Probably cooling from the austenitic field through the critical temperature was too slow to prevent the separation of excess carbide in the form of envelopes around the austenitic grains. The subsequent spheroidization treatment broke up the continuity of the carbide envelopes but left a "string of beads" of carbide in a network form. This structure is not eliminated by hardening from the usual temperature between the A_{c_1} and A_{cm} lines; the coarser carbides, aligned as grain boundary envelopes, are not dissolved, and their residual presence in a network results in a more brittle tool, subject to chipping at the cutting edge or other difficulties which are summarized in the words "poor tool performance."

Plate XI, Fig. 4. S.A.E. 4335 steel (1.8 per cent Ni, 0.8 per cent Cr, 0.3 per cent Mo, 0.35 per cent C); ×1,000; Nital etch. This structure is that of the steel after quenching in oil from 1550°F. and tempering to a hardness of C50. Employed in an antiaircraft gun, this steel is used for a part subjected to battering impact loads. The section is too large to be "austempered," yet hardness is vital and as much toughness as possible is desired.

This nickel-chromium-molybdenum steel has considerably greater toughness at a Rockwell of C50 than most other available carbon or alloy types.

Plate XI, Fig. 5. Overhardened S.A.E. 52100 steel (1.25 per cent Cr, 1.00 per cent C); ×1,000; Nital etch. This steel, originally developed for ball bearings, is now widely used where high hardness and good depth of hardening is essential. The structure shown was from a defective part in an aircraft-engine clutch; this section showed brittle chipping of corners which had been designed with rounded edges to avoid such trouble. The brittleness is undoubtedly related to the extremely coarse martensite which must have been derived from very coarse austenite. This structure shows no residual carbides although it is strongly hypereutectoid (1.25 per cent chromium lowers the eutectoid carbon content to about 0.70 per cent), and it is believed the part was heated above 1800°F. The steel part had been heated, by a commercial heat treater, in a salt bath and it is hypothesized that a high-speed steel bath with a minimum operating temperature of about 1750°F. was employed in order to avoid the trouble and expense of changing to a normal steel hardening salt bath, the type required for treating this steel at the proper temperature of 1550°F.

Plate XI, Fig. 6. Properly hardened S.A.E. 52100 steel; ×1,000; Nital etch. This structure is of the same steel when the original stock was quenched in oil from 1550°F. and drawn to the same hardness as above, Rockwell C62. The background is extremely fine black martensite (it might be called troostite except for the high hardness) which would be much tougher than the overheated coarse martensite. In addition, the presence of residual, undissolved carbides (the white spheroids) considerably increases resistance to abrasion.

Plate XI, Fig. 7. S.A.E. 3140 steel (0.40 per cent C, 0.75 per cent Mn, 1.25 per cent Ni, 0.60 per cent Cr), section from a generator axle broken in service; ×10; Nital etch. This macrograph, taken at the base of a keyway notch on a 2-in. shaft, may be interpreted as follows: The original keyway was cut somewhat oversize. To correct the error, a layer of ordinary low-carbon steel was deposited by welding at the base. Subsequent machining apparently disclosed porosity, or other defects, in the first deposit, so a second layer of metal was welded over the first. The right-hand edge of the micrograph represents the base of the

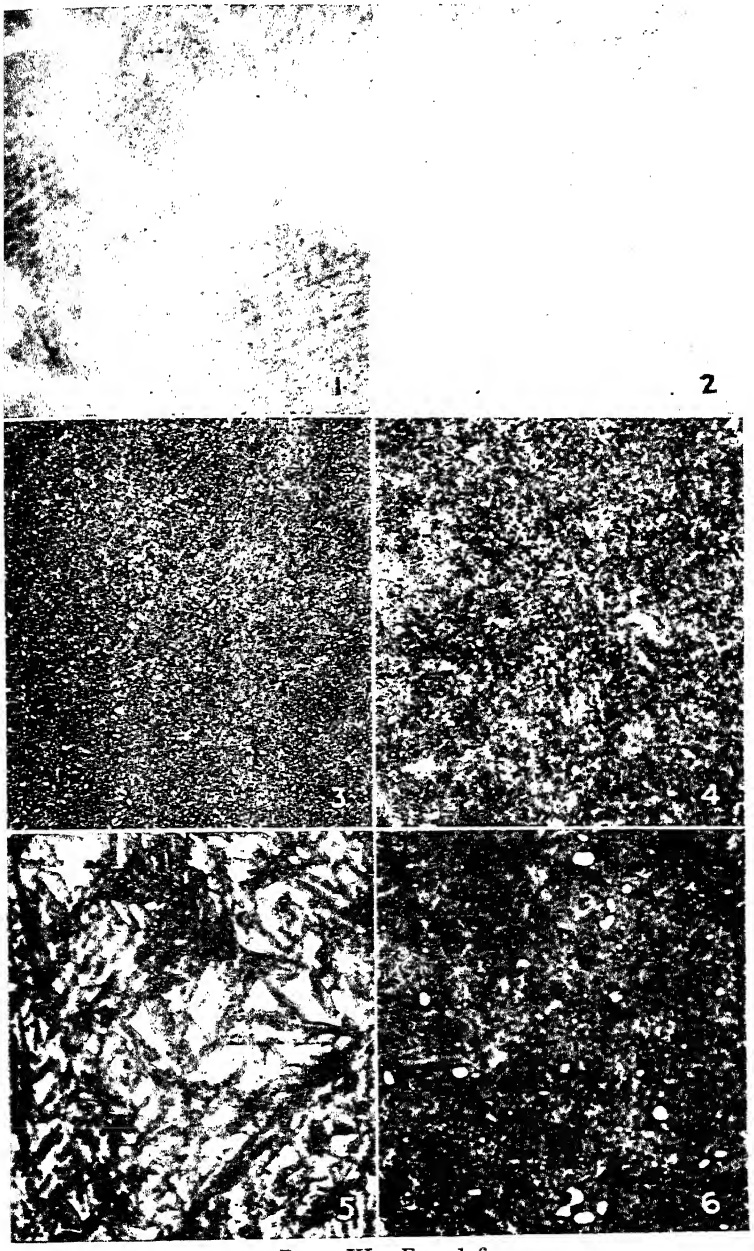

PLATE XI. FIGS. 1–6.

keyway, and ¼ in. to the left of this, an open line *A* shows the poor junction of the first and second weld deposits (weld metal, of low-carbon steel, is white). About 2 in. further to the left, at *B*, a sharp discontinuity in shading indicates the junction between the alloyed steel base and the first weld deposit. To the immediate right of *B*, a higher magnification disclosed evidence of carbon diffusion from the base metal into the low-carbon weld metal. To the left of *B*, there is a dark zone which shows a sharp transverse crack, followed at *C* by the normal base metal. This zone (*B* to *C*) was heated to the austenitic state by the first welding operation, and cooled rapidly by the mass of the main section, it became martensitic and probably highly stressed as well. The second weld deposit and thermal gradients related to the rapid localized heating probably initiated the crack in the martensitic structure which also was tempered to its present dark etching state before finally cooling again to room temperature.

Plate XI, Fig. 8. Section in vicinity of *C* from Fig. 7; ×1,000; Nital etch. A higher magnification of a section in the vicinity of *C* shows an area to the right in which the alloy became completely austenitic and cooled rapidly enough to become martensitic. It is in this section (although farther to the right, beyond this field) in which the crack shown in the micrograph above was formed. In between the martensitic section and the unaffected base metal at the left, there is a zone of metal which apparently became austenitized at a sufficiently high temperature for grain growth to have occurred, as evidenced by the ferrite which separated at the austenitic boundaries on cooling. The separation of the ferrite is in itself evidence that this narrow zone cooled slowly enough to avoid martensitization. Here, within a narrow zone of about 0.003 in., relatively unaffected metal, an area of grain growth, and an area of tempered martensite are visible.

Plate XI, Fig. 9. Oxidation-resistant stainless steel (20 per cent Cr, 12 per cent Ni) at a welded joint; ×50; etched with 1:2:3 parts of HNO_3, HCl, and glycerin. In this micrograph, the dark, fine-grained structure at the right side represents the weld deposit (also of 20:12 steel), while at the left the original structure of the base metal sheet is visible. In the intermediate zone, the structure shows the effect of being heated close to its melting point. This steel is largely austenitic, although some alloyed ferrite or body-centered iron is visible as the darker structure, showing a

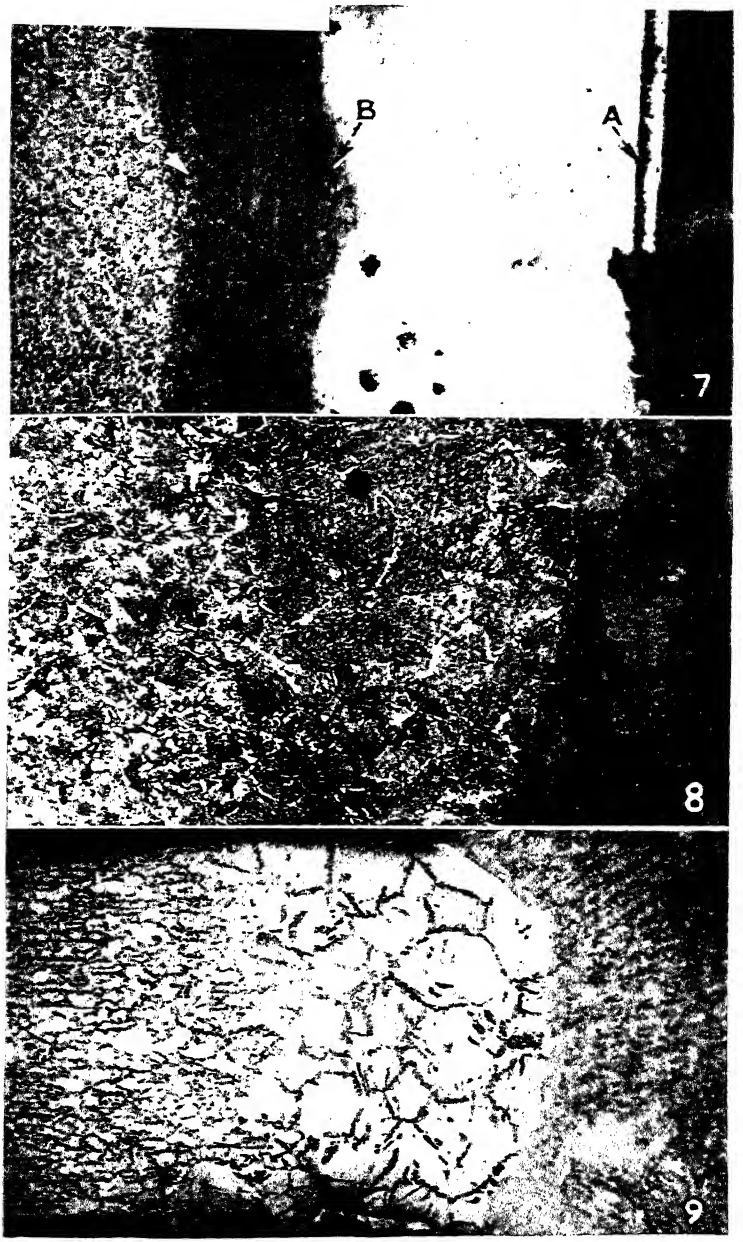

PLATE XI. FIGS. 7–9.

grain boundary network distribution. In the heat-affected zone there has been a pronounced grain growth and, associated with this, a weakening of the structure. This is the reason why in most tests of sound, welded specimens, fractures occur in the coarsened structure adjacent to the weld, rather than in the fine-grained, or equivalently, the chill-cast weld deposit.

Plate XI, Fig. 10. Fine-grained high-speed steel (Type II or 6:6), quenched from 2250°F.; ×1,000 Nital etch; C66. After quenching from this hardening temperature, slightly below the normal value of 2275°F., many residual, undissolved alloy carbides of $(Fe, W, Mo, Cr, V)_6C$ are present in the structure, and the austenite grain size is considerably smaller than for the specimen shown in Plate XI, Fig. 12. Although this structure is predominantly martensitic, the needlelike or acicular characteristic is not noticeable.

Plate XI, Fig. 11. The fine-grained high-speed steel (Fig. 10) after tempering 2 hr. at 1050°F.; ×1,000; Nital etch; C64. The precipitation of alloy carbides and decomposition of residual austenite result in this structure's etching more rapidly than Fig. 10 and to a black aggregate in which the martensitic needles are too small to be evident. The white spheroids are the residual, undissolved alloy carbides, unaffected by the tempering treatment. Since a Nital etch of a tempered high-speed steel will not reveal the size of the former austenitic grains, a special etch (Snyder's reagent, 7 per cent HCl and 3 per cent HNO_3 in alcohol) may be used to show the former austenitic grain boundaries and yield evidence as to the actual temperature attained in hardening a specific part.

Plate XI, Fig. 12. Coarse-grained high-speed steel (Type II or 6:6), as quenched from 2325°F.; ×1,000; Nital etch; C61. There are only a few undissolved alloy carbides in this martensitic-austenitic structure. Some traces of eutectic melting are visible at the austenitic grain boundaries although the burning is not very pronounced and would not be detectable in the tempered structure (next micrograph). Quenched from a higher temperature than the specimen of Plate XI, Fig. 10, and thus with more carbon in solution in the austenite, this specimen has more retained austenite and is, therefore, softer.

Plate XI, Fig. 13. The coarse-grained high-speed steel after tempering 2 hr. at 1050°F.; ×1,000; Nital etch; C66. Martensite

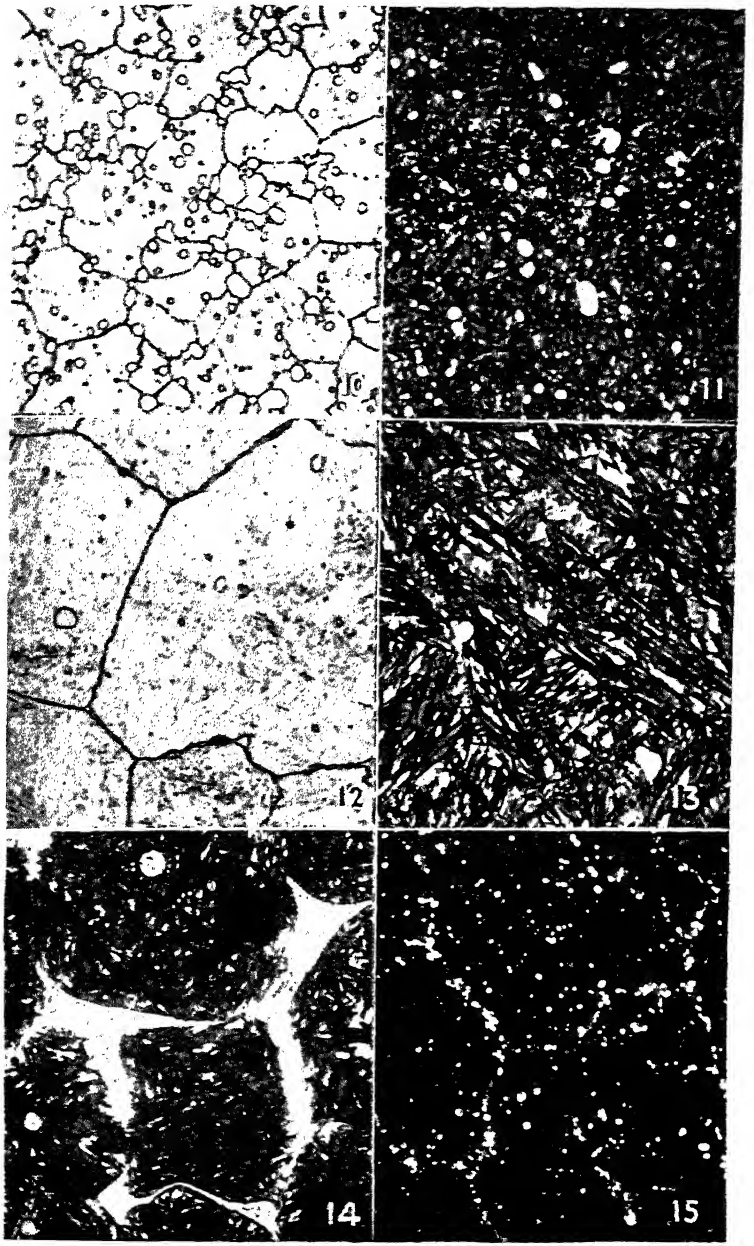

PLATE XI. FIGS. 10–15.

needles forming in a coarse-grained austenite are always more readily resolved than the needles in a fine-grained structure. Although more evident and preferable for demonstrating the nature of martensite, they are decidedly not preferable for most uses. This structure is evidence that the tool was *overhardened*, *i.e.*, heated at the upper limit of the permissible range. It would have better cutting properties than Plate XI, Fig. 11, if the greater brittleness of this structure did not cause chipping or crumbling of the cutting edge or if the tool did not snap under an impact load. The special etch (Snyder's reagent) would reveal the grain size of this structure better than it would that of a fine-grained aggregate and would also reveal the incipient melting.

Plate XI, Fig. 14. Overheated or burnt high-speed steel (Type III or 2:8 W-Mo) quenched from 2350°F. and tempered at 1050°F.; ×1,000; Nital etch; C65. When high-speed steel is heated above its eutectic temperature, the liquid phase which forms at grain boundaries is of nearly eutectiferous composition and upon quenching solidifies as a brittle eutectic in which the carbide is the continuous phase. This structure, formed by quenching, is naturally much finer than, and readily distinguished from, the eutectic present in the cast alloy or in inadequately hot-worked metal. As in all cases of *burning*, the eutectic is predominantly located at grain boundaries, particularly at the junction of three grains, although some spherical liquid pools, formed within the grains, now show a *rosette* eutectic structure. Note the coarse austenitic grain size (now, largely coarse martensite). The brittle eutectic network makes the entire structure brittle, and the metal is ruined as a tool. It cannot be readily reclaimed and is ordinarily useful only as scrap for remelting.

Plate XI, Fig. 15. Properly hardened (2275°F.) and tempered (1050°F.) high-speed steel, Type II (6:6); ×1,000; Nital etch; C64. This structure shows an undesirable distribution of the coarse carbides, present originally in the form of a eutectic network which surrounded the austenitic grains during solidification. Since these carbides cannot be completely dissolved in the solid alloy, hot-working (forging and upsetting) must be relied upon to break up this distribution and, in this specimen, the hot-working apparently was insufficient. In some very inadequately hot-worked (or cast) structures, these carbides may be seen in the

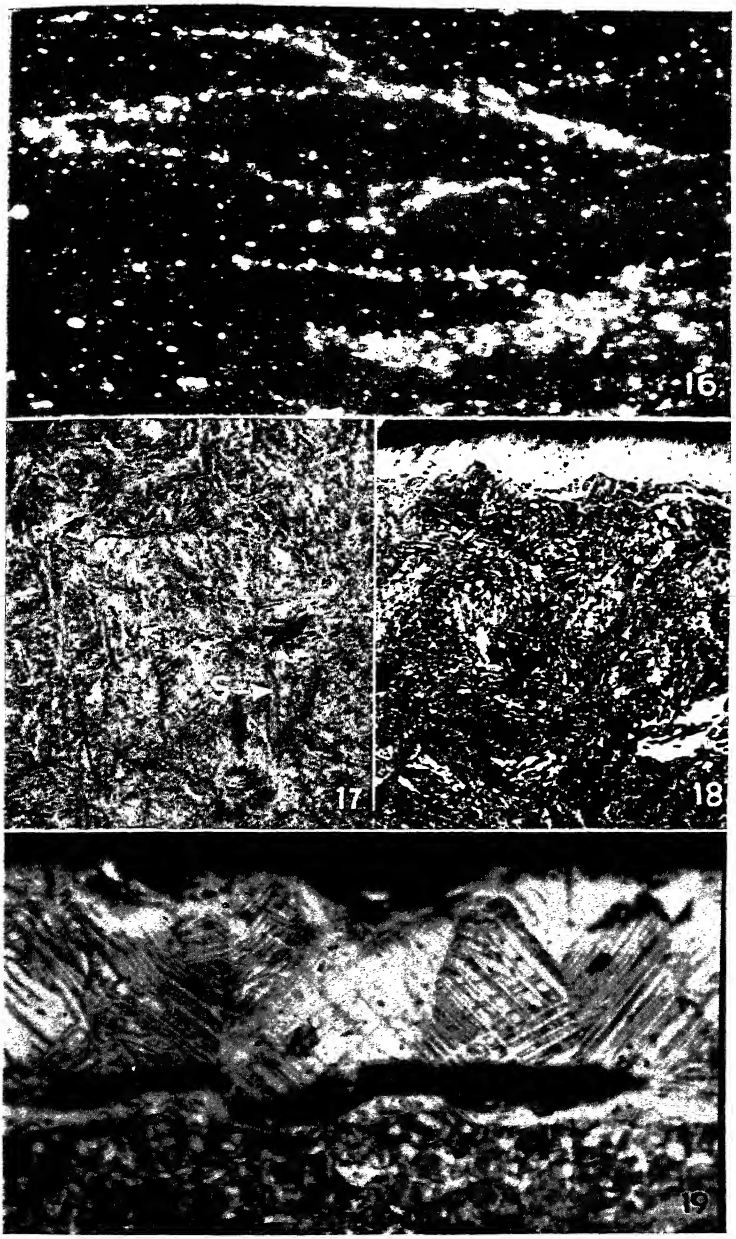

PLATE XI. FIGS. 16–19.

form of a coarse eutectic. This is a transverse section of a broach made from a 2 in. diameter bar.

Plate XI, Fig. 16. A longitudinal micrograph of the same specimen as Fig. 15; ×1,000; Nital etch. The transverse section of the tool showed an equiaxed grain boundary distribution of undissolved carbides. This is a view of the same tool but with the polished section parallel to the long axis of the broach (longitudinal). The carbide distribution is, of coarse, an indication of the direction of hot-working, and here the envelopes, instead of indicating an equiaxed structure, show characteristically elongated grains. The structure is frequently termed *hooked* carbides.

Plate XI, Fig. 17. Carburized free-machining steel, S.A.E.-X1315 (0.15 per cent C, 1.5 per cent Mn, 0.128 per cent S); the case after hardening and tempering; ×500; Nital etch; C60. This low-carbon, high-manganese free-cutting steel after carburizing, quenching, and drawing shows a typical tempered martensitic structure in the case, together with some manganese sulphide inclusions (*S*).

Plate XI, Fig. 18. Case of nitrided steel (0.24 per cent C, 0.55 per cent Mn, 1.20 per cent Al, 1.10 per cent Cr, 0.25 per cent Mo, 3.50 per cent Ni) after normal ammonia treatment of 48 hr. at 975°F.; ×200; Nital etch. This represents a good nitrided case with an extremely high degree of hardness. The immediate surface shows a characteristic white layer of somewhat lesser hardness than the nitrided zone immediately below it. It is believed that the atomic nitrogen, which diffuses into the metal during the ammonia treatment, forms an aluminum nitride with a high degree of dispersion (aluminum is always present in amounts of about 1 per cent in steel which is to be nitrided). This particular grade of steel for nitriding has age-hardening characteristics which seem to be associated with the combination of nickel and aluminum. Not only does the long nitriding treatment at 975°F. increase the hardness of the surface to an extent comparable with other grades but, simultaneously, precipitation of a phase (of unknown character) occurs in the body of the metal not reached by nitrogen. This results in an increase of mechanical strength and hardness of the core which accompanies the surface hardening (*e.g.*, tensile strength of 130,000 p.s.i. increased to 190,000 p.s.i., Brinell hardness from 275 to 415).

Plate XI, Fig. 19. Nitrided case of same grade of steel as Fig. 18 but on an originally severely decarburized surface; ×200; Nital etch. A decarburized steel, slowly cooled from above the A_1 temperature, usually shows columnar grains of ferrite extending until they encounter the normal pearlitic structure. This does not mean that decarburization removes all the carbon to a certain depth at which it suddenly increases to the normal value, but, when a structure with a carbon gradient cools slowly, ferrite forms first at the point in the structure which has the highest A_3 point (compare with banding, page 130) and continues to grow, forcing carbon away from the austenite-ferrite interface, until the entire structure transforms. When the decarburized, columnar ferrite grains are subsequently nitrided, *growth* of the structure causes a strong outward force to develop. If the structure is weak, as in this case, the net result may be *spalling* of the case. Note how spalling (or cracking of the case) follows the grain boundaries at the decarburization interface. The very large ferrite grains permitted very coarse nitride needles to form during cooling from the treatment.

PROPERTIES

Physical properties of the multitudinous alloy steels cannot be discussed here. The "Metals Handbook" contains charts of properties of the S.A.E. types as affected by the standard heat treatments. Differences among the steels are related to the disposition of the alloying elements, whether dissolved in the ferrite or in the carbide phase (or both), and to their effects on the distribution, particle size, and inherent properties of these phases. The question of substitutes for alloy steels is determined by the same basic considerations. Recent improvements in the quality of carbon steels, particularly with regard to freedom from inclusions and attainment of uniformly fine-grained structures, have permitted the substitution of plain carbon steels for alloyed steels in many uses. Moreover, low alloy steels now offer deep, oil-hardening characteristics which formerly were attainable only in steels with a higher alloy content. (See reference on p. 120 regarding the National Emergency (N.E.) steels.)

The physical properties desired in quenched and tempered tool steel are strength or rigidity, toughness, hardness, and abrasion resistance at maximum cutting or operating temperatures. It is

not customary to employ the usual tension test because a slight eccentricity of loading would not be relieved by localized deformations in this nonplastic material and premature rupture would result from stress concentrations. Torsion tests, in which the stresses are distributed over a comparatively long distance, however, are of great value, and when the angle of twist is multiplied by the ultimate torque a useful indicator of "toughness" is obtained. The minimum degree of toughness required should enable the tool to resist the stresses that normally occur in manufacture and use and prevent undue cracking, chipping, or crumbling of the cutting edge. Hardness is usually determined by the Rockwell method, although file tests can be very useful in this field. The wearing quality, or resistance to abrasion, must be determined by some form of test simulating service conditions. Thus, there are a great variety of cutting tests in which the material is made into drills, milling cutters, saw blades, etc., and made to perform heavy-duty service under strict control.

CARBON STEELS[1]

Carbon tool steel still maintains a wide usefulness and well-deserved popularity for a large variety of cutting tools. Some of its valuable attributes are: The high hardness which can be imparted to it, greater than that of many of its alloyed competitors; toughness, especially under shock; ease of fabrication; the readily varied degree of hardness or temper; and finally, its low cost. These valuable qualities have firmly entrenched it for hand tools, tools subject to severe shock, and tools which encounter only low operating temperatures.

Steels containing up to 0.75 per cent chromium or 0.25 per cent vanadium are usually regarded commercially as carbon tool steels. Chromium in this low range imparts the quality of hardening uniformly to a greater depth. Consequently, carbon-steel drills in sizes larger than 1 in. in diameter are usually made from this grade of steel. Vanadium increases toughness and widens the permissible hardening temperature range by refining the grain size or restricting austenitic grain growth.

[1] More detailed information on carbon and alloy tool steels is available in articles by Gill (*Metal Progress*, November, 1934) and Emmons (*Metal Progress*, December, 1933), from which a part of this discussion has been abstracted.

INTERMEDIATE ALLOY STEELS

Chromium, tungsten, molybdenum, and manganese in amounts of 1 per cent or higher are frequently added to tool steels. The objective is sometimes to increase the cutting quality and sometimes to make the steel hardenable by oil-quenching. Commercial tools made of such steels are frequently marketed as "carbon" tools. At times, carbon tool steels containing less than 3 per cent tungsten have been marketed as semihigh-speed steels, a classification to which they are not entitled (the prefix *semi* is generally meaningless when applied to metallurgical products).

Tool steel containing from 1 to 1.5 per cent chromium is oil-hardening and develops a good degree of hardness and excellent toughness together with a high resistance to wear. An unusually wide range of useful properties can be imparted to it by variations in heat treatment. Its ease of fabrication and its low cost also contribute to its popularity.

Tool steel containing from 1 to 1.5 per cent manganese is also oil-hardening and is frequently used for intricate tools where there is great danger of warping or cracking if made from plain carbon steel and quenched in brine. It has been particularly popular for die work and for forging tools.

Other intermediate alloy steels of higher alloy content are used for special requirements. A good example is the steel with about 4 per cent tungsten, 1 per cent chromium, and 1.4 per cent carbon, used for fine finishing tools taking only light cuts, and also for dies where great resistance to wear is required under low operating temperatures. Some makers also add small amounts of vanadium to this steel. Molybdenum steels are used to some extent in this field, intermediate between carbon and high-speed steels.

HIGHLY ALLOYED TOOL MATERIALS

A recently introduced type of oil-hardening steel employs 12 per cent or more chromium and 1.5 per cent carbon; in air-hardening varieties minor additions of vanadium, cobalt, or molybdenum are made. Such steels are used for thread rolling and forming dies where great resistance to wear is desired. They have been found to be quite resistant to moderate operating temperatures.

The familiar 18-4-1 (Type I) composition predominates in the field of high-speed steels (at least, until the war caused a shortage

in tungsten). It is used for the majority of mass-production operations and is a universal standard of comparison for cutting quality. The peculiar property distinguishing high-speed steel from carbon or low-alloy steels is its ability to maintain its hardness, strength, and cutting quality at high temperatures, up to 1100°F. (about 600°C.), or a low red heat, while carbon-steel tools start to soften at operating temperatures in the vicinity of 400°F. (about 205°C.).

High-speed steels containing cobalt are harder but not as tough as the standard types (I, II, and III, page 171). They may be hardened by treatment throughout a wider range of temperature with less likelihood of damage by grain growth upon overheating. These steels, however, tend to develop a soft skin as a result of surface decarburization during heat-treating so that the working surfaces must be ground after hardening. They are particularly adapted for cutting hard, gritty, or scaly material.

In the field of high-speed steels, molybdenum has long been known to be a possible substitute for tungsten, but it is only in the last 10 years that the low-tungsten, high-molybdenum types have come to be widely used. The chief deterrent was the decarburization of the surface of these steels (particularly in the 1.5 per cent W, 8 per cent Mo type) occurring at the hardening temperature of about 2250°F. (It may also occur to some extent when the steel is being preheated at about 1500°F.) This difficulty has been overcome in most cases by the use of a thin film of borax which, even though liquid at the hardening temperature, restricts the counter diffusion of oxygen and carbon atoms at the surface sufficiently to prevent noticeable removal of carbon. The use of borax (or other surface coatings) is messy; borax drippings in a furnace may alter the temperature distribution; the film on the quenched tool is difficult to remove; the steel is more sensitive to temperature variations at the high heat than the 18–4–1; these and other minor factors have contributed to a reluctance on the part of toolmakers and users to accept high-molybdenum types. The new 4 to 6 per cent tungsten and 4 to 6 per cent molybdenum type more closely resembles 18–4–1 in its heat treatment, with regard both to decarburization and temperature, and is therefore coming into wide use since it enables a saving of about two-thirds of the tungsten used in the basic high-speed type. It is impossible to distinguish between the structures of the three grades *when each*

has been properly heat-treated. The difference in properties, particularly cutting performance, is also minute or absent. Long studies in plants of large users have indicated a tendency for one grade to be superior for one type of cutting operation while a different grade might show a slight superiority for a different operation. The differences are usually small, apparent only from statistical studies, and might be far outbalanced by variability in the heat treatment or structure of any one type or by improper tool design and maintenance.

Other materials besides high-speed steel are available for cutting operations at elevated temperature. The *Stellite* type of alloy containing cobalt, chromium, and tungsten must be cast and ground to shape and is more expensive than the steels. It requires no heat treatment and maintains useful cutting hardness at temperatures far above those permitted by the use of high-speed steel.

Carbide compositions, such as Carboloy or Firthite, generally contain approximately 94 per cent tungsten carbide particles, held in position by about 6 per cent of cobalt. The alloy cannot be produced with a useful structure by melting and casting, but powders of the constituents, tungsten (or tantalum, boron, etc.) carbide, and cobalt are mixed, pressed to approximately final shape, and then sintered by heating to a high temperature in a hydrogen atmosphere. The aggregate possesses great hardness (closely approaching that of the diamond, which is the hardest material known), high compressive strength, but a relatively low order of toughness. Tools made of carbides have often been seen machining glass or porcelain in popular demonstrations. These tools are almost requisite in cutting abrasive materials of relatively low strength which rapidly dull the edges of other tools—such as aluminum-silicon alloys (page 95), white cast iron, graphite, hard rubber, slate or asbestos compositions. Carbide tools will cut cast irons at exceptionally high speeds which produce very high temperatures at the tool edge. In many types of machining work, they will remove metal from forgings, castings, etc., at rates far surpassing the best attainable with high-speed-steel tools. The brittleness of the material, however, sometimes limits its applicability since a high clearance angle cannot be employed. It has occasionally been found inferior to high-speed steels in machining some types of highly alloyed steels.

and it is usually inferior on machines subject to excessive vibration by either tool or work.

QUESTIONS

1. (*a*) What heat treatment would you recommend for spheroidizing the cementite of steel containing 1.0 per cent carbon? (*b*) What is the effect of a coarse spheroidal carbide structure on the subsequent hardening heat treatment?

2. A steel shows a microstructure consisting of approximately 50 per cent free ferrite and 50 per cent coarse spheroidal carbides in a ferritic matrix. (*a*) What is the probable carbon content of the steel? (*b*) Describe two different heat treatments that might have resulted in this structure. (*c*) How could the structure be changed to show smaller spheroidal carbides *uniformly* dispersed in ferrite?

3. A coarsely spheroidized 1.0 per cent carbon steel gives trouble in an intricate machining operation. It is desired to test the machinability of specimens with the following structures: (*a*) coarse pearlite + some spheroidized carbides, (*b*) entirely fine pearlite, (*c*) entirely fine spheroidal carbides, (*d*) moderately coarse pearlite + ferrite, (*e*) partially spheroidized moderately fine pearlite. Describe the heat treatments required, in terms of temperatures and cooling rates, to produce these structures (if they can be obtained).

4. (*a*) What quenching media are used for cooling steels from the austenitic range? (Arrange in order of decreasing cooling rates.) (*b*) What advantages would be gained by quenching a ½-in. section of carbon steel into brine, then, as soon as the exterior has cooled below 1000°F., transferring the section into an oil bath? (*c*) After removing from the brine, holding in air a few seconds, and then replacing in the brine, what might the final surface structure be?

5. How might a large screwdriver be treated, using an external source of heat but once, to develop a fine pearlitic structure in the shank and a troostitic structure at the tip?

6. What difficulties are associated with the hardening of dies used for cutting threads? How would you suggest heating a large high-speed steel wedge so as to bring the heavy section up to the proper hardening temperature without "burning" the thin edge?

7. Since neither the hardness nor the toughness of a high-speed-steel cutting tool is usually increased by tempering at 1050°F., why should it be given this treatment?

REFERENCES

"Metals Handbook," section on Heat Treatment.
BAIN, "Alloying Elements in Steel," A.S.M., 1939.
FRENCH, "Alloy Constructional Steels," A.S.M., 1942.
GILL, "Tool Steels," A.S.M., 1934.

CHAPTER XII

CAST IRONS

The iron-carbon phase diagram of page 110 is applicable to the interpretations of cast-iron structures when modifying factors, such as undercooling and impurity effects, are considered. In the discussion of that diagram, it was pointed out that the phase in stable equilibrium with ferrite or austenite is graphite, not carbide, although the positions of important boundary lines, such as the eutectic, A_{cm} and A_1 lines, are not materially displaced in the stable system. Cast irons, containing from 2.0 to 4. per cent carbon show ferrite, graphite, and carbide in their structures at room temperature, depending on the variables to be discussed.

COMPOSITION

Cast irons are essentially pig iron from a blast furnace, remelted with additions of cast-iron scrap and, occasionally, of steel scrap and perhaps some ferro-alloys to modify the composition to that finally desired. The original pig iron is usually made particularly for foundry use; analyses of some typical grades are:

Trade name	Per cent C	Per cent Si	Per cent S		Mn
No. 1—soft	3.00	3.00	0.05	0.3–1.5	0.1–1.0
No. 1—fdry	3.25	2.50	0.05	0.3–1.5	0.1–1.0
No. 2—fdry	3.50	2.00	0.06	0.3–1.5	0.1–1.0
No. 3—fdry	3.75	1.50	0.065	0.3–1.5	0.1–1.0

Stoughton, "*Metallurgy of Iron and Steel*" McGraw-Hill, 1934.

Silicon is the most important element in controlling the degree to which the cast iron develops a stable structure, in which carbon is present as graphite rather than cementite. The mechanism by which silicon forces carbon into the graphitic form is not well known nor is it certain whether, during solidification of a normal, hypoeutectic cast iron, the eutectic reaction is Liquid $\rightarrow \gamma + Fe_3C$ with a simultaneous breakdown of Fe_3C in the manner

$$Fe_3C \rightarrow 3Fe\ (\gamma) + C\ (\text{graphite})$$

or whether the graphite forms directly in the eutectic reaction Liquid $\rightarrow \gamma$ + graphite. At any rate, assuming for the moment that other elements are present in low concentrations and that the cooling rate is moderately rapid, the absence of silicon causes the alloy immediately after solidification to contain only primary austenite with eutectiferous austenite and carbide (ledeburite). A critical concentration of silicon (the amount required will be affected by other elements and the cooling rate) will cause the structure to be "mottled"—a mixture of austenite, ledeburite, and graphite—while further additions of silicon will cause the stable system to be attained, and the structure will then be austenite and graphite. Further cooling below the A_1 temperature causes the austenite to transform eutectoidally, and again the silicon content (together with the other variables) will determine which of the following reactions occurs:

$$(a)\ \gamma \rightarrow \alpha + Fe_3C \qquad \text{or} \qquad (b)\ \gamma \rightarrow \alpha + C\ \text{(graphite)}$$

If the silicon content is just enough to graphitize completely the eutectic reaction, reaction (a) may predominate at the eutectoid, and the final structure becomes pearlite plus graphite. A large excess of silicon forces the eutectoid reaction to proceed as (b), leaving a final structure of ferrite and graphite. Intermediate silicon contents may permit both reactions to occur in different parts of the structure, which results in a mixture of ferrite, pearlite, and graphite. The physical distribution of these phases is naturally of vital importance with respect to the physical properties of the aggregate. Under most conditions, the maximum graphitization effect comes at silicon concentrations of about 3 per cent. Further additions may again tend to stabilize carbide, as well as cause iron silicides to appear.

Manganese is in itself a moderately strong carbide-forming element, and its presence in cast iron tends to stabilize carbide or prevent graphitization. For example, if just enough silicon is present to give a completely graphitic structure under specific controlled conditions, a slight increase in manganese may make the iron "mottled" (partly carbide in the eutectic) or a large increase in manganese may cause the iron to solidify completely in the metastable or carbide condition. This effect is postulated on the absence of sulphur.

Sulphur chemically acts to stabilize iron carbide although it does not participate in the carbide formation. It has a very strong influence; it is ordinarily considered that each 0.01 per cent sulphur is sufficient to neutralize the graphitizing influence of 0.15 per cent silicon. However, sulphur has a strong affinity for manganese to form a manganese sulphide compound (page 25) which has little influence on carbide or graphite formation. Therefore, the first additions of sulphur to an iron with a moderately high manganese content have an indirect graphitizing tendency by removing the carbide-stabilizing manganese; vice versa, the first additions of manganese to a moderately high sulphur iron remove some of the sulphur from an active to an inactive role and thus promote graphitization. Although the sulphur content of foundry pig iron may be in the vicinity of 0.05 per cent, sulphur present in the coke enters the iron with which is is in contact. This may result in a considerable increase in sulphur content when high-sulphur coke is used and, in setting up a furnace charge, necessitates a compensating adjustment in silicon or manganese contents.

Phosphorus chemically acts to promote carbide formation. Physically, it forms a phosphide eutectic with a melting point below that of iron and carbon. This causes the $\gamma + Fe_3C$ eutectic to solidify over a temperature range which increases the critical time available for silicon to promote graphitization. With moderately low phosphorus contents, the physical effect predominates and graphitization is encouraged, but large amounts of phosphorus cause it to act chemically as a carbide stabilizer.

Gaseous elements, particularly hydrogen and oxygen, may enter cast iron during melting and will affect the cast structure. Hydrogen seems to stabilize carbides (Boyles) and, when combined with oxygen as steam or moisture, is quite active in preventing graphitization during solidification but does not seem to have any effect on graphitization of the solid iron. Oxygen, as iron oxide, seems to promote graphitization during solidification and retard the process in the solid alloy[1] (during malleabilizing, page 203).

Of the *alloying elements*, nickel, which like silicon dissolves completely in ferrite, also acts as a graphitizer while the carbide-forming elements, specifically chromium and molybdenum, tend

[1] BOEGEHOLD, *Trans. A.S.M.*, **26**, 1084, 1938.

to stabilize carbide. The effect of alloying elements on the mode of dispersion and particle size of the basic phases, ferrite, carbide, and graphite, is the chief reason for the use of alloy cast irons.

UNDERCOOLING

In general, very slow cooling tends to permit equilibrium conditions to be attained in alloy systems. In the iron-carbon system, graphitization is assisted by slow freezing and retarded or prevented altogether by rapid freezing, or chill-casting, unless the composition is adjusted by increasing silicon and decreasing manganese and sulphur. If such an adjustment is made, the graphitic structure would be expected to be finer grained by reason of the more rapid nucleation of crystallization in undercooled liquids.

Since both ferrite and carbide are white, the broken surface of a cast iron that contains only these phases shows a white fracture and the metal is called a *white iron*. A cast iron that contains only ferrite and graphite (or even pearlite and graphite) breaks along the graphite phase. Even though the graphite is discontinuous, a fractured surface contains enough sooty graphite to have a gray color, and the metal is called a *gray iron*. The *mottled* structure already spoken of is a result of the iron's being graphitic in some areas and carbidic in others.

The relation between the color of the fracture and the structure of a cast iron makes it quite easy to test an iron of a specific composition for degree of graphitization. The degree of undercooling may be varied by pouring the liquid iron in a wedge-shaped mold. At the thin end of a wedge, less hot liquid metal and more heat-abstracting material are present, and the cooling rate is quite rapid. As the thickness of the wedge increases, the cooling rate is correspondingly slower. The fracture of the cast wedge will show at what thickness of a casting having varied sections, mottled or white iron is likely to be encountered.

MICROSTRUCTURES (PLATE XII)

Plate XII, Fig. 1. Commercial white cast iron (about 2.50 per cent C); ×50; Picral etch. This specimen shows a hypoeutectic structure in which the gray background was chiefly primary austenite but transformed on later cooling to pearlite. The white masses are iron carbide. The eutectic structure of γ and

Fe_3C is not very evident since the austenite part of the eutectic was alongside, and indistinguishable from, the primary austenite. Although white iron is ordinarily considered to be brittle, hard, and unmachinable, this structure is sufficiently low in carbide for the pearlite to be nearly continuous; the iron showed a slight ductility in the tension test and could be machined.

Plate XII, Fig. 2. Same white iron; ×1,500; Picral etch. At a high magnification, details of the pearlitic background and massive carbides become readily visible. Although in this hypoeutectic structure three different forms of carbide should exist, specifically, eutectic Fe_3C, Fe_3C separating out from γ along the A_{cm} line, and eutectoid carbide, only the first and last are visible. Presumably, Fe_3C separating out from austenite along the A_{cm} line formed on the massive, eutectiferous Fe_3C already present rather than at the austenitic boundaries. This form of preferred nucleation, or in reality, growth of present large nuclei, is rather frequently encountered in all alloys where a comparable condition may exist. Here, the eutectoid reaction was normal and all of the eutectoid carbon apparently formed pearlitic carbide.

Plate XII, Fig. 3. High-carbon white cast iron (about 4.0 per cent C); ×50; Picral etch. This structure appears to be completely eutectiferous, showing only ledeburite. Again the white structure is carbide, appearing in this chill-cast structure in a needlelike form. The background was austenite as the eutectic solidified.

Plate XII, Fig. 4. Same white iron; ×800; Picral etch. At a higher magnification, details of the ledeburite structure become evident. The white carbides stand in relief with ferrite in between, since the intervening austenite did not normally transform to pearlite. The carbide forming from austenite along the A_{cm} line built up on the eutectiferous carbide masses, as in Plate XII, Fig. 2, but in addition, carbide from the pearlite reaction also tended to form on the Fe_3C already present. In some areas, this has resulted in a completely abnormal structure (see page 156) where only ferrite and massive carbides are visible while, in other places, some small areas of fine pearlite (dark masses) are visible.

Plate XII, Fig. 5. Standard malleable cast iron; ×50; Nital etch. If the white cast iron of Fig. 1 were heated long enough below the eutectic temperature, the carbide would decompose to

graphite by the reaction $Fe_3C \rightarrow 3Fe\ (\gamma) + C$ (graphite). The graphite forming in a solid structure grows in all directions from nuclei in the carbide to form *nodular graphite* or *temper carbon* particles in austenite. Very slow cooling through the eutectoid, with sufficient amounts of dissolved silicon present, causes the eutectoid reaction to be in the form, $\gamma \rightarrow \alpha + C$ (graphite), and this additional graphite forms on the nodules already present. The end structure shown here consists of a continuous, moderately fine-grained ferrite containing irregular, randomly dispersed graphite nodules.

Plate XII, Fig. 6. Malleable cast iron; ×300; Nital etch. At a higher magnification, details of the ferritic matrix and nodular (or "temper") carbon particles are more evident.

Plate XII, Fig. 7. Chill-cast gray iron from an automotive hydraulic brake cylinder; ×100; Nital etch (very light). This structure is recognizable immediately as hypoeutectic, with primary dendrites surrounded by a continuous eutectic structure. The primary dendrites were austenite which subsequently transformed to pearlite, but the light etch has not darkened the pearlitic structure. The black eutectic structure is of pearlite (γ during the eutectic reaction) and very small graphite flakes. The eutectic structure is fine as a result of the chill-casting. In order to chill-cast the iron and still obtain a graphitic structure, the silicon content must be quite high, with manganese and sulphur low or balanced.

Plate XII, Fig. 8. Chill-cast iron (Fig. 7) at ×1,000; light Nital etch. This high manification shows the pearlitic character of the primary dendrites (which solidified as austenite) and the very fine (as compared to normal cast iron, Plate XII, Fig. 9) graphitic carbon flakes. The white structure *P* with small holes is a eutectic structure of iron phosphide, called *steadite*.

Plate XII, Fig. 9. Gray cast iron at ×50; as polished with no etch. The graphite flake structure of ordinary cast irons is most readily visible in the unetched structure since the black "grooves" representing the graphite show up best against a white background. The size of these flakes is evidently about twenty times those of the chill-cast iron (Plate XII, Fig. 8). Until fairly recently, most photographs of cast iron appeared to have tremendously greater amounts of graphite than actually were present. This exaggeration occurred when polishing with the usual cloths

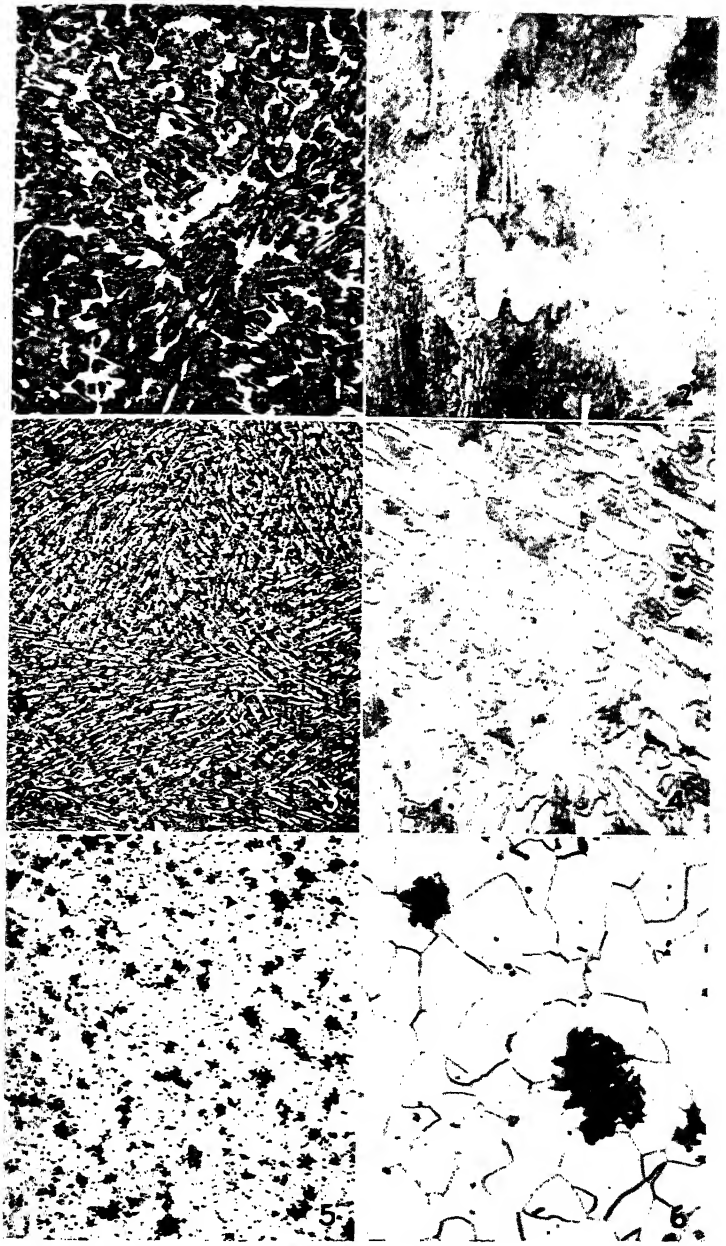

PLATE XII. FIGS. 1–6.

having a long "nap"; cloth fibers dug out the soft graphite, and the abrasive powder on the cloth gradually widened the narrow channel formerly occupied by graphite. Short-napped cloths, such as silk, or lead laps containing a fine abrasive leave more scratches but give a truer indication of the size and distribution of graphite.

Plate XII, Fig. 10. Gray cast iron at ×50; light Nital etch. This is a somewhat different iron from Fig. 9, having more and larger graphite flakes. The white area adjacent to the graphite is generally ferrite (with silicon, etc., in solid solution). Light-gray areas are pearlite.

Plate XII, Fig. 11. Soft gray cast iron at ×300; Nital etch. At this high magnification, the pearlitic part of the background of the iron is resolved. The pearlite in ordinary moderately soft cast irons is coarser than in steels, because of slower cooling through the critical temperature and the higher silicon content and coarser grain size of the austenite. The white structure adjacent to the graphite is ferrite (α) and, in addition, some steadite is visible (P).

Plate XII, Fig. 12. Relatively hard roll iron at ×300; Nital etch. This iron is used for cast-iron rolls employed in rubber mills. It is noticeably harder and more abrasion resistant than ordinary soft iron, for two reasons; (a) there is more carbon in the combined form as pearlite, and (b) there is a much higher phosphorus content and the iron contains large areas of the hard, white phosphide eutectic (marked P).

Plate XII, Fig. 13. High-strength gray cast iron; ×100; unetched. This iron with a low silicon content was melted in a special (Bracklesburg) furnace and then treated with powdered ferro-silicon just before casting. The structural effect is similar to that of sodium added to aluminum-silicon alloys before casting (see page 88), but the mechanism is different. Here, the total silicon content is sufficient to cause the iron to be graphitic and relatively free from large carbides, even in thin sections, and the addition of the ferro-silicon at the proper time provides many more nuclei for solidification with a resultant refinement in structure. The size of these graphite flakes should be compared with those of Figs. 9 and 10.

Plate XII, Fig. 14. High-strength cast iron (Fig. 13) at ×1,000; Nital etch. The matrix structure of the high-strength


P
8
9
10
α
P
11
P
P
12

iron is almost completely pearlitic although a few small ferrite areas are visible (α), as well as some steadite, (P).

Plate XII, Fig. 15. High-strength alloy (Ni, Cr, and Mo) cast iron; ×100; unetched. Additions of nickel, chromium, and molybdenum, with the carbide-stabilizing effect of the chromium and molybdenum balanced by the graphitizing effect of nickel and silicon, result in a greater refinement of graphite flakes than can be achieved by iron-silicon inoculation. Note in this structure that the graphite shows an interdendritic form of dispersion. This iron at ×1,000 has a structure very similar to that of Plate XII, Fig. 14; pearlite, a few ferrite areas, and fine graphite.

Plate XII, Fig. 16. Alloy cast iron; ×50; Picral etch. This iron has less alloy content than Fig. 15; it contains 3.0 per cent C, 1.70 per cent Ni, and 0.6 per cent Mo (trade name, Ni-Tensyl). The graphite flake size is decidedly smaller than ordinary gray iron, while the matrix is a eutectoidal ferrite-carbide aggregate.

Plate XII, Fig. 17. Heat- and corrosion-resistant alloy cast iron; ×50; Nital etch. This is a highly alloyed austenitic iron of the following composition: 2.75 per cent C, 14. per cent Ni, 2 per cent Cr, 6. per cent Cu (trade name, Ni-Resist). Variations in shading of the austenite (from white to light brown) show coring in the solid-solution austenitic dendrites. The small, bent, black streaks are graphite flakes, and the fine eutectiferous network represents carbides.

Plate XII, Fig. 18. Abrasion-resistant alloy cast iron (Ni-Hard); 3.5 per cent C, 4.5 per cent Ni, 1.7 per cent Cr; ×100; Nital etch. This structure is also clearly hypoeutectic with primary dendrites surrounded by a fine eutectic structure. The highly alloyed austenite is so sluggish in transformation that it becomes martensitic at ordinary cooling rates in the mold after casting. In addition, the eutectic structure contains an alloy carbide. The aggregate is hard and unmachinable; it can be cut only by grinding.

PROPERTIES

Structurally, the matrices of gray cast irons resemble steels in that they contain varying proportions of ferrite and pearlite. The ferrite may be a little stronger than that of most carbon steels, because of the dissolved silicon, but the pearlitic part of the structure may be softer as a result of its somewhat greater

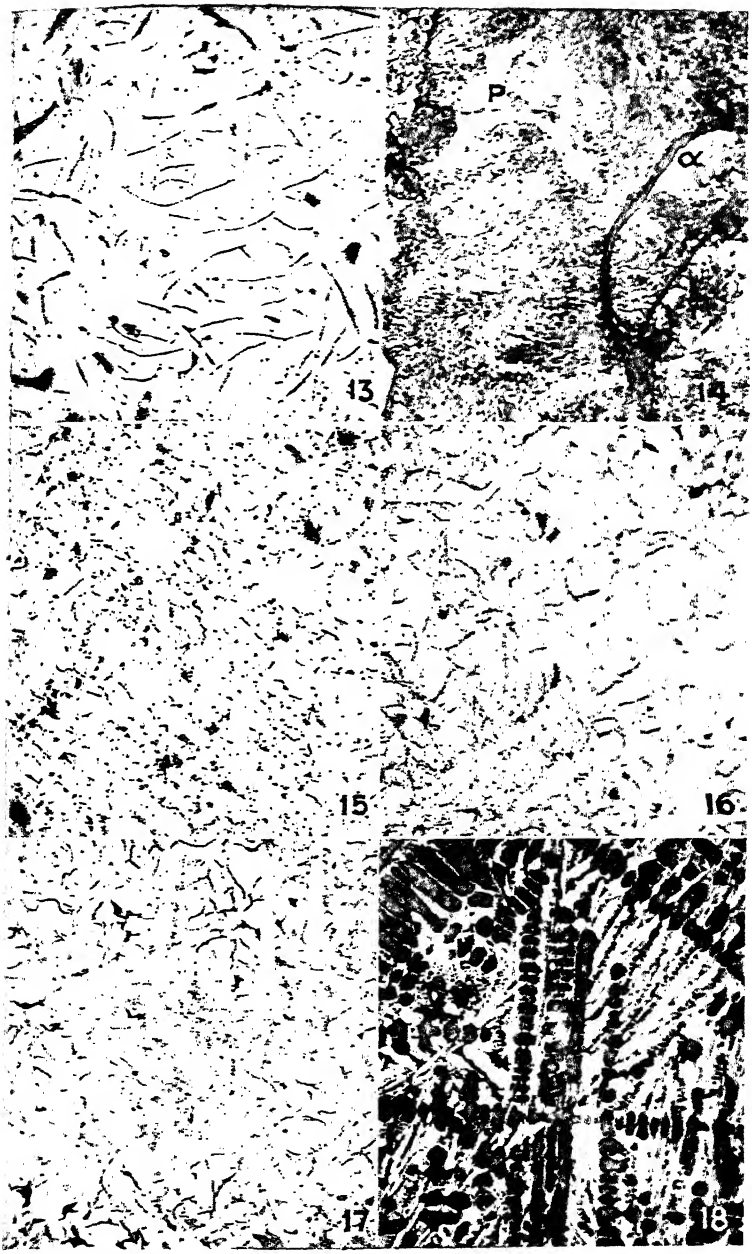
P
α
13
14
15
16
17
18

coarseness. Overbalancing both of these factors is the weakening and embrittling effect of a relatively large amount (3 per cent by weight corresponds to 12 per cent by volume) of the soft, brittle graphite flakes which disrupt the continuity of the plastic matrix. The edges of the flakes are likely to be comparatively sharp, and each acts as an internal notch which, upon deformation, tends to initiate a crack in the plastic matrix. For this reason, gray cast irons break with a brittle fracture and, until the past decade, at stresses of only 20,000 to 30,000 p.s.i. In recent years, strengths have been increased until around 60,000 p.s.i. is a common value. Some foundries have been pouring iron for several years with no test bars in the 60,000-p.s.i. class ever breaking below this value. There are classifications of 30,000, 40,000, 50,000, and 60,000 p.s.i. cast iron. The higher strengths have been achieved in two ways; by greatly refining the graphite flake size (*e.g.*, Plate XII, Figs. 13 and 15) and by attaining a fine, completely pearlitic matrix. Success in achieving this structural condition is dependent on close control of the chemical composition of the iron and of pouring temperatures.

Aside from strength properties, gray cast irons have several other features which fit them particularly well for certain applications. The relatively low melting point and ready castability of irons makes them relatively cheap, although, naturally, costs will be increased if high-strength specifications require laboratory control and use of alloying elements. More important in some applications is the fact that the internal structural discontinuities offer sites for the local dissipation of vibrational energy. This is equivalent to saying that gray cast irons have a high internal friction or damping capacity. Used as a base for machinery or any equipment subject to vibration, the structure of the iron permits the vibrations to be absorbed internally. Machine bases, or piano frames, could be made of welded steel assemblies, but these assemblies would not so readily absorb external vibrations and, at frequencies approaching the natural vibration period of the structure, the amplitude of vibration might well increase to the point where the structure would break by fatigue stressing. The great importance of this feature of cast irons is just coming to be recognized and more fully utilized; *e.g.*, in the Ford cast crankshaft.

Malleable iron castings are of intermediate cost and properties between gray iron and steel.[1] The nodular form of graphite, or temper carbon, does not interrupt the continuity of the ferritic matrix, and the aggregate may show strengths of around 55,000 p.s.i. combined with elongation values in the vicinity of 12 to 18 per cent. Two fairly recent developments have been of engineering significance. Closer control of composition and pouring temperatures (sometimes achieved by the use of special melting furnaces) has given a metal that is consistently white in the as-cast form and yet quickly graphitizes upon reheating. This possibility of quicker graphitization has been successfully utilized by the development of new annealing furnaces in which castings need not be packed in an insulating carbonaceous material (to protect them from excessive scaling) and require a week to heat, to hold, and to cool from the annealing temperature but in which the malleabilizing treatment can be completed in 48 hr. or less. Uniform results can be achieved only by uniformity of heating during annealing, a requirement best met by long, continuous furnaces of small cross section. A second development has been of malleable cast iron containing temper carbon nodules in a pearlitic rather than a ferritic matrix. The pearlitic structure enables the iron to show strengths in the vicinity of 70,000 to 80,000 p.s.i. and good elongation, 6 to 12 per cent. Some foundries call this material *semisteel*, but the disrepute of this meaningless word has led to the use of the more exact descriptive term *Pearlitic Malleable*.

Heat treatment of cast irons will not affect the graphite structure, at least not that representing carbon in excess of the amount soluble in austenite. (This is the reason that malleable cast iron must be entirely "white" as cast; graphite forming as flakes at a high temperature cannot be changed to the nodular form.) However, reheating of pearlitic malleable or gray cast iron above the critical temperatures develops austenite of eutectoidal carbon

[1] In many applications, pearlitic malleable cast iron and cast steel may be used interchangeably, and in these cases, malleable iron enjoys a competitive advantage. While its heat treatment may be more expensive, there is a lesser cost from: (*a*) scrap lost in risers and (*b*) cost of removing risers (the risers can be knocked off the original white iron castings with a hammer while they must be cut from steel casting).

content. This austenite will behave on cooling in a manner nearly identical to that of an eutectoid steel (see Chap. X); it may be quenched to martensite and then tempered, it may be "austempered" to hard but tough bainite structures, it may be air-cooled to develop a finer pearlite than was originally present, or it may be very slowly cooled to effect a more complete graphitization and, consequently, a softer structure.

There are several cast irons for special applications. A high-silicon cast iron (trade name, Duriron) resists sulphuric acid attack at all concentrations as well as many other chemicals. The martensitic cast iron (Plate XII, Fig. 18) shows particularly high resistance to wear and is applicable for many uses in which white cast iron or Hadfield manganese steel do not show sufficient service life.

QUESTIONS

1. What structural characteristics and consequent properties may be developed by the use of "chills" on the treads of freight-car wheels during casting of a normally gray iron?

2. What factors are responsible for the widespread use of cast-iron pipe for water or gas conduction?

3. In what respect might the structure of gray cast iron be considered suitable for use as a bearing material?

4. Gray cast-iron brake linings for busses may show cracks after hard service, in which localized frictional heat momentarily raises the surface layer to a temperature well above the critical (A_1) point. What would be the cause of the localized crack formation, where would the cracks appear in relation to the surface structure and what micrographic constituents would probably be visible in this zone (refer to Question 6 (*b*), page 164)?

5. Compare the normal and optimum mechanical properties of unalloyed gray cast iron, malleable cast iron, and cast steel.

6. If chromium or molybdenum is added to iron, why is nickel usually added also and in somewhat greater amounts?

7. Compare a nickel-molybdenum cast iron with plain gray iron with regard to: (*a*) machinability, (*b*) strength, (*c*) structure, (*d*) applications.

REFERENCES

"Metals Handbook," Cast Iron, Malleable Iron, Pearlitic Malleable Iron.

MERICA, "Progress in Improvement of Cast Iron and Use of Alloys in Iron," *Trans. A.I.M.E.*, **125**, p. 13, 1937.

CHAPTER XIII

MONOTECTICS; SINTERED METAL POWDERS

There are many binary alloy systems in which the component metals do not show complete mutual solubility in the liquid form. Examples of this type include: Fe-Sn, Cu-Pb, Ni-Pb, Cu-Cr, Cu-Co, Cu-Mo, Cu-W, Cu-S, Cu-Se, Cu-Te, Ag-Ni, Ag-W, Ag-Mo, Al-Cd, Al-Pb, Zn-Pb, Zn-Bi, etc. In a few of these, such as the silver-molybdenum system, the metals seem to show almost no liquid solubility. In most of the others, however, the two liquid metals show some mutual solubility at temperatures near the melting point of the more refractory constituent and form a homogeneous liquid if the temperature is increased to a sufficiently high value.

PHASE DIAGRAM

The silver-nickel phase diagram (Fig. 13, page 206), shows two horizontal lines, at 960.5°C. (0.5° above the melting point of silver) and at 1435°C. (17° below the melting point of nickel). At 960.5°, an α solid solution consisting of almost pure silver (containing only about 0.1 per cent of nickel) forms by a peritectic reaction between liquid silver and the $\alpha_{(Ni)}$ phase. The peritectic concentration is so near to pure silver in composition that it cannot be shown in the figure. At 1435°, a liquid of 95 per cent nickel reacts to form a small amount of liquid containing about 97 per cent silver and a large amount of the $\alpha_{(Ni)}$ phase, containing 4 per cent silver in solid solution. The reaction, written in the form

$$\text{Liquid}_{(95\%\ Ni)} \rightarrow \text{liquid}_{(3\%\ Ni)} + \alpha_{(Ni)}$$

is called a *monotectic*. It consists, essentially, of a considerable change in the composition and proportionate amount of a liquid phase, occurring at a constant temperature, as a result of the

rejection of a solid phase. Above the monotectic horizontal, there is always a dome-shaped field (not reproduced completely in the figure), and alloys at temperatures and concentrations within this field consist of two liquid phases. Since there is usually a considerable difference in specific gravity of the two liquids, they tend to separate into two liquid layers in a manner

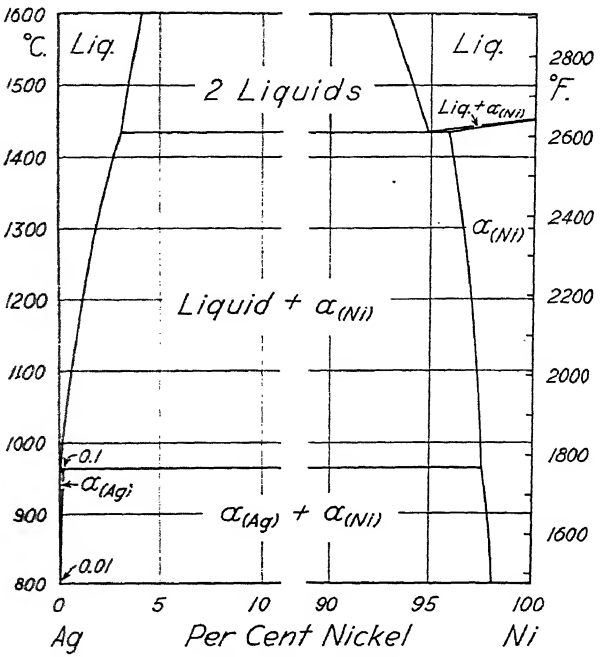

FIG. 13.—Phase diagram of the silver-nickel alloy system showing a monotectic horizontal at 1435°C. and a peritectic at 960.5°C. The diagram between 10 and 90 per cent Ni has been omitted since the phasial relations indicated on the diagram apply throughout this section.

similar to oil and water. Thus, binary alloys of compositions under the "dome" cannot usually be melted and cast, particularly in large sections, without serious liquid segregation which results in a nonuniform distribution of the ultimate solid phases. Alloys of this type are successfully produced by mixing metal powders and sintering at a temperature under that of the monotectic (although this is not the only field of application of powder metallurgical methods).

MICROSTRUCTURES (PLATE XIII)[1]

Plate XIII, Fig. 1. Alloy of 60 per cent Ag, 40 per cent Ni; ×1,000. Powders of the two metals were mixed in the specified proportions, pressed into the desired shape, and then sintered at a temperature slightly below the melting point of the silver. The gray irregular shapes represent the original nickel powder, while the continuous, dark matrix is the silver phase. (The relative areas of $\alpha_{(Ni)}$ and $\alpha_{(Ag)}$ shown in this small section are not representative.) Slow cooling from the sintering temperature permitted nickel, which had dissolved (up to 0.1 per cent) in the silver, to precipitate as the $\alpha_{(Ni)}$ phase and caused the silver-rich phase to appear dark *except* for light areas adjacent to the nickel; here nucleation for precipitation was furnished by the nickel particles (an effect discussed in several previous sections, *e.g.*, *abnormal* steel structures).

Plate XIII, Fig. 2. Alloy of 60 per cent Ag, 40 per cent Ni; rolled; ×1,000. The continuous ductile silver matrix of the previous specimen permitted the specimen to be rolled, after which it was reheated to the sintering temperature and rapidly cooled. This micrograph of a section transverse to the rolling direction shows much less than the expected amount of nickel, perhaps because of segregation resulting from inadequate mixing of the powders. The harder, gray nickel particles stand in relief while the annealing twins in the silver matrix are evidence of the working and heating. The primary purpose of rolling the original sintered aggregate was to eliminate porosity and attain a sound, dense structure.

Plate XIII, Fig. 3. Alloy of 60 per cent Ag, 40 per cent Mo; ×1,000. Powdered metals of these two components were mixed, pressed, sintered, rolled, and resintered. In this system, there is practically no mutual liquid solubility. The silver again forms a continuous ductile matrix phase which permitted the sintered compact to be rolled without breaking. Twins in the silver phase again are evidence of the deformation and subsequent reheating. In addition, the elongated stringers of the gray molybdenum

[1] The photomicrographs in this section, together with pertinent information regarding preparation of the specimens, were supplied by Professor G. J. Comstock of the Stevens Institute of Technology.

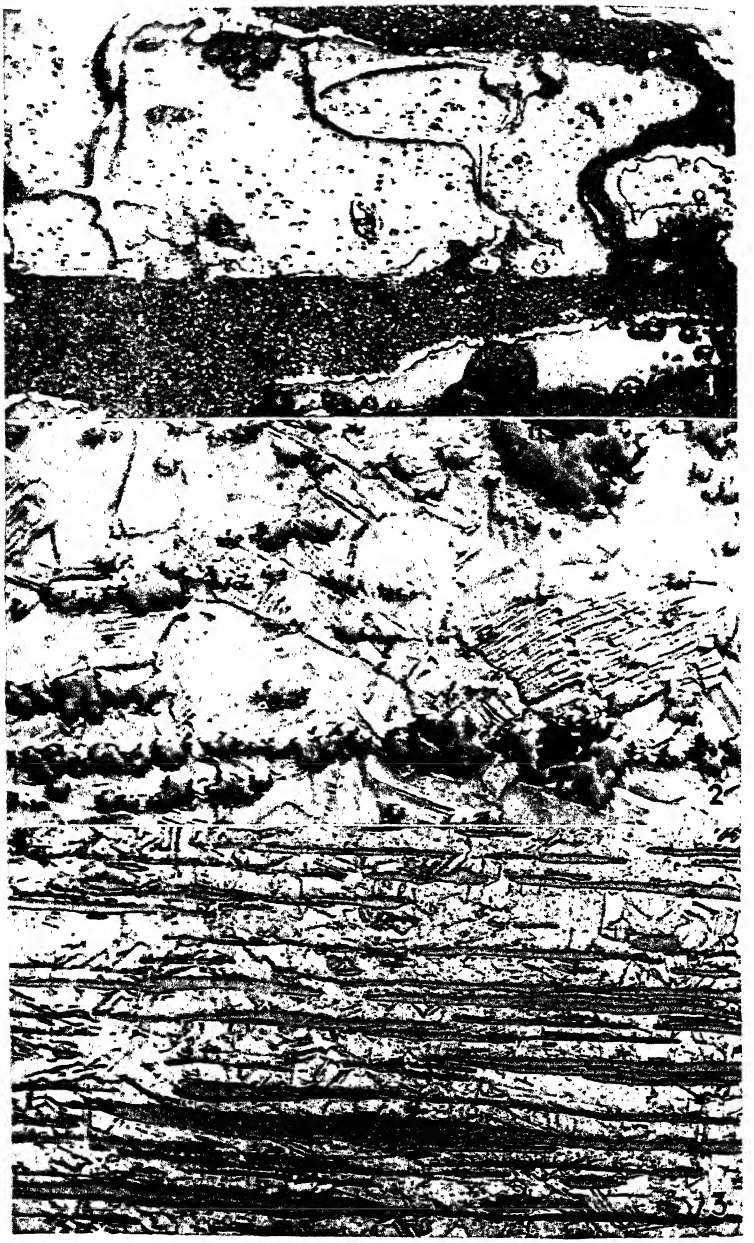

PLATE XIII. FIGS. 1–3.

phase are evidence of deformation (*cf.* slag stringers in wrought iron, page 17).

Plate XIII, Fig. 4. Alloy of 94 per cent tungsten carbide, 6 per cent cobalt; ×2,000. Powders of the carbide (dark gray) and cobalt (light matrix) were mixed by grinding together in a ball mill for many hours. After grinding, the external shape of the carbide particles is quite different from that shown here; the milling of the brittle carbide resulted in a form characteristic of such materials, with little evidence of crystallinity. The milled powder mixture was then pressed to approximate final shape and sintered in a hydrogen atmosphere at a temperature above the melting point of the cobalt but below that of the carbide. There were too many of the solid, interlocking carbide particles for any "floating" segregation to occur, but the liquid cobalt phase dissolved tungsten carbide to an amount of about 18 per cent of its own weight (thus, the proportion was about 93 per cent solid carbide and 7 per cent liquid). On cooling, most of the carbide which was dissolved in the liquid cobalt precipitated on the undissolved carbides already present (again, preferred nucleation) and left the final particles in this characteristic crystalline form.

Plate XIII, Fig. 5. Sintered carbon steel; ×1,000. Carburized iron powder was compacted at 50,000 p.s.i., sintered 1 hr. at 1120°C. (2050°F.), and slowly cooled. The structure is that of an annealed steel containing about 0.30 per cent carbon; it shows ferrite and coarse pearlite. In addition, a few oxides are visible and some small pores.

Plate XIII, Fig. 6. Diffusion of Zn into Cu powder; ×1,000. Zinc and copper powders were heated together (without pressing) at a temperature at which no melting occurred and the loose powders did not sinter. The large particle shows a core of copper, a narrow zone of α and a wide zone of β brass. Small particles in this field have been completely converted to the β phase. All of these structures resulted from an inward diffusion of zinc, in the form of a vapor, from the surface of the copper particles.

PROPERTIES AND APPLICATIONS

The silver-nickel and silver-molybdenum alloys shown here cannot be produced with the proper distribution of the two phases except by powder metallurgical methods. The alloys have particular application as contact materials in electrical circuit

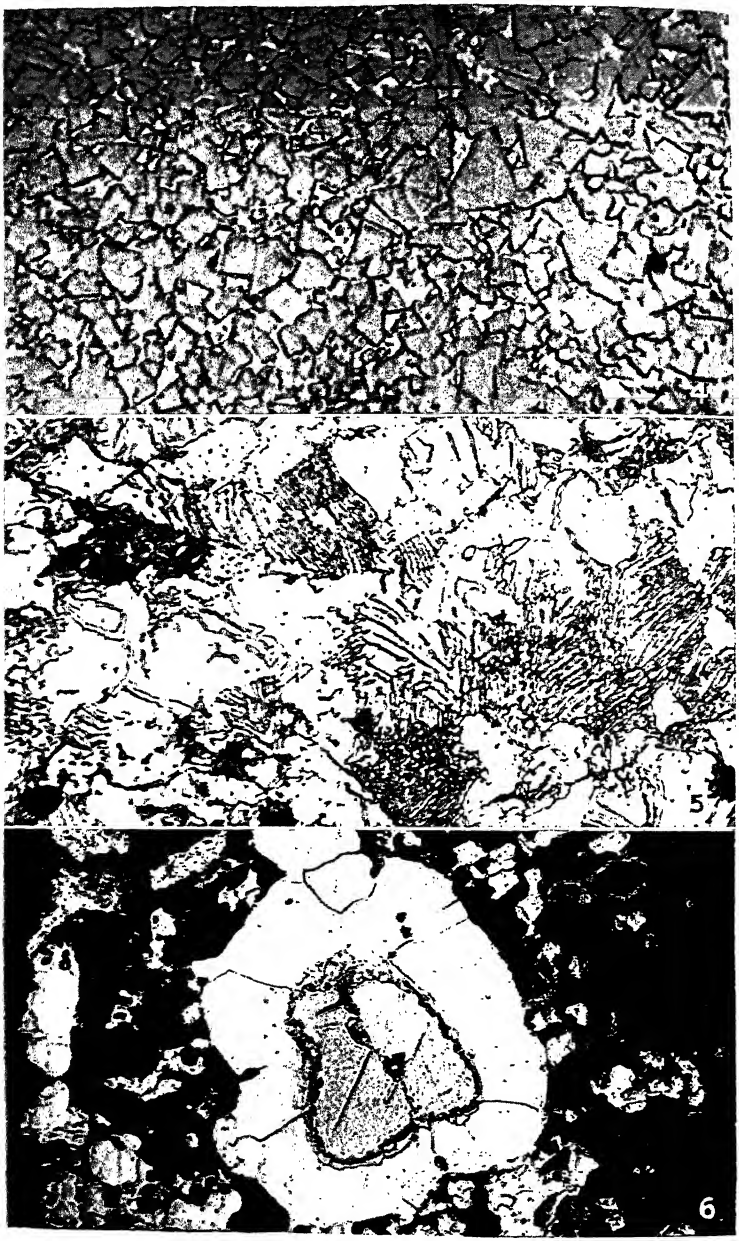

PLATE XIII. FIGS. 4–6.

breakers and other similar uses. The silver, constituting the continuous phase, has a very high electrical conductivity and is present in amounts sufficient to prevent heating of the contacts under closed circuit conditions. At the same time, the silver areas are so small that, even though they fuse in spots, the contact-opening mechanism can readily break these small, fused areas. The second phase of a refractory metal prevents fusion of large areas under the action of an accidental electrical arc.

The tungsten carbide material represents another specific structure that cannot be obtained by ordinary melting and casting procedures. This alloy can be melted and cast without segregation, but the brittle tungsten carbide phase solidifies to form a *continuous* structure. Thus, the aggregate is too brittle to be used in the cast form and the structure cannot be hot-worked or modified by heat treatment. When powders are mixed and sintered, the *cobalt* forms a practically continuous structure enveloping each carbide particle. It is possible to modify the thermal conductivity and other properties of the sintered carbides by altering the amount or composition of the matrix cobalt. Other sintered carbides than tungsten have been produced by similar techniques and successfully employed as cutting tools (*cf.* page 189).

The other structures reproduced here are of alloys customarily prepared by normal metallurgical methods. However, powdered iron (sometimes in a slightly carburized condition) is being processed by pressing and sintering to make gears and other similar parts. The basis of this application is purely economic; powder methods can produce a large number of articles to a close dimensional tolerance at a low unit cost if the metal powders are not too expensive. The additional cost of metal in a powdered form and of pressing and sintering equipment may frequently be more than offset by the saving in the gross weight of metal and the costs of removing excess by machining of forgings or castings.

While brass is ordinarily cast or wrought, the micrograph showing diffusion of zinc into copper particles is illustrative of the diffusion process, occurring during sintering, which converts pure metal powders into alloyed aggregates. Powdered copper-base alloys were mentioned on page 70 as being of importance in the field of bearings, and, in this application, structures can be obtained with a degree of porosity greater than any foundry can

produce. Of course, the important aspect is a *controlled* dispersion of porosity for soaking up oil without having large areas with no supporting metal underneath. The spot-welding industry owes its economic usefulness very largely to the development of a copper-molybdenum alloy, necessarily produced from powders, for tips on the contact electrodes. As in the silver-molybdenum alloy, the copper is continuous and supplies the required conductivity while the refractory molybdenum prevents the material being welded from fusing to the electrodes with an associated sticking, tearing, and necessity for frequent tip-redressing.

Finally, it is possible to produce from powders aggregates of metals and nonmetals, such as asbestos, to meet specific service requirements not attainable otherwise. It is not within the scope of this book to discuss all of these possibilities or to dwell on the actual forming and sintering methods employed in producing the structures. The size and shape of the original metal-powder particles, the pressing temperature and pressure, the sintering temperature and time, are all factors affecting the final density and structure and are subjects of active experimentation. It is sufficient to say here that, under optimum conditions, dispersions of two or more phases can be created in a form not attainable by normal methods of casting, working, and heat-treating. Consequently the aggregates may have unusual and very valuable properties for specific applications. However, the structures are still amenable to reasoning based on phasial relationships, deformational characteristics, etc., as covered in this book.

REFERENCES

W. D. Jones, "Principles of Powder Metallurgy," Longmans, 1937.
John Wulff (Ed.), "Powder Metallurgy," ASM, 1942.

CHAPTER XIV

GENERALIZATIONS

Nonferrous metals differ among themselves, as well as from irons and steels, in their response to alloying and to mechanical and thermal treatments. However, the differences are essentially in the degree, not in the kind, of reactions encountered; all metals and alloys have been found to follow the same general pattern of behavior. Variations in the details of the pattern are shown to a considerable extent by the specific alloy phase diagrams although, it should be emphasized, these deal with the constitutional or phasial relationships and not directly with structures. Structures may be varied, by mechanical or thermal treatments, without disturbing the phasial equilibrium in a chemical sense (*e.g.*, cold-working, or spheroidization of carbides in a steel). In other cases, a high-temperature treatment may be required to change the number or kind of phases present, in order to obtain a new and controlled distribution of these phases. The constitutional diagrams are highly useful in disclosing the basic structural elements available, as a function of the alloy composition, and frequently are useful in realizing the potential values of the alloy.

BINARY PHASE DIAGRAMS

1. Between two separate single-phase fields, there is always a region, in concentration and temperature, of alloys containing a mixture of the two phases.

2. At a given temperature T in a two-phase field, the *equilibrium* composition of each of the two phases is given by the intersections of a horizontal line, drawn at T, with the two-phase field boundary lines. By Gibbs's phase rule, when the temperature of an alloy in this field is varied, the composition of each phase is automatically fixed.

3. The relative proportions of the two phases for a specific alloy at T are given by the lever rule (see page 49).

4. At all compositions along a horizontal line of the diagram, three (and only three) phases can coexist. The situation is most simply represented by an equation in which the phase meeting the horizontal in the form of a notch, somewhere along its length, is in equilibrium with the two phases at the ends of the horizontal (example: eutectic, Chap. V; peritectic, Chap. VII; eutectoid, Chap. VIII; monotectic, Chap. XIII). In a binary alloy, the coexistence of three phases is possible only at a fixed temperature; *i.e.*, the period of their coexistence is indicated by a constant temperature on a cooling curve.

5. Equilibrium conditions may be attained only upon extremely slow heating or cooling and, in general, *time* may approach *temperature* in importance when considering metallurgical reactions. The phase diagram enables one to predict qualitatively the direction of departures from equilibrium encountered in commercial alloys. Specific cases are discussed in Chaps. IV to VIII and X.

MICROSTRUCTURES

1. Homogeneous single-phase alloys show a uniform structure with grain boundaries (or twins) as the only distinguishable detail. In etched nonhomogeneous (cored) solid solutions, the dendrites in the cast structure may efface grain boundaries (see Chap. IV).

2. In hypo- or hypereutectic alloys, the eutectic, if present in sufficient amounts (usually 5 to 10 per cent of the structure is enough), appears as a *continuous*, two-phase structure surrounding primary dendrites of the excess phase (Chaps. V, VI, XII).

3. When a second phase forms in a solid alloy under circumstances requiring diffusion, it appears first, or in greatest quantities, at grain boundaries of the phase already present, unless the alloy is in an unstable or cold-worked condition, when nucleation may be quite general (Chaps. VI to VIII, X). If formation of the new phase does not involve diffusion, as in the martensite transformation, nucleation is general throughout the structure.

4. The orientation of a new solid phase must be crystallographically related to that of its parent solid phase as a result of the necessity of lattice matching during nucleation of the new phase. When the new structure grows in the form of plates, needles, or polyhedra, these form a geometrical pattern which is called a Widmanstätten structure.

5. Undercooling tends to increase the nucleation rate of a reaction, whether it be a solidification process or the separation of one or more new phases from the solid state, with a corresponding decrease in grain or particle size. Reactions involving diffusion of two elements may be entirely suppressed by rapid cooling with the appearance of metastable or transitional phases. The alloy concentration of eutectics and eutectoids may be increased, decreased, or widened to a range by undercooling.

6. The structure obtained by heating any alloy to a specific temperature T is stable and will remain unchanged for any lower temperature, regardless of the cooling rate, *unless* the phase diagram indicates a change of composition or structure occurring between T and room temperature. Thus, a structure may be stabilized by heating to a temperature slightly above that encountered in service.

7. Disperse particles of a second phase are subject to growth, generally in a spherical form, if heated for long periods of time at a high temperature unless (*a*) the phase is completely insoluble, or (*b*) it is completely soluble, in which case, the particles disappear.

PROPERTIES

1. The strength and hardness of metals are increased by:

a. Decreasing the grain size (effect small, except for extremely fine grains, see Chap. III).

b. Cold deformation (effect moderately strong, see Chap. III).

c. Adding another element in solid solution (effect generally small but variable for different solute elements and concentrations and greatest when the solution is inhomogeneous or cored, see Chap. IV).

d. The presence of a second phase in a moderately coarse form (effect moderate, see Chaps. V to VIII).

e. The presence of a second phase in an extremely fine dispersion (effect very strong, see Chaps. VI, VII, X).

2. Ductility properties generally decrease to an extent proportional to the increase in strength (important exceptions; a few solid solutions such as α brass, Chap. IV, certain age-hardenable alloys, Chap. VI, and a part of the range of *pearlite* and *bainite* structures, Chap. X).

3. In two-phase alloys, the mechanical properties (particularly plasticity) are basically determined by those of the *continuous*

phase in the structure even though it is present in relatively small proportions (for example, hypoeutectic aluminum-silicon and aluminum-copper alloys, Chap. VI). A general quantitative law has been proposed[1] stating that the resistance to deformation of a two-phase structure consisting of a plastic matrix and a disperse hard constituent varies linearly with the logarithm of the average length of uninterrupted path through the continuous phase.

4. Physical as well as mechanical properties are affected by structural variations. For example, both thermal and electrical conductivities are decreased by addition elements in solid solution. When an element is added in amounts exceeding the solubility limit, the effect of the second phase appearing in the structure will depend on the conductivity of that phase and its dispersion; if it has a low conductivity and forms a *continuous* structure, it will have an effect disproportionate to the amount present. Other physical properties, such as magnetism, are frequently more related to atomic structure than to the visible microstructure.

5. Corrosion properties are not amenable to many generalizations, but one of considerable importance, associated with structure, is: the localized precipitation of a second phase at grain boundaries of the matrix solid solution may result in a severe, electrolytic-cell type of corrosion at the boundary areas with a considerably more serious diminution in strength properties than an equivalent corrosion distributed uniformly over the entire surface.

6. Failure to achieve the expected service life from a metal may often be traced to faulty mechanical details rather than to internal flaws or improper microstructures. Considerable internal porosity may be tolerated in a casting if the porosity occurs in areas subjected to low stresses, *e.g.*, in the center of a section subjected to bending forces. Surface defects, such as scratches, tool marks, or intergranular corrosion "notches," cause high localized stress concentrations; if the surface is a very plastic material, such as annealed copper or aluminum on Duralumin (Alclad), localized plastic flow may reduce the stress concentration to the point where it is insignificant. An equivalent stress concentration at the surface of a less plastic material may seriously reduce the impact or fatigue strength of the metal even when there is no apparent reduction in the ordinary tensile strength.

[1] GENSAMER *et al.*, *A.S.M. Preprint*, 1941.

INDEX

A

D

E

F

G

H